

**IMPROVING OIL RECOVERY BY WATERFLOODING  
IN SUPHAN-BURI BASIN OF THAILAND**

**Miss Suwannee Rattanapranudej**

**A Thesis Submitted in Partial Fulfillment of the Requirements for the  
Degree of Master of Engineering in Geotechnology  
Suranaree University of Technology**

**Academic Year 2004**

**ISBN 974-533-415-4**

# การเพิ่มการผลิตน้ำมันโดยขั้วด้วยน้ำในแอ่งสุพรรณบุรีของประเทศไทย

นางสาวสุวรรณณี รัตนภานุเดช

วิทยานิพนธ์นี้เป็นส่วนหนึ่งของการศึกษาตามหลักสูตรปริญญาวิศวกรรมศาสตรมหาบัณฑิต

สาขาวิชาเทคโนโลยีธรณี

มหาวิทยาลัยเทคโนโลยีสุรนารี

ปีการศึกษา 2547

ISBN 974-533-415-4

**IMPROVING OIL RECOVERY BY WATERFLOODING  
IN SUPHANBURI BASIN OF THAILAND**

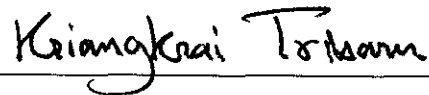
Suranaree University of Technology has approved this thesis submitted in partial fulfillment of the requirements for a Master's Degree.

Thesis Examining Committee



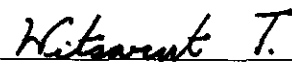
(Asst. Prof. Thara Lekuthai)

Chairperson



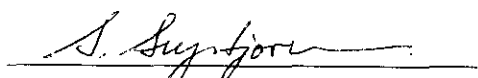
(Asst. Prof. Kriangkrai Trisarn)

Member (Thesis Advisor)




(Dr. Wisarut Thungsuntonkhun)

Member



(Assoc. Prof. Dr. Sarawut Sujitjorn)

Vice Rector for Academic Affairs



(Assoc. Prof. Dr. Vorapot Khompis)

Dean of Institute of Engineering

สุวรรณณี รัตนภรานุเดช : การเพิ่มการผลิตน้ำมัน โดยขับด้วยน้ำในแอ่งสุพรรณบุรีของ  
ประเทศไทย (IMPROVING OIL RECOVER BY WATERFLOODING IN SUPHAN-  
BURI BASIN OF THAILAND) อาจารย์ที่ปรึกษา : ผู้ช่วยศาสตราจารย์ เกรียงไกร ไตรสาร,  
205 หน้า. ISBN 974-533-415-4

การวิจัยนี้มีวัตถุประสงค์เพื่อเพิ่มปริมาณการผลิตน้ำมัน โดยขับด้วยน้ำในแหล่งน้ำมันของแอ่ง  
สุพรรณบุรีของประเทศไทย ปัจจุบันความต้องการใช้น้ำมันมีมากขึ้นเนื่องจากการพัฒนาและการ  
ขยายตัวทั้งในด้านอุตสาหกรรมและเกษตรกรรม ดังนั้นการเพิ่มปริมาณการผลิตน้ำมัน โดยการขับด้วย  
น้ำจึงเป็นวิธีหนึ่งที่น่าสนใจ ในการศึกษาประกอบด้วย (1) การศึกษาค่าความพรุนและค่าความซึม  
ผ่านได้ของหินทรายในยุคเทอร์เชียรีในห้องปฏิบัติการทดลอง (2) การศึกษาเปรียบเทียบของการผลิต  
โดยการขับด้วยน้ำในกรณีต่างๆ โดยใช้แบบจำลองทางแหล่งกักเก็บเพื่อหาค่าต่างๆของการผลิตน้ำมัน  
โดยการขับด้วยน้ำ อาทิเช่นค่าประสิทธิภาพในการผลิตน้ำมัน, อัตราการผลิตน้ำมัน, และประสิทธิภาพ  
ในการแทนที่เป็นต้น (3) การวิเคราะห์ค่าทางเศรษฐกิจเพื่อใช้ในการตัดสินใจเลือกกรณีที่เหมาะสมและ  
มีค่าทางเศรษฐกิจที่มีประสิทธิภาพเพื่อใช้ในการพัฒนาต่อไป ค่าความพรุนที่วัดได้มีค่าเฉลี่ยที่ 11.7%  
และค่าความซึมผ่านได้มีค่าเฉลี่ยเท่ากับ 5.2 มิลลิเดาร์ซี ในการศึกษาแบบจำลองแหล่งกักเก็บได้ถูกแบ่ง  
ออกเป็น 5 กรณีคือ กรณีที่ 1 ไม่มีการอัดด้วยน้ำ และ อีก 4 กรณีมีการอัดด้วยน้ำโดยมีแบบหลุมอัดน้ำที่  
แตกต่างกัน ในการผลิตขั้นแรกก่อนการมีการขับด้วยน้ำสามารถผลิตน้ำมันได้เพียง 0.58 ล้านบาร์เรล  
หรือ 10% ของปริมาณของน้ำมันดิบทั้งหมดที่มีอยู่ในแหล่งกักเก็บเป็นเวลา 3 ปี และได้มีการผลิต  
ต่อไปอีก 15 ปีโดยในกรณีที่ 1 สามารถเพิ่มการผลิตน้ำมันได้อีก 11.93% โดยไม่มีการอัดด้วยน้ำ แต่อีก  
4 กรณีซึ่งมีการผลิตโดยการขับด้วยน้ำสามารถเพิ่มการผลิตได้ถึง 17.59%, 34.69%, 36.10%, และ  
36.55% ตามลำดับ เราจะพบว่ากรณีที่ 1 ซึ่งไม่มีการอัดด้วยน้ำมีค่าประสิทธิภาพในการผลิตน้ำมันน้อย  
ที่สุดในทางตรงกันข้ามกรณีที่ 4 และ 5 ซึ่งมีหลุมอัดน้ำจำนวน 4 หลุมสามารถผลิตน้ำมันได้มากที่สุด  
ถึง 3.20 และ 3.23 ล้านบาร์เรล ตามลำดับในกรณีของการขับด้วยน้ำเราสามารถคำนวณค่าประสิทธิภาพ  
ในการแทนที่ได้ดังต่อไปนี้ 0.55, 0.58, 0.60, และ 0.59 ตามลำดับ ในการวิเคราะห์ค่าทางเศรษฐกิจพบว่า  
กรณีที่ 4 และ 5 แม้ว่าสามารถผลิตน้ำมันได้มากที่สุด แต่เนื่องจากมีค่าการลงทุนที่สูงกว่ากรณีอื่นๆ จึง  
ทำให้ไม่เหมาะที่จะนำมาพัฒนา ดังนั้นกรณีที่ 3 จึงเป็นกรณีที่ดีที่สุดที่จะนำมาใช้เป็นแผนพัฒนา  
เนื่องจากให้ค่าทางเศรษฐกิจที่ดีกว่ากรณีอื่นๆ ประโยชน์ ที่ได้รับจากการศึกษาครั้งนี้เพื่อนำไป  
ปรับปรุงความรู้ในการผลิตน้ำมันโดยการขับด้วยน้ำรวมถึงความ สามารถในการใช้แบบจำลอง แหล่ง  
กักเก็บเพื่อใช้ในการศึกษาการเพิ่มปริมาณการผลิตโดยการขับด้วยน้ำในแหล่งน้ำมันอื่นๆ ต่อไป

สาขาวิชาเทคโนโลยีธรณี  
ปีการศึกษา 2547

ลายมือชื่อนักศึกษา \_\_\_\_\_  
ลายมือชื่ออาจารย์ที่ปรึกษา \_\_\_\_\_

SUWANNEE RATTANAPRANUDEJ : IMPROVING OIL RECOVERY BY  
WATERFLOODING IN SUPHAN-BURI BASIN OF THAILAND.

THESIS ADVISOR : ASST. PROF. KRIANGKRAI TRISARN.

205 PP. ISBN 974-533-415-4

WATERFLOODING/AREAL SWEEP EFFICIENCY/DISPLACE  
EFFICIENCY/RECOVERY FACTOR/RESERVOIR SIMULATION

The objective of the research is to improve and increase oil recovery by waterflooding in Suphan-Buri Basin of Thailand. At the present, the petroleum demand is increasing due to Thai economic has expanded and developed both industry and agriculture. Therefore Increasing oil recovery by waterflooding is the most interesting method. The research effort includes (1) the porosity and permeability measurements of Tertiary sandstone in laboratory (2) study comparison of waterflooding cases by using reservoir simulation to estimate waterflood performances such as oil recovery factor, water cut, and displacement efficiency etc. (3) economic analysis study to make alternative economic cases for suitable development plan. The porosity and permeability are determined in laboratory. Average porosity is 11.7% and average permeability is 5.2 md respectively. The reservoir simulation study is divided into 5 cases; case 1 has no water injection and four cases which have water injection in different flood patterns. For three years, it can be produced about 0.58 MMSTB or 10% of original oil in place (OOIP). After that, the field has been continued to produce oil for 15 years. For case 1 without waterflooding, it can be increased oil recovery factor by 11.93%. The other 4 cases with waterflooding production, they are increased by 17.59%, 34.69%, 36.10%, and

36.55% respectively. It shows that case 1 has no water injection; it provides the minimum of oil recovery factor. On the other hands, case 4 and 5 which have four injection wells, they can be produced a largest amount of oil production about 3.20 and 3.23 MMSTB. In four cases of waterflooding, they can be calculated the displacement efficiencies about 0.55, 0.58, 0.60, and 0.59 respectively. In economic analysis, for case 4 and 5 can be produced maximum of oil production but there is higher investment than other cases. As a result, they are not suitable for development. Therefore case 3 is the best case operation in development plan due to economic values which are more favorable than the other cases. The benefits of this study will improve the knowledge of waterflooding including the ability to use reservoir simulation. The simulation model and results can be applied for study of improving oil recovery by waterflooding in other fields

School of Geotechnology

Academic Year 2004

Student's Signature \_\_\_\_\_

Advisor's Signature \_\_\_\_\_

## **ACKNOWLEDGEMENTS**

The author wishes to acknowledge the support from the PTT Exploration and Production Public Company Limited (PTTEP) who has provided funding for this research and DMF (Department of Mineral Fuel) who supports software to use run simulator.

Asst. Prof. Kriangkrai Trisarn is the thesis advisor, Asst. Prof. Thara Lekuthai and Dr. Wisarut Thungsuntonkhun are the thesis committee.

Suwannee Rattanapranudej

# TABLE OF CONTENTS

	<b>PAGE</b>
ABSTRACT (THAI) .....	I
ABSTRACT (ENGLISH).....	III
ACKNOWLEDGEMENTS.....	IV
TABLE OF CONTENTS .....	V
LIST OF TABLES.....	XI
LIST OF FIGURES .....	XIII
LIST OF ABBREVIATIONS.....	XXII
<b>CHAPTER</b>	
<b>I INTRODUCTION .....</b>	<b>1</b>
1.1 Objectives .....	1
1.2 Problem and rationale .....	2
1.3 Scopes and limitations of research .....	3
1.4 Research methodology.....	3
1.5 Expected results .....	5
<b>II LITERATURE REVIEW .....</b>	<b>6</b>
2.1 Site geology .....	6
2.2 Porosity and permeability measurement.....	9
2.3 Case study of waterflooding in development plans .....	11



## TABLE OF CONTENTS (Continued)

	<b>PAGE</b>
<b>III    LABORATORY EXPERIMENT .....</b>	<b>25</b>
3.1 Objectives .....	26
3.2 Sample collection and preparation .....	26
3.3 Porosity measurement .....	30
3.3.1 The porosimeter calculations.....	30
3.4 Permeability measurement .....	38
3.4.1 The overburden permeability calculations .....	40
3.5 Conclusions and discussion.....	43
<b>IV    WATERFLOODING ANALYSIS.....</b>	<b>44</b>
4.1 Microscopic displacement efficiency .....	44
4.2 Macroscopic displacement efficiency of a linear waterfood.....	45
4.2.1 Development of equation description multi-phase flow in porous media.....	45
4.2.2 Flow equation for each phase.....	46
4.2.3 Steady-state solutions to fluid-flow equations in Linear system.....	46
4.2.4 Buckley-Leverett method .....	49
4.3 Immiscible displacement in two dimensions-Areal .....	54
4.3.1 Craig-Geffen-Morse correlation (CGM).....	54

## TABLE OF CONTENTS (Continued)

	<b>PAGE</b>
4.3.2 Stream tube models .....	55
4.4 Estimating waterflooding performance with 3D model and reservoir simulators .....	56
4.5 Waterflooding patterns .....	57
4.6 Recovery efficiency.....	61
<b>V RESERVOIR SIMULATION .....</b>	<b>63</b>
5.1 Theory of reservoir simulation .....	63
5.1.1 Simulation solution procedures .....	63
5.1.2 Classification of reservoir simulation.....	64
5.1.3 Other classification.....	65
5.1.4 Fluid representation .....	65
5.1.5 Reservoir model geometry .....	65
5.1.6 Transmissibility conventions.....	66
5.1.7 Formulation of the equations.....	70
5.1.8 Benefits of reservoir simulation .....	74
5.2 Objective.....	75
5.3 Reservoir model characteristic .....	76
5.4 Inputting data for the reservoir modeling.....	80
5.4.1 Grid section data.....	80
5.4.2 PVT section data.....	81

## TABLE OF CONTENTS (Continued)

	<b>PAGE</b>
5.4.3 SCAL section data.....	85
5.4.4 Initialization section data.....	89
5.4.5 Well data.....	90
5.5 Results of reservoir simulation.....	95
5.5.1 Case 1 (No water injection).....	95
5.5.2 Case 2 (One injection well).....	95
5.5.3 Case 3 (Two injection wells).....	96
5.5.4 Case 4 (Four injection wells).....	97
5.5.5 Case 5 (Four injection wells in aquifer).....	98
5.6 Frontal advanced analysis.....	110
<b>VI ECONOMIC EVALUATION</b> .....	<b>116</b>
6.1 Objective.....	116
6.2 Assumption of economic study.....	116
6.3 Calculation of cash flow.....	118
6.3.1 Payout time.....	119
6.3.2 Profit to investment ratio (PIR).....	119
6.3.3 Present Worth net profit.....	119
6.3.4 Internal Rate of Return (IRR).....	119
6.4 Results of economic evaluation.....	120



**TABLE OF CONTENTS (Continued)**

	<b>PAGE</b>
APPENDIX H WELL RESULTS OF CASE 1.....	175
APPENDIX I WELL RESULTS OF CASE 2.....	181
APPENDIX J WELL RESULTS OF CASE 3.....	187
APPENDIX K WELL RESULTS OF CASE 4.....	193
APPENDIX L WELL RESULTS OF CASE 5.....	199
<b>BIOGRAPHY</b> .....	<b>205</b>

## LIST OF TABLES

TABLE		PAGE
2.1	The porosity and permeability of Mid Tertiary Sandstone.....	10
3.1	The porosity values in different types of reservoir rock.....	32
3.2	The volumes of the matrix cup billets that are used with the porosimeter. The volume of the billet removed should be approximately equal to the pore volume of the sample test .....	34
3.3	Summary of the porosity measurement results of sandstone specimens .....	36
3.4	Summary of the permeability measurement results of sandstone specimens .....	41
4.1	Characteristics of waterflood patterns.....	60
5.1	PVTO (The Oil Properties) .....	82
5.2	PVDG (The Dry Gas Fluid Property).....	83
5.3	PVTW (The Water properties), Density and Rock properties .....	84
5.4	SOF <sub>3</sub> (Oil Saturation Function) .....	86
5.5	SGFN (Gas Saturation Function) .....	87
5.6	SWFN (Water Saturation Function).....	88
5.7	Summarizes of the results of simulation at the end of production life in five cases.....	109

**LIST OF TABLES (Continued)**

<b>TABLE</b>		<b>PAGE</b>
5.8	Relative permeability and fractional flows.....	111
5.9	The calculated resulted from frontal advanced analysis .....	114
5.10	The WORs at the end of the production life .....	115
6.1	Economic parameters .....	117
6.2	Economic evaluation of case 1 .....	121
6.3	Economic evaluation of case 2 .....	123
6.4	Economic evaluation of case 3 .....	125
6.5	Economic evaluation of case 4 .....	127
6.6	Economic evaluation of case 5 .....	129
6.7	Summary of calculations of economic evaluation .....	131

## LIST OF FIGURES

FIGURE	PAGE
2.1 U-Thong oil field location map .....	8
3.1 Location of Chiang Muan Basin in northern part of Thailand .....	26
3.2 Location of Li Basin, and Mae Moe Basin in northern part of Thailand.....	27
3.3 The drilling machine is used to drill core specimens using diamond impregnated bit.....	28
3.4 The core specimens are cut to obtain the desired length .....	29
3.5 Some Tertiary sandstone specimens for measurements.....	29
3.6 The oven is used to heat the core specimens about at $50 - 60^{\circ}\text{C}$ .....	31
3.7 Porosimeter instrument is used to measure the porosity the specimens.....	31
3.8 The overburden poro-perm cell instrument is used to measure the permeability of the specimens .....	39
4.1 Schematic of steady two-phase flow in a porous rock.....	48
4.2 Oil-Water relative permeability .....	52
4.3 Fraction water flow .....	52
4.4 Determination of average water saturation at breakthrough.....	53
4.5 Flood patterns .....	58
5.1 Block corner transmissibility .....	67



## LIST OF FIGURES (Continued)

FIGURE	PAGE
5.2	Corner point transmissibility .....69
5.3	The contour of top surface .....77
5.4	Cross- section area of reservoir model .....77
5.5	Reservoir Modeling in Top View .....78
5.6	Reservoir Modeling in Bottom View .....78
5.7	Reservoir Modeling in Front View .....79
5.8	Reservoir Modeling in Back View .....79
5.9	Graph shows relationship of bubble-point pressure, ( $P_{\text{bub}}$ ) VS oil formation volume factor, (FVF) and solution gas-oil ratio, ( $R_s$ ) .....82
5.1	Graph shows relationship of pressure VS gas formation volume factor and gas viscosity .....83
5.11	Graph of oil saturation plots with oil-water relative permeability and oil- water-gas relative permeability .....86
5.12	Graph of gas saturation plots with gas relative permeability.....87
5.13	Graph of water saturation plots with water relative permeability .....88
5.14	Location of producing wells with no injection well in case 1 .....92
5.15	Location of producing wells one injection well which inverting from producing well (P1). in case 2 .....92
5.16	Location of six producing wells and two injection wells in case 3 .....93
5.17	Location of six producing wells and four injection wells in case 4.....93

## LIST OF FIGURES (Continued)

<b>FIGURE</b>	<b>PAGE</b>
5.18 Location of six producing wells and four injection wells in aquifer in case 5 .....	94
5.19 Oil, Gas, and Water In Place versus Time .....	99
5.20 Oil Recovery Factor and Cumulative Oil Production versus Time, (Case 1) .....	99
5.21 Oil Production Rate versus Cumulative Oil Production, (Case 1).....	100
5.22 Field Pressure versus Time, (Case 1) .....	100
5.23 Cumulative Oil, Gas, and Water Production versus Time,(Case1) .....	101
5.24 Oil Recovery Factor and Cumulative Oil Production versus Time, (Case 2) .....	101
5.25 Oil Production Rate versus Cumulative Oil Production, (Case2).....	102
5.26 Field Pressure versus Time, (Case 2) .....	102
5.27 Cumulative Oil, Gas, and Water Production versus Time, (Case 2) .....	103
5.28 Oil Recovery Factor and Cumulative Oil Production versus Time, (Case 3) .....	103
5.29 Oil Production Rate versus Cumulative Oil Production, (Case 3) .....	104
5.30 Field Pressure versus Time, (Case 3) .....	104
5.31 Cumulative Oil, Gas, and Water Production versus Time, (Case 3) .....	105
5.32 Oil Recovery Factor and Cumulative Oil Production versus Time, (Case 4) .....	105

## LIST OF FIGURES (Continued)

<b>FIGURE</b>	<b>PAGE</b>
5.33 Oil Production Rate versus Cumulative Oil Production, (Case 4) .....	106
5.34 Cumulative Oil, Gas, and Water Production versus Time, (Case 4) .....	106
5.35 Oil Recovery Factor and Cumulative Oil Production versus Time, (Case 5) .....	107
5.36 Oil Production Rate versus Cumulative Oil Production, (Case 5) .....	107
5.37 Field Pressure versus Time, (Case 5).....	108
5.38 Cumulative Oil, Gas, and Water Production versus Time, (Case 5) .....	108
5.39 The fractional flow curve with tangent drawn to find $S_{wf}$ .....	112
A.1 Porosity distribution of first layer .....	141
A.2 Porosity distribution of second layer .....	141
A.3 Porosity distribution of third layer.....	142
A.4 Porosity distribution of fourth layer.....	142
A.5 Porosity distribution of fifth layer.....	143
A.6 Porosity distribution of sixth layer.....	143
A.7 Porosity distribution of seventh layer .....	144
A.8 Porosity distribution of eighth layer .....	144
B.1 Permeability distribution in x and y direction of first layer.....	146
B.2 Permeability distribution in x and y direction of second layer .....	146
B.3 Permeability distribution in x and y direction of third layer.....	147
B.4 Permeability distribution in x and y direction of fourth layer .....	147

## LIST OF FIGURES (Continued)

<b>FIGURE</b>	<b>PAGE</b>
B.5 Permeability distribution in x and y direction of fifth layer .....	148
B.6 Permeability distribution in x and y direction of sixth layer .....	148
B.7 Permeability distribution in x and y direction of seventh layer .....	149
B.8 Permeability distribution in x and y direction of eighth layer .....	149
B.9 Permeability distribution in z direction of first layer.....	150
B.10 Permeability distribution in z direction of second layer.....	150
B.11 Permeability distribution in z direction of third layer.....	151
B.12 Permeability distribution in z direction of forth layer .....	151
B.13 Permeability distribution in z direction of fifth layer .....	152
B.14 Permeability distribution in z direction of sixth layer .....	152
B.15 Permeability distribution in z direction of seventh layer.....	153
B.16 Permeability distribution in z direction of eighth layer .....	153
C.1 Distribution of oil saturation in July 1991 .....	155
C.2 Distribution of oil saturation in January 1993 .....	155
C.3 Distribution of oil saturation in January 1995 .....	156
C.4 Distribution of oil saturation in January 2000 .....	156
C.5 Distribution of oil saturation in January 2005 .....	157
C.6 Distribution of oil saturation in January 2009 .....	157
D.1 Distribution of oil saturation in July 1991 .....	159

## LIST OF FIGURES (Continued)

<b>FIGURE</b>	<b>PAGE</b>
D.2    Distribution of oil saturation in January 1993 .....	159
D.3    Distribution of oil saturation in January 1995 .....	160
D.4    Distribution of oil saturation in January 2000 .....	160
D.5    Distribution of oil saturation in January 2005 .....	161
D.6    Distribution of oil saturation in January 2009 .....	161
E.1    Distribution of oil saturation in July 1991 .....	163
E.2    Distribution of oil saturation in January 1993 .....	163
E.3    Distribution of oil saturation in January 1995 .....	164
E.4    Distribution of oil saturation in January 2000 .....	164
E.5    Distribution of oil saturation in January 2005 .....	165
E.6    Distribution of oil saturation in January 2009 .....	165
F.1    Distribution of oil saturation in July 1991 .....	167
F.2    Distribution of oil saturation in January 1993 .....	167
F.3    Distribution of oil saturation in January 1995 .....	168
F.4    Distribution of oil saturation in January 2000 .....	168
F.5    Distribution of oil saturation in January 2005 .....	169
F.6    Distribution of oil saturation in January 2009 .....	169
G.1    Distribution of oil saturation in July 1991 .....	171
G.2    Distribution of oil saturation in January 1993 .....	171
G.3    Distribution of oil saturation in January 1995 .....	172

## LIST OF FIGURES (Continued)

<b>FIGURE</b>	<b>PAGE</b>
G.4 Distribution of oil saturation in January 2000 .....	172
G.5 Distribution of oil saturation in January 2005 .....	173
G.6 Distribution of oil saturation in January 2009 .....	173
H.1 Cumulative Oil Production versus Time .....	175
H.2 Cumulative Water Production versus Time.....	175
H.3 Cumulative Gas Production versus Time .....	176
H.4 Water Cut versus Time .....	176
H.5 Oil, Water, and Gas Production Rate of Well P1 versus Time.....	177
H.6 Oil, Water, and Gas Production Rate of Well P2 versus Time.....	177
H.7 Oil, Water, and Gas Production Rate of Well P3 versus Time.....	178
H.8 Oil, Water, and Gas Production Rate of Well P4 versus Time.....	178
H.9 Oil, Water, and Gas Production Rate of Well P5 versus Time.....	179
H.10 Oil, Water, and Gas Production Rate of Well P6 versus Time.....	179
I.1 Cumulative Oil Production versus Time .....	181
I.2 Cumulative Water Production versus Time.....	181
I.3 Cumulative Gas Production versus Time .....	182
I.4 Water Cut versus Time .....	182
I.5 Oil, Water, and Gas Production Rate of Well P1 versus Time.....	183
I.6 Oil, Water, and Gas Production Rate of Well P2 versus Time.....	183

## LIST OF FIGURES (Continued)

<b>FIGURE</b>	<b>PAGE</b>
I.7 Oil, Water, and Gas Production Rate of Well P3 versus Time.....	184
I.8 Oil, Water, and Gas Production Rate of Well P4 versus Time.....	184
I.9 Oil, Water, and Gas Production Rate of Well P5 versus Time.....	185
I.10 Oil, Water, and Gas Production Rate of Well P6 versus Time.....	185
J.1 Cumulative Oil Production versus Time .....	187
J.2 Cumulative Water Production versus Time.....	187
J.3 Cumulative Gas Production versus Time .....	188
J.4 Water Cut versus Time .....	188
J.5 Oil, Water, and Gas Production Rate of Well P1 versus Time.....	189
J.6 Oil, Water, and Gas Production Rate of Well P2 versus Time.....	189
J.7 Oil, Water, and Gas Production Rate of Well P3 versus Time.....	190
J.8 Oil, Water, and Gas Production Rate of Well P4 versus Time.....	190
J.9 Oil, Water, and Gas Production Rate of Well P5 versus Time.....	191
J.10 Oil, Water, and Gas Production Rate of Well P6 versus Time.....	191
K.1 Cumulative Oil Production versus Time .....	193
K.2 Cumulative Water Production versus Time.....	193
K.3 Cumulative Gas Production versus Time .....	194
K.4 Water Cut versus Time .....	194

## LIST OF FIGURES (Continued)

<b>FIGURE</b>	<b>PAGE</b>
K.5 Oil, Water, and Gas Production Rate of Well P1 versus Time.....	195
K.6 Oil, Water, and Gas Production Rate of Well P2 versus Time.....	195
K.7 Oil, Water, and Gas Production Rate of Well P3 versus Time.....	196
K.8 Oil, Water, and Gas Production Rate of Well P4 versus Time.....	196
K.9 Oil, Water, and Gas Production Rate of Well P5 versus Time.....	197
K.10 Oil, Water, and Gas Production Rate of Well P6 versus Time.....	197
L.1 Cumulative Oil Production versus Time .....	199
L.2 Cumulative Water Production versus Time.....	199
L.3 Cumulative Gas Production versus Time .....	200
L.4 Water Cut versus Time .....	200
L.5 Oil, Water, and Gas Production Rate of Well P1 versus Time.....	201
L.6 Oil, Water, and Gas Production Rate of Well P2 versus Time.....	201
L.7 Oil, Water, and Gas Production Rate of Well P3 versus Time.....	202
L.8 Oil, Water, and Gas Production Rate of Well P4 versus Time.....	202
L.9 Oil, Water, and Gas Production Rate of Well P5 versus Time.....	203
L.10 Oil, Water, and Gas Production Rate of Well P6 versus Time.....	203



## LIST OF ABBREVIATIONS

$A$	=	cross-sectional area of plug
$a$	=	distance between wells in line in regular pattern
$A_{12}$	=	the interface area between the two cells in the x direction
$A_{X12}$	=	the x projections of the interface area of cells 1 and 2
$A_{Y12}$	=	the y projections of the interface area of cells 1 and 2
$A_{Z12}$	=	the z projections of the interface area of cells 1 and 2
$BP$	=	barometric pressure
$B_{oi}$	=	oil formation volume factor at pressure $\bar{p}_1$ , bbl/STB
BBL	=	barrel
$B_g$	=	gas formation volume factor
$B_o$	=	oil formation volume factor
BPD	=	barrel per day
$B_w$	=	water formation volume factor
$C_t$	=	total aquifer volume
$C$	=	the Darcy constant conditions
$D$	=	cell center depth
$d$	=	distance from an injector to the line connecting two production wells
$D_{12}$	=	dip direction

## LIST OF ABBREVIATIONS (Continued)

$dM$	=	the mass per unit surface density, accumulated during the current time step, $dt$
$dP$	=	potential difference ( $dP_{gni}$ is the gas potential difference between cells $n$ and $i$ )
$DX_1$	=	the x components of the distance between the center and x face of cell
$DY_1$	=	the y components of the distance between the center and y face of cell
$DZ_1$	=	the z components of the distance between the center and z face of cell
$E_{Abt}$	=	areal sweep efficiency at breakthrough of the displacing fluid
$E_A$	=	areal sweep efficiency of the displacing fluid
$E_D$	=	displacement efficiency within the volume swept by water
$E_R$	=	overall recovery efficiency
$E_t$	=	vertical or invasion sweep efficiency
$E_V$	=	volumetric actually, the fraction of the reservoir volume actually swept by water
$f_{wf}$	=	fraction of water flowing at the flood front

## LIST OF ABBREVIATIONS (Continued)

$f_{w2}$	=	fraction of water flowing at the producing end of the system
$F$	=	the net flow rate into neighboring grid blocks
$f'_{sw2}$	=	derivative of fractional flow of water to $S_w$ at $x_2$
ft.	=	feet
$f_w$	=	fractional flow of water
GOR	=	gas-oil ratio
$G$	=	acceleration due to gravity (0.00694 in field units)
$G_j$	=	shape factor in the Higgens – leignton model, $(L_j / A_j)$
$h_i$ and $h_a$	=	cell depth and aquifer datum depth respectively average saturation of residual oil.
$H$	=	hydrostatic head correction
$H_{wj}$	=	well pore pressure head between the connection and the well's
$I$	=	number of injection wells
$J_w$	=	aquifer productivity index
$K$	=	permeability
$k_b$	=	base permeability for relative permeability
$K_{gas}$	=	gas permeability
$km^2$	=	square kilometer

## LIST OF ABBREVIATIONS (Continued)

$k_o$	=	oil permeability
$K_r$	=	relative permeability
$k_{rg}$	=	relative water permeability
$k_{ro}$	=	relative oil permeability
$k_{rw}$	=	relative water permeability
$k_w$	=	water permeability
$L$	=	length of the specimen
MMSTB	=	million of stock tank oil barrel
$M_{pj}$	=	phase mobility at the connection
$N_{pw}$	=	oil displaced by water
NTG	=	net to gross
$P_f$	=	equilibrated pressure
$P_{a0}$	=	initial aquifer pressure
$P_{ob}$	=	reference pressure
$P_{of}$	=	reference pressure
$P_{os}$	=	the reference chamber of the clean and dried core sample with helium is filled 100 psi
$P_b$	=	the reference chamber pressure and equilibrated pressure of the sample chamber

## LIST OF ABBREVIATIONS (Continued)

$P_s$	=	the stabilized pressure the helium is introduced into matrix cup and pressure is allowed to stabilize.
$P_1$	=	upstream pressure
$P$	=	number of production wells
$P_a$	=	aquifer pressure at time $t$
$P_{bh}$	=	the bottom hole pressure
$p_c$	=	capillary pressure
$P_i$	=	cell press at time $t$
$P_j$	=	nodal pressure in the grid block containing the connection $p_i$
	=	pressure at injection well
$p_{oi}$	=	initial oil-phase pressure
$p_p$	=	pressure at production well
psi	=	pound square inches
$PV$	=	pore volume
$P_w$	=	bottom hole pressure head between the connection
$p_{wi}$	=	water-phase pressure at inlet of linear core
$Q$	=	flow rate
$Q_i^*$	=	number of water contact PV's injected
$Q_{ai}$	=	inflow rate from aquifer to cell $i$

## LIST OF ABBREVIATIONS (Continued)

$q_{pj}$	=	the volumetric flow rate of phase $p$ in connection $j$ at stock tank
$q_t$	=	total production rate
$(R_g)_i$	=	the gas residual in cell $i$
$(R_o)_i$	=	the oil residual in cell $i$
$(R_w)_i$	=	the water residual in cell $i$
$R_{fl}$	=	non-linear residual
$R_s$	=	solution gas-oil ratio
RV	=	reference volume
$R_v$	=	vapor oil-gas ratio
$\overline{S}_w$	=	average water saturation after breakthrough
$S_{wbt}$	=	average water saturation at breakthrough
$\overline{S}_{wf}$	=	average water saturation at breakthrough
$\overline{S}_{w5}$	=	average water saturation in five spot
$S_{wc}$	=	connate water saturation
$S_{or}$	=	residual oil, fraction
$\overline{S}_{o1}$	=	volumetric average oil saturation at the beginning of the waterflood, where the average pressure is $\overline{p}_1$
$S_{wf}$	=	water saturation at the flood front
$S_{wor}$	=	water saturation at the residual oil saturation

## LIST OF ABBREVIATIONS (Continued)

SCF	=	standard cubic feet
$S_g$	=	gas saturation
$S_o$	=	oil saturation
STB/D	=	stock tank barrel per day
$S_w$	=	water saturation
$S_{w2}$	=	water saturation at $x_2$
$S_{wi}$	=	initial water saturation
$V_{2bil}$	=	the billet volume which filled in the excess space in case that the sample is short
$T_{12}^x$	=	the x direction transmissibility between (I, J, K) and (I+1, J, K)
T	=	temperature
$T_{ni}$	=	transmissibility between cells $n$ and $i$
$T_{wi}$	=	well connection transmissibility factor
$T_{wj}$	=	the connection transmissibility factor
$V_{w0}$	=	initial aquifer volume
$V_{pw}$	=	pore volume that has been swept by water to volumetric
$V_P$	=	pore volume within rock.
$V_{bil}$	=	volume of the billet
$W_{ai}$	=	cumulative influx from aquifer to cell $i$

**LIST OF ABBREVIATIONS (Continued)**

$W_i$	=	cumulative water injection
$W_{ibt}$	=	cumulative water injection at breakthrough
WOR	=	water-oil ratio
$\phi$	=	porosity (fraction)
$\Delta x$	=	length
$\bar{\lambda}_{ro}$	=	average relative mobility of the oil phase in cell j
$\alpha_i$	=	area fraction for cell i
$\bar{\lambda}_{rw}$	=	average relative mobility of the water phase in cell j
$\mu$	=	fluid viscosity, (cp)
$\mu_{N_2}$	=	viscosity of nitrogen, cp
$\rho$	=	fluid density



# CHAPTER I

## INTRODUCTION

### 1.1 Objectives

The primary objective of this research is to improve oil recovery by reducing the residual oil left in the reservoir Suphan Buri Basin of Thailand. The method used in this study is the waterflooding technique which is one of the enhanced oil recovery techniques. In a suitable reservoir condition and proper flooding design waterflooding can help to increase 20 to 30 percent of primary production. This research is to study waterflooding plans which are the most suitable in Suphan-Buri Basin. The research effort includes laboratory testing in Tertiary sandstone sample for estimating porosity and permeability and running reservoir simulation by using "ECLIPSE" software to design the flooding pattern. Since typical waterflood project involves both technical and economical considerations. Thus, in this study for technical part in order to understand reservoir characteristic the petrophysical parameters: porosity and permeability were determined and analyzed in the laboratory. Then the production efficiency and reserve for both primary recovery and waterflooding were computed and the results were compared. Furthermore, the economic consideration regarding on flooding pattern, optimum injection and production rates, optimum time to start injection water, and abandonment rate were studied. Therefore, the results of this research may be supporting information for

exploration and production company to develop and/or improve oil recovery in Thailand.

## **1.2 Problem and Rationale**

Petroleum is the most important energy sources for social and economic development in Thailand. At the present, the demand of petroleum is increasing due to that the expansion of Thai economics for both industry and agriculture. Even though indigenous oil and gas production is accounted about 44 percents of petroleum consumption in Thailand and exploration and development in petroleum fields are moderately successful, it is still not enough especially when oil prices continue to increase discoveries of new oil fields are less and less. Nowadays, oil fields in Thailand can be produced oil only 10-30 percent of oil in place in primary production. The oil production is only 15 percents of the country's consumption and the less has to be imported.

Since the reserves of hydrocarbon in Thailand are limited. Therefore, the use of this hydrocarbon is important. This can be achieved either by discovery of new oil fields or by increasing the recovery from the existing ones. The discovering of new oil field has risk and high investment. On the other hands, large quantity of residual oil has remained in the oil reservoirs and they can be developed. Thus, increasing oil recovery from existing fields with the cheapest and available method becomes everybody (concessionaires, operators, oil and gas companies, and Department of Mineral Fuels). Enhanced Oil Recovery (EOR) is a method that refers to any method used to recover more oil from a reservoir than would be produced by primary recovery. The waterflooding is the most successful and widely used commercial

recovery process. This is because water is available and inexpensive when it relates to other fluids. Additionally, flooding involves low capital investment and operating costs and favorable economics (Thakur and Satter).

The reservoir simulation has been studied to consider waterflooding plan development. The computer software named “ECLIPSE”; it is used to be tool for operating. The reservoir model is constructed as hypothetical model. Some data from U-Thong field, which is in Suphan-Buri Basin, is used for reservoir simulator. Different flooding scenarios are simulated in order to consider the most optimum flooding scenario for Suphan-buri Basin.

### **1.3 Scopes and Limitations of the Study**

Suphan-Buri Basin, U-Thong Field is the studied area to improve oil recovery by waterflooding. It is constructed as hypothetical model while its geological, petrophysical and production data are based on the data from this field. This reservoir model is used to analyze characteristic and behaviors of reservoir process that cannot be easily observed. Additionally, the study and experiment work will be scoped in the existing oil field (U-Thong field) and in the laboratory. The rock samples are collected from outcrop in coal mines which are represented in Tertiary sandstone due to out crops of Tertiary sandstone in central part of Thailand are rarely found.

## **1.4 Research Methodology**

### **1.4.1 Literature Review**

Literature review has been carried out to study the state-of-art of waterflooding technique. The review will include detail of geological information,

production data, theory of waterflood, and case study of waterflooding. The sources of information are from Social Petroleum Engineering (SPE), Journal of Petroleum Technology (JPT), technical report and conference papers. A summary of the literature review is given in this thesis.

#### **1.4.2 Sample Collection and Preparation**

Rock samples have been collected from outcrops of coal mines in northern part of Thailand. The rock samples of Tertiary sandstone are used to determine porosity and permeability values. Sample preparation has been carried out in the laboratory at the Suranaree University of Technology.

#### **1.4.3 Experiment Work in Laboratory**

In laboratory, collected rock samples are cut and shaped in the cylinder form. The properties of Tertiary sandstone are the porosity – a measure of the void space in the rock; the permeability – a measure of fluid transmissibility of rock. Poroperm meter in the laboratory will be used to measure the porosity and permeability and to do rock description.

#### **1.4.4 Reservoir Simulation**

The reservoir simulators are complex computer program that simulate multiphase displacement processed in two or three dimensions. Coats 1982 defines simulation as the use of calculation to predict reservoir performance and to forecast recovery method. It solves the fluid-flow equation by using numerical techniques to estimate saturation distribution, pressure distribution, and flow of each phase at discrete points in a reservoir. ECLIPSE is simulation software which is used to study waterflood performances.

#### **1.4.5 Economic Evaluation**

Economic evaluation is calculated from results of reservoir simulator; optimum oil gas and water production rate, ultimate recovery, and other factors of investment were determined. Different waterflood scenarios were analyzed to determine the potentially most economically viable project.

#### **1.4.6 Data Analysis**

Collecting petrophysics data and the results from laboratory experiment were analyzed and compared with results from well logs data.

### **1.5 Expected Results**

The research involves in improving of the oil recovery and minimizing oil left in the reservoir by using waterflooding technique. Simulation results are useful as supporting information to study improved oil recovery in inshore fields in Thailand. Researcher is earned the valuable experience in term of programming application, simulation modeling, computer software and using apparatus in laboratory. Specially, the result of the research will be informatively support for the oil companies to perform more waterflood projects which can help to increase oil reserves for the country. In addition, the waterflood project can also help minimizing environment issue from produces water by re-injecting the produced water back into the reservoir to enhance more oil production.

## **CHAPTER II**

### **LITERATURE REVIEW**

#### **2.1 Site Geology**

The U-Thong Field is situated in the Suphan-Buri Basin which lies in the southern part of the central plain of Thailand. The field is located in Amphoe U-Thong, 20 km west of Amphoe Muang, Suphan-Buri province and approximately 80 km north-west of Bangkok. The Suphan-Buri Basin is a Tertiary half graben of approximately 800 sq. km with over 3 km thick of sediments (Praditarn *et al*). The reservoir is separated into three parts by relatively main structure of the basin namely, active margin, basin center, and passive margin. Eight depositional sequences (S10-S80) have been identified (Triamwichanan, 2000).

The U-Thong oil Field was discovered by well UT 1-3 in May 1987. It is situated on the western part of Suphan-Buri Basin (Figure 2.1). The field lies on the western, fault-controlled basin flank. The field structure formed as a rollover on a low angle north-south trending fault during the deposition. The reservoir interval is Miocene fluvio-lacustrine sediments. These sediments were deposited on an alluvial braided plain fringing lake cut and filled by channel conglomeratic sandstones.

During 1986-1988, 12 explorations and appraisal wells were drilled in this basin. The results of stratigraphic and exploration wells data in Suphan-Buri Basin showed that oil accumulation was presented only in the western part of the basin (U-Thong Field). While oil shows in the eastern and central basin are insignificant. The

reservoir in U-Thong Field (KR1-1 to KR2-8) can be categorized into two zones, the upper (KR1-1 to KR 2-5) and the lower zone (KR2-6 to KR2-8). The primary drive mechanism for the upper zone is depletion drive with low recovery factor about 5 percent. The water drive mechanism was predominantly represented in lower zone with recovery factor of 30 percent. The primary recovery of the field is in the range of 2.87 to 3.16 MMSTB. At the present, U-Thong Field has nine production wells and one injection well (UT 1-7/D1). Oil production rate is at 550-600 bbl/day.

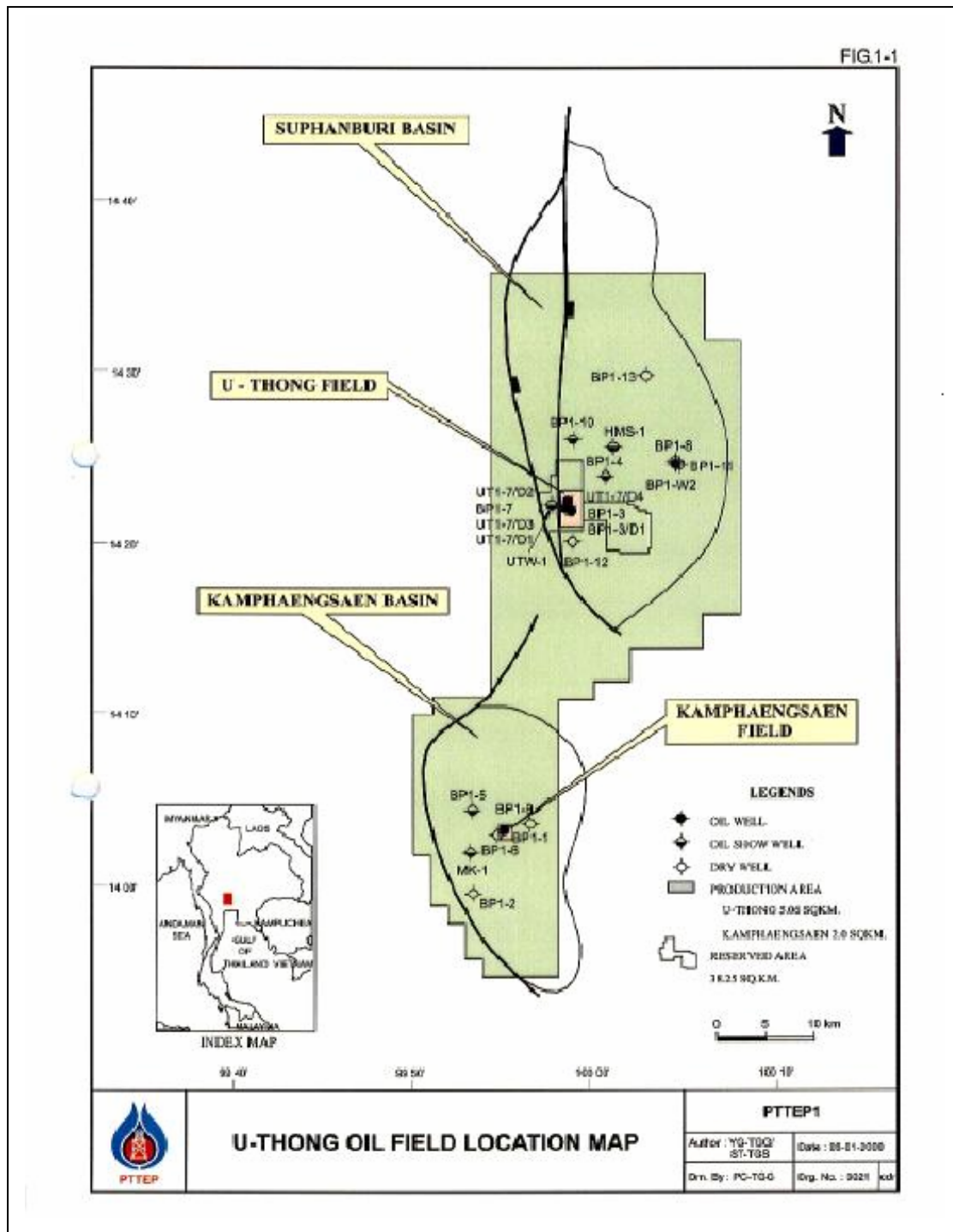


Figure 2.1 U-Thong Oil Field Location Map.



## 2.2 Porosity and Permeability Measurement

Baoxing *et al* (1995) described porosity and permeability evaluation of Tertiary sandstone reservoirs, western Qiongdongnan Basin, South China Sea. The main productive rocks are Mid Tertiary sandstones. Sandstone reservoirs are buried in the depth of 3500-4500 m. The average porosity is 13 percent and maximum permeability up to  $16213 \times 10^{-3} \mu\text{m}^2$ . Core analysis of porosity and permeability from 2341 samples shows that porosity ranges from < 1 % to 26 % (Table 2.1).

Aziz *et al* (1995) determined permeability by using core and log analysis. Core analysis provided direct measurement of permeability which can be performed either under controlled laboratory conditions or reservoir conditions. Two types of permeability can be measured on core samples in the laboratory: absolute and relative permeability. A practical way to incorporate these factors in the core analysis method is to combine absolute-permeability measurements at in-situ pressure with relative-permeability data. Wireline log measurements have three methods for obtaining permeability. (1) Empirical Correlation, which used to predict the permeability of formation. (2) NML Measurements provides two specific products that can be indirectly related to formation permeability; 1)  $I_f$  is a measure of movable ratio and 2)  $t_f$  is spin-lattice relation time. (3) MDT Measurements (Modular Formation Dynamic Tester), which is a similar tool to Repeat Formation Tester (RFT) tool but has wider application in wireline logging.

The interrelationships among the wireline-log and core analysis permeability depend on three important factors: measurements scale, environment, and physics.

**Table 2.1** The porosity and permeability of Mid Tertiary Sandstone.

Formation	Porosity (%)			Permeability		
	Average	Range	Samples	Average (md)	Range (md)	No. of Samples
Meison	7.54	2.8-26	96.00	0.29	0.01-4.5	96.00
Linshui	13.02	0.14-23.7	1379.00	240.15	0.01-4.5	1363.00
Yacheng	5.60	0.2-20.7	1008.00	37.61	0.002-208	882.00

## **2.3 Case Study of Waterflooding in Development Plans**

In early 1880, Carll discovered that it might be possible to increase oil recovery by injecting water to displace oil in the reservoir (Willhite, 1986). Waterflooding began accidentally producing in Bradford Field, PA in 1880's. Many wells were abandoned in Bradford Field by pulling casing without plugging while in some wells casings were left in the wells, thus they were corroded. Therefore, water from shallow horizons could enter the producing interval. The practical water injection began, perhaps as early as 1890, when operators realized that water entering the productive formation was stimulating oil production. Then in 1907, the practice of water injection had an impact on oil production from the Bradford Field. The first flooding pattern was a circle flood and it was developed continuously until the present there are many patterns which use in waterflooding.

Waterflooding, called secondary recovery because the process yields a second batch of oil after a field was depleted by primary production. The slow growth of water injection was caused by several factors. In the early days, waterflooding was understood poorly. Interest in waterflooding developed in the late 1940's and early 1950's as reservoir approached economic limits and operators needed to increase reserves. Nowadays waterflooding is practiced extensively throughout the world. In the U.S. as much as half of the current oil production is thought to be the result of water injection.

### **2.3.1 The Sirikit Oilfield (Wongsirasawad, 2002):**

The oilfields in the Sirikit Area are situated within Phitsanulok Basin. The basin has an areal extent in order of 6,000 km<sup>2</sup> formed as a result of the relative movement of the Shan Tai and Indonesian Blocks. The main reservoir formations are

Lan Krabu (LKU) and Pradu Tao (PTO) formations. The Sirikit oilfield is geologically very complex. The geological complexity is a product of the multi-phased structural history and the interaction between faulting and deposition through time. However, the complexity and uncertainties of the Sirikit oilfield will always be the key factor to determine the successful projects in the future. The waterflooding is one of the successful projects which have been developed in the Sirikit oilfields. The waterflood project started as early as 1983. A small pilot project in a small area of LKU-E block was designed to test the viability of injecting water into the complex sand shale inter-bedded layers of the Lan Krabu formations. It was proved that the pilot test could maintain pressure under a non-fracturing condition. So it was indicated that the waterflooding of Lan Krabu reservoir was feasible. However, the waterflooding study was initiated lower than plan due to problems with deliverability of source-water. Moreover, the responses in the reservoirs were very slow. The waterflooding project had studies again during 1993-1994. It gave a boost to the confidence in recovery factor of the field, which increased over 20 percent for the first time. The discovery of oil in Pradu Tao and Yom reservoirs during 1997-1998 gave another upgrade to the recovery factor to a level of around 25 percent. The implementation of the previous waterflood project encountered many operational difficulties, but proved waterflood to be a technically viable secondary recovery technique in the Sirikit complex reservoirs. Reviews and studies of reservoir performances and simulations of the Sirikit reservoirs indicated that a reserves volume is recoverable only through waterflood of the Sirikit reservoirs. Recent disappointing results of new infill wells confirmed that the plans to drill hundreds of infill wells would not be as effective as waterflooding. With the advanced of computer modeling techniques

compared to 10 years ago, the confidence of successfully implementing waterflooding projects in the Sirikit Field has been reviewed.

### **2.3.2 The Benchamas Oilfield (Graves *et al*, 2001):**

Benchamas Development in the Gulf of Thailand is an oil play predominantly gas condensate region. This development is unique in that the operator has significant oil reserves of high pour-point crude oil in several zones. The project has developed as a waterflood with horizontal and monobore producers and injectors. The initial phases of horizontal producers were completed with sand exclusion capability, consisting of multi-layered sintered screens. This has so far proved to be effective. The Benchamas waterflood project is comprised of eight stacked in sandstone reservoirs. This sandstone is fluvial channels and is discontinuous. The waterflood is designed to maintain oil viscosity and gas cap location in order to maximize recovery. The economic impact of this waterflood is estimated to increase the recovery from 12-18 percent (primary) to 25-35 of the OOIP.

### **2.3.3 The West Seminole Field (Harpole, 1980):**

The West Seminole Field in west central Grained County, Texas, produces from the San Andres formation. A large primary gas cap covers most of the field area. The West Seminole Field was discovered in June 1948. Initial field development consisted of 54 wells drilled on approximately 40-acre spacing. Most of the wells were completed open-hole with casing set to just below the gas/oil contact. The gas injection into the gas cap was started in 1964 to reduce the rapid pressure decline in the reservoir. The water injection was established to assist in pressure maintenance during 1969-1971. Most of these injection wells were injected directly into the oil zone and might result in loss of large quantities of oil into the gas cap.

Significant communication between porosity zones in the oil leg and those in the gas cap could have an effect on waterflood performance in this reservoir. So Harpole (1980) studied the vertical communication between porosity zones by using black oil simulation with three dimensions, and three phases. The study area for the simulation consisted of only the main dome portion of the reservoir. After the reservoir description data had been digitized and incorporated into model grid system in order to do history matching. Individual well performance was matched wherever the data were available and considered to be valid. Significant aspect of the history-matching work was to quantify the approximate effective injection in to peripheral water injection wells. However, the peripheral water injection program was not effective due to two major factors.

- 1) The peripheral injection wells were completed well below the water/oil contact, and as a result, the injection interval was separated vertical from the reservoir by several of the tight “barrier” zones.

- 2) Pay continuity was not sufficient in these lower zones.

The simulator was run next in prediction made to project future field performance. A comprehensive reservoir study using a black-oil simulation model showed that control of vertical movement of oil into the gas cap under waterflood operations was the key to maximizing oil recovery from this West Texas San Andres reservoir. Recovery of an additional 4 MMSTB of oil is expected as a result of a reservoir management plan which includes a 46 infill wells.

#### **2.3.4 The Mean Field (Stiles and Magruder, 1992):**

The Means Field in Andrews County, Texas, was discovered in 1934 and developed on 40-acre spacing in early 1950's. Production is from the Grayburg

and San Andres formation at depths ranging from 4,200 to 4,800 ft. The Grayburg is about 400 ft. thick with the basal 100 to 200 ft. considered gross pay. Production from Grayburg was by solution-gas drive with the bubble point at the original reservoir pressure of 1,850 psi. The waterflood program was initiated after the operators in the area authorized a major reservoir study to evaluate secondary recovery. Highlights of this study included one of Humble's first full-field computer simulations. For this study, additional data had to be accumulated, including logging, fluid sampling and core data. It was recommended that waterflooding should be initiated on a peripheral pattern that would encompass the more prolific Lower San Andres. A five-spot pattern was implemented later when needed. For the Grayburg, a lease-line pilot with the portion of the field west of the unit was recommended. In 1963, the field was unitized and water injection began with 36 wells, forming a peripheral pattern. The reservoir study was reviewed again in 1969 due to the peripheral injection pattern could no longer provide sufficient pressure support. Barber (Stile and Magruder, 1992) reported the results of a detailed engineering and geologic study conducted during 1968-1969 to determine a new depletion plan more consistent with capacity production. Analysis of pressure data from the pressure observation wells indicated that parts of the South Dome were not receiving adequate pressure support from the peripheral injectors. This study recommended interior injection with a three-to one-line drive following implementation of this program. Production increased from 13,000 BPD in 1970 to more than 18,000 BPD in 1972. After peaking in 1972, production began to decline again. An in-depth reservoir study indicated that all the pay was not being flooded effectively by the three-to-one

line drive pattern. Hence the geologic study provided that the basis for a secondary surveillance program and later to design and implement of the CO<sub>2</sub> tertiary project.

### **2.3.5 The Fahud Field (Nicholls *et al*, 2000):**

A fracture model was constructed for the Natih-E reservoir unit of the Fahud Field in north Oman. The fracture model indicates that the current gas/oil gravity drainage (GOGD) recovery mechanism is an inefficient oil recovery method for a large part of the lower Natih-E. The optimum well pattern for a waterflood development within two Natih-E subunits is proposed on the basis of simulation results. Nicholls *et al* (2000) studies the fracture modeling and they expected that the oil recovery is increased from 17 percent under GOGD to 40 percent for the waterflood. A fracture model that includes information from well production and injection performance, borehole-image data, structural map, and fault data has been constructed for the Natih-E containing sparse and widely spaced fractures. A pilot water injection cell of two horizontal procedures and one injector well oriented parallel to the bedding strike has shown that water injection is a viable alternative to GOGD.

### **2.3.6 The Statfjord Field (Haugen *et al*, 1988):**

Haugen *et al*. (1988) described reservoir development strategies and field experiences to increase production rate and reservoir. The Statfjord Field is the largest producing oil field in Europe. The field was discovered in March 1974. The Statfjord Field, which is 15 miles long and averages 2.5 miles in width, is located in a westerly tilted and eroded Jurassic fault block. About 75% of the main recoverable reserves are located in the middle Jurassic Brent group, while the remaining 25% is in the Lower Jurassic/ Upper Triassic Statfjord formation. The estimated ultimate



recovery is around 3,000 MMBBL of oil and 3.0 TSCF of gas. Both Brent and Statfjord reservoir contain highly undersaturated low sulfur crude oil. The one of reservoir development strategy is to develop the Upper and Lower Brent as separate reservoirs with pressure maintenance by water injection. The Brent reservoir had a common initial oil/water contact (WOC) and equal reservoir pressure. The original reservoir pressure was 5,561 psia, about 1,550 psia higher than the bubble point pressure. The average reservoir pressure is maintained at around 4,500 psia by balancing total fluid production with water injection. All wells are anticipated to produce with flowing BHP above the BP. In fact, the minimum reservoir pressure was reached in late 1986 if there is no waterflood. The maximum oil production is around 630,000 STB/D and 1,050,000 B/D of water is injected into the Brent reservoir.

### **2.3.7 The Jay-LEC Field (Willhite, 1986):**

The Jay-LEC Field has produced from the Smackover carbonate and Norphlet sand formations at depth about 15,400 ft. An oil/water contact is located at a sub-sea depth of 15,480 ft. More than 90% of the oil in place is in Smackover. The reservoir study indicated that natural water drive would not be effective source of reservoir energy. Thus, waterflood was selected among other possible processes to maintain pressure for increasing oil recovery. The waterflooding plan in Smackover formation was developed by using a two-dimensional (2-D) simulation to compare alternative flooding schemes. Four waterflood plans were evaluated: (1) peripheral flood, (2) five-spot pattern (3) a 3:1 staggered line-drive pattern and (4) a combination of peripheral wells and five-spot patterns. From the results of the 2D simulator indicated that the peripheral flood was not effective. For the remaining three waterflooding plans, the 3:1 staggered line-drive plan was recovered more than 200

MMBBL. The 3:1 plan yielded 9.8 MMBBL incremental oil recoveries over the five-spot plan and 14.4 MMBBL over the combination pattern. Moreover the 3:1 plan also has advantages for development plan and economic potential.

### **2.3.8 The Judy Creek Field** (Thakur and Satter, 1998):

The Judy Creek Field in central Alberta produces from a Devonian reef. The field was discovered in 1959 and original oil in place was estimated at 830 MMBBL. Because the field is not connected to a large aquifer so a peripheral flood was initiated in 1962 for pressure maintenance. By 1973, the waterflood was ineffective due to permeability barrier existed within the reservoir that prevented communication between peripheral wells and other parts of the reservoir. A combined engineering and geologic study indicated that the reservoir was subdivided into three units; S3, S4, and S5 that corresponded to three periods of reef growth. The detailed engineering and geological evaluation led to two major's conclusions (1) a pattern waterflood should be installed to flood unit S5; and (2) discontinuous bed in unit S4 were not waterflooded effectively by peripheral and bottom-water injection. The study also resulted in the opening of several zones in unit S4 in wells behind the flood front that were through to be flooded out.

### **2.3.9 Nine-Fields in Texas, Oklahoma, and Illinois** (Barber *et al*, 1983):

Barber et al. (1983) studied the production history of infill drilling program in nine-fields in Texas, Oklahoma, and Illinois in order to determine the maximum well spacing that will effectively drain oil and gas reserves. This infilling drilling study is concluded that (1) oil recovery increased from the drilling of 870 infill wells in 9 fields ranges from 56% to 100% of their well-bore production (2) total

additional reserves from these wells will be 61.8 MMBBL oil and (3) pay zones after infill drilling are more discontinuous than before infill drilling.

#### **2.3.10 The Kuparak River Field** (Chapman and Thompson, 1989):

Chapman and Thompson (1989) described the computer-aided waterflood surveillance method used in the Kuparak River Field. It is a useful tool that has enabled detailed analysis of large amounts of data. The program enables engineers to gain a more thorough understanding of waterflood progress. This procedure is especially useful in mature waterflood that do not have a good production and injection log history. From the results indicated the EOR process should begin in an area where waterflood performance was the best to reduce risk from factors such as poor reservoir continuity and low overall conformance.

#### **2.3.11 The Postle Area** (Irwin *et al*, 1972):

Irwin et al. (1972) described the reservoir simulator model to use monitoring project performance, designing pressure maintenance program and changing the operational guide lines for a second project. The geologic and engineering study had reviewed again before starting reservoir simulator model. The results of the reservoir simulator studies have been used to design one pressure maintenance program and to change the operational program in a second project. The operational changes consisted of well conversions, producing and injection well drilling, unit enlargement, and acceleration of the injection and production rates. Implementation of the pressure maintenance programs are based on the results of the simulator studies. They expected to increase ultimate oil recovery by 15 percent.

### **2.3.12 The Meren Field (Thakur, 2004):**

Thakur (2004) described the waterflood surveillance to improve oil recovery and maintain pressure reservoir in Meren Field. Meren Field is located in OML-95 of the Niger Delta. The primary production is gas cap expansion, solution gas drive and water drive. The drive mechanism was dependent on the location of the reservoirs. The ultimate recovery factor from the primary depletion was estimated as 27%. The study used reservoir simulation techniques available the (2-D areal and 2-D cross-sectional) and analytical methods to evaluate different schemes for optimizing oil recovery. From results of reservoir simulator passed on the observed trends. The current ultimate recovery factor is estimated at 59%, which is significantly higher than estimated recovery of 45-52% used to justify the project.

### **2.3.13 The McElroy Field (Thakur, 2003):**

McElroy Field was discovered in 1962 during the initial exploration along the Central Basin Platform. This case provides an innovative approach of modeling and successfully history matching the primary and waterflood phase in vuggy portion of the carbonate reservoir (Thakur, 2003). CHEARS (Chevron Extended Application Reservoir Simulator) was utilized for primary and waterflood simulation. The reservoir simulator is very good match with history. The results show oil saturations greater than 50% in the model at initial time, after primary recovery and after waterflood. It also shows the gas saturation greater than 20% after primary recovery and water sat greater than 65% after waterflood. The areas of high water saturation indicate that vuggy zones play.

#### **2.3.14 The Kaybob Beaverhill Laker “A” Pool (Thakur 1998):**

Kaybob Beaverhill Lake “A” Pool, a carbonate reef contains an OOIP of about 250 million barrels. It produces 5% OOIP under primary production from discovery in 1957 to the start of line drive water injection in 1964. By 1978, the recovery increased to 26%, at which time the waterflood was converted to pattern flood. The recovery factor increased to 39% by 1988, the waterflood performance in Kaybob has been very good with ultimate recovery estimated at about 46% OOIP. One of the favorable factors for the waterflood is the oil water viscosity ratio of 0.40.

#### **2.3.15 The Acheson D-3A Pool (Thakur, 1998):**

The Acheson D-3A pool was discovered in 1950 and has been produced in primary waterflood and secondary hydrocarbon miscible flood (HCMF). The pool contains Devonian dolomites reef. Both of vuggy and matrix porosity is an average of about 11 percent. The excellent reservoir performance results from low  $S_{or}$  to waterflood (~29%) and miscible flood (~7%), high volumetric sweep efficiency of over 90 percent and gravity-stable vertical displacement efficiencies. The original oil in place of pool was about 69 percent ultimately. The miscible flood injected a 29 percent HCPV solvent slug. Follow by chase gas to push solvent downward in a gravity stable manner. Two simulation models were used to design the cycling scheme in the water flooded area and to develop the operating and monitoring strategies. The first included a full-field cross-sectional model, and the second, a detailed geo-statistical cross-sectional model. An expected value method was utilized to investigate uncertainties in a number of economic variables.

### **2.3.16 The Intistar “A” Field (DesBrisay, 1972):**

Intistar “A” Field has been selected to studied waterflooding plan by limiting the geology of the reservoir. In this field, unique geology properties permitted the use of a bottom-water drive to deplete the reservoir. The carbonate reef reservoir is at depths of 8,900 to 10,000ft. This reservoir has gross thickness about 1,002 ft. at the thickest point. Log analyses indicated that the oil column was essentially continuous from the oil/water contact (OWC) to the top of the reef. Primary recovery from this reservoir was below because the oil was highly under-saturated. Although there was OWC at the base of the reef, all of the reservoir energy was not supplied by the aquifer. The reservoir energy was thought to be limited to fluid and rock expansion in addition with solution gas drive. A bottom-water injection program was started for pressure maintenance in this field. Water was injected below the OWC in the 29 wells. For a bottom-water flood to be effective, the reservoir must have good communication in horizontal and vertical directions with no barriers to vertical flow. The ratio of vertical to horizontal permeability was about 0.75, which indicated good communication in both horizontal and vertical directions. Reservoir pressure declined rapidly with fluid withdrawal before water injection; it had decreased from 4,352 to 3,700 psig. And cumulative production was 40 MMBBL. The pressure decline had changed in about 2 years after water injection began in 1968. This study also included reservoir pressure computed in December, 1982 using a reservoir simulator. At end of 1983, the field had produced 683 MMBBL of oil and 1.17 MMMBBL of water had been injected. Ultimate recovery is estimated to be 750 MMBBL which is almost 50 percent of the stock-tank oil original oil in place.

### **2.3.17 The Madison Reservoir in The Elk Basin (Willhite, 1986):**

The Madison reservoir in the Elk basin is anticlinal reservoir. Performance during the first 10 years was characteristic of a strong water drive in that a small pressure decline was observed. The reservoir was considered homogeneous with tight streaks. In developing plan, interpretation of well logs led to a definition of the reservoir with four distinct zones A, B, C, and D. Later on when new wells were drilled in separate zones, it was realized that zone A did not have any water influx and had low reservoir pressure, whereas zones B, C, and D responded as expected under a water drive. Moreover study of extensive reservoir characterization from core, log, and production data, zone A is characterized by high permeability, low lateral continuity of the pay zones, and a lack of a natural water drive. Zones B, C, and D are characterized by low permeability, a higher degree of lateral continuity and strong water drive. The revised reservoir description combined with results of the initial water injection program was used to alter the water injection program and to drill new producing wells in underdeveloped areas. In the initial water injection program, water breakthrough was rapid in interior wells and caused scaling problems which resulted in production rate declines in production wells. The performance history of the Elk Basin Madison from this analysis was studied again. This results in an increase in ultimate recoverable reserves of 62 million barrels, or 8% of original oil in place. The Elk Basin Madison reservoir illustrates the importance of obtaining extensive reservoir data during field development so that waterflooding can be implemented effectively as soon as practical.

### **2.3.18 The Denver Unit in Wasson San Andres Field (Ghauri, 1980):**

The Denver Unit Waterflooding is in Wasson San Andres Field of West Texas. This field is discovered in 1963 and produces from the San Andres carbonate at a depth of about 5,000 feet. The formation thickness varies from 300 to 500 feet. The primary producing mechanism was solution gas drive. Primary development was on 40-acre spacing in the early 1940's. The initial design was the peripheral flood. Water was injected below oil/water contact. Because the reservoir was considered continuous vertically and laterally and thus believed that the injected water from below the oil/water contact would displace oil effectively. The result of the peripheral waterflooding was failed because edge wells selected for water injection often had the poorest-quality reservoir rock. Moreover production wells located 3 to 4 miles from the injection wells did not respond to water injection. These results indicated that pattern flooding would be required. The reservoir characterization concept of the Denver Unit changed and as a result of the peripheral waterflooding. A detailed geological study indicates that total vertical section was made up of 10 distinct zones. Zones were mapped vertically and laterally over distances of several well location discovery was that some pay members were not continuous over large distances and would not be flooded on the 40-acre spacing. Further study led to infill drilling on 20 acre spacing to increase the fraction of continuous pay under waterflooding. The inverted nine-spot pattern was developed in this field. The performance curve of this field shows a decreasing gas/oil ratio (GOR), increasing water injection rate, and reservoir voidage and oil production rate. These performance characteristics clearly indicate the successful performance of the waterflooding.



## **CHAPTER III**

### **LABORATORY EXPERIMENT**

#### **3.1 Objectives**

Laboratory experiment has been performed to determine porosity and permeability of Tertiary sandstone. The sample preparation, test methods, results and discussion of experiment work are described in the following sections

#### **3.2 Sample Collection and Preparation**

Tertiary sandstone samples used in this research are obtained from coal mine in northern part of Thailand. These rock samples are collected from three locations; Li Basin, Mae Moa Basin, and Chiang Muan Basin (Figure 3.1 and Figure 3.2). They are represented to Tertiary sandstone because the outcrops of Tertiary sandstone in central part of Thailand are rarely discovered. Most of samples are collected as rock samples. Exceptionally in Mae Moa Basin, there are both rock samples and core samples. The rock samples and core samples are drilled by core drilling machine as core specimens and they are cut by cutting machine (Figure 3.3 and Figure 3.4). They are cylindrical shaped with 38.55 millimeters (1.5 inches) in diameter and 51.17 millimeters (2 inches) in length. Some of Tertiary sandstone samples are shown in Figure 3.5. All specimens are measured to determine the precise dimension to the nearest 0.01 inches. They are cleaned and dried before they are measured

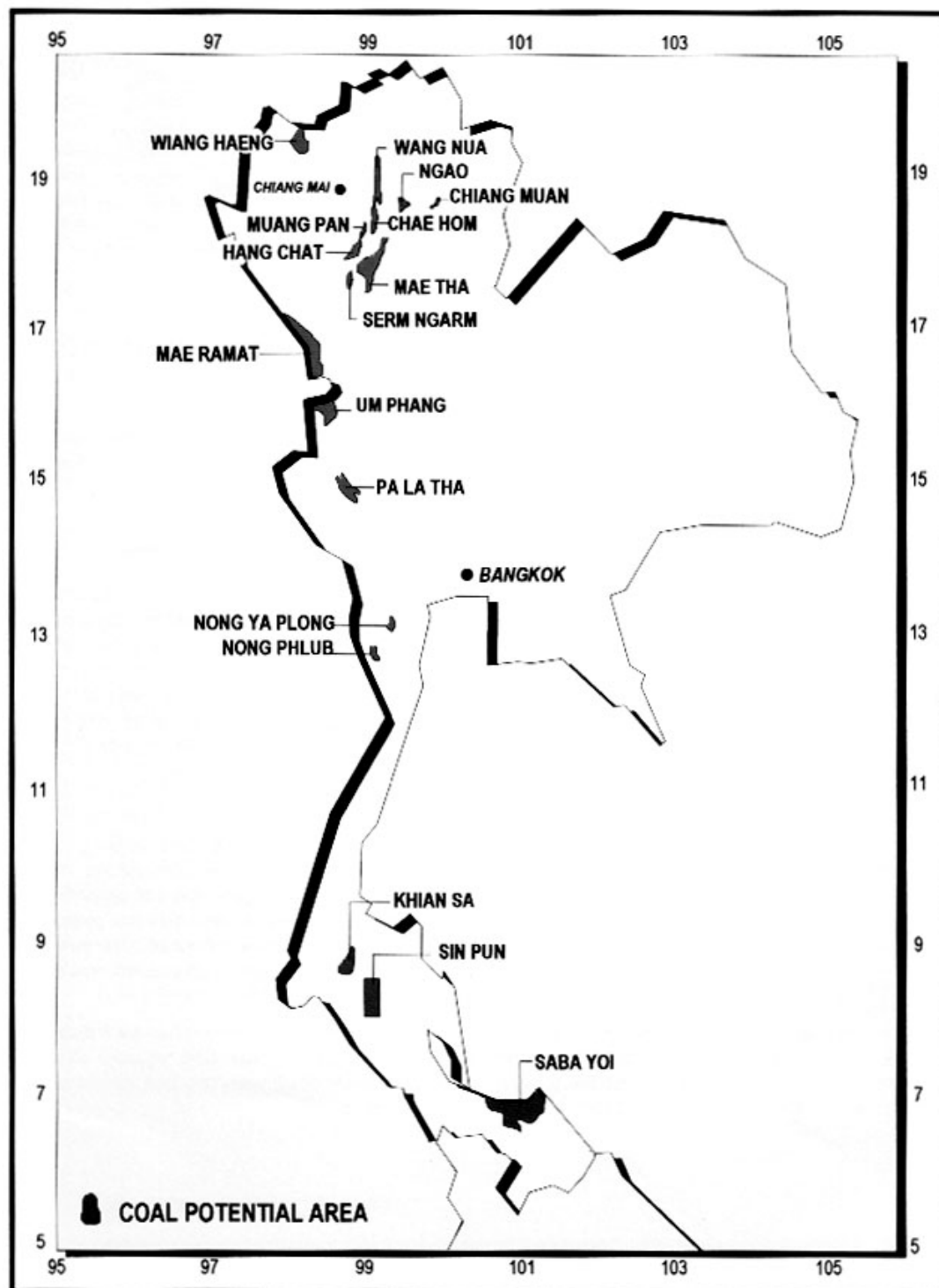


**Figure 3.1** Location of Chiang Muan Basin in Northern Part of Thailand.

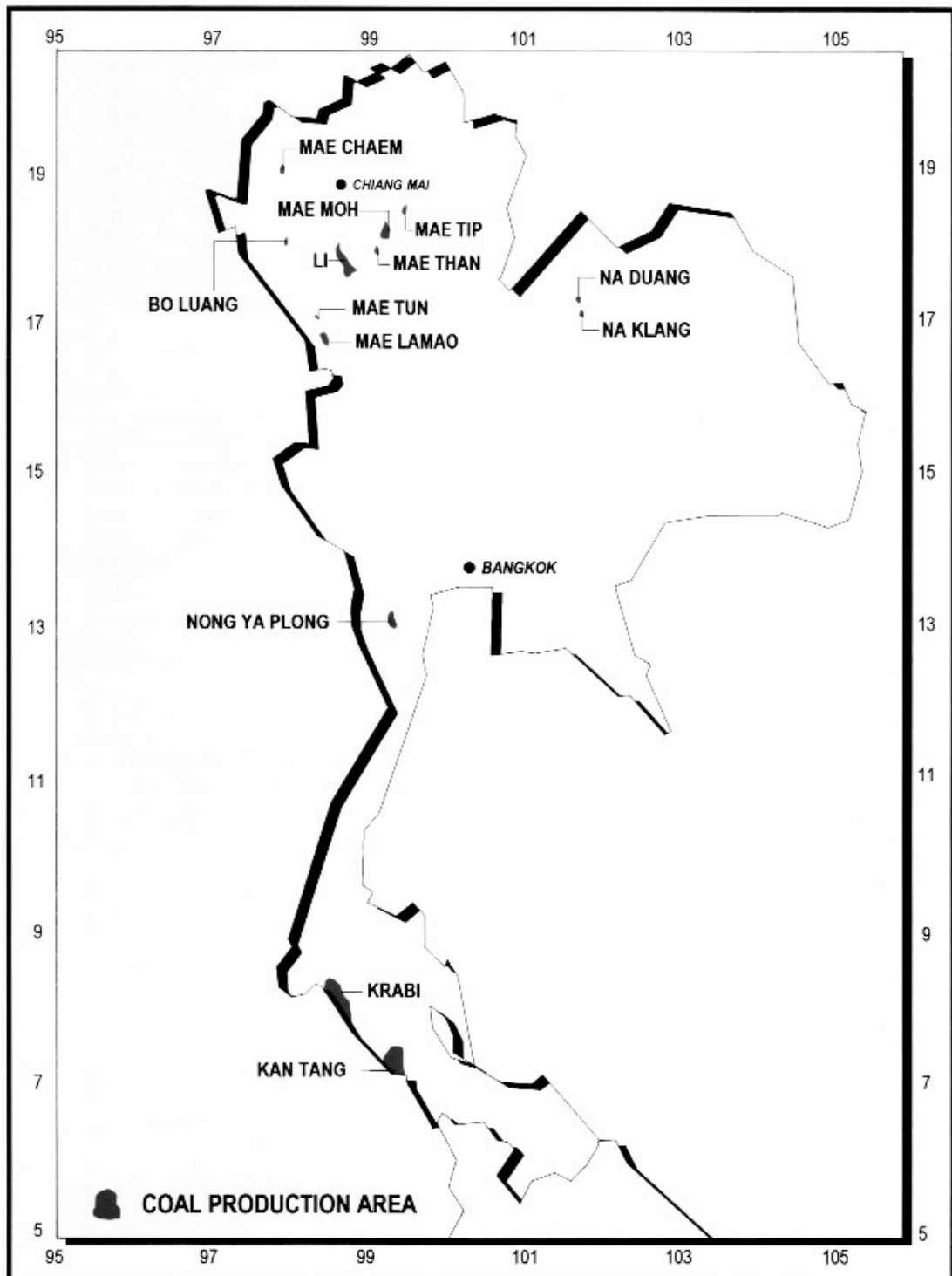


**Figure 3.2** Location of Li Basin, and Mae Moe Basin in Northern Part of Thailand.



**Figure 3.3** The drilling machine is used to drill core specimens using diamond impregnated bit.



**Figure 3.4** The core specimens are cut to obtain the desired length.

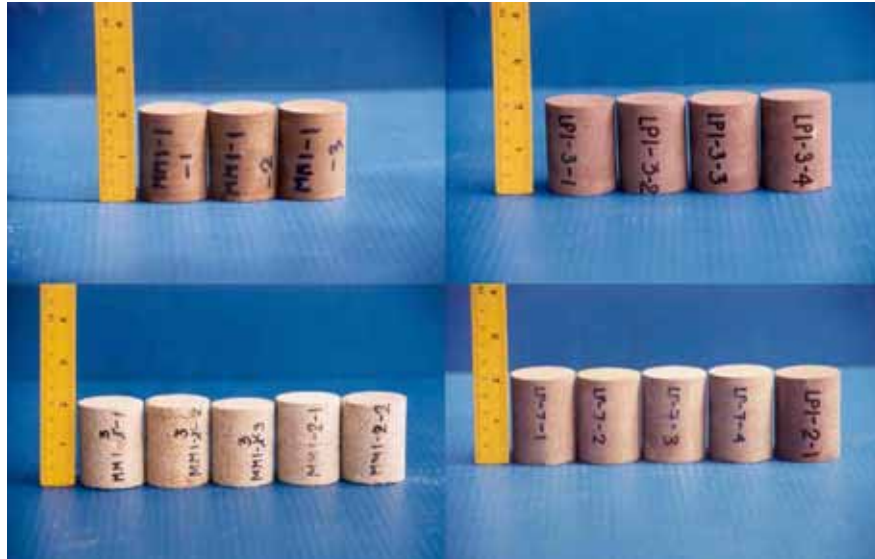


**Figure 3.5** Some Tertiary sandstone specimens for measurements.

Figure 3.6 shows oven which used to heat the specimens about at 50-60 °C for 24 hours.

### 3.3 Porosity Measurement

Porosity is the fraction of a porous of rock that is pore space. The pore space in the bulk volume that is not occupied by rock grains. Therefore, porosity is the ratio of pore volume to bulk volume.

$$\phi = \frac{V_P}{V_B} \quad (3.1)$$

Where  $\phi$  = porosity (fraction)

$V_P$  = pore volume within rock.

$V_B$  = bulk volume of rock.

There are two types of porosity. Primary porosity is the original porosity a porous medium that results from sediment deposition. Secondary porosity is the incremental increase in primary porosity due to chemical dissolution of reservoir rock. Table 3.1 shows values in different types of reservoir rock (Fanchi, 2000).

#### 3.3.1 The Porosimeter Calculations

The porosimeter is the instrument to measure the porosity of the specimens. It is shown in Figure 3.7. Helium is used for this test. It is more advantages than other gases; (1) the small size of helium allows it to penetrate micro-poro rapidly than other gases, (2) it does not affect the instrument. The porosity in clean and dried specimen is determined by a combination of the three properties that are grain volume (GV), bulk volume (BV), and pore volume (PV).



**Figure 3.6** The oven is used to heat the core specimens about at  $50 - 60^{\circ}\text{C}$ .



**Figure 3.7** Porosimeter instrument is used to measure the porosity the specimens.

**Table 3.1** The porosity values in different types of reservoir rock.

Reservoir Rock Type	Porosity Range, %	Typical Porosity, %
Sandstone	15-35	25
Unconsolidated Sand	20-35	30
Carbonate		
- Intercrystalline limestone	5-20	15
- Oolitic limestone	20-35	25
- Dolomite	10-25	20



The reference volume of the reference chamber (RV) is determined by

$$RV = \frac{V_{bil}}{\frac{P_{ob}}{P_b} - \frac{P_{of}}{P_f}} \quad (3.2)$$

Or if  $P_{ob}$  and  $P_{of} = 100$  psi

$$RV = \frac{P_b V_{bil} \left( \frac{P_f}{100} \right)}{P_f - P_b} \quad (3.3)$$

Where

- $P_{of}$  = reference pressure, always uses 100 psi
- $P_f$  = equilibrated pressure, psi
- $V_{bil}$  = volume of the billet (Table 3.2),  $cm^3$
- $P_b$  = the reference chamber pressure and equilibrated pressure of the sample chamber, psi
- $P_{ob}$  = reference pressure, (if  $P_{ob} = 100$  psi)

Through knowledge of the previously RV, the  $P_s$  is used to calculate the grain volume.

**Table 3.2** The volumes of the matrix cup billets that are used with the porosimeter.

The volume of the billet removed should be approximately equal to the pore volume of the samples test.

<b>1" Billets</b>	<b>Billet Number</b>	<b>Volume (<math>cm^3</math>)</b>
	1	4.63
	2	4.59
	3	9.22
	4	18.49
<b>1 1/2' Billets</b>	<b>Billet Number</b>	<b>Volume (<math>cm^3</math>)</b>
	1	10.18
	2	10.2
	3	20.39
	4	40.74

The grain volume is determined by

$$GV = V_{2bil} + RV \left[ \frac{P_{of}}{P_f} - \frac{P_{os}}{P_s} \right] \quad (3.4)$$

Where  $V_{2bil}$  = the billet volume which filled in the excess space in case that the sample is short.

$P_{os}$  = the reference chamber of the clean and dried core sample with helium is filled 100 psi.

$P_s$  = the stabilized pressure the helium is introduced into matrix cup and pressure is allowed to stabilize.

$P_{of}$  = reference pressure, always uses 100 psi

$P_f$  = equilibrated pressure, psi

The bulk volume is determined by;

$$BV = \pi L \left( \frac{D}{2} \right)^2 \quad (3.5)$$

Sample weight is determined by using the weight balance for measuring the dry weight of specimens. The sample is weighed to two decimal places.

$$\text{Immersed weight} = 13.54166 \times BV \quad (3.6)$$

Pore volume is the different value of BV. and GV.

$$PV = BV - GV \quad (3.7)$$

And porosity is calculated by

$$\phi(\%) = \frac{PV}{BV} \times 100 \quad (3.8)$$

Table 3.3 summarizes the measurement results of porosity.

**Table 3.3** Summary of the porosity measurement results of sandstone specimens.

<b>Number</b>	<b>Sample</b>	<b>Grain Volume</b>	<b>Bulk Volume</b>	<b>Pore Volume</b>	<b>Porosity (%)</b>
1	CM1-5	57.65	60.13	2.48	4.13
2	CM1-6	48.42	51.52	3.10	6.02
3	CM2-1	58.53	59.70	1.17	1.96
4	CM2-2	58.32	60.30	1.98	3.28
5	MM1-1-1	52.97	58.99	6.03	10.22
6	MM1-1-2	52.79	59.19	6.40	10.81
7	MM1-2-1	52.29	59.71	7.42	12.43
8	MM1-2-2	51.92	55.72	3.80	6.83
9	MM1-3-1	51.90	58.50	6.60	11.28
10	MM1-3-2	50.54	58.47	7.93	13.56
11	MM1-3-3	48.15	55.38	7.24	13.07
12	MM1-4-1	42.17	48.45	6.29	12.97
13	MM1-4-2	41.30	51.65	10.35	20.04
14	MM1-4-3	54.37	60.29	5.92	9.82
15	MM2-1	49.30	58.53	9.23	15.77
16	MM2-5	38.62	49.65	11.03	22.21
17	LP1-1	39.65	49.44	9.80	19.81
18	LP1-2	46.42	56.33	9.91	17.60
19	LP2-1	56.72	58.65	1.93	3.30
20	LP3-1	56.06	59.95	3.89	6.48

**Table 3.3** Summary of the porosity measurement results of sandstone specimens

(continued).

<b>Number</b>	<b>Sample</b>	<b>Grain Volume</b>	<b>Bulk Volume</b>	<b>Pore Volume</b>	<b>Porosity (%)</b>
21	LP3-2	57.41	60.42	3.01	4.99
22	LP3-3	56.78	60.15	3.37	5.60
23	LP3-4	56.98	60.86	3.88	6.37
24	LP4-1	59.36	60.18	0.82	1.36
25	LP4-2	58.69	59.39	0.70	1.18
26	LP5-1	29.22	45.12	15.90	35.24
27	LP5-2	41.32	45.12	3.80	8.43
28	LP5-3	30.77	48.52	17.75	36.58
29	LP6-1	41.19	52.38	11.19	21.37
30	LP7-3	57.15	60.07	2.92	4.86
31	LP7-4	59.09	61.02	1.93	3.16
32	LP8-1	51.64	61.02	9.38	15.38
33	LP-8-2	52.98	59.05	6.07	10.27
34	LP9-1	46.79	59.62	12.83	21.53

### 3.4 Permeability Measurement

The flow of fluids in a porous medium depends on the connectivity of pores. Permeability is a measure of pore connectivity in the equations describing fluid flow in a porous media (Fanchi, 2000). Darcy's equation for single phase flow is

$$Q = -0.001127 \frac{KA \Delta p}{\mu \Delta x} \quad (3.9)$$

Where	$Q$	=	flow rate, (bbl/ddy)
	$K$	=	permeability, (md)
	$A$	=	cross-sectional area, (ft <sup>2</sup> )
	$\mu$	=	fluid viscosity, (cp)
	$\Delta x$	=	length, (ft)

The overburden poro-perm cell is shown in Figure 3.8. It has been designed to perform porosity and permeability measurements on specimens under simulated reservoir conditions. It uses an air actuated hydraulic pump to achieve a simulated reservoir confining pressure on specimens. The permeability determination of specimens is used nitrogen (N<sub>2</sub>) which is specified initial pressure (upstream pressure) let flow through the length of specimen. The specimen is sealed along its length so that nitrogen cannot leave from the specimen. The flow rate of air from the other end of specimen is measured. The permeability of the specimen is calculated by using the upstream pressure and flow rate during the test, the atmospheric pressure, viscosity of nitrogen and the length and cross sectional area of specimen. Permeability is indicator of ability of porous medium to transmit fluids. Unit of permeability is required in md.



**Figure 3.8** The overburden poro-perm cell instrument is used to measure the permeability of the specimens.

### 3.4.1 The Overburden Permeability Calculations

The following equation is applied from Darcy's Law equation to calculate the permeability of specimens. All pressure needs to be unit of atmosphere (atm).

$$K_{gas} = \frac{2000 \times BP \times \mu_{gas} \times Q \times L}{\left[ (P_1 \times 0.06805 + BP)^2 - (BP)^2 \times A \right]} \quad (3.10)$$

$$K_{gas(actual)} = K_{gas(apparent)} \times 0.9716^* \quad (3.11)$$

Where

$BP$  = barometric pressure, atm, ( $BP_{atm} = BP_{millibar} \times 0.0009896$ )

$\mu_{N_2}$  = viscosity of nitrogen, cp

$Q$  = flow rate,  $cm^3 / sec$

$L$  = length of the specimen, cm

$P_1$  = upstream pressure, psi

0.6805 = conversion factor, (converting psi to atm)

$A$  = cross-sectional area of plug,  $cm^2$

0.9716\* = conversion factor the expansion of air due to saturation with water vapor in the bubble tube.

$$\mu_{air} = -8 \times 10^{-7} T^2 + 8 \times 10^{-5} T + 0.171$$

$$\mu_{N_2} = -8 \times 10^{-7} T^2 + 8 \times 10^{-5} T + 0.0158$$

Where

$T$  = temperature,  $^{\circ}C$

Table 3.4 summarizes the measurement results of permeability.



**Table 3.4** Summary of the permeability measurement results of sandstone specimens.

Number	Sample	P <sub>1</sub> (psi)	Volume (cm <sup>3</sup> )	Time (second)	Length (mm)	Diameter (mm)	Permeability (md)
1	CM1-5	49.99	3.0	546.67	5.17	3.85	0.005
2	CM1-6	57.98	1.0	356.44	4.45	3.82	0.002
3	CM2-1	56.59	1.0	468.28	5.15	3.84	0.002
4	CM2-2	49.87	10	88.17	5.19	3.85	0.113
5	MM1-1-1	57.59	0.1	21.41	5.18	3.81	0.004
6	MM1-1-2	49.32	0.1	23.85	5.17	3.82	0.004
7	MM1-2-1	50.08	50	6.00	5.15	3.84	8.19
8	MM1-2-2	49.97	50	10.00	5.15	3.84	4.930
9	MM1-3-1	49.99	100	12.00	5.04	3.84	8.05
10	MM1-3-2	50.00	50	5.00	5.06	3.84	9.63
11	MM1-3-3	50.00	50	2.00	4.84	3.82	23.05
12	MM1-4-1	50.25	10	304.89	4.17	3.85	0.026
13	MM1-4-2	49.87	10	88.17	4.50	3.83	0.098
14	MM1-4-3	49.98	3.0	126.67	5.20	3.84	0.024
15	MM2-1	50.07	10	24.00	5.26	3.76	0.437
16	MM2-5	50.64	10	41.00	4.51	3.74	0.218
17	LP1-1	50.05	10	33.62	4.53	3.73	0.275
18	LP1-2	50.16	10	28.67	5.18	3.72	0.368
19	LP2-1	55.32	1.0	157.39	5.08	3.83	0.005
20	LP3-1	56.93	1.0	158.22	5.17	3.84	0.005

**Table 3.4** Summary of the permeability measurement results of sandstone specimens  
(continued).

Number	Sample	P <sub>1</sub> (psi)	Volume (cm <sup>3</sup> )	Time (second)	Length (mm)	Diameter (mm)	Permeability (md)
21	LP3-2	54.19	1.0	294.93	5.19	3.85	0.003
22	LP3-3	49.95	1.0	245.99	5.17	3.85	0.004
23	LP3-4	58.27	1.0	211.64	5.23	3.85	0.004
24	LP4-1	49.99	1.0	165.67	5.23	3.83	0.006
25	LP4-2	49.99	1.0	152.33	5.18	3.82	0.007
26	LP5-1	50.00	80	2.00	4.45	3.60	38.90
27	LP5-2	50.04	50	4.00	4.45	3.60	12.14
28	LP5-3	50.11	100	5.00	4.53	3.70	18.68
29	LP6-1	49.92	50	1.00	4.92	3.68	51.38
30	LP7-3	57.61	1.0	156.10	5.17	3.85	0.005
31	LP7-4	57.51	1.0	57.84	5.25	3.85	0.014
32	LP8-1	49.98	10	59.33	5.13	3.83	0.167
33	LP-8-2	49.98	10	68.67	5.17	3.83	0.146
34	LP9-1	57.59	0.1	21.41	5.00	3.77	0.004

### 3.5 Conclusion and Discussion

From summarization of porosity and permeability measurements in Table 3.3 and 3.4, the range porosity is 1.18-36.58 % and average porosity is 11.7 %. Whereas the permeability values are ranged from 0.002 to 51.38 md and its average is 5.2 md. The porosity range of U-Thong field is 11-23% and permeability is 0.1-500 md (Thongpenyai, *et al*). Comparison of results obtained from U-Thong field with rock samples testing indicates that the values of porosity from rock samples are closely valued of U-Thong field but permeability of rock samples are more different from U-Thong field. This is because of many reasons; (1) errors which have occurred as measuring such as lower pressure when measured and water supply maybe leak to sample (2) the rock samples are collected from different formations although they are the same Tertiary sandstone. (3) difference of the vary conditions which used in measurement; overburden pressure, atmospheric pressure, and temperature.

## CHAPTER IV

### WATERFLOODING ANALYSIS

#### 4.1 Microscopic Displacement Efficiency

Displacement efficiency is influenced by rock and fluid properties. It can be determined by laboratory floods, frontal advances theory and empirical correlations. The microscopic displacement efficiency of a waterflood,  $E_D$  is defined as follows

$$E_D = 1 - \frac{S_{or}}{\bar{S}_{o1}} \quad (4.1)$$

Where  $S_{or}$  = residual oil, fraction  
 $\bar{S}_{o1}$  = volumetric average oil saturation at the beginning of the waterflood, where the average pressure is  $\bar{p}_1$ , fraction

The oil displaced by a waterflood of reservoir in which  $V_{pw}$  has been swept to an average oil saturation of  $S_{or}$  is given by equation (4.2)

$$N_{pw} = E_D V_{pw} \frac{\bar{S}_{o1}}{B_{o1}} \quad (4.2)$$

Where  $N_{pw}$  = oil displaced by water, STB  
 $V_{pw}$  = pore volume that has been swept by water to volumetric average saturation of residual oil.

$B_{oi}$  = oil formation volume factor at pressure  $\bar{p}_1$ , bbl/STB

## 4.2 Macroscopic Displacement Efficiency of a Linear Waterflood

Macroscopic efficiency is the term used to describe the displacement efficiency of a waterflood in a specified volume of reservoir rock. Macroscopic displacement efficiency also changes with time. Solution of these equations for specified reservoir geometries yield displacement rate/time estimated. In some cases, partial mathematical solutions can be obtained with a desk calculator and graph paper. Large problems in heterogeneous reservoirs may be solved only with the use of numerical simulators.

### 4.2.1 Development of Equations Describing Multiphase Flow in Porous Media.

The flow of fluids through porous media is described by the continuity equation which is the partial differential equation describing the law of conservation of mass at every point in the porous media. Considering the flow of two fluids-oil and water, Darcy flow is assumed.

**Mass in – Mass out = Remaining**

$$-\frac{\partial}{\partial x}(\rho_o u_x) - \frac{\partial}{\partial y}(\rho_o u_y) - \frac{\partial}{\partial z}(\rho_o u_z) = \frac{\partial}{\partial t}(\rho_o S_o \phi) \quad (4.3)$$

Similarly, for the water phase,

$$-\frac{\partial}{\partial x}(\rho_w u_x) - \frac{\partial}{\partial y}(\rho_w u_y) - \frac{\partial}{\partial z}(\rho_w u_z) = \frac{\partial}{\partial t}(\rho_w S_w \phi) \quad (4.4)$$

These equations assume that there is no dissolution of oil in the water phase.

### 4.2.2 Flow Equations for Each Phase

The continuity equations, while conceptually correct, are expressed in velocities that cannot be measured. Darcy's law is applied to each phase.

$$\frac{\partial}{\partial x} \left( \frac{\rho_o^2 k_{ox}}{\mu_o} \frac{\partial \Phi_o}{\partial x} \right) + \frac{\partial}{\partial y} \left( \frac{\rho_o^2 k_{oy}}{\mu_o} \frac{\partial \Phi_o}{\partial y} \right) + \frac{\partial}{\partial z} \left( \frac{\rho_o^2 k_{oz}}{\mu_o} \frac{\partial \Phi_o}{\partial z} \right) = \frac{\partial}{\partial t} (\rho_o S_o \phi) \quad (4.5)$$

Where,  $\Phi_o =$  the oil phase potential

$$\frac{\partial \Phi_o}{\partial x} = \frac{\partial}{\partial x} \left[ g(z - z_d) + \int_{p_{od}}^{p_o} \frac{dp_o}{\rho_o} \right] = g \frac{\partial z}{\partial x} + \frac{1}{\rho_o} \frac{\partial \rho_o}{\partial x} \quad (4.6)$$

For oil (law of conservation of mass)

$$\frac{\partial}{\partial x} \left( \frac{\rho_o k_{ox}}{\mu_o} \frac{\partial \rho_o}{\partial x} \right) + \frac{\partial}{\partial y} \left( \frac{\rho_o k_{oy}}{\mu_o} \frac{\partial \rho_o}{\partial y} \right) + \left[ \frac{\partial}{\partial z} \frac{\rho_o k_{oz}}{\mu_o} \left( \frac{\partial \rho_o}{\partial z} + \rho_o g \right) \right] = \frac{\partial}{\partial t} (\rho_o S_o \phi) \quad (4.7)$$

Water is similar to oil phase.

$$\frac{\partial}{\partial x} \left( \frac{\rho_w k_{wx}}{\mu_w} \frac{\partial \rho_w}{\partial x} \right) + \frac{\partial}{\partial y} \left( \frac{\rho_w k_{wy}}{\mu_w} \frac{\partial \rho_w}{\partial y} \right) + \left[ \frac{\partial}{\partial z} \frac{\rho_w k_{wz}}{\mu_w} \left( \frac{\partial \rho_w}{\partial z} + \rho_w g \right) \right] = \frac{\partial}{\partial t} (\rho_w S_w \phi) \quad (4.8)$$

### 4.2.3 Steady-State Solutions to Fluid-Flow Equations in Linear System.

These equations are solved in order of increasing complexity, beginning with the problem of steady flow of two phases in linear porous rock. Steady flow of two phases is of interest primarily for interpretation of laboratory experiments to determine relative permeability.

#### 1. Steady Linear Flow

Flow is considered steady when there are no changes with time. For the purposes of this section, we assume flow is in the  $x$  direction and flow is one-dimensional (1D) in the horizontal plane. These equations are represented the steady flow of oil and water in  $x$  direction.

$$\frac{\partial}{\partial x} \left( \frac{\rho_o k_{ox}}{\mu_o} \frac{\partial p_o}{\partial x} \right) = 0 \quad (4.9)$$

$$\frac{\partial}{\partial x} \left( \frac{\rho_w k_{wx}}{\mu_w} \frac{\partial p_w}{\partial x} \right) = 0 \quad (4.10)$$

In equation of 4.9 and 4.10, oil and water densities and viscosities are function of pressure and temperature. Temperature is constant while pressure gradient is usually small. If both oil and water densities and viscosities are considered constants. The term of incompressible is used to describe the assumption of constant densities.

$$\int \frac{\partial}{\partial x} \left( \frac{\rho_o k_{ox}}{\mu_o} \frac{\partial p_o}{\partial x} \right) = 0$$

$$\frac{d}{dx} k_o \frac{dp_o}{dx} = 0 \quad (4.11)$$

$$\frac{d}{dx} k_w \frac{dp_w}{dx} = 0 \quad (4.12)$$

Oil and water phase pressure are assumed to be correlated through the capillary pressure curve for the specific saturation path.

## 2. Capillary End Effect

A phenomenon known as the capillary end effect occurs under certain conditions in laboratory experiments involving the steady flow of two immiscible phases. Oil and water phases are in capillary equilibrium throughout the porous rock. The difference between the oil and water phase pressures is given by the capillary pressure curve corresponding to the saturation path (drainage or imbibition) and the water saturation.

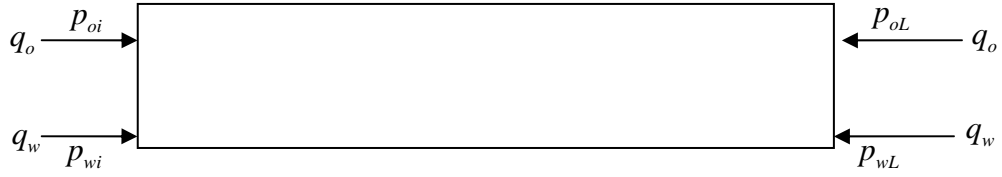


**Figure 4.1** Schematic of steady two-phase flow in a porous rock.

At the inlet ( $S_w$ ) of the core,

$$p_c = P_{oi} - P_{wi} \quad (4.13)$$

At the exit,

$$p_c = 0 \quad (4.14)$$

In actually  $p_c \neq 0$  in strongly water wet core on the imbibition path. Recall the definition of the capillary pressure.

$$\frac{dp_c}{dx} = \frac{dp_o}{dx} - \frac{dp_w}{dx} = \frac{q_w \mu_w}{Ak_w} - \frac{q_o \mu_o}{Ak_o} \quad (4.15)$$

$p_c$  curve is a function of water saturation,  $S_w$

$$\frac{\partial p_c}{dx} = \frac{\partial p_c}{\partial S_w} \frac{dS_w}{dx} \quad (4.16)$$

$$\left( \frac{\partial p_c}{\partial S_w} \right) \left( \frac{dS_w}{dx} \right) = \frac{q_w \mu_w}{Ak_w} - \frac{q_o \mu_o}{Ak_o} \quad (4.17)$$

$$k_o = \frac{q_o \mu_o L}{A \Delta p}, \quad k_w = \frac{q_w \mu_w L}{A \Delta p}$$



$$k_w^* = k_w \left( \frac{1}{1 - \frac{P_{c1} - P_{c2}}{P_{o1} - P_{o2}}} \right) \quad (4.18)$$

The displacement of one fluid by another fluid is an unsteady-state process because the saturations of the fluids change with time. This causes changes in relative permeability and either pressure or phase. Two methods to predict displacement performance will be presented. The first method is the Buckley-Leverett, or frontal advance, model, which can be solved easily with graphical techniques. The second method is the generalized treatment of two-phase flow leading to a set of partial equations that can be solved on a digital computer with numerical techniques.

#### 4.2.4 Buckley-Leverett Model

The Buckley-Leverett model was developed by application of the law of conservation of mass to the flow of two fluids (oil and water) in one direction ( $x$ ).

$$\left( \frac{dx}{dt} \right)_{S_w} = \frac{qt}{\phi A} \left( \frac{\partial f_w}{\partial S_w} \right)_f \quad (4.19)$$

Equation 4.19 is the Buckley-Leverett equation. It is also called the frontal advance which state that in a linear displacement process. Three assumptions were made in developing in equation 4.19.

1. Incompressible flow.
2. The fractional flow of water is a function only of a water saturation.
3. No mass transfer between phases.

From (4.19)

$$\int_0^{X_{S_w}} dx S_w = \frac{qt}{A\phi} \int_0^t \left( \frac{\partial f_w}{\partial S_w} \right)_t dt \quad (4.20)$$

When  $\partial f_w / \partial S_w$  is only function  $S_w$ .

$$X_{S_w} = \frac{q_t t}{A\phi} \left( \frac{\partial f_w}{\partial S_w} \right)_{S_w} \quad (4.21)$$

$$\frac{X}{L} = \frac{q_t t}{A\phi L} \left( \frac{\partial f_w}{\partial S_w} \right)_{S_w} \quad (4.22)$$

Where  $q_t t$  = Total fluid injected

$A\phi L$  = Total pore volume

This velocity,  $\left( \frac{dx}{dt} \right)_{S_w}$  is determined uniquely by the water saturation through the

fractional flow equation as follows.

$$f_w = \frac{1}{1 + \left( \frac{k_o}{k_w} \right) \left( \frac{\mu_w}{\mu_o} \right)} + \frac{1.127 k_{oA} (\rho_o - \rho_w) g \sin \alpha}{\mu_o q_t \left[ 1 + \left( \frac{k_o}{k_w} \right) \left( \frac{\mu_w}{\mu_o} \right) \right]} \quad (4.23)$$

When  $x$  is the horizontal plane,  $\alpha = 0$  and there is no gravity term.

$$f_w = \frac{1}{1 + \left( \frac{k_o}{k_w} \right) \left( \frac{\mu_w}{\mu_o} \right)} \quad (4.24)$$

Using the oil-water relative permeability data shown in Figure 4.2 and an oil-water viscosity ratio, calculated fractional flow curve is shown in Figure 4.3 and Figure 4.4 show determination of average water saturation at breakthrough. The frontal advance equation can be used to derive the expressions for average water saturation as follows:

At breakthrough,

$$\overline{S}_{wbt} - S_{wc} = \left( \frac{\partial S_w}{\partial f_w} \right)_f = \frac{S_{wf} - S_{wc}}{f_{wf}} \quad (4.25)$$

After breakthrough,

$$\bar{S}_w - S_{w2} = \frac{1 - f_{w2}}{\left( \frac{\partial f_w}{\partial S_w} \right)_{S_{w2}}} \quad (4.26)$$

Where

- $f_{wf}$  = fraction of water flowing at the flood front
- $f_{w2}$  = fraction of water flowing at the producing end of the system
- $\bar{S}_w$  = average water saturation after breakthrough, fraction
- $S_{wf}$  = water saturation at the flood front, fraction
- $S_{wbt}$  = average water saturation at breakthrough, fraction
- $S_{wc}$  = connate water saturation, fraction
- $S_{w2}$  = water saturation the producing end of the system, fraction

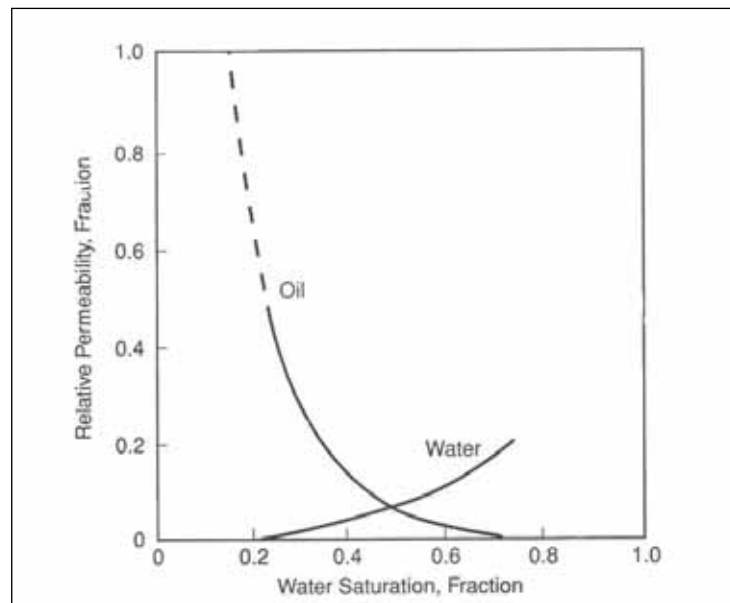


**Figure 4.2** Oil-Water Relative Permeability.

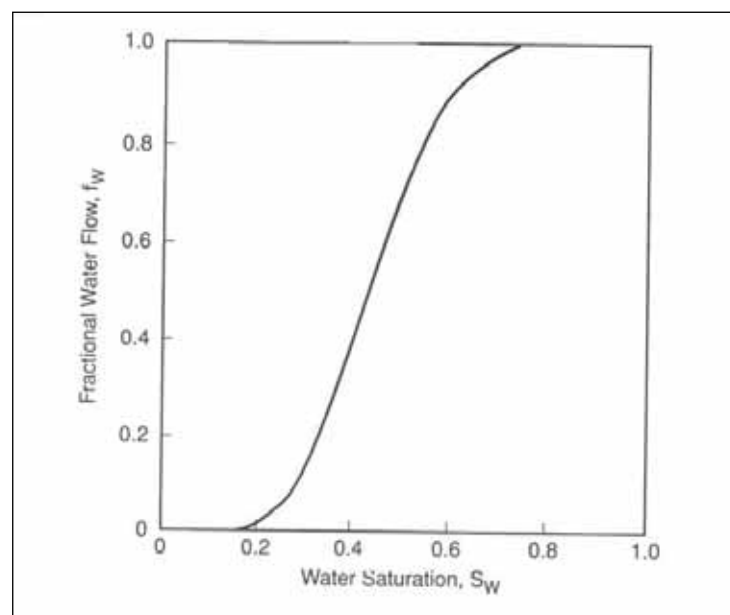


**Figure 4.3** Fraction Water Flow

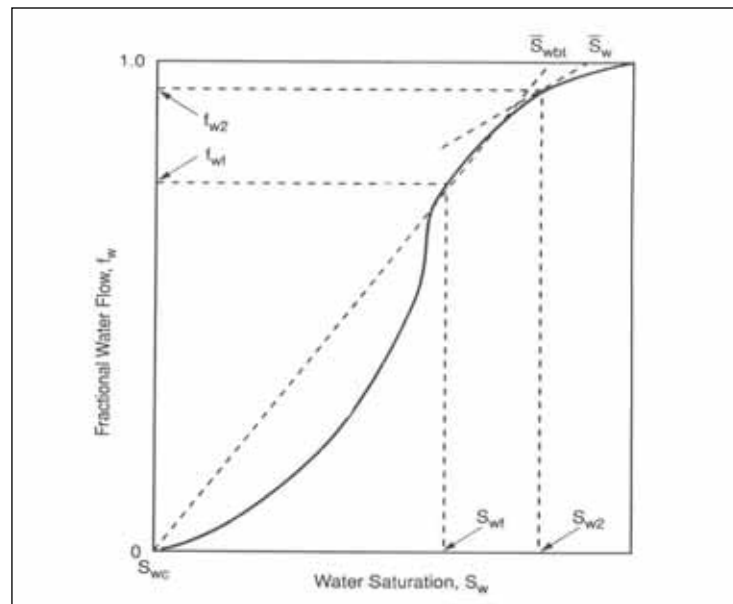


**Figure 4.4** Determination of Average Water Saturation at Breakthrough.

### 4.3 Immiscible Displacement in Two Dimensions – Areal

#### 4.3.1 Craig–Geffen–Morse Correlation (CGM)

Craig *et. al* obtained experimental data in horizontal laboratory models representing a quadrant of a five-spot. Experimental data for a variety of oil and aqueous systems were correlated empirically (Willhite, 1986).

At and after breakthrough

$$E_A = E_{Abt} + 0.274 \ln \frac{W_i}{W_{ibt}} \quad (4.27)$$

Where  $E_{Abt}$  = areal sweep efficiency at breakthrough of the displacing fluid.

$E_A$  = the fraction of the area that has been swept to an average  $S_w$  of  $S_{wf}$ .

The development of the model considers the displacement of oil by water in a five-spot pattern with no  $S_{gi}$ .

$$N_{pbt} = E_{Abt} (\bar{S}_{wf} - S_{wi}) V_p \quad (4.28)$$

Where  $\bar{S}_{wf}$  = the average displacing-phase saturation at breakthrough

Production after breakthrough is estimated from equation (4.30).

$$N_p = E_A (\bar{S}_{w5} - S_{iw}) V_p \quad (4.29)$$

Where  $\bar{S}_{w5}$  is the average water saturation in a region swept by the injected fluid. The key to this model is the assumption made to evaluate  $\bar{S}_{w5}$ . A new variable,  $Q_i^*$ , is defined to represent the number of water-contacted PV's in the five spot pattern-that

is,  $Q_i^*$  equals the volume of water injected divided by the volume of the five-spot contacted by the injected water.

At breakthrough

$$Q_i^* = \frac{W_{ibt}}{E_{Abt} V_p} = \overline{S}_{wf} - S_{iw} \quad (4.30)$$

$$f'_{Sw5} = \frac{1}{Q_i^*} \quad (4.31)$$

Thus when  $Q_{i2} = Q_i^*$

$$f'_{Sw2} = f'_{Sw5} \quad (4.32)$$

and

$$\overline{S}_{w5} = S_{w2} + f_{o2} Q_i^* \quad (4.33)$$

Value of  $f_{o2}$  and  $S_{w2}$  are obtained from the frontal advanced solution at

$$f'_{Sw2} = \frac{1}{Q_i^*} \quad (4.34)$$

### 4.3.2 Stream tube Models

Higgins and Leighton (1986) approximate solution of displacement problems can often be obtained without resorting to mathematically complex and expensive numerical simulators. Stream tube is paths followed by fluid particles as they traverse from an injection well to production well. Stream tube models assume that immiscible displacement processed of a homogeneous fluid in the porous media.

Before breakthrough at the end of the last cell,  $q_o = q_t$

$$q_t = \frac{k_b (p_I - p_p) h}{\sum_{j=1}^k \frac{G_j}{(\overline{\lambda}_{ro} + \overline{\lambda}_{rw})_j} + \sum_{j=k+1}^n \frac{G_j}{\lambda_{roi}}} \quad (4.35)$$

After breakthrough,

$$q_t = \frac{k_b (p_i - p_p) h}{\sum_{j=1}^n \frac{G_j}{(\bar{\lambda}_{ro} + \bar{\lambda}_{rw})_j}} \quad (4.36)$$

Where  $\bar{\lambda}_{ro}$  = average relative mobility of the oil phase in cell j  
 $\bar{\lambda}_{rw}$  = average relative mobility of the water phase in cell j  
 $G_j$  = shape factor in the Higgens – leighton model,  $(L_j / A_j)$

#### **4.4 Estimating Waterflooding Performance with 3D Models and Reservoir Simulators.**

Reservoirs are 3D geologic deposits that have properties that may throughout the deposit. Frequently, the amount of variation is not known until revealed by analysis of displacement performance. Thus, simulation of displacement performance may be limited by knowledge of reservoir properties as well as available reservoir models. Three-dimensional simulation of displacement processed may be required when there are significant changes in reservoir properties (permeability, porosity, and thickness), or saturations or when cross flow or gravity segregation are important. Solution of fluid- flow equation in 3D, including the effects of rock and fluid compressibility is possible with numerical techniques for almost any reservoir geometry.



## **4.5 Waterflooding Patterns**

Selection of the waterflooding plan is determined by factors that often unique to each reservoir. Pattern flooding, an alternative to pressure maintenance, may be selected because reservoir properties will not permit waterflooding through edge wells at desired injection rates. In pattern flooding, injection and withdrawal rates are determined by well spacing as well as reservoir properties. The selection of possible waterflooding depends on existing wells that generally must be used because of economics. Finally, selected flooding pattern to use waterflooding a reservoir must be determined by comparison of the economics of alternative flooding schemes. Injection-production well arrangements are shown in Figure 4.5 and their characteristics are given in Table 4.1.

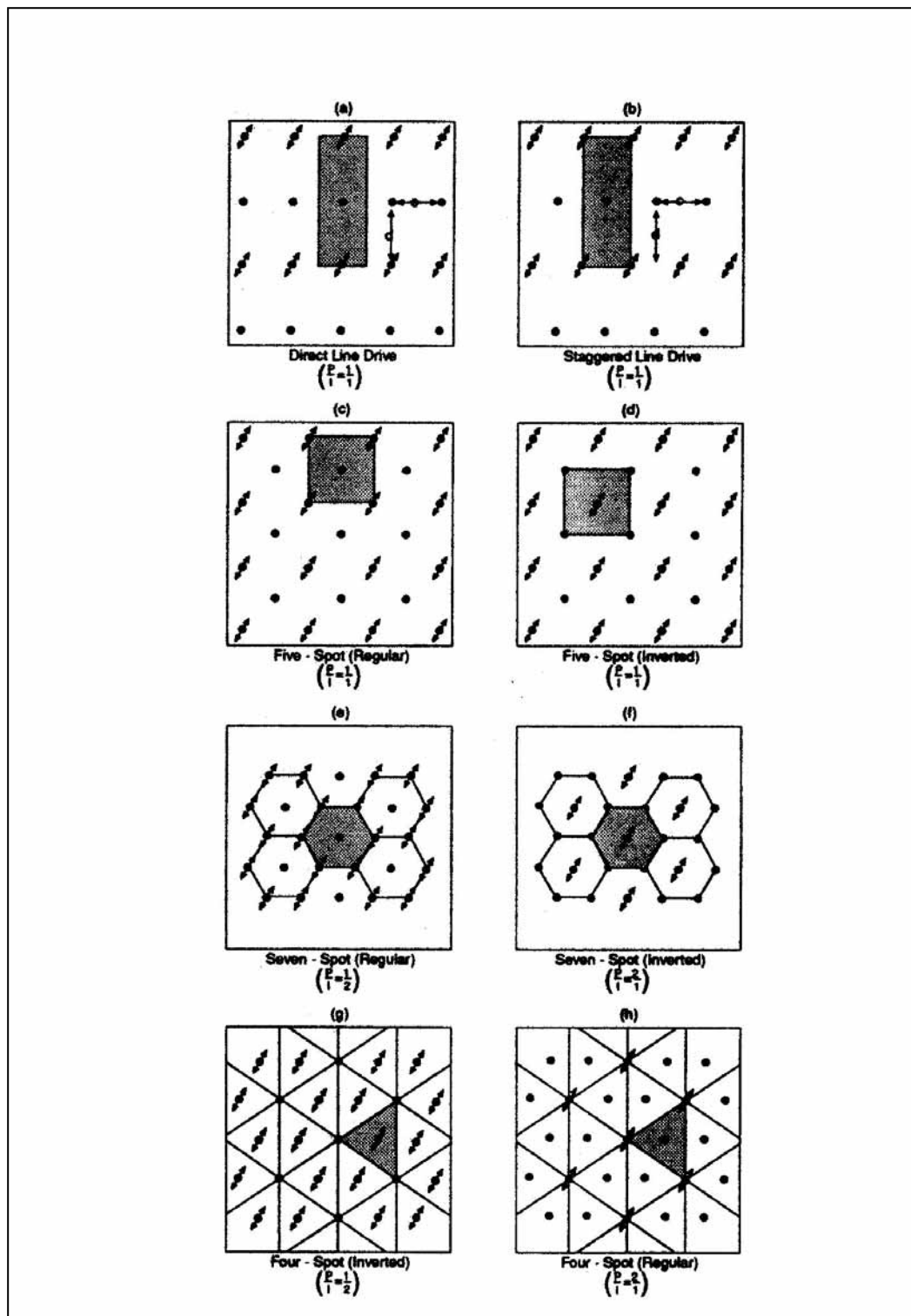


Figure 4.5 Flood Patterns

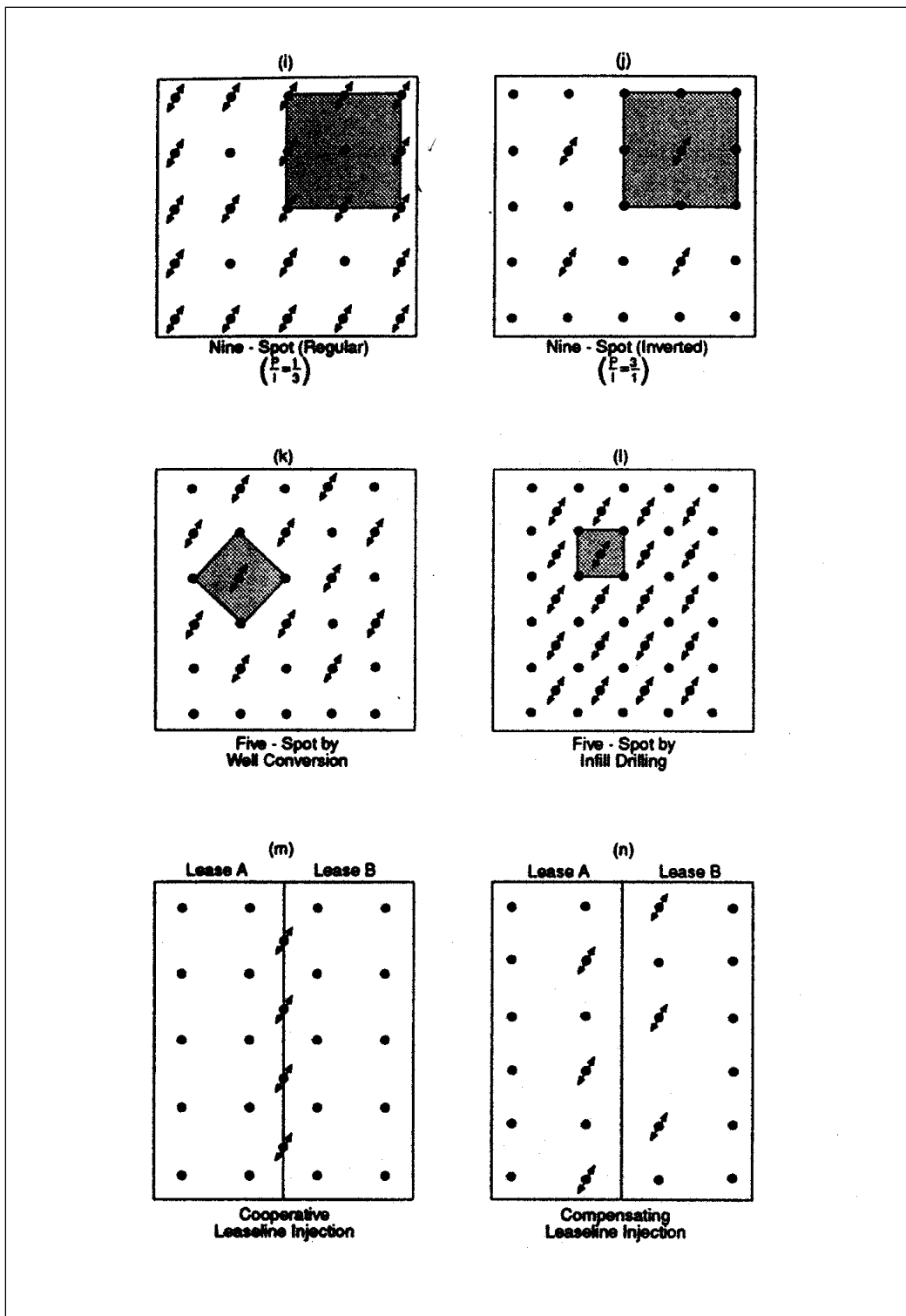


Figure 4.5 Flood Patterns (continued).

**Table 4.1** Characteristics of waterflood patterns.

Pattern	P/I Regular	P/I Inverted	d/a	$E_A$ , %
Direct Line Drive	1	-	1	56
Staggered Line drive	1	-	1	78
4-spot	2	1/2	0.866	-
5-spot	1	1	1/2	72
7-spot	1/2	2	0.866	-
9-spot	1/3	3	1/2	~80

P = number of production wells

I = number of injection wells

d = distance from an injector to the line connecting two production wells

a = distance between wells in line in regular pattern

$E_A$  = areal sweep efficiency at water breakthrough at a producing well for a

= water-oil mobility ratio = 1

## 4.6 Recovery Efficiency

The overall waterflood recovery efficiency is given by

$$E_R = E_D \times E_V \quad (4.37)$$

Where  $E_R$  = overall recovery efficiency, fraction or %

$E_D$  = displacement efficiency within the volume swept by water, fraction or %

$E_V$  = volumetric actually, the fraction of the reservoir volume actually swept by water, fraction or %

Displacement efficiency that is governed by rock and fluid properties is given by:

$$E_D = \frac{S_{wor} - S_{wi}}{1 - S_{wi}} \quad (4.38)$$

Where  $S_{wor}$  = water saturation at the residual oil saturation which can be determined from the fractional flow curve for given fractional water flow

Volumetric sweep efficiency is defined by:

$$E_V = E_A \times E_I \quad (4.39)$$

Where  $E_A$  = areal sweep efficiency, fraction

$E_I$  = vertical or invasion sweep efficiency, fraction

Areal sweep efficiency for various patterns has been studied using both physical and mathematical models. Whereas vertical sweep efficiency is influenced by reservoir heterogeneity, mobility ratio, cross-flow, gravity and capillary forces. Permeability variation has the greatest influence on vertical sweep efficiency. Horizontal permeability varies with depth due to change in depositional environments

and subsequent geologic events. The injected water moves preferentially through zones of higher permeability. In a preferentially water-wet rock, water is imbibed into the adjacent lower permeable zones from the higher permeable zones because of capillary forces. Also, injected water tends to flow to the bottom of the reservoir due to gravity segregation. The net effect of these factors is to influence the vertical sweep efficiency of a water flood project.

# **CHAPTER V**

## **RESERVOIR SIMULATION**

### **5.1 Theory of Reservoir Simulation**

Numerical reservoir simulators are used widely; primary because they can solve problems that cannot be solved in any other ways. Simulation is the only way to describe quantitatively the flow of multi-phases in a heterogeneous reservoir having a production schedule determined not only by the properties of the reservoir, but also by market demand, investment strategy, and government regulations. Reservoir modeling is the application of computer simulation system to the description of fluid flow in a reservoir. The area of reservoir simulation applies the concepts and techniques of mathematical modeling to the analysis of the behavior of petroleum reservoir system.

#### **5.1.1 Simulation Solution Procedures**

Fluid flow equations are a set of non-linear partial differential equations that must be solved by computer. The partial derivatives are replaced with finite differences, which are in turn derived from Taylor's series. The two most common solution procedures in use today are following:

1. Newton-Raphson (Fully Implicit Techniques)

The terms in finite difference form of the flow equations are expanded in the Newton-Raphson procedure as the sum of each term at the current iteration level, plus a contribution due to a change of each term with respect to the

primary unknown variables over the iteration. The derivatives are stored in matrix called the acceleration matrix or the Jacobian. The Newton-Raphson technique leads to a matrix equation  $J \circ \delta X = R$  that equates the product of the acceleration matrix  $J$  and a column vector  $\delta X$  of changes to the primary unknown variables to the column vector of residual  $R$ . It is solved by matrix algebra to yield the changes to the primary unknown variables  $\delta X$ . These changes are added to the value of the primary unknown variables at the beginning of the iteration. If the changes are less than a specified tolerance, the iterative Newton-Raphson technique is considered complete and the simulator proceeds to the next time step. The three primary unknown variables for an oil-water-gas system are oil phase pressure, water saturation ( $S_w$ ) and either gas saturation ( $S_g$ ), or solution gas-oil ratio.

## 2. IMplicit Pressure-Explicit Saturation (IMPES)

The IMPES procedure solves for pressure at the new time level using saturations at the old time level, then uses the pressure at the new time level to explicit calculate saturations at the new time level. The iterative IMPES technique takes longer to run than the non-iterative techniques technique but generates less material balance error (Fanchi, 1997).

### 5.1.2 Classification of Reservoir Simulation

1. Single phase reservoir simulator (liquid or gas)
2. Multiphase reservoir simulator
  - Black-oil simulator
  - Compositional simulator



### **5.1.3 Other classification**

1. Type of Reservoir
  - 1.1 Gas reservoir simulator
  - 1.2 Black-oil reservoir simulator
  - 1.3 Compositional reservoir simulator
2. Recovery Process
  - 2.1 Primary recovery
    - Solution gas drive
    - Gas cap expansion
    - Gravity drainage
    - Water influx
  - 2.2 Secondary recovery
    - Gas injection
    - Water injection
  - 2.3 Enhanced oil recovery
    - Chemical flood
    - Miscible displacement
    - Thermal recovery

### **5.1.4 Fluid Representation**

1. Compositional
2. Non-compositional

### **5.1.5 Reservoir Model Geometry**

There are two ways to define dimensions and depths of each grid cell.

### 1. Block-Centered (BC) Geometry

It required for each cell a top depth plus a cell size in the x, y, and z directions. The upper and lower faces are flat and horizontal and the cell sides are flat and vertical. The cells are all rectangular.

### 2. Corner Point Geometry

It is based on the notion of co-ordinate lines and corner depths. A co-ordinate line defines each edge of each column of cells. Co-ordinate lines are always straight but need not be vertical. The x, y, and z locations of one point above and one point below the grid define each co-ordinate line. Cells are then defined by fixing their corners at set elevation along each co-ordinate line. This permits the cells to have any physically valid shape: sloping surfaces, fault planes, pitchouts and erosion surfaces can be represented correctly.

The type of model geometry depends on a number of factors including;

1. Extent of the area to be modeled
2. Level of detail required in the study
3. Level of detail of available data
4. Complexity of faulting structure
5. Formation continuity across faults
6. Presence of sloping and/or listric (slump) faults
7. Time available for model construction

#### **5.1.6 Transmissibility Conventions**

The transmissibility is a property shared by connected cells. It controls the amount of fluid flow from cell to cell. In a system of discrete grid cells fluid flow is calculated between the centers of grid blocks. The extent of this flow is determined

by the transmissibility and mobility between connected cells, and now those quantities are calculated and assigned. All transmissibility calculations, however, are in the upstream direction i.e. the transmissibility assigned to cell (I, J, K) govern the flows to cells (I+1, J, K) and (I, J, K+1).

### 1. Block Center Transmissibility Calculations

In this case, x and y direction transmissibility values in the cartesian case are obtained using cell center and cross sectional area obtained from DX, DY, and DZ with a dip direction.

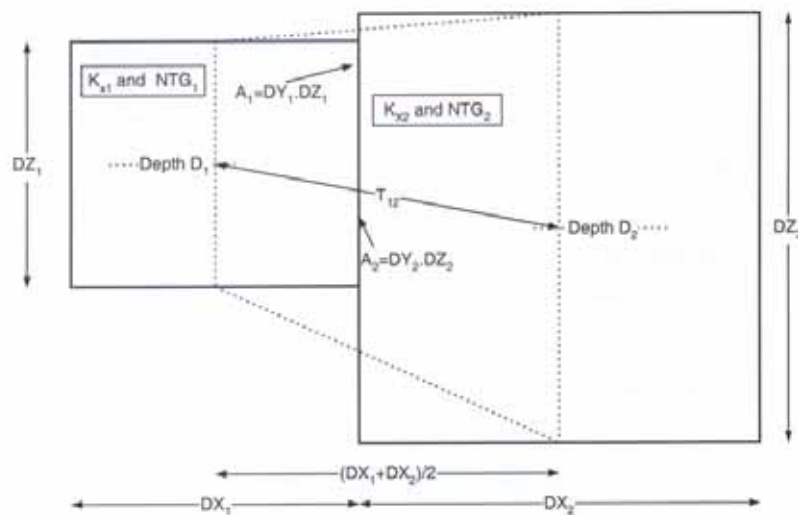


**Figure 5.1** Block Corner Transmissibility.

It takes the form

$$T_{12}^x = \frac{CA_{12}D_{12}}{B_{12}} \quad (5.1)$$

Where  $T_{12}^x$  = the x direction transmissibility between (I, J, K) and (I+1, J, K)

$C$  = the Darcy constant

$A_{12}$  = the interface area between the two cells in the x  
direction

$D_{12}$  = dip direction

$A_{12}$ ,  $D_{12}$  and  $B_{12}$  are given, respectively, by

$$A_{12} = \frac{DX_1 DY_1 DZ_1 NTG_1 + DX_2 DY_2 DZ_2 NTG_2}{DX_1 + DX_2} \quad (5.2)$$

$$D_{12} = \frac{\left(\frac{DX_1 + DX_2}{2}\right)^2}{\left(\frac{DX_1 + DX_2}{2}\right)^2 + (D_1 - D_2)^2} \quad (5.3)$$

Where  $D_1$  and  $D_2$  are cell center depths and

$$B_{12} = \frac{1}{2} \left[ \frac{DX_1}{K_{x1}} + \frac{DX_2}{K_{x2}} \right] \quad (5.4)$$

Then the transmissibility is

$$T_{12}^x = CD_{12} \left[ \frac{DX_1 DY_1 DZ_1 NTG_1 + DX_2 DY_2 DZ_2 NTG_2}{DX_1 + DX_2} \right] \frac{2}{\frac{DX_1}{K_{x1}} + \frac{DX_2}{K_{x2}}} \quad (5.5)$$

or

$$T_{12}^x = \frac{2CD_{12}}{(DX_1 + DX_2)} \left( \frac{DX_1 A_1 NTG_1 + DX_2 A_2 NTG_2}{DX_1 + DX_2} \right) \left[ \frac{(DX_1 + DX_2)}{\left(\frac{DX_1}{K_{x1}} + \frac{DX_2}{K_{x2}}\right)} \right] \quad (5.6)$$

$$T_{12}^x = \frac{2CD_{12}}{(DX_1 + DX_2)} \bar{A} \cdot \bar{K} \quad (5.7)$$

Note that the dimensions used here are simple those supplied by dx, dy, and dz.

## 2. Corner Point Transmissibility Calculations

The transmissibility is calculated from the x, y, and z projections of the interface area of the cells. Using a vector distance from the cell center to the face automatically incorporated a dip direction.

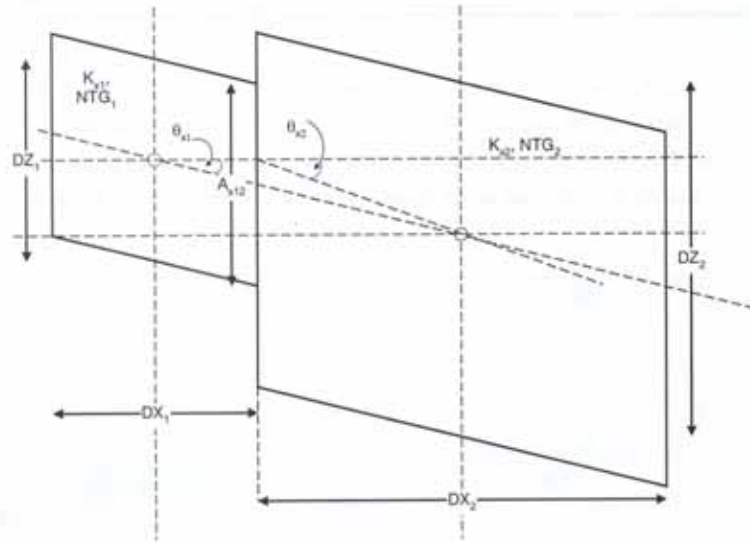


**Figure 5.2** Corner Point Transmissibility.

The x direction transmissibility takes the form

$$T_{12}^x = \frac{C}{\left(\frac{1}{T_1^x}\right) + \left(\frac{1}{T_2^x}\right)} \quad (5.8)$$

$$T_1^x = \frac{K_{X1} NTG_1 A_{X12} DX_1 + A_{Y12} DY_1 + A_{Z12} DZ_1}{DX_1^2 + DY_1^2 + DZ_1^2} \quad (5.9)$$

Where  $A_{X12}$ ,  $A_{Y12}$ , and  $A_{Z12}$  are the x, y and z projections of the interface area of cells 1 and 2.

$DX_1, DY_1,$  and  $DZ_1$  are the x, y, and z components of the distance between the center and x face of cell 1.

For a rectangular cell the y and z projections and components are zero. The x component of the distance from the cell centre to the x direction face is horizontal.

$$T_1^x = \frac{K_{x1}NTG_1A_{x12}}{\frac{DX_1}{2}} \quad (5.10)$$

$$\text{Or } T_1^x = \frac{2K_{x1}NTG_1\text{COS}\theta_{x1}}{DX_1} \quad (5.11)$$

Where  $A_{12}$  = the shared interface area

### 5.1.7 Formulation of the Equations

The non-linear residual,  $R_{fl}$ , for each fluid component in each grid block at each time step is

$$R_{fl} = \frac{dM}{dt} + F + Q \quad (5.12)$$

Where  $dM$  = the mass per unit surface density, accumulated during the current time step,  $dt$

$F$  = the net flow rate into neighboring grid blocks

$Q$  = the net flow rate into wells during the time step

$R_{fl}$  = defined for each cell and fluid in the study

In the black-oil case the fluid are oil, water, and gas in the compositional case they are hydrocarbon components and water. In order to solve the residual equations, we require a set of solution variables. The number of independent variables must be equal to the number of residual conditions.

The primary solution variables  $x$  are pressure,  $p$  and two saturations for a three phases black-oil study. The water saturation,  $S_w$  and either  $S_g$ ,  $R_s$ , or  $R_v$  are chosen to complete the set. From a three component black-oil system (oil, water, and gas). The residual  $R$  and the solution  $X$  are three component vectors in each grid block. By default, the solution procedure is fully explicit.

$$R = \begin{bmatrix} R_o \\ R_w \\ R_g \end{bmatrix} \quad (5.13)$$

$$X = \begin{bmatrix} P_o \\ S_w \\ S_g \text{ or } R_s \text{ or } R_v \end{bmatrix} \quad (5.14)$$

And the Jacobian,  $J = \frac{dR}{dX}$ , take the form

$$\frac{dR_i}{dX_j} = \begin{bmatrix} \frac{dR_o}{dP_o} & \frac{dR_o}{dS_w} & \frac{dR_o}{dS_g} \\ \frac{dR_w}{dP_o} & \frac{dR_w}{dS_w} & \frac{dR_w}{dS_g} \\ \frac{dR_g}{dP_o} & \frac{dR_g}{dS_w} & \frac{dR_g}{dS_g} \end{bmatrix}_{ij} \quad (5.15)$$

The mass change during the time step,  $dt$  is then

$$dM = M_{t+dt} - M_t \quad (5.16)$$

$$\text{With } M = PV \begin{bmatrix} \frac{S_o}{B_o} + \frac{R_v S_g}{B_g} \\ \frac{S_w}{B_w} \\ \frac{S_g}{B_g} + \frac{R_s S_o}{B_o} \end{bmatrix} \quad (5.17)$$

Where	$PV$	=	pore volume
	$B_o$	=	oil formation volume factor
	$B_w$	=	water formation volume factor
	$B_g$	=	gas formation volume factor
	$R_s$	=	solution gas-oil ratio
	$R_v$	=	vapor oil-gas ratio

The New solver aims to reduce the residuals  $R(X)$  to zero. This is the material balance error. For a three-component system we have

$$\sum_i (R_o)_i = \sum_i \left( \frac{dM_o}{dt} \right)_i + \sum_i (Q_o)_i \quad (5.18)$$

$$\sum_i (R_w)_i = \sum_i \left( \frac{dM_w}{dt} \right)_i + \sum_i (Q_w)_i \quad (5.19)$$

$$\sum_i (R_g)_i = \sum_i \left( \frac{dM_g}{dt} \right)_i + \sum_i (Q_g)_i \quad (5.20)$$

Where	$\sum_i$	=	refers to the sum over all reservoirs cell
	$(R_o)_i$	=	the oil residual in cell $i$
	$(R_w)_i$	=	the water residual in cell $i$
	$(R_g)_i$	=	the gas residual in cell $i$

The flow rate into cell  $i$  from a neighboring cell  $n$ ,  $F_{ni}$  is

$$F_{ni} = T_{ni} \begin{bmatrix} \frac{K_{ro}}{B_o \mu_o} & 0 & \frac{R_v K_{rg}}{B_g \mu_g} \\ 0 & \frac{K_{rw}}{B_w \mu_w} & 0 \\ \frac{R_s K_{ro}}{B_o \mu_o} & 0 & \frac{K_{rg}}{B_g \mu_g} \end{bmatrix}_u \times \begin{bmatrix} dP_{oni} \\ dP_{wni} \\ dP_{gni} \end{bmatrix} \quad (5.21)$$



Where

$$dP_{oni} = P_{on} - P_{oi} - \rho_{oni}G(D_n - D_i)$$

$$dP_{ni} = P_{on} - P_{oi} - \rho_{oni}G(D_n - D_i)$$

$$= P_{on} - P_{oi} - \rho_{oni}G(D_n - D_i) - P_{cown} + P_{cowi}$$

$$dP_{gni} = P_{gn} - P_{gi} - \rho_{gni}G(D_n - D_i)$$

$$= P_{on} - P_{oi} - \rho_{oni}G(D_n - D_i) + P_{cogn} - P_{cogi}$$

$T_{ni}$  = transmissibility between cells  $n$  and  $i$

$K_r$  = relative permeability

$\mu$  = viscosity

$dP$  = potential difference

( $dP_{gni}$  is the gas potential difference between cells  $n$  and  $i$ )

$\rho$  = fluid density

$G$  = acceleration due to gravity (0.00694 in field units)

$D$  = cell center depth

The net flow rate from cell  $i$  into neighboring cells is obtained by summing over the neighboring cells,  $F_i = \sum_n F_{ni}$

The rate of flow into a production well from cell  $i$  is

$$Q_i = -T_{wi} (P_{oi} - H_{iw} - P_{bh}) \left[ \frac{\frac{K_{ro}}{B_o \mu_o} + \frac{R_v K_{rg}}{B_g \mu_g}}{\frac{K_{rw}}{B_w \mu_g} + \frac{K_{rg}}{B_o \mu_o} + \frac{R_s K_{ro}}{B_o \mu_o}} \right] \quad (5.22)$$

Where  $T_{wi}$  = well connection transmissibility factor

$H$  = hydrostatic head correction

$P_{bh}$  = the bottom hole pressure

The inflow performance relationship is written in terms of the volumetric production rate of each phase at stock tank conditions.

$$q_{p,i} = T_{wi} M_{pj} (P_j - P_w - H_{wj}) \quad (5.23)$$

Where  $q_{pj}$  = the volumetric flow rate of phase  $p$  in connection  $j$  at stock tank conditions. (The flow is taken as positive from the formation into well, and negative from the well into the formation)

$T_{wj}$  = the connection transmissibility factor

$M_{pj}$  = phase mobility at the connection

$P_j$  = nodal pressure in the grid block containing the Connection

$P_w$  = bottom hole pressure head between the connection

$H_{wj}$  = well pore pressure head between the connection and the well's bottom hole datum depth

### 5.1.8 Benefits of Reservoir Simulation

1. Compile all data pertinent to a reservoir into one compact database.
2. Provide opportunity to produce the reservoir before commencing
3. Can produce the reservoir several times to examine alternatives.
4. Can be utilized as a management tool for selecting development plan and operational changes
5. Present a common ground between companies and regulatory agencies that deal with petroleum resources.

## 5.2 Objective

Reservoir Stimulation, like material balance calculation, is a form of numerical modeling which is used to quantify and interpret physical phenomena with the ability to extend these to project future performance. The objective of the reservoir stimulation study is to be reservoir management tool. It is use of calculations to predict reservoir performance, forecast recovery, or compare economics of waterflooding. The study of waterflooding performances is made for the following operating scenarios in order to determine the optimum development plan

Case 1 : Producing oil with no injection well.

Case 2 : Producing oil with one injection well, inverting producing well (P1) to injection well.

Case 3 :Producing oil with 2 injection wells.

Case 4 : Producing oil with 4 injection wells.

Case 5 : Producing oil with 4 injection wells in aquifer area.

There are six producing wells in this field which are produced by water drive mechanism and they are on 60-acre spacing. The waterflooding start at above slightly bubble point pressure. The solutions of this study are submitted for reservoir model, with coarse grid and use/ fully implicit procedure runs performance using ECLIPSE 100. The ECLIPSE 100 is defines as black-oil reservoir simulation; which is based on the assumption that the saturated phase properties of two HC phases (oil and gas) depend on pressure only. The limitation of ECLIPSE office is not able to a Fast Restart (LOAD) data set on import and display multi-lateral wells in 2D.

### **5.3 Reservoir Model Characteristic**

The reservoir model is hypothetical model which based on available data of U-Thong field and some of data assumptions. The reservoir model is a three-phase model that has a simple 3-D dimensional model with domal structure, no faults and simple geometry. The reservoir is under-saturated reservoir and it is underlain by small aquifer. Figure 5.3 and Figure 5.4 shows the contoured of top surface and cross-section area. The dimensions of the model are 3,960 feet in long by 3,960 feet in wide by 85 feet in thick. The scale grid is 20x20x8 with uniform size for each of the grid blocks. The reservoir model is described on a regular Cartesian grid and geometry of model is corner point. The small aquifer is defined by analytical model. The oil/water contact is depth of 4,050 feet. The top surface of the model is at 4179.9 feet with initial pressure at this point of 1,800 psia.

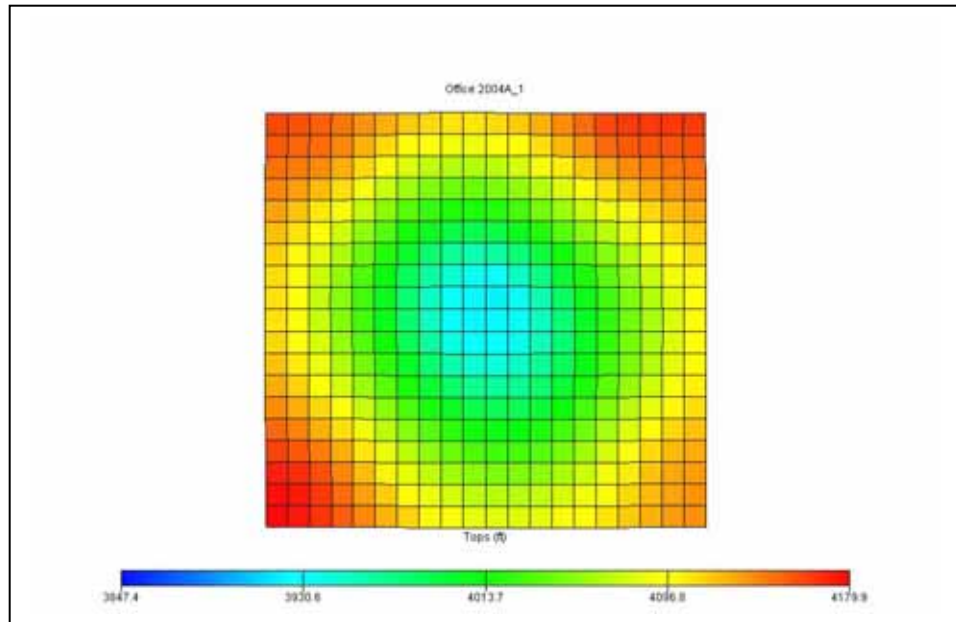


**Figure 5.3** The contour of top surface.

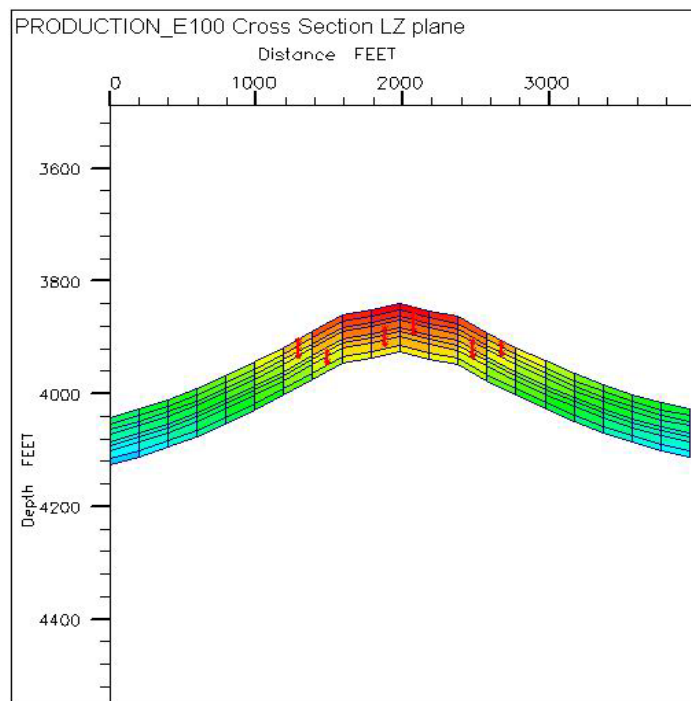


**Figure 5.4** Cross- section area of reservoir model.



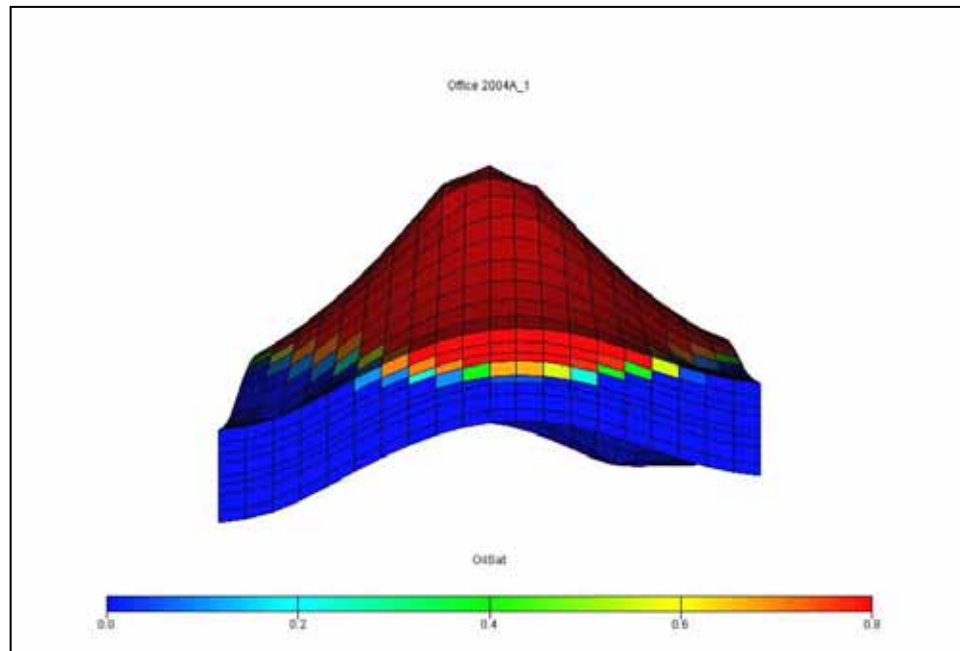


**Figure 5.7** Reservoir Modeling in Front View.

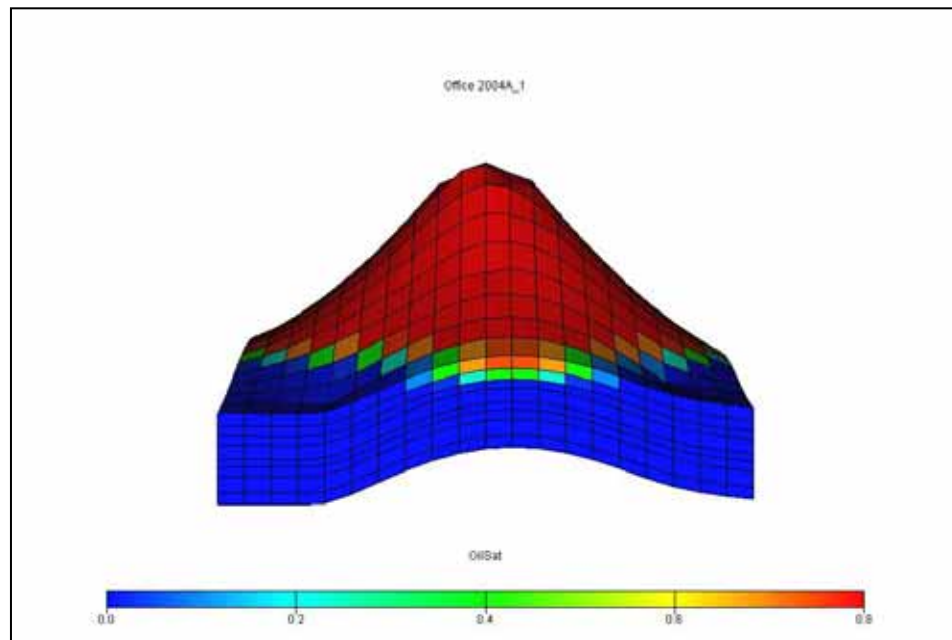


**Figure 5.8** Reservoir Modeling in Back View.

## 5.4 Inputting Data for the Reservoir Modeling.

The data input in the reservoir model are received from available data of U-Thong field data. They are composed of fluid and rock properties such as porosity, permeability, pressure, etc. Some data are not available from U-Thong data so they are assumed for using in the modeling. However, these data are also based on U-Thong field. The data input in the ECLIPSE Office 100 are classified in section of grid, PVT, SCAL, Initialization, and well data.

### 5.4.1 Grid Section Data

The data input in this section, which contains of COORD (Grid Block Coordinate Lines), ZCORN (Grid Block Corner), porosity and permeability distribution, and NTG (Net-to-Gross Ratio). The COORD and ZCORN are described in shaped and geometry of reservoir model. The porosity distributions are generated by Surfer Version 7.0. Using an equation from porosity-permeability scatter program, generate a geo-statistical permeability distribution. This equation is followed as:

$$\text{Log}(k)=0.2023 \times \phi - 2.3475 \quad (5.24)$$

The conclusion of the data in grid section is following:

Average porosity, (%)	19.0
Average permeability in x and y direction, (mD)	60.12
Average permeability in z direction	0.60
Depth of Top Surface, (feet)	3850
Gross Thickness, (feet)	85
Net-to-Gross Ratio	0.4

The porosity and permeability distributions of all layers are shown in Appendix A and Appendix B.



#### 5.4.2 PVT Section Data

This section provides the fluid formation volume factors, viscosities, densities, gas-oil ratio, and rock and water compressibility. PVT data are the results of laboratory analysis of reservoir fluids. This data is required to describe the phase behavior of reservoir fluids at all times and to calculate the density of each phase.

The data input in PVT section is:

Rock Type of reservoir	Consolidated Sandstone
Oil gravity, (API Oil)	33
Gas gravity, (Sg_Air_1)	0.74
Bubble-point pressure, (psi)	300
Referenced pressure, (psi)	1,800
Porosity, (%)	19.0
Salinity, (fraction)	0.01
Fraction of H <sub>2</sub> S	0.17
Fraction of CO <sub>2</sub>	0.06
Fraction of N <sub>2</sub>	0.03
Standard temperature, (°F)	60
Standard pressure, (psi)	14.7

From the input data, ECLIPSE Office provides an extensive set of property correlations that can be used to define PVT section data. Three Tables from PVT correlations are shown in Table 5.1 through 5.3 and plot to view data graphically in Figure 5.9 through 5.10.

**Table 5.1** PVTO (The Oil Properties).

$R_s$ , Mscf/stb	$P_{bub}$ , psia	$B_o$ , rb/stb	$\mu_o$ , cp
0.00116	14.7	1.0573	2.5551
	300	1.0453	2.7309
	466.57	1.0451	2.9009
	692.51	1.045	3.1884
	918.45	1.0449	3.5386
	1144.38	1.0449	3.9527
	1370.32	1.0448	4.4349
	1596.25	1.0448	4.9905
	1800	1.0448	5.5598
	2048.13	1.0448	6.3484
	2274.06	1.0448	7.1655
	2500	1.0448	8.0854
	0.04386	300	1.0752
466.57		1.0698	2.0074
692.51		1.0666	2.0724
918.45		1.065	2.157
1144.38		1.0641	2.2586
1370.32		1.0634	2.3757
1596.25		1.063	2.5076
1800		1.0626	2.6389
2048.13		1.0623	2.8144
2274.06		1.0621	2.9889
2500		1.0619	3.1777

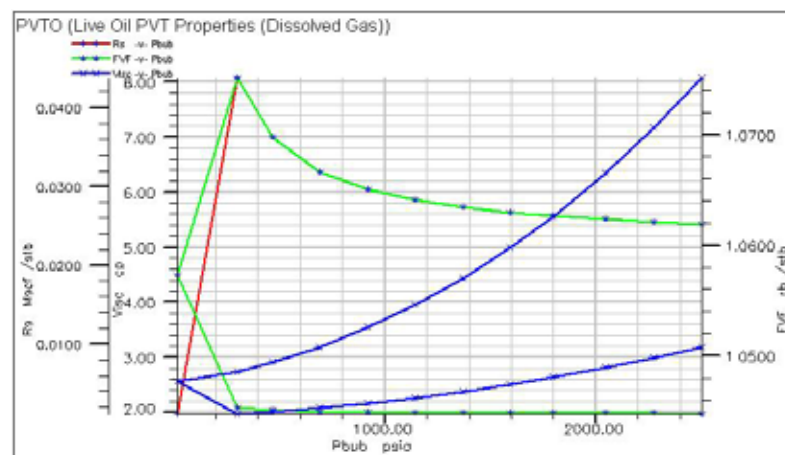


**Figure 5.9** Graph shows relationship of bubble-point pressure, ( $P_{bub}$ ) VS oil formation volume factor, (FVF) and solution gas-oil ratio, ( $R_s$ ).

**Table 5.2** PVDG (The Dry Gas Fluid Property).

Pressure, psi	$B_g$ , rb/Mscf	$\mu_g$ , cp
14.7	218.535	0.01265
300	10.3776	0.01289
466.57	6.555	0.0131
692.51	4.3151	0.01346
918.45	3.1837	0.01389
1144.38	2.5052	0.0144
1370.32	2.0564	0.01498
1596.25	1.7405	0.01564
1800	1.5285	0.01629
2048.13	1.3331	0.01714
2274.06	1.1973	0.01798
2500	1.0904	0.01885

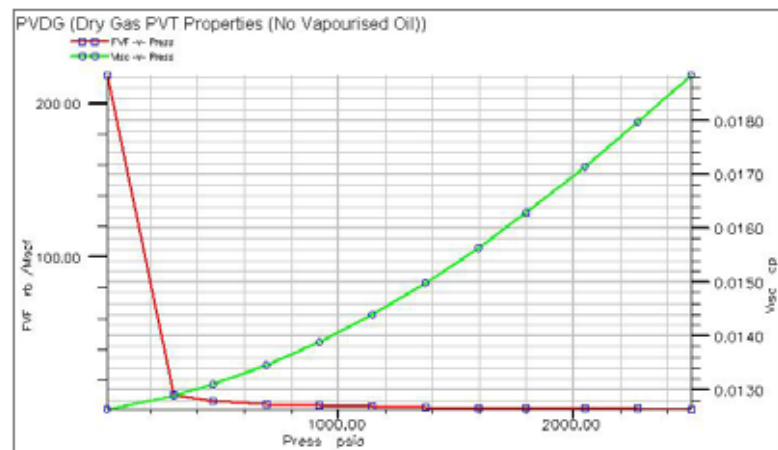


**Figure 5.10** Graph shows relationship of pressure VS gas formation volume factor and gas viscosity.

**Table 5.3** PVTW (The Water properties), Density and Rock properties.

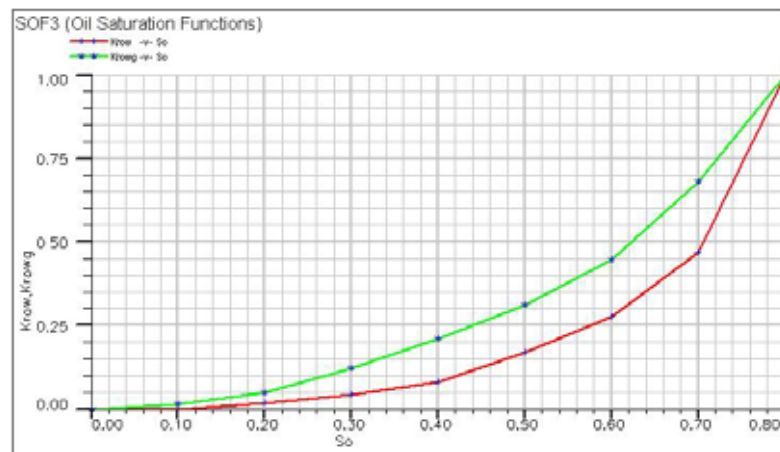
<b>PVTW:</b>	
Pressure References	1800 psi
$B_w$ at $P_{ref}$	1.107 rb/stb
Water compressibility	$3.093 \times 10^{-6} \text{psi}^{-1}$
Water viscosity at $P_{ref}$	0.3499 cp
Water viscosibility	$2.499 \times 10^{-6} \text{psi}^{-1}$
<b>Density:</b>	
Oil density	53.65 lb/ft <sup>-3</sup>
Water density	62.43 lb/ft <sup>-3</sup>
Gas density	0.05 lb/ft <sup>-3</sup>
<b>Rock Properties:</b>	
Pressure References	1800 psi
Rock compressibility	$1.546 \times 10^{-6} \text{psi}^{-1}$

### 5.4.3 SCAL Section Data

The SCAL section refers to the term of rock properties which is sets of input tables of relative permeability versus saturation. Effectively this defines the connate (or irreducible), critical and maximum saturation of each phase supplies information for defining the transition zone and defines the conditions of flow of phases relative to one another. The Table 5.4 and Table 5.5 show fluid saturation and plot to graphically view the saturation versus relative permeability curves in Figure 5.11 through 5.13. From these graph, it shows that the initial water saturation is 0.2 and critical water saturation is 0.3. Whereas the initial gas saturation is 0.04 and critical gas saturation is 0.1.

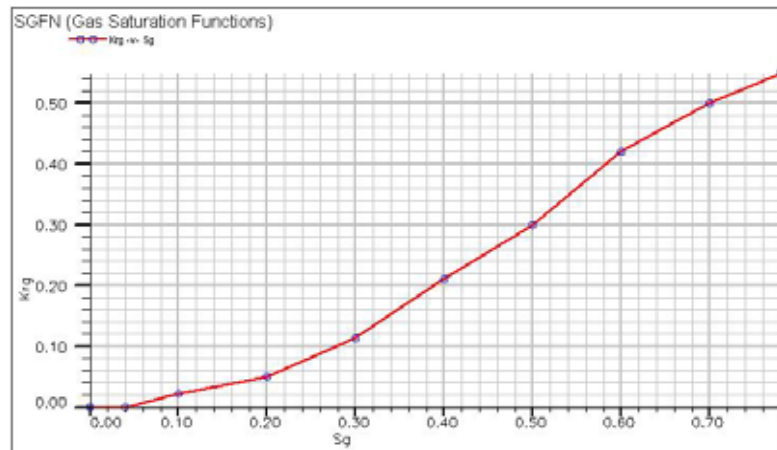
**Table 5.4** SOF<sub>3</sub> (Oil Saturation Function).

$S_o$	$K_{row}$	$K_{rowg}$
0	0	0
0.1	0	0.015
0.2	0.018	0.05
0.3	0.044	0.123
0.4	0.082	0.211
0.5	0.17	0.311
0.6	0.277	0.4449
0.7	0.47	0.68
0.8	1	1

**Figure 5.11** Graph of oil saturation plots with oil-water relative permeability and oil-water-gas relative permeability.

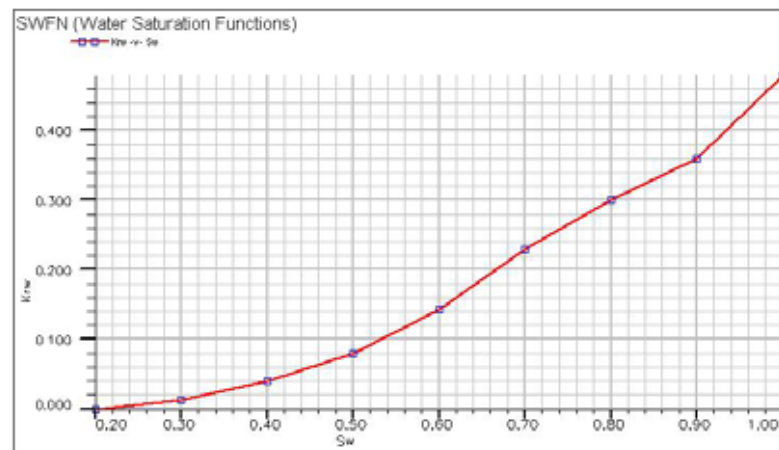
**Table 5.5** SGFN (Gas Saturation Function).

$S_g$	$K_{rg}$
0	0
0.04	0
0.1	0.022
0.2	0.05
0.3	0.113
0.4	0.21
0.5	0.3
0.6	0.42
0.7	0.5
0.78	0.55

**Figure 5.12** Graph of gas saturation plots with gas relative permeability.

**Table 5.6** SWFN (Water Saturation Function).

$S_w$	$K_{rw}$
0.2	0
0.3	0.0126
0.4	0.04
0.5	0.08
0.6	0.1435
0.7	0.23
0.8	0.3
0.9	0.36
1	0.48

**Figure 5.13** Graph of water saturation plots with water relative permeability.



#### 5.4.4 Initialization Section Data

Initialization refers to defining the initial conditions of the simulation. The initial conditions are defined by specifying the OWC (Oil-Water contact) depths and the pressure at a known depth. ECLIPSE uses this information in conjunction with much of the information from previous stages to calculate the initial hydrostatic pressure gradients in each zone of the reservoir model and allocate the initial saturation of each phase in every grid cell prior to production and injection. The data of equilibration is following:

Datum depth, (feet)	3,850
Pressure at datum depth, (psi)	1,800
WOC depth, (feet)	4,050
The bubble-point at datum depth, (psi)	300

The Fetkovich aquifers are defined in this section. The Fetkovich aquifers are based on a pseudo-steady state productivity index and material balance between aquifer pressure and cumulative influx. The flow is modeled by the equations 5.2.

$$\overline{Q}_{ai} = \alpha_i J (P_a - P_i + \rho g (h_i - h_a)) \left[ \frac{1 - \exp(-J\Delta t / C_t V_{w0})}{-J\Delta t / C_t V_{w0}} \right] \quad (5.24)$$

The subscripts a and i denote the aquifer and grid cell I, respectively.

Where $\overline{Q}_{ai}$	=	inflow rate from aquifer to cell i
$J_w$	=	aquifer productivity index
$\alpha_i$	=	area fraction for cell i
$P_a$	=	aquifer pressure at time t
$P_i$	=	cell press at time t

$\rho$	=	aquifer water density
$h_i$ and $h_a$	=	cell depth and aquifer datum depth respectively
$W_{ai}$	=	cumulative influx from aquifer to cell i
$C_t$	=	total aquifer volume
$V_{w0}$	=	initial aquifer volume
$P_{a0}$	=	initial aquifer pressure

#### 5.4.5 Well data

Well data provide well and completion locations, production and injection rates of wells and other data such as skin factors, well radius, and well controls, etc. The well data which use in producing wells and injection wells as following;

Diameter of well bore	0.71	feet
Skin factor	-1	
Effective $K_h$ in producing well	200	mD
Effective $K_h$ in injection well	100	mD

Case 1, there are six producing wells which are produced on 60-acre spacing. The locations of wells are shown in Figure 5.9. Well names are P1, P2...to P6. The oil production rates of six producing wells are 300, 300, 350, 300, 150 and 150 BPD respectively. The well economic of production well does not exceed 0.9 of water cut. These wells are produced oil in upper zones (layer1-4). In this case, there is no water injection and it is produced by nature flow.

Case 2, there is one injection well which is inverting producing well (P1) to injection well (W1). It is shown in Figure 5.11. At starting date, the water

injection rate of well (W1) is 2,000 BPD and it is changed to 1,200 BPD on January 1, 1996.

Case 3, two injection wells are located in the remaining high oil saturation zone. They are shown in Figure 5.12. at starting date, water injection rate in each well (W1 and W2) is 1,000 BPD and it is reduced to 600 BPD on January 1, 1996. Well P4 and P5 are shut April 1998 at water cut about 0.78.

Case 4 and 5, in both cases have four injection wells but they are different locations. They are shown in Figure 5.13 and 5.14. they started injection water at 500 BPD/well and they have changed water injection rate to 300 BPD since January 1, 1996.

All cases of waterflooding were started to inject water on December 17, 1993. The water is injected in lower zones (layer 7-8). Exceptionally, in case 5, water is injected to aquifer (layer 1-8). The well economic of water injection wells limits is minimum rate of 50 BPD.

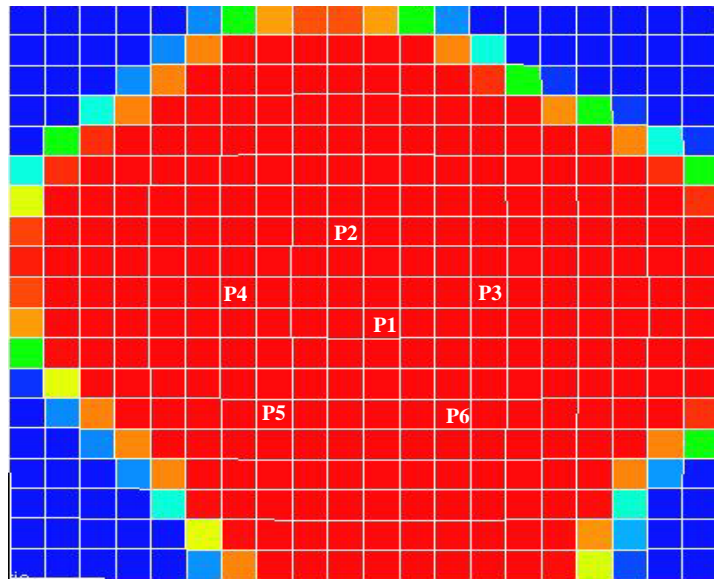


**Figure 5.14** Location of producing wells with no injection well in case 1.

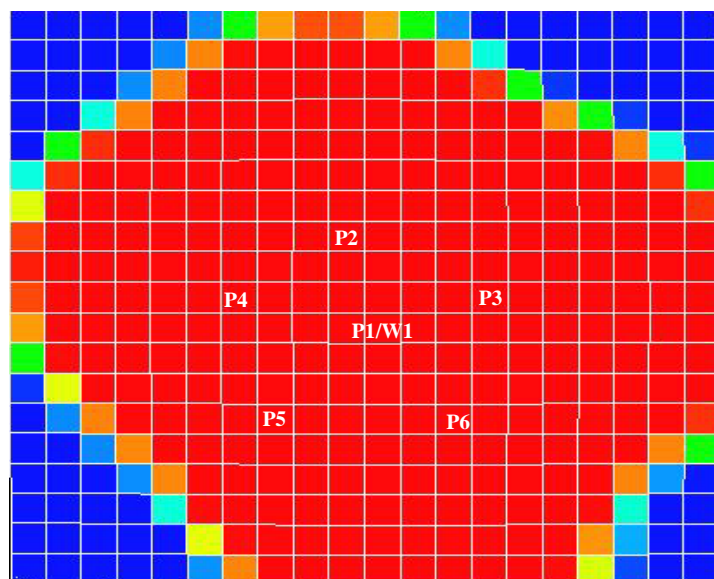


**Figure 5.15** Location of producing wells one injection well which inverting from producing well (P1). in case 2.

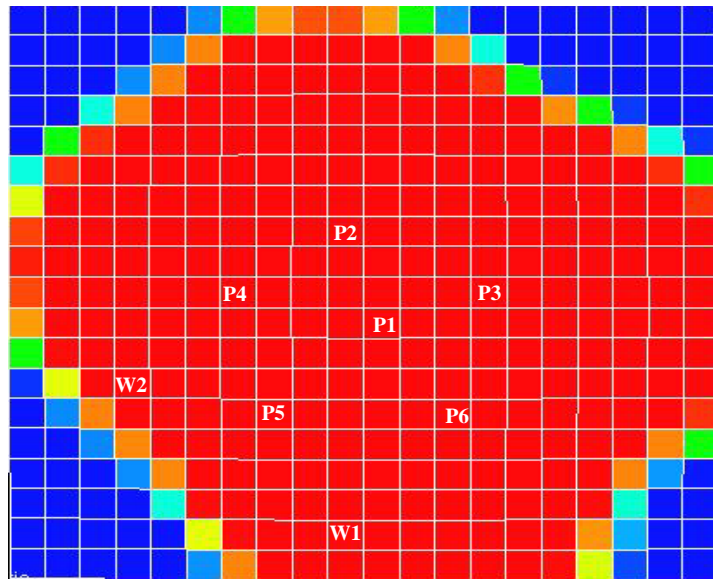


**Figure 5.16** Location of six producing wells and two injection wells in case 3.

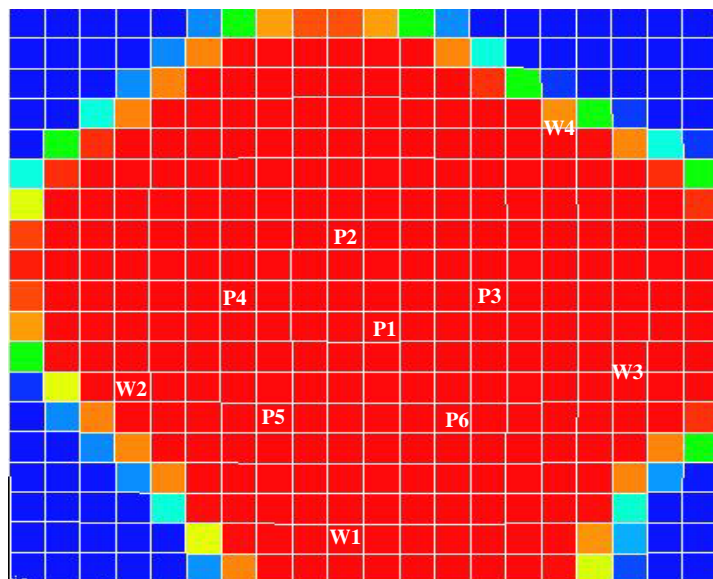


**Figure 5.17** Location of six producing wells and four injection wells in case 4.

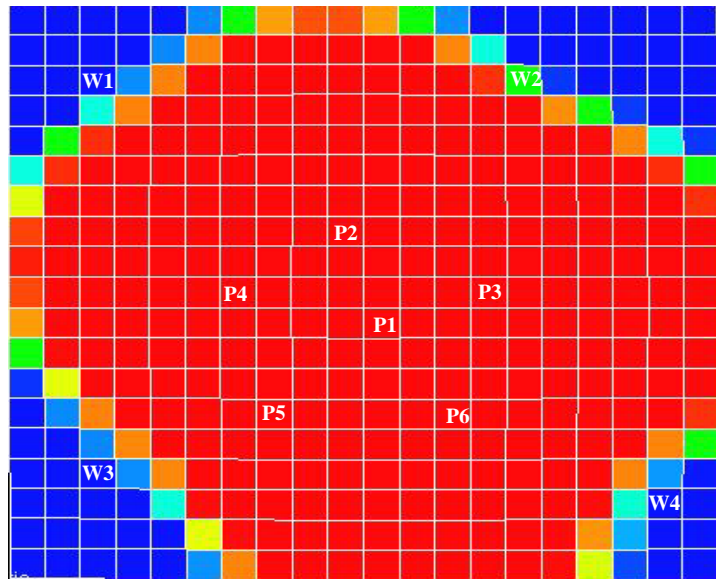


**Figure 5.18** Location of six producing wells and four injection wells in aquifer in case 5.

## **5.5 Results of Reservoir Simulation**

Figure 5.19 represents the field in place. The original oil, gas, and water in place are computed to be 6.98 MMSTB, 300 MCSF, and 9.57 MMSTB respectively. In all cases the primary production is begun in July 1991. The primary recovery before waterflooding is about 10% of OOIP (Original Oil in Place) and oil production is estimated 0.701 MMSTB.

### **5.5.1 Case 1 (No water injection)**

This case has produced oil without water injection. In Figure 5.20 cumulative oil production is estimated about 1.52 MMSTB or about 21.93% of OOIP. Figure 5.22 shows field pressure which declines rapidly. The pressure has been below the bubble point pressure since 1994-2008. As a result, gas-oil ratio is increasing from 0.04 to 0.58 MCSF/STB and gives maximum gas-oil ratio about 1.88 MSCF/STB in well P1. There is no water production in all wells which are shown in figure of well water rate (Figure H-5 through Figure H-10). Figure 5.21 represents ultimate oil recovery which is produced at rate of 30 STB/DAY.

### **5.5.2 Case 2 (One injection well)**

The oil producing well (P1) is inverted to water injection well (W1). As a result, an increase in production of oil about 600 STB/DAY is shown in Figure 5.24 and it has led to an increase in ultimate reserves of 1.119 MMSTB or about 12 %. The ultimate recovery is about 1.92 MMSTB shown in Figure 5.25. In Figure 5.26, the pressure is maintained above bubble-point pressure after it can peak at 1,130 psi so it provides the gas-oil ratios of all producing wells are constant at 0.04 MSCF/STB. On the other hands, well water cut is increased in all wells which show in Figure I-4. Well P2 and P3 provides about 0.95 of maximum water cut. In Figure I-2, the water

production begin in well P2 but it starts to produce in small quantity of water. In well P2 has produced more water rate than other well at maximum rate of 420 STB/DAY. After reaching peak, water rate begins decline and gradually constant at rate 318 STB/DAY of water. Figure D-1 through D-6 shows the distribution of oil saturation. The water breakthrough began in well P2 and P3 in September 1994 after they have produced for three years. Well P5 is the latest well which has water breakthrough in January 2000. In this case, water breakthrough occurs in the early waterflooding. This is because water injection rate is so high at 2,000 BPD and location between producing wells and injection well are closed. Well P2 provides the highest WOR (water-oil ratio) at 16.59 due to it is the nearest producing well with injection well where well P5 provides the lowest WOR at 5.58. However, average WOR of the field is 9.43. From frontal advanced analysis, it can calculate the displacement and areal sweep efficiency about 0.34 and 0.55 respectively.

### **5.5.3 Case 3 (Two injection wells)**

Two water injection wells are drilled in remaining higher saturation. It is observed from 3D of oil saturation model. The ultimate oil recovery is estimated about 3.10 MMSTB or about 44.68% of OOIP. It is shown in Figure 5.28. After waterflooding, the oil production is increased from 0.701 to 3.10 MMSTB. The oil production rate increases from 457 to 1,260 STB/DAY in 1995. After reaching a peak in 1995, the oil production rate again begin decline. Figure 5.30 is shown the pressure in this field is still above the bubble point pressure although the oil production is declined. The well water cut of all wells are over 0.75. The maximum water cut is 0.94 of well P4 and minimum water cut is 0.775 of well P3. These are shown in Figure J-4. In Figure E-3, it shows that water saturation begins to increase



in well P4 and P5 to 0.345 and 0.395 respectively in 1996. Well P4 and P5 are shut at 0.78 of water cut in April 1998 due to high WOR. As a result, it can increase oil production about 1.15 MSTB and also decrease water production about 155.10 MSTB. The well P6 is the first well to have water breakthrough in July 1999. Whereas well P3 is the latest well this is occurred water breakthrough in January 2003. This well is slower breakthrough than other wells due to it is far from injection wells. In this case, well P6 provides the maximum of WOR at 10.01 due to water breakthrough occurs quicker than other wells. On the other hands, well P3 also provides the minimum of WOR at 4.89. Average WOR of this case is about 7.66 at the end of the production.

#### **5.5.4 Case 4 (Four injection wells)**

Well W3 and W4 are infilled drilling additionally in case 3. In Figure 5.32, the ultimate oil recovery is estimated about 3.20 MMSTB or about 46.10% of OOIP at rate 150 STB/DAY of oil. An increase oil recovery from primary production is 2.5 MMSTB or 36.10%. In Figure 5.34, the pressure is increased from 305.5 to 1,415 psi after waterflooding. The oil production rate can peak at 1,270 STB/DAY and then it again begins to decline about 140 STB/DAY. In this case, the water cut of all wells are close to values which are over 0.85. In Figure F-3, it shows that well P3 and P4 begin to change of water saturation from initial value ( $S_{wi} = 20\%$ ) to 0.307 and 0.315 respectively. But other wells are still not changed in this time. However, well P4 begin breakthrough firstly in January 1999 and well P3 and P5 occurs water breakthrough in April 1999. Maximum of WOR is about 9.15 in well P5 and minimum of WOR is about 6.23 in well P2. From the frontal advanced analysis, it

can be calculated the displacement and areal sweep efficiency of 0.60 and 0.56 respectively.

#### **5.5.5 Case 5 (Four injection wells in aquifer)**

In case 5, four wells are drilled in location of aquifer. The ultimate oil recovery is 3.23 MMSTB or 46.55% of OOIP shown in Figure 5.36. The oil recovery factor is increased to 36.55% from primary production. In Figure 5.37, the oil production rate can peak at 1,285 STB/DAY in 1994 after water injection and it declines to about 150 STB/DAY in 2008. Well P5 gives maximum water cut of 0.95 but well P1 gives the minimum water cut of 0.87. This is shown in Figure L-4. Well P2 is produced water about at 110 STB/DAY in 1996 and it also provides the maximum water rate is at 205 STB/DAY at the end of production life. The cumulative water production in Figure 5.6 is estimated 4.22 MMSTB. In Figure G-3, it shows that the water saturation has been changed in well P3 and P5 since 1996. The first well has occurred water breakthrough is well P5 in May 1998. The well P1 is the latest well which water breakthrough has occurred since July 2003. Well P5 provides the maximum of WOR at 11.03 due to water breakthrough occurs earlier than other wells, whereas well P1 provides the minimum of WOR about 5.02. In this case, the displacement and areal sweep efficiency are estimated at 0.57 and 0.59 respectively.

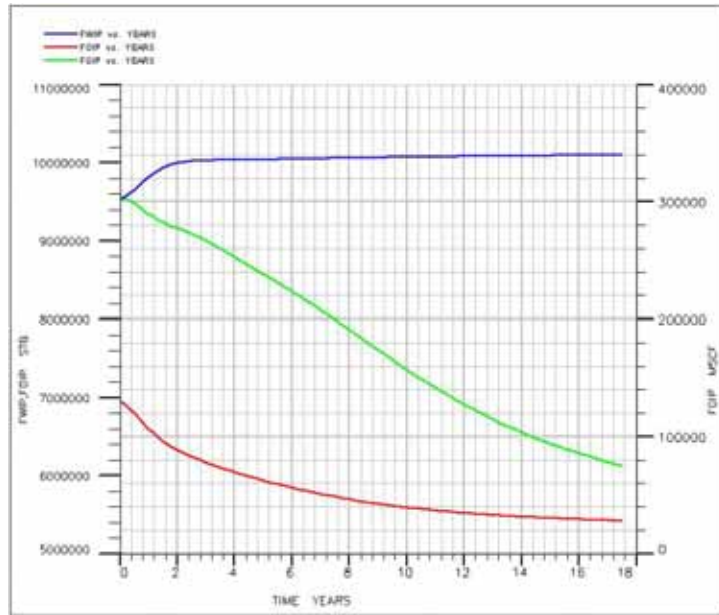


**Figure 5.19** Oil, Gas, and Water In Place versus Time.

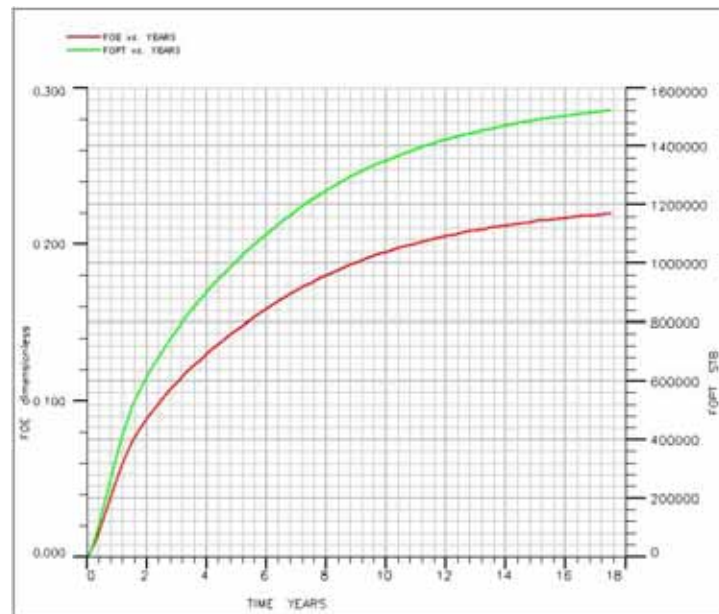


**Figure 5.20** Oil Recovery Factor and Cumulative Oil Production versus Time, (Case 1).

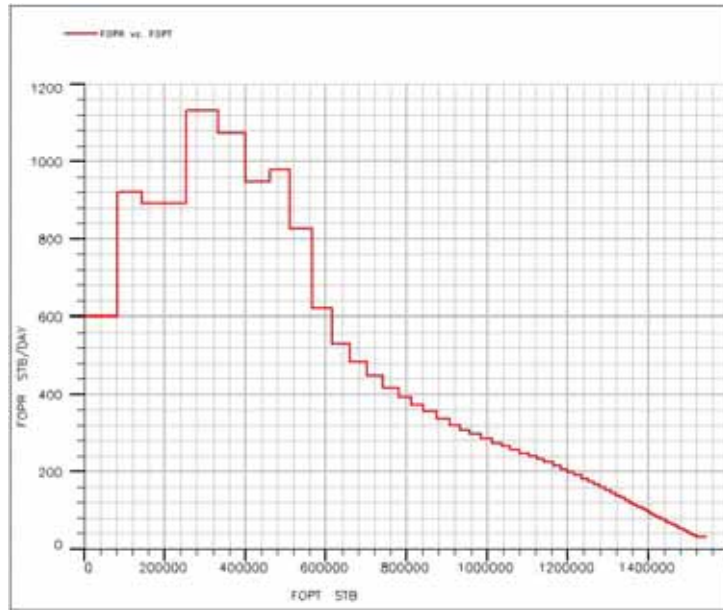


**Figure 5.21** Oil Production Rate versus Cumulative Oil Production, (Case 1).

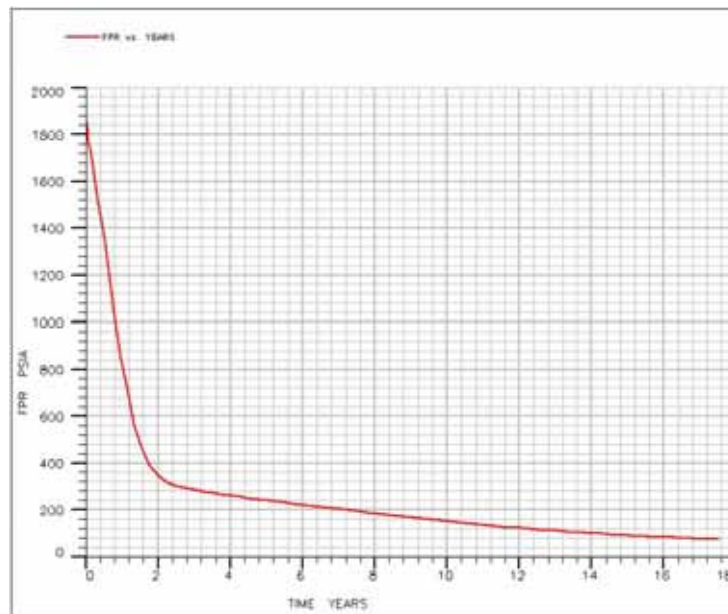


**Figure 5.22** Field Pressure versus Time, (Case 1).

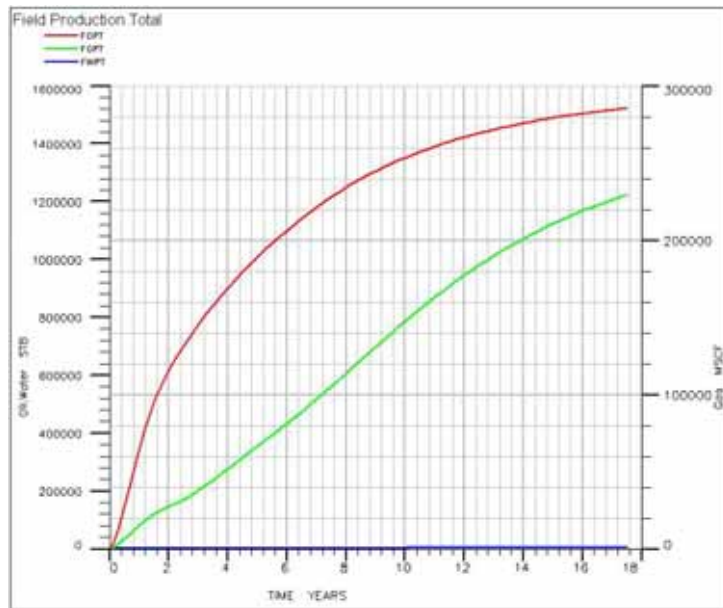


**Figure 5.23** Cumulative Oil, Gas, and Water Production versus Time, (Case 1).

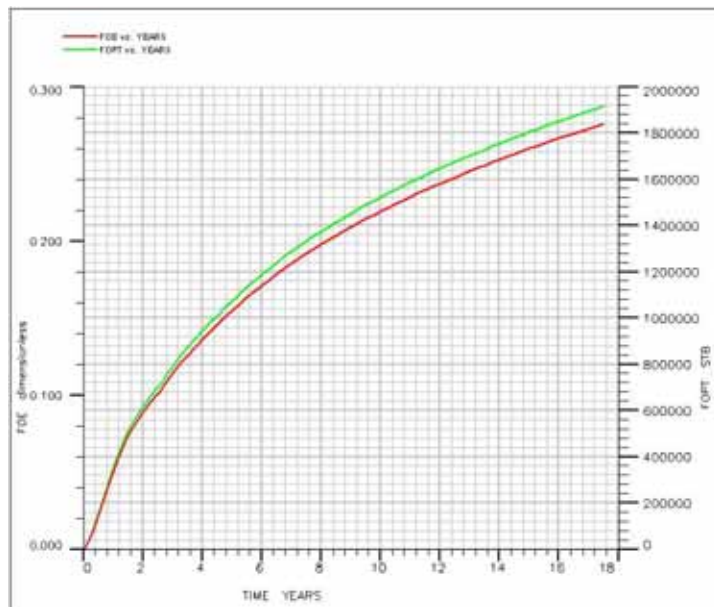


**Figure 5.24** Oil Recovery Factor and Cumulative Oil Production versus Time, (Case 2).

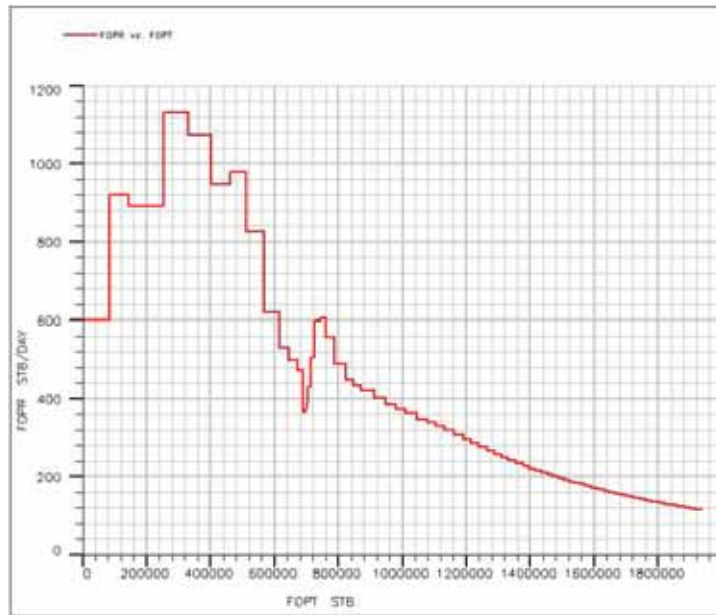


**Figure 5.25** Oil Production Rate versus Cumulative Oil Production, (Case 2).

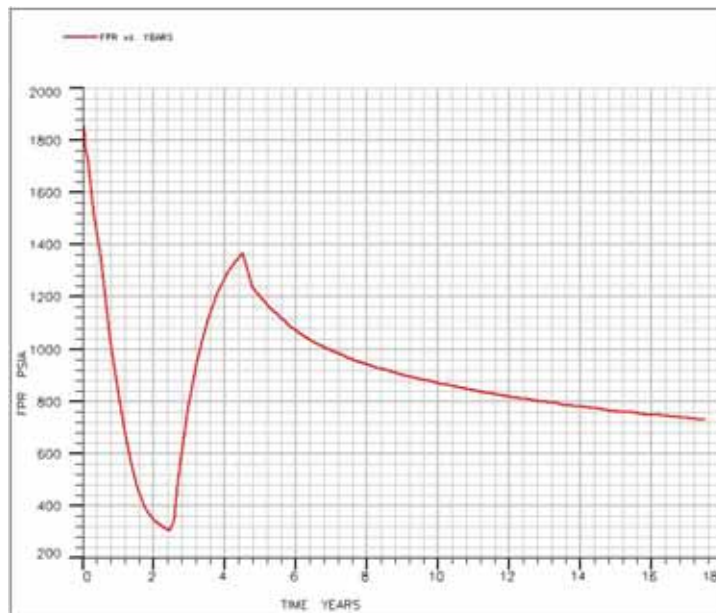


**Figure 5.26** Field Pressure versus Time, (Case 2).

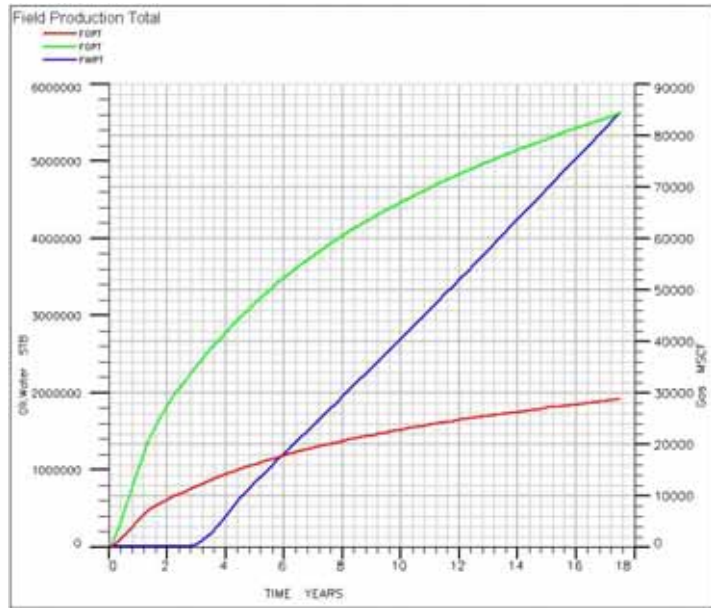


**Figure 5.27** Cumulative Oil, Gas, and Water Production versus Time, (Case 2).

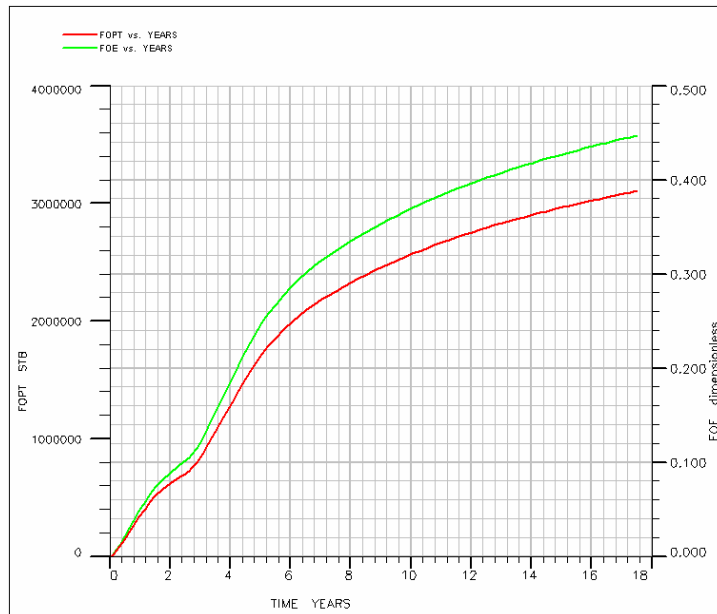


**Figure 5.28** Oil Recovery Factor and Cumulative Oil Production versus Time, (Case 3).

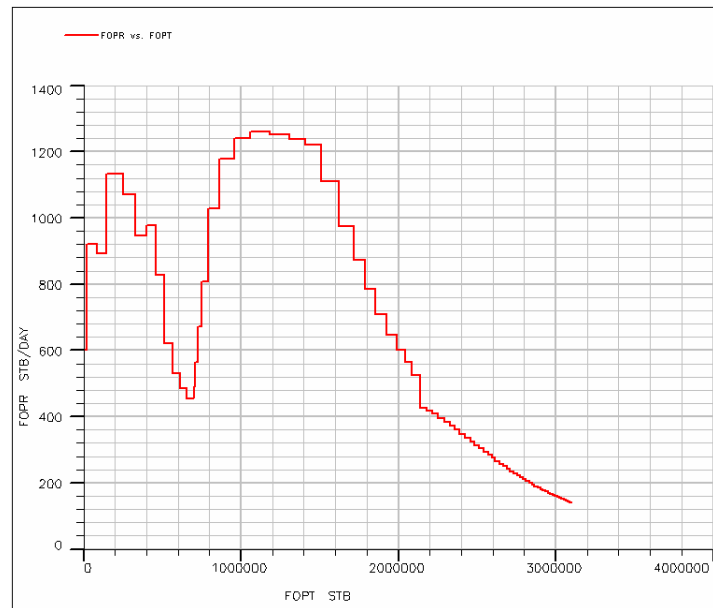


**Figure 5.29** Oil Production Rate versus Cumulative Oil Production, (Case 3).

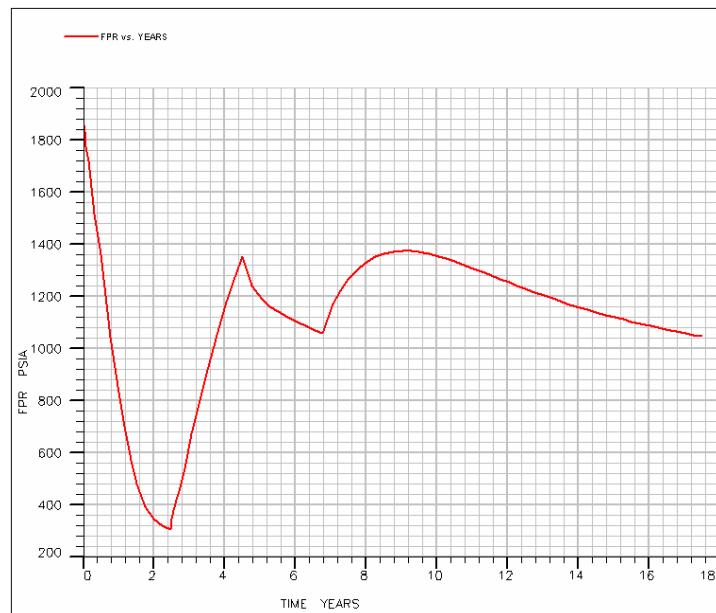


**Figure 5.30** Field Pressure versus Time, (Case 3).



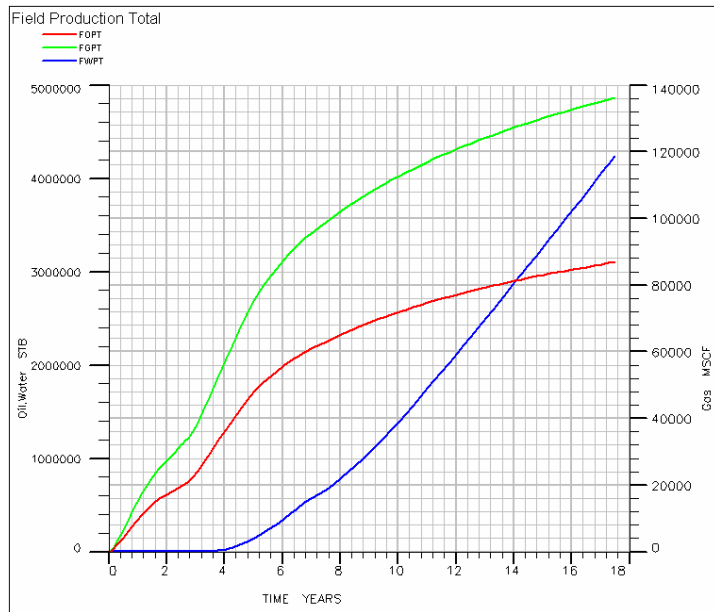


**Figure 5.31** Cumulative Oil, Gas, and Water Production versus Time, (Case 3).

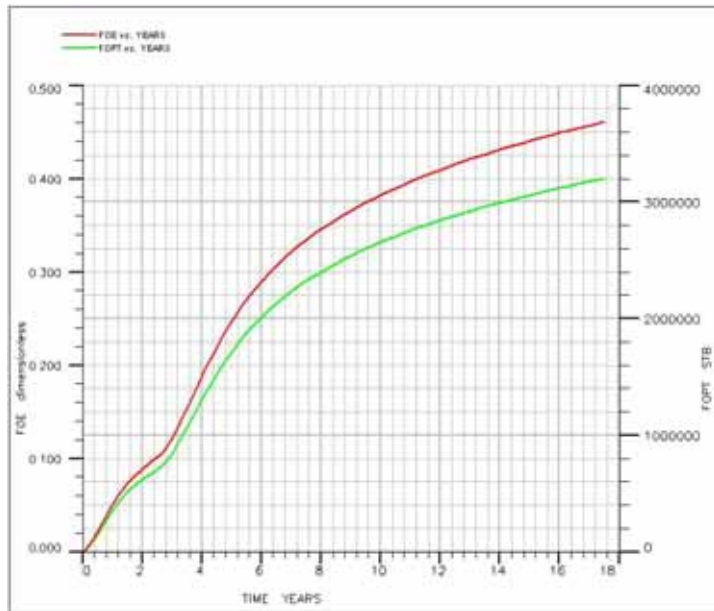


**Figure 5.32** Oil Recovery Factor and Cumulative Oil Production versus Time, (Case 4).

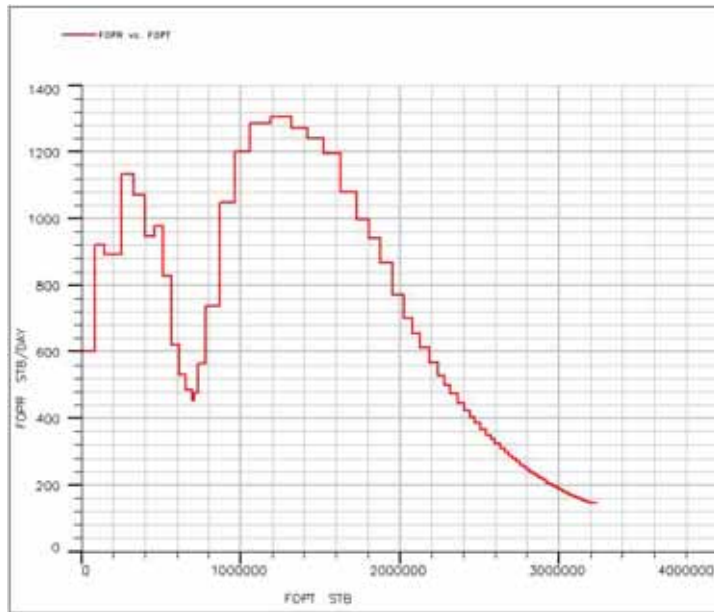


**Figure 5.33** Oil Production Rate versus Cumulative Oil Production, (Case 4).

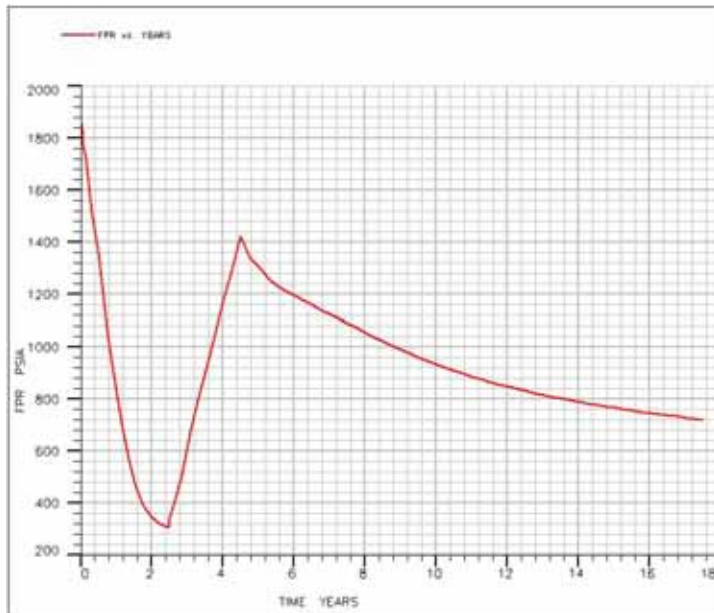


**Figure 5.34** Cumulative Oil, Gas, and Water Production versus Time, (Case 4).

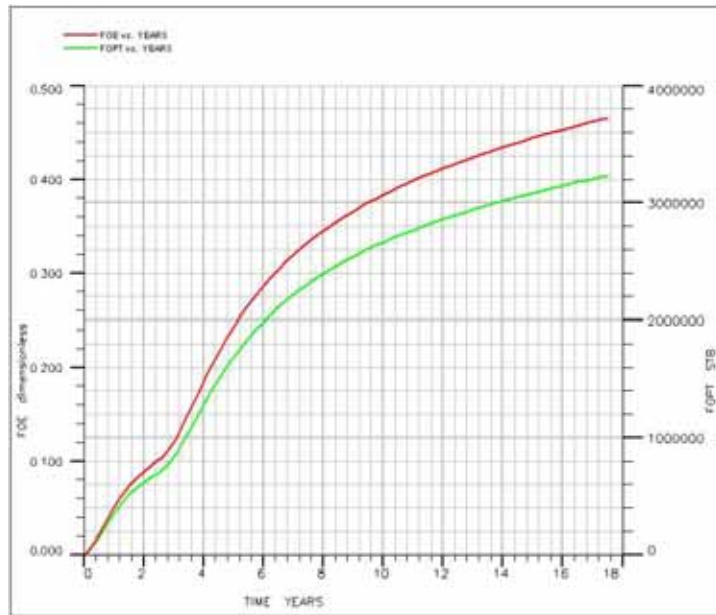


**Figure 5.35** Oil Recovery Factor and Cumulative Oil Production versus Time, (Case 5).

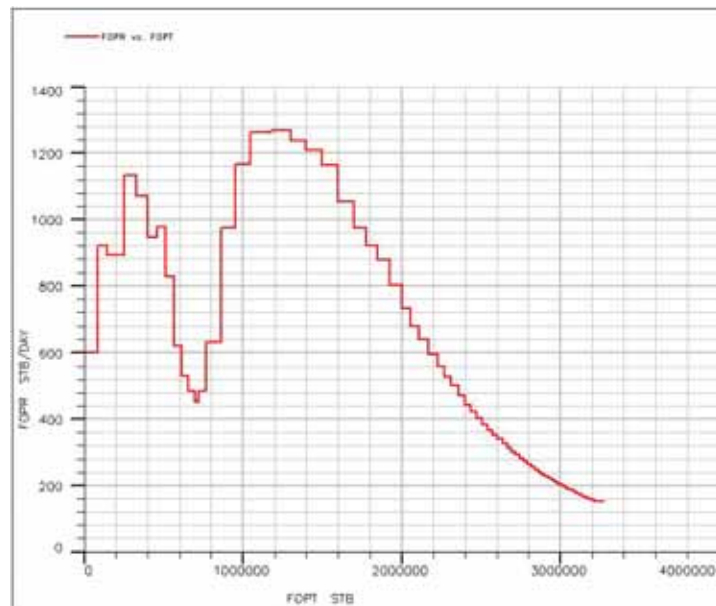


**Figure 5.36** Oil Production Rate versus Cumulative Oil Production, (Case 5).

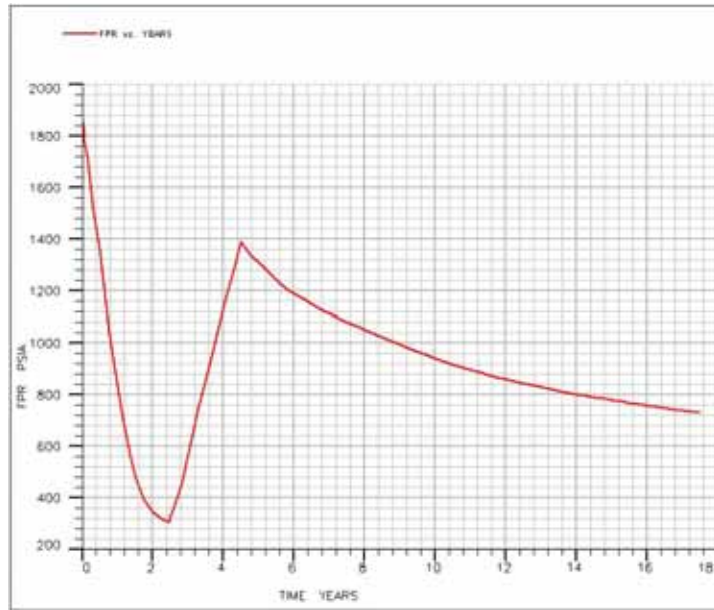


**Figure 5.37** Field Pressure versus Time, (Case 5).

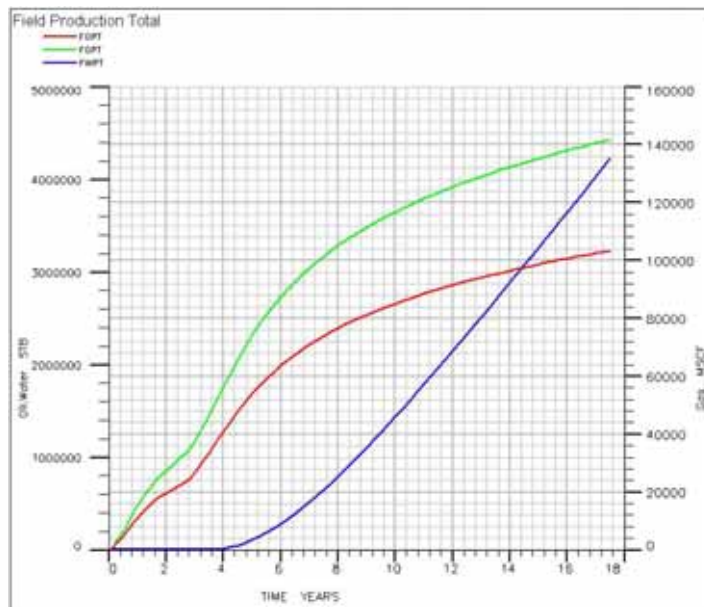


**Figure 5.38** Cumulative Oil, Gas, and Water Production versus Time, (Case 5).

**Table 5.7** Summarizes of the results of simulation at the end of production life in five cases.

Case	FOPT, MSTB	FWPT, MSTB	FGPT, MMSCF	FWCT, %	FOE, %	Increased FOE from primary production, %
1	1522.91	0.4807	229.51	0.9	21.93	11.93
2	1915.8	5635.25	84.26	90.4	27.59	17.59
3	3102.31	4395.88	136.09	88.4	44.68	34.68
4	3201.21	4275.97	140.42	88.1	46.10	36.10
5	3232.24	4223.96	141.78	87.7	46.55	36.55

**Note** Case 1 has no water injection.

## 5.6 Frontal Advanced Analysis

Using the oil-water relative permeability data are shown in Table 5.4 and Table 5.6, calculated fractional flow by equation 4.25. Whereas  $f'_w$  are calculated by following equation

$$f'_w = b(f_w^2 - f_w) \quad (5.25)$$

$$b = \frac{\ln \left( \frac{\left( \frac{K_{ro}}{K_{rw}} \right)_2}{\left( \frac{K_{ro}}{K_{rw}} \right)_1} \right)}{S_{w2} - S_{w1}} \quad (5.26)$$

Values of  $f_w$  and  $f'_w$  computed at water saturation increments of 0.1 are represented in Table 5.8 Graph of  $f_w$  versus water saturation are represented in Figure 5.40. A tangent drawn in Figure 5.40 from  $S_{wi} = 0.2$  intersect the fractional flow curve at  $S_w = 0.45$ .

$\overline{S_{w5}}$  is calculated by selecting of  $S_{w2} = 0.55$  and determine  $f_{w2} = 0.87$ ,  $f'_{w2} = 1.37$ , and  $Q_i = 1.73$ . These values are substituting into equation 5.26;

$$\overline{S_{w5}} = S_{w2} + Q_i f'_{o2} \quad (5.27)$$

The areal sweep efficiency can be calculated by

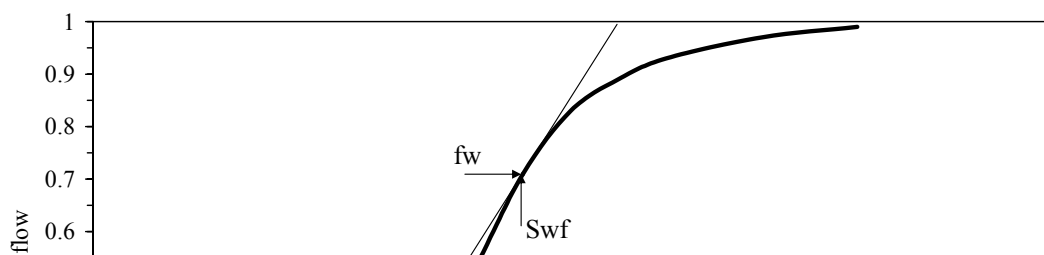
$$E_A = \frac{N_p}{(\overline{S_{w5}} - S_{wi})V_p} \quad (5.28)$$

And the displacement efficiency can be also calculated by

$$E_D = \frac{\frac{S_{oi}}{B_{oi}} - \frac{S_{or}}{B_{or}}}{\frac{S_{oi}}{B_{oi}}} \quad (5.29)$$

**Table 5.8** Relative Permeability and Fractional Flows.

$S_w$	$K_{ro}$	$K_{rw}$	$f_w$	$f'_w$
0.2	1	0	0	0
0.3	0.47	0.013	0.17	1.97
0.4	0.277	0.04	0.53	3.47
0.5	0.17	0.08	0.78	2.39
0.6	0.082	0.144	0.93	0.91
0.7	0.044	0.23	0.97	0.405
0.8	0.018	0.30	0.99	0.14
0.9	0	0.36	0	0



The overall waterflood recovery efficiency is given by .



$$E_R = E_D \times E_v \quad (5.30)$$

Where , the volumetric efficiency,  $E_v$  is assumed that 0.70.

Water-oil ratio (WOR) is a measure of the efficiency of the displacement at a point in the process. In production operations, it represents the volume of water that must be handled to produce a unit volume of oil. Equation 5.29 defines the WOR;

$$WOR = \frac{q_w}{q_o} \quad (5.31)$$

The mobility ratio is about 0.206 that it is calculated by

$$\text{Mobility Ratio} = \frac{\mu_o}{\mu_w} \cdot \frac{K_{rw}}{K_{ro}} \quad (5.32)$$

The values of  $E_D$ ,  $E_A$ ,  $E_R$ , and WOR in each case are shown in Table 5.9 and values of WORs of each wells are shown in Table 5.10.

**Table 5.9** The calculated resulted from frontal advanced analysis.

	$E_A$ , (fraction)	$E_D$ , (fraction)	$E_R$ from Frontal Advance, (fraction)	$E_R$ from Reservoir Simulation, (fraction)	WOR
Case 2	0.34	0.55	0.385	0.275	9.43
Case 3	0.55	0.58	0.406	0.446	7.66
Case 4	0.56	0.60	0.420	0.461	7.38
Case 5	0.57	0.59	0.413	0.465	7.10

**Table 5.10** The WORs at the end of the production life.

	Case 2	Case 3	Case 4	Case 5
P1	-	9.81	6.75	5.02
P2	16.59	6.00	6.23	8.23
P3	15.67	4.89	7.57	6.61
P4	6.18	-	7.39	7.87
P5	5.58	-	9.15	11.03
P6	8.95	10.01	7.96	6.19

# CHAPTER VI

## ECONOMIC EVALUATION

### 6.1 Objective

The objective of this study is to use economic evaluation to provide the answer to making the best case decision to maximize profits. The five cases are analyzed to determine the potentially most economically viable development plan.

### 6.2 Assumption of Economic Study

The data required for economic study can be generally classified as production, injection, investment and operating costs, financial, and economic data. In this economic study use 7.25 percent of discount rate of money, oil price is at 40 \$/bbl, and income tax is 50 percent of revenue. The Table 6.1 summarized the economic parameters which is used to evaluation economic decision. Assumption data of Capital investment and operational costs are used in economic evaluation as following data:

Drilling and completion production well	1,000,000 \$/well
Drilling and completion injection well	850,000 \$/well
Facility costs of injection well	200,000 \$/well
Facility costs of production well	350,000\$/well
Abandonment cost	12,000 \$/well

**Table 6.1** Economic parameters.

	<b>Case 1</b>	<b>Case 2</b>	<b>Case 3</b>	<b>Case 4</b>	<b>Case 5</b>
<b>Capital Investment Cost</b>					
Number of Production wells, (well)	6	6	6	6	6
Number of Injection wells, (well)	0	1	2	4	4
Drilling and completion costs of production well, (MM\$)	6.0	6.0	6.0	6.0	6.0
Drilling and completion costs of injection well, (MM\$)	0	1	1.7	3.4	3.4
Facility cost of production well, (MM\$)	2.1	2.1	2.1	2.1	2.1
Facility cost of injection well, (MM\$)	0.0	0.2	0.4	0.8	0.8
Abandonment cost, (MM\$)	0.072	0.072	0.096	0.12	0.12
Capital Investment, (MM\$)	8.172	8.372	10.296	12.42	12.42
<b>Annual operating costs</b>					
Production wells, (\$/BBL)	12.0	12.0	12.0	12.0	12.0
Injection wells, (MM\$)	0.0	0.1	0.2	0.5	0.5

Operational costs of Production well	12 \$/bbl
Operational cost of Injection well	120,000 \$/well

### 6.3 Calculation of Cash Flow

The tables of cash flow in each case are shown in Table 6.3 to 6.7. These tables of cash flow are estimated by using Microsoft excel. The details of table are described as following:

Column	Detail
A	= Production Date
B	= Oil Production per year (MSTB/Year)
C	= Oil Price (US\$/BBL) constant over the contact
D	= Oil revenue sale income (MM\$)
	= $(B * C) / 1000$
E	= Production tax = 50% of Oil Revenue
F	= Capital investment (MM\$), from Table 6.1
G	= Discount factor @ 7.25 %
H	= Discounted capital investment (MM\$)
	= $F * G$
I	= Production operating cost (MM\$)
	= $(B * 12) / 1000$
J	= Injection operating cost (MM\$), from Table 6.1
K	= Total operating cost (MM\$) = (I+J)
L	= Total cost (MM\$)
	= $E + F + K$

M	=	Undiscounted cash flow (MM\$)	=	(D-L)
N	=	Discounted cash flow @ 7.25% (MM\$)		
O	=	Cumulative discounted cash flow @ 7.25 % (MM\$)		

### **6.3.1 Payout Time**

The time needed to recover the investment is defined as the payout time. It is the time when the undiscounted or discounted cash flow (CF = revenue-capital investment-operating expenses) is equal to zero.

### **6.3.2 Profit to Investment Ratio (PIR)**

Profit to investment ratio is the total undiscounted cash flow without capital investment divided by the total investment. Unlike the payout time, it reflects total profitability; however, it does not recognize the time value of money.

### **6.3.3 Present Worth Net Profit**

Present worth net profit is the present value if the entire cash flow discounted at a specified discount rate.

### **6.3.4 Internal Rate of Return (IRR)**

Internal rate of return is the maximum discount rate which needs to be charged for the investment capital to produce a break even venture, i.e., the discount rate at which the present worth net profit is equal to zero. This can be also expressed as the discount rate at which the total discounted cash flow excluding investments is equal to the discounted in investments over the life of the project.

## 6.4 Results of Economic Evaluation

Tables 6.2 through Table 6.6 show the results of cash flow analysis for the five cases. Note that the royalty are not taken into account. This table contains of internal rate of return (IRR), profit to investment ratio (PIR), payout time, and present worth net profits. These values are variable to make economic decision. In case 3, payout time is 5.9 which provides the least time. So investment in this case will return in a shorter time than other cases. Additionally in case 3 also gives the highest value of IRR and PIR about 17.0% and 0.44 respectively. Present worth net profits are 0.818, 2.474, 4.234, 0.958, and 1.017 respectively. Whereas the smallest values are 10.30% and 0.11 respectively which are represent in case 1. Present worth net profits of all cases are positive. It represents that investment should be made operation. From the all variable economic data are shown in Table 6.7. It can indicate that case 3 gives the most economically viable project. Due to it can provide better value than other cases such as IRR, PIR and payout time etc.



**Table 6.2** Economic Evaluation of Case 1.

<b>A</b>	<b>B</b>	<b>C</b>	<b>D</b>	<b>E</b>	<b>F</b>	<b>G</b>	<b>H</b>
Date	Oil Production (MSTB)	Oil Price (MM\$)	Total Revenue (MM\$)	Producing Tax (MM\$)	Capital Investment (MM\$)	Discounted Factor@ 7.25%	Discounted Capital Investment (MM\$)
1/7/1991	0.000	40.00	0.000	0.000	8.100	0.932	7.552
1/7/1992	343.674	40.00	13.747	6.873		0.869	
1/7/1993	272.350	40.00	10.894	5.447		0.811	
1/7/1994	158.903	40.00	6.356	3.178		0.756	
1/7/1995	126.822	40.00	5.073	2.536		0.705	
1/7/1996	106.735	40.00	4.269	2.135		0.657	
1/7/1997	92.156	40.00	3.686	1.843		0.613	
1/7/1998	80.038	40.00	3.202	1.601		0.571	
1/7/1999	68.036	40.00	2.721	1.361		0.533	
1/7/2000	56.850	40.00	2.274	1.137		0.497	
1/7/2001	46.821	40.00	1.873	0.936		0.463	
1/7/2002	38.613	40.00	1.545	0.772		0.432	
1/7/2003	31.901	40.00	1.276	0.638		0.403	
1/7/2004	26.485	40.00	1.059	0.530		0.375	
1/7/2005	21.905	40.00	0.876	0.438		0.350	
1/7/2006	18.222	40.00	0.729	0.364		0.326	
1/7/2007	15.214	40.00	0.609	0.304		0.304	
1/7/2008	12.796	40.00	0.512	0.256	0.072	0.284	0.020
<b>Total</b>			60.701	30.350	8.172		7.573

**Table 6.2** Economic Evaluation of Case 1 (Continued).

<b>A</b>	<b>I</b>	<b>J</b>	<b>K</b>	<b>L</b>	<b>M</b>	<b>N</b>	<b>O</b>
Date	Production Operation Cost (MM\$)	Injection Operation Cost (MM\$)	Total operation Cost (MM\$)	Total Cost (MM\$)	Undiscounted Cash Flow (MM\$)	Discounted Cash Flow (MM\$)	Cumulative Discounted Cash Flow @ 7.25% (MM\$)
1/7/1991	0.000	0.000	0.000	8.100	-8.100	-7.552	-7.552
1/7/1992	4.124	0.000	4.124	10.99	2.749	2.390	-5.162
1/7/1993	3.268	0.000	3.268	8.715	2.179	1.766	-3.396
1/7/1994	1.907	0.000	1.907	5.085	1.271	0.961	-2.435
1/7/1995	1.522	0.000	1.522	4.058	1.015	0.715	-1.720
1/7/1996	1.281	0.000	1.281	3.416	0.854	0.561	-1.159
1/7/1997	1.106	0.000	1.106	2.949	0.737	0.452	-0.708
1/7/1998	0.960	0.000	0.960	2.561	0.640	0.366	-0.342
1/7/1999	0.816	0.000	0.816	2.177	0.544	0.290	-0.052
1/7/2000	0.682	0.000	0.682	1.819	0.455	0.226	0.174
1/7/2001	0.562	0.000	0.562	1.498	0.375	0.173	0.347
1/7/2002	0.463	0.000	0.463	1.236	0.309	0.133	0.481
1/7/2003	0.383	0.000	0.383	1.021	0.255	0.103	0.584
1/7/2004	0.318	0.000	0.318	0.848	0.212	0.080	0.663
1/7/2005	0.263	0.000	0.263	0.701	0.175	0.061	0.724
1/7/2006	0.219	0.000	0.219	0.583	0.146	0.048	0.772
1/7/2007	0.183	0.000	0.183	0.487	0.122	0.037	0.809
1/7/2008	0.154	0.000	0.154	0.481	0.030	0.009	0.818
<b>Total</b>	18.210		18.210	56.73	IRR=10.3%	0.818	

**Table 6.3** Economic Evaluation of Case 2.

<b>A</b>	<b>B</b>	<b>C</b>	<b>D</b>	<b>E</b>	<b>F</b>	<b>G</b>	<b>H</b>
Date	Oil Production (MSTB)	Oil Price (MM\$)	Total Revenue (MM\$)	Producing Tax (MM\$)	Capital Investment (MM\$)	Discounted Factor@ 7.25%	Discounted Capital Investment (MM\$)
1/7/1991	0.000	40.00	0.000	0.000	8.300	0.932	7.739
1/7/1992	343.674	40.00	13.747	6.873		0.869	
1/7/1993	272.364	40.00	10.895	5.447		0.811	
1/7/1994	175.665	40.00	7.027	3.513		0.756	
1/7/1995	151.101	40.00	6.044	3.022		0.705	
1/7/1996	130.122	40.00	5.205	2.602		0.657	
1/7/1997	114.365	40.00	4.575	2.287		0.613	
1/7/1998	99.114	40.00	3.965	1.982		0.571	
1/7/1999	86.927	40.00	3.477	1.739		0.533	
1/7/2000	77.903	40.00	3.116	1.558		0.497	
1/7/2001	70.618	40.00	2.825	1.412		0.463	
1/7/2002	64.851	40.00	2.594	1.297		0.432	
1/7/2003	59.966	40.00	2.399	1.199		0.403	
1/7/2004	55.962	40.00	2.238	1.119		0.375	
1/7/2005	52.229	40.00	2.089	1.045		0.350	
1/7/2006	49.162	40.00	1.966	0.983		0.326	
1/7/2007	46.487	40.00	1.859	0.930		0.304	
1/7/2008	44.262	40.00	1.770	0.885	0.072	0.284	0.020
<b>Total</b>	1894.771		75.791	41.685	8.372		7.759

**Table 6.3** Economic Evaluation of Case 2 (continued).

<b>A</b>	<b>I</b>	<b>J</b>	<b>K</b>	<b>L</b>	<b>M</b>	<b>N</b>	<b>O</b>
Date	Production Operation Cost (MM\$)	Injection Operation Cost (MM\$)	Total operation Cost (MM\$)	Total Cost (MM\$)	Undiscounted Cash Flow (MM\$)	Discounted Cash Flow (MM\$)	Cumulative Discounted Cash Flow @ 7.25% (MM\$)
1/7/1991	0.000	0.00	0.000	8.30	-8.300	-7.739	-8.075
1/7/1992	4.124	0.00	4.124	10.998	2.749	2.390	-5.684
1/7/1993	3.268	0.00	3.268	8.716	2.179	1.766	-3.918
1/7/1994	2.108	0.12	2.228	5.741	1.285	0.971	-2.947
1/7/1995	1.813	0.12	1.933	4.955	1.089	0.767	-2.179
1/7/1996	1.561	0.12	1.681	4.284	0.921	0.605	-1.574
1/7/1997	1.372	0.12	1.492	3.780	0.795	0.487	-1.087
1/7/1998	1.189	0.12	1.309	3.292	0.673	0.384	-0.703
1/7/1999	1.043	0.12	1.163	2.902	0.575	0.306	-0.396
1/7/2000	0.935	0.12	1.055	2.613	0.503	0.250	-0.146
1/7/2001	0.847	0.12	0.967	2.380	0.445	0.206	0.060
1/7/2002	0.778	0.12	0.898	2.195	0.399	0.172	0.232
1/7/2003	0.720	0.12	0.840	2.039	0.360	0.145	0.377
1/7/2004	0.672	0.12	0.792	1.911	0.328	0.123	0.500
1/7/2005	0.627	0.12	0.747	1.791	0.298	0.104	0.604
1/7/2006	0.590	0.12	0.710	1.693	0.273	0.089	0.693
1/7/2007	0.558	0.12	0.678	1.608	0.252	0.077	0.770
1/7/2008	22.206	0.12	23.886	24.843	4.824	1.369	2.036
<b>Total</b>			47.772	94.040	IRR=13.2%	2.474	

**Table 6.4** Economic Evaluation of Case 3.

<b>A</b>	<b>B</b>	<b>C</b>	<b>D</b>	<b>E</b>	<b>F</b>	<b>G</b>	<b>H</b>
Date	Oil Production (MSTB)	Oil Price (MM\$)	Total Revenue (MM\$)	Producing Tax (MM\$)	Capital Investment (MM\$)	Discounted Factor@ 7.25%	Discounted Capital Investment (MM\$)
1/7/1991	0.00	40.00	0.000	0.000	10.2	0.932	9.510
1/7/1992	343.67	40.00	13.747	6.873		0.869	
1/7/1993	272.35	40.00	10.894	5.447		0.811	
1/7/1994	224.11	40.00	8.964	4.482		0.756	
1/7/1995	445.38	40.00	17.815	8.908		0.705	
1/7/1996	417.00	40.00	16.680	8.340		0.657	
1/7/1997	277.82	40.00	11.113	5.556		0.613	
1/7/1998	195.43	40.00	7.817	3.909		0.571	
1/7/1999	146.84	40.00	5.874	2.937		0.533	
1/7/2000	129.59	40.00	5.184	2.592		0.497	
1/7/2001	112.79	40.00	4.512	2.256		0.463	
1/7/2002	98.92	40.00	3.957	1.978		0.432	
1/7/2003	87.32	40.00	3.493	1.746		0.403	
1/7/2004	78.08	40.00	3.123	1.562		0.375	
1/7/2005	70.18	40.00	2.807	1.404		0.350	
1/7/2006	63.99	40.00	2.560	1.280		0.326	
1/7/2007	58.90	40.00	2.356	1.178		0.304	
1/7/2008	54.85	40.00	2.194	1.097	0.096	0.284	0.027
<b>Total</b>	3077.24		123.090		10.296		9.538

**Table 6.4** Economic Evaluation of Case 3 (continue).

<b>A</b>	<b>I</b>	<b>J</b>	<b>K</b>	<b>L</b>	<b>M</b>	<b>N</b>	<b>O</b>
Date	Production Operation Cost (MM\$)	Injection Operation Cost (MM\$)	Total operation Cost (MM\$)	Total Cost (MM\$)	Undiscounted Cash Flow (MM\$)	Discounted Cash Flow (MM\$)	Cumulative Discounted Cash Flow @ 7.25% (MM\$)
1/7/1991	0.000	0.00	0.000	10.200	-10.200	-9.510	-9.510
1/7/1992	4.124	0.00	4.124	10.998	2.749	2.390	-7.120
1/7/1993	3.268	0.00	3.268	8.715	2.179	1.766	-5.354
1/7/1994	2.689	0.24	2.929	7.412	1.553	1.174	-4.180
1/7/1995	5.345	0.24	5.585	14.492	3.323	2.342	-1.839
1/7/1996	5.004	0.24	5.244	13.584	3.096	2.034	0.196
1/7/1997	3.334	0.24	3.574	9.130	1.983	1.215	1.410
1/7/1998	2.345	0.24	2.585	6.494	1.323	0.756	2.166
1/7/1999	1.762	0.24	2.002	4.939	0.935	0.498	2.664
1/7/2000	1.555	0.24	1.795	4.387	0.797	0.396	3.060
1/7/2001	1.354	0.24	1.594	3.849	0.662	0.307	3.367
1/7/2002	1.187	0.24	1.427	3.405	0.551	0.238	3.605
1/7/2003	1.048	0.24	1.288	3.034	0.459	0.185	3.789
1/7/2004	0.937	0.24	1.177	2.738	0.385	0.144	3.934
1/7/2005	0.842	0.24	1.082	2.486	0.321	0.112	4.046
1/7/2006	0.768	0.24	1.008	2.288	0.272	0.089	4.135
1/7/2007	0.707	0.24	0.947	2.125	0.231	0.070	4.205
1/7/2008	0.658	0.24	0.898	2.091	0.103	0.029	4.234
<b>Total</b>			40.527	112.368	IRR=17.0%	4.234	

**Table 6.5** Economic Evaluation of Case 4.

<b>A</b>	<b>B</b>	<b>C</b>	<b>D</b>	<b>E</b>	<b>F</b>	<b>G</b>	<b>H</b>
Date	Oil Production (MSTB)	Oil Price (MM\$)	Total Revenue (MM\$)	Producing Tax (MM\$)	Capital Investment (MM\$)	Discounted Factor@ 7.25%	Discounted Capital Investment (MM\$)
1/7/1991	0.00	40.00	0.000	0.000	12.300	0.932	11.469
1/7/1992	343.67	40.00	13.747	6.873		0.869	0.000
1/7/1993	272.35	40.00	10.894	5.447		0.811	0.000
1/7/1994	224.27	40.00	8.971	4.485		0.756	0.000
1/7/1995	456.53	40.00	18.261	9.131		0.705	0.000
1/7/1996	414.50	40.00	16.580	8.290		0.657	0.000
1/7/1997	301.63	40.00	12.065	6.033		0.613	0.000
1/7/1998	217.23	40.00	8.689	4.345		0.571	0.000
1/7/1999	169.00	40.00	6.760	3.380		0.533	0.000
1/7/2000	138.52	40.00	5.541	2.770		0.497	0.000
1/7/2001	116.39	40.00	4.656	2.328		0.463	0.000
1/7/2002	100.36	40.00	4.015	2.007		0.432	0.000
1/7/2003	88.20	40.00	3.528	1.764		0.403	0.000
1/7/2004	78.97	40.00	3.159	1.579		0.375	0.000
1/7/2005	71.27	40.00	2.851	1.425		0.350	0.000
1/7/2006	65.23	40.000	2.609	1.305		0.326	0.000
1/7/2007	60.22	40.00	2.409	1.204		0.304	0.000
1/7/2008	56.17	40.00	2.247	1.123	0.120	0.284	0.034
<b>Total</b>	3174.52		126.981		12.420		11.503

**Table 6.5** Economic Evaluation of Case 4 (continued).

<b>A</b>	<b>I</b>	<b>J</b>	<b>K</b>	<b>L</b>	<b>M</b>	<b>N</b>	<b>O</b>
Date	Production Operation Cost (MM\$)	Injection Operation Cost (MM\$)	Total operation Cost (MM\$)	Total Cost (MM\$)	Undiscounted Cash Flow (MM\$)	Discounted Cash Flow (MM\$)	Cumulative Discounted Cash Flow @ 7.25% (MM\$)
1/7/1991	0.000	0.000	0.000	12.30	-12.300	-11.469	-11.469
1/7/1992	4.124	0.000	4.124	10.99	2.749	2.390	-9.078
1/7/1993	3.268	0.000	3.268	8.715	2.179	1.766	-7.312
1/7/1994	2.691	0.480	3.171	7.657	1.314	0.993	-6.319
1/7/1995	5.478	0.480	5.958	15.08	3.172	2.236	-4.083
1/7/1996	4.974	0.480	5.454	13.74	2.836	1.863	-2.220
1/7/1997	3.620	0.480	4.100	10.13	1.933	1.184	-1.036
1/7/1998	2.607	0.480	3.087	7.431	1.258	0.719	-0.317
1/7/1999	2.028	0.480	2.508	5.888	0.872	0.464	0.147
1/7/2000	1.662	0.480	2.142	4.913	0.628	0.312	0.459
1/7/2001	1.397	0.480	1.877	4.204	0.451	0.209	0.668
1/7/2002	1.204	0.480	1.684	3.692	0.323	0.139	0.808
1/7/2003	1.058	0.480	1.538	3.302	0.226	0.091	0.899
1/7/2004	0.948	0.480	1.428	3.007	0.152	0.057	0.955
1/7/2005	0.855	0.480	1.335	2.761	0.090	0.032	0.987
1/7/2006	0.783	0.480	1.263	2.567	0.042	0.014	1.001
1/7/2007	0.723	0.480	1.203	2.407	0.002	0.001	1.001
1/7/2008	0.674	0.480	1.154	2.397	-0.151	-0.043	0.958
<b>Total</b>			45.294	121.2	IRR=9.4%	0.958	



**Table 6.6** Economic Evaluation of Case 5.

<b>A</b>	<b>B</b>	<b>C</b>	<b>D</b>	<b>E</b>	<b>F</b>	<b>G</b>	<b>H</b>
Date	Oil Production (MSTB)	Oil Price (MM\$)	Total Revenue (MM\$)	Producing Tax (MM\$)	Capital Investment (MM\$)	Discounted Factor@ 7.25%	Discounted Capital Investment (MM\$)
1/7/1991	0.000	40.00	0.000	0.000	12.300	0.932	11.469
1/7/1992	343.674	40.00	13.747	6.873		0.869	0.000
1/7/1993	272.353	40.00	10.894	5.447		0.811	0.000
1/7/1994	218.075	40.00	8.723	4.362		0.756	0.000
1/7/1995	443.939	40.00	17.758	8.879		0.705	0.000
1/7/1996	404.079	40.00	16.163	8.082		0.657	0.000
1/7/1997	305.941	40.00	12.238	6.119		0.613	0.000
1/7/1998	227.391	40.00	9.096	4.548		0.571	0.000
1/7/1999	178.249	40.00	7.130	3.565		0.533	0.000
1/7/2000	145.034	40.00	5.801	2.901		0.497	0.000
1/7/2001	121.946	40.00	4.878	2.439		0.463	0.000
1/7/2002	105.190	40.00	4.208	2.104		0.432	0.000
1/7/2003	92.364	40.00	3.695	1.847		0.403	0.000
1/7/2004	82.596	40.00	3.304	1.652		0.375	0.000
1/7/2005	74.495	40.00	2.980	1.490		0.350	0.000
1/7/2006	68.068	40.00	2.723	1.361		0.326	0.000
1/7/2007	62.685	40.00	2.507	1.254		0.304	0.000
1/7/2008	58.314	40.00	2.333	1.166	0.120	0.284	0.034
<b>Total</b>	3204.38		128.176	64.088	12.420		11.503

**Table 6.6** Economic Evaluation of Case 5 (continue).

<b>A</b>	<b>I</b>	<b>J</b>	<b>K</b>	<b>L</b>	<b>M</b>	<b>N</b>	<b>O</b>
Date	Production Operation Cost (MM\$)	Injection Operation Cost (MM\$)	Total operation Cost (MM\$)	Total Cost (MM\$)	Undiscounted Cash Flow (MM\$)	Discounted Cash Flow (MM\$)	Cumulative Discounted Cash Flow @ 7.25% (MM\$)
1/7/1991	0.000	0.000	0.000	12.30	-12.300	-11.469	-11.469
1/7/1992	4.124	0.000	4.124	10.99	2.749	2.390	-9.078
1/7/1993	3.268	0.000	3.268	8.715	2.179	1.766	-7.312
1/7/1994	2.617	0.480	3.097	7.458	1.265	0.956	-6.356
1/7/1995	5.327	0.480	5.807	14.68	3.072	2.165	-4.192
1/7/1996	4.849	0.480	5.329	13.41	2.753	1.809	-2.383
1/7/1997	3.671	0.480	4.151	10.27	1.968	1.205	-1.178
1/7/1998	2.729	0.480	3.209	7.756	1.339	0.765	-0.413
1/7/1999	2.139	0.480	2.619	6.184	0.946	0.504	0.091
1/7/2000	1.740	0.480	2.220	5.121	0.680	0.338	0.429
1/7/2001	1.463	0.480	1.943	4.382	0.496	0.229	0.658
1/7/2002	1.262	0.480	1.742	3.846	0.362	0.156	0.815
1/7/2003	1.108	0.480	1.588	3.436	0.259	0.104	0.919
1/7/2004	0.991	0.480	1.471	3.123	0.181	0.068	0.987
1/7/2005	0.894	0.480	1.374	2.864	0.116	0.041	1.027
1/7/2006	0.817	0.480	1.297	2.658	0.065	0.021	1.048
1/7/2007	0.752	0.480	1.232	2.486	0.021	0.007	1.055
1/7/2008	0.700	0.480	1.180	2.466	-0.133	-0.038	1.017
<b>Total</b>				122.2	IRR=9.47%	1.017	

**Table 6.7** Summary of calculations of economic evaluation.

	Case 1	Case 2	Case 3	Case 4	Case 5
Capital Investment, MM\$ 0	8.172	8.322	10.296	12.42	12.42
Reserves, MMSTB	1.517	1.894	3.077	3.174	3.204
Project Life, Years	18	18	18	18	18
Payout, Years	9.23	9.24	5.9	8.68	8.82
Internal Rate of Return, %	10.30	13.2	17.0	9.4	9.47
Present Worth Net Profits, MM\$	0.818	2.474	4.234	0.958	1.017
Profit-to-Investment Ratio	0.11	0.252	0.446	0.083	0.088

# CHAPTER VII

## CONCLUSIONS AND RECOMMENDATIONS

### 7.1 Conclusions

The main objective of the research is to improve and increase oil recovery by waterflooding in Suphan-Buri Basin of Thailand. The research effort includes laboratory experiments, reservoir simulation and economic evaluation. The porosity and permeability measurements are performed on cylindrical specimens in laboratory. The reservoir simulator is a reservoir management tool to use calculation of waterflood performance and predicting recovery. In economic evaluation, it provides to make economic decision.

Tertiary sandstone used in the laboratory experiments are obtained from coal mine in northern part of Thailand; Li Basin, Mae Moa Basin, and Chiang Muan Basin. These rock samples are represented to Tertiary sandstone of Suphan-Buri Basin. Due to outcrops of Suphan-Buri Basin is rarely to discovered. The core specimens are in cylindrical shaped with 38.55 millimeters in diameter and 51.17 millimeter in length. The core specimens are measured to find porosity and permeability. The permeability is ranged of 0.002 to 51.38 md and average permeability is 5.2 mD. Whereas porosity is averaged at 11.7% and it is ranged of 1.18-36.58 %. From this result, some values are too high or low value this is because (1) errors which have been occurred as measuring, (2) core specimens are not cleaned or dried and (3) calibrating before measuring.

The study uses reservoir simulation to evaluate different cases for optimizing oil recovery. Performance forecasts for oil recovery are made for five cases in order to determine the optimum development plan. The reservoir simulation study used the reservoir and fluid data from data of U-Thong Field. But some data are not available so they are assumed that based on U-Thong data. All cases have the same total production life time (18 years). In case 1, which has no water injection well, this result shows that there is no change of oil saturation at anytime. On the other hands, gas can be more production than other cases due to reservoir pressure is below the bubble point pressure. As a result, case 1 is also produced in a large amount of gas. Whereas all cases of waterflooding, the reservoir pressure has been maintained above the bubble point pressure. This field can be produced oil about 10% of OOIP before waterflooding. Case 1 has been increased oil production without waterflooding about 11.93% since July 1993 when it is the starting date of waterflooding. This case shows the least oil recovery factor. Case 2 has only one injection well which is inverted from producing well (P1) to injection well (W1). It has been increased oil recovery factor from primary production is about 17.59% after waterflooding. The displacement and areal sweep efficiency of this case is the lowest value ( $E_D = 0.55$  and  $E_A = 0.34$ ). Moreover, water breakthrough occurs earlier than other cases. First wells of this case (well P2 and P3) have begun breakthrough since 1994. As a result, it provides water-oil ratio (WOR) at 9.43 that is the highest value. This is because the water injection rate is too high and the spacing of producing wells and injection well are also closed. Case 3 has two injection wells and it is increased oil recovery factor from primary production is 34.69%. Whereas, case 4 and 5 which have four injection wells, they are increased oil recovery factor from primary production about 36.10%

and 36.55% respectively. The displacement efficiencies of case 3, 4 and 5 are 0.58, 0.60, and 0.59 respectively. The areal sweep efficiencies of three cases are 0.55, 0.56, and 0.57 respectively. These values are closed due to reservoir is homogeneous and continuity. However, case 4 and 5 can provide more production than case 3. Case 3 also gives higher WOR than case 4 and 5. The values of WOR are 7.66, 7.38, and 7.10 respectively. From the results, it is concluded that water breakthrough is occurred early because (1) water injection rate per well is too high and (2) spacing of production wells and injection well are closed. The results also show significantly higher recoveries in case 4 and 5 which have more injection wells than other cases. Or in the other words, recoveries are directly related to the number of injection wells. Three dimensional reservoir simulation studies of this field indicate that high water cut is increased continuously after waterflooding. The reservoir pressure in all cases of waterflooding has been maintained above the bubble point pressure. However, oil recovery with more injection wells may not provide the best economically viable case. That can only be determined by economic analysis of the cases.

From the results of the economic evaluation, case 3 provides the least payout time at 5.9 years and case 2 provides the most payout time at 9.24 years. It is indicated that investment in the case 3 will be return in shorter than other cases. Additionally, case 3 still gives the highest values of internal rate of return (IRR), profit to investment (PIR), and present worth net profits, about 17%, 0.446, and 5.234 MM\$ respectively. On the other hands, case 4 gives the lowest of IRR and PIR about 9.4% and 0.083 respectively. This is because case 4 has the highest amount of investment. Whereas case 1 gives the lowest of present worth net profits about 0.818 MM\$ due to this case has produced in the smallest amount of oil recovery reserves.

However, present worth net profits of these cases can still be positive so the project should be operated. Finally, from the results, it is indicated that case 3 should be the best case of this field due to it can provides the best values of economics.

## **7.2 Recommendations for Future Research Study**

In laboratory experiments, the actual outcrops of Tertiary sandstone are needed for the determination of porosity and permeability. The specimens should be obtained from Suphan-Buri Basin. They should be collected from core-logging because it can provide more accuracy. The reservoir simulation, the researcher should read and learn the manual of simulation program (ECLIPSE) before working. Reliability of simulation results depends on the accuracy of the input data of simulators. The history matching should be defined in the reservoir simulation because it is necessary step for more accuracy of results. Moreover, more known reservoir data help to be more accuracy of results. In the waterflooding study, the locations of water injection wells are considered to be careful the earlier water breakthrough. The water injection rate should be also balanced with total oil production rate because high water injection rate is results of high water production. the researcher should understand in reservoir characteristics of this field before running reservoir simulation.

## REFERENCES

- Ascope Technical Committee Paper. "Tertiary Sedimentary Basins of The Gulf Thailand and South China Sea," **The 5<sup>th</sup> Council on Petroleum Conference and Exhibition,**" November 2-6, 1993. p.1
- Aziz, A. Kadir, A., Hamid, M.F., and Ikhan, A. "Permeability Prediction: Core and Log-Derived Values," **International Conference on Geology, Geotechnology and Mineral Resources of Indochina (Geo-Indo'95),** November 22-25, 1995, Khon Kaen, Thailand.
- Barber, Jr. A.H., Stile, L.H., and Thompson, B.B. "Infill Drilling to Increase Reserves Actual Experience in Nine Fields in Texas, Oklahoma, and Illinois," **Journal of Petroleum Technology** (August 1983): 1530-1538.
- Baoxing, Y. Guohua, Z., and Zhongqiang L. "Porosity Evolution and Prediction of Tertiary Sandstone Reservoirs, Western Qiongdongnan Basin, South China Sea," **International Conference on Geology, Geotechnology and Mineral Resources of Indochina (Geo-Indo'95),** November 22-25, 1995, Khon Kaen, Thailand.
- Chapman, L.R., and Thompson, R.R. "Waterflood Surveillance In Kuparak River Unit with Computerized Pattern Analysis," **Journal of Petroleum Technology** (March 1989): 277-282.
- Chrichlow, H.B. "**Modern Reservoir Engineering – A Simulation Approach,**" Prentice-Hall, Eaglewood Cliffs, New Jersey, (1977).
- Craft, B.C., and Hawkins, M.F. "**Applied Petroleum Reservoir Engineering,**" second edition, Pentice Hall, Eaglewood Cliffs, N.J, (1990).



- Crichlow, H.B. “**Advanced Reservoir Engineering,**” Oklahoma, (1994).
- Dandona, A.K., Alston, R.B., and Braun, R.W. “Definebg Data Requirements for a Simulation Study,” **Paper SPE 22357 presented at the SPE International Meeting on Petroleum Engineering, Beijing, China, March 24-27, 1992.**
- DesBrisay, C.L. “Supplemental Recovery Development of the Intisar “A” and “D” Reef Fields, Libyan Arab Republic,” **Journal of Petroleum Technology** (July 1972): 785-796.
- Franchi, J.R. “**Integrated Flow Modeling,**” Elsevier, Netherlands, (2000).
- Franchi, J.R. “**Principles of Applied Reservoir Simulation,**” Gulf, Houston, Texas, (1997).
- Ghauri, W.K. “Production Technology Experience in a Large Carbonate Waterflood, Denver Unit, Wason San Andres Field,” **Journal of Petroleum Technology** (September 1980): 1493-1502.
- Graves, K.S., Valentine, A.V., Dolma, M.A., and Morton, E.K. “Design and Implementation of Horizontal Injector Program for the Benchamas Waterflood –Gulf of Thailand,” **The 6<sup>th</sup> Mining, Metallurgical, and Petroleum Engineering Coference,** Bangkok, October 24-26, 2001.
- Harpole, K.J. “Improved Reservoir Characterization – A Key to Future Reservoir Management for the West Seminole San Andres Unit,” **Journal of Petroleum Technology** (November 1980): 2009-2019.
- Hugen, S.A., Lund, O., and Hoyland, L.A. “Statfjord Field: Development Strategy and Reservoir Management,” **Journal of Petroleum Technology** (July 1988): 863-873.

- Irwin, R.A., Tucker, C.W., and Jr. H.E.S. "A Case History of the Postle Area – Computer Production Control and Reservoir Simulation," **Journal of Petroleum Technology** (July 1972): 775-781.
- Mattax, C.C., and Dalton, R.L. "**Reservoir Simulation**," SPE, First Printing, Richardson, TX, (1990).
- Mian, M.A. "**Petroleum Engineering Handbook for the Practicing Engineer**," Volume 1, Penn Well Book, Tulsa, OK, (1992).
- Nicholls, C.A., Boom, W., Geel, J. Khodori, S.A., and Lawati, M.A. "Fracture Modeling as a Key to Waterflood Development," **Paper SPE 53211 presented at the 1999 SPE Middle East Oil Show**, Bahrain, 20-23 February, 1999.
- Praditarn, S., Jaroonsitha, S., and Gonecome, Y. "Petroleum Systems of The Petroliferous Basin in Thailand," **Symposium on Mineral, Energy, and Water Resources of Thailand: Towards to the year 2000**, October 28-29, 1999, Bangkok, Thailand: 557-559.
- Pisutha-Arnond, S., Ukkakimapan, J., and et al. "Predicting Oil and Water Interval in U-Thong Field using Thermal Extraction Pyrolysis Gas Chromatography," **International Conference on Stratigraphy and Tectonic Evaluation of Southeast Asia and the South Pacific**, August 10-24, 1997, Bangkok, Thailand: 543-558.
- Simon, V. "Petroleum Resources and Potential in Thailand: Central Plains," **108<sup>th</sup> Anniversary of Department of Mineral resources**, August 16, 2000.
- Stiles, L.H., and Magruder, J.B. "Reservoir Management in the Means San Andres Unit," **Journal of Petroleum Technology** (April 1992): 469-475.

- Smith, J.T., and Cobb, W.M. **“Predicting Waterflood Recovery Performance,”**  
Based on a workshop sponsored by PTTC’s Midwest Region on February 17-21, 1997, Evansville, IN.
- Talash, A.W. “An Overview of Waterflood Surveillance and Monitoring,” **Journal of Petroleum Technology** (December 1988): 1539-1543.
- Thakur, G.C. “A 5-Phase Methodical Approach of Identifying Selecting, Developing, Implementing and Operating a Pressure Maintenance Scheme for and Offshore Field,” **Paper OTC conference**, Houston, Texas, May 5-8, 2003.
- Thakur, G.C. “The Role of Reservoir Management in Carbonate Waterfloods,” **Paper SPE 39519 presented at the 1998 SPE India Oil and Gas Conference and Exhibition**, New Delhi, India, February 10-12, 1998.
- Thakur, G.C. **“Achieving Excellence in Waterflooding,”** presented at Central Sofitel Hotel, February 6, 2004, Bangkok, Thailand.
- Thakur, G.C. “Waterflood Surveillance Techniques – A Reservoir Management Approach,” **Journal of Petroleum Technology** (October 1991):1180-1188.
- Thakur, G.C., and A. Satter. **“Integrated Waterflood Asset Management,”** Penn Well Book, Tulsa, OK, (1998).
- Triamwichanon, H. “Reservoir Characterization Using Porosity Distribution in Suphan Buri Basin Thailand,” **Symposium on Mineral, Energy, and Water Resources of Thailand: Towards to the year 2000**, October 28-29, 1999, Bangkok, Thailand: 545-556.
- Uttamo, W., Nichols, G.J., and Elders, C.F. “The Tertiary Sedimentary Basins of Northern Thailand,” **Symposium on Mineral, Energy, and Water**

**Resources of Thailand: Towards to the year 2000**, October 28-29, 1999,  
Bangkok, Thailand: 668-674.

Willhite, G.P. **“Waterflooding,”** SPE Textbook Series, Volume 3, Richardson, TX,  
(1986).

Wongsirasawad, L. “20 Successful Years of Sirikit Oilfield,” **Thailand Petroleum  
Conference 2002**, Bangkok.

APPENDIX A  
POROSITY DISTRIBUTION

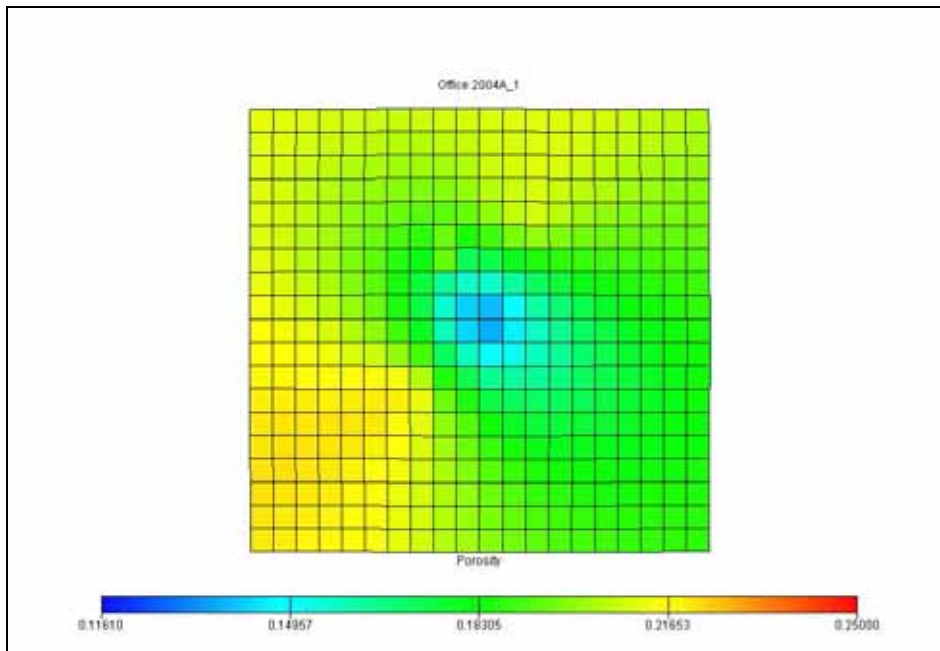


**Figure A-1** Porosity distribution of first layer.

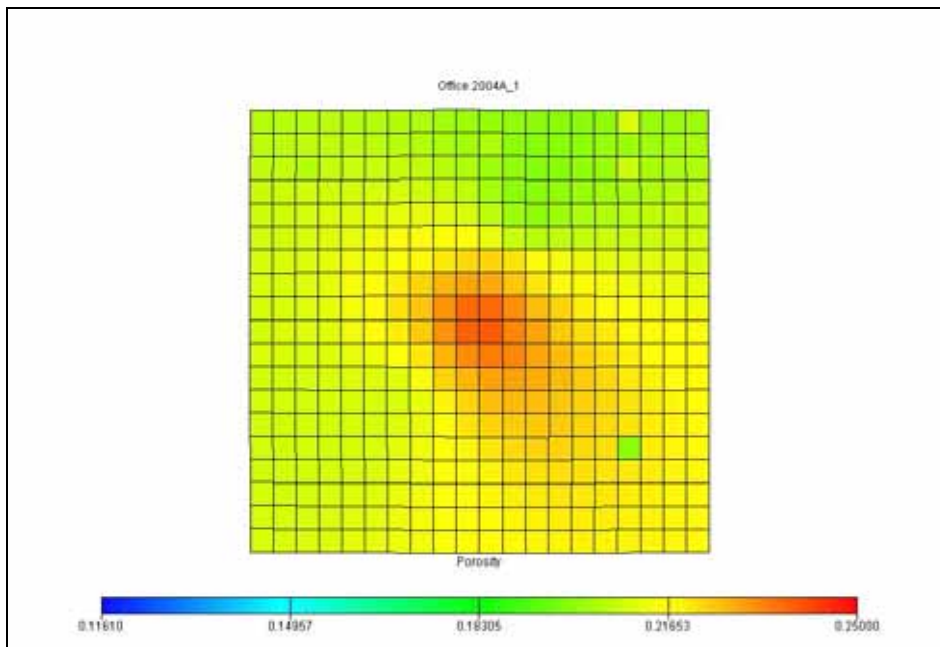


**Figure A-2** Porosity distribution of second layer.

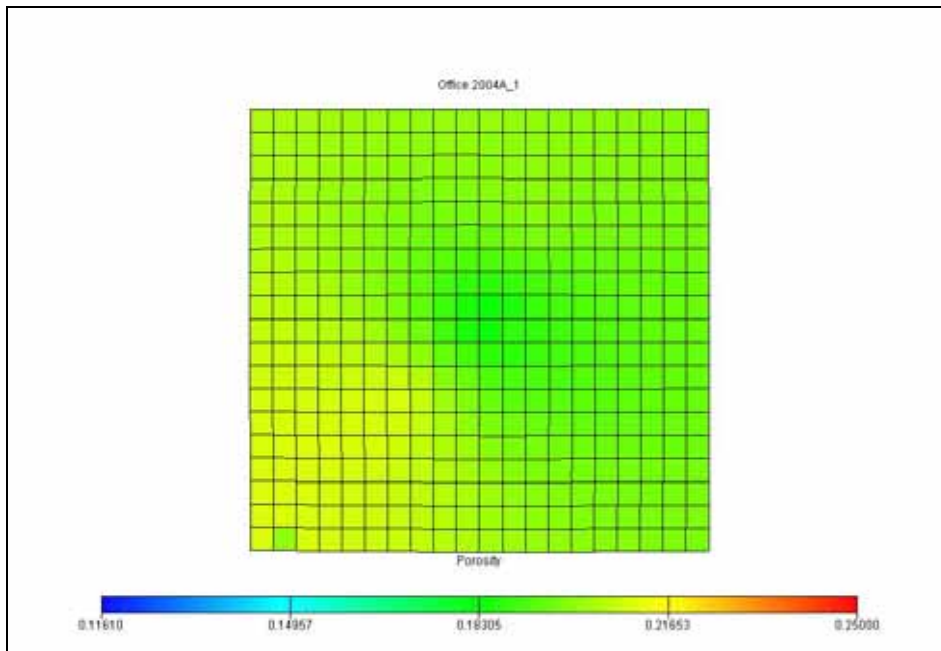


**Figure A-3** Porosity distribution of third layer.

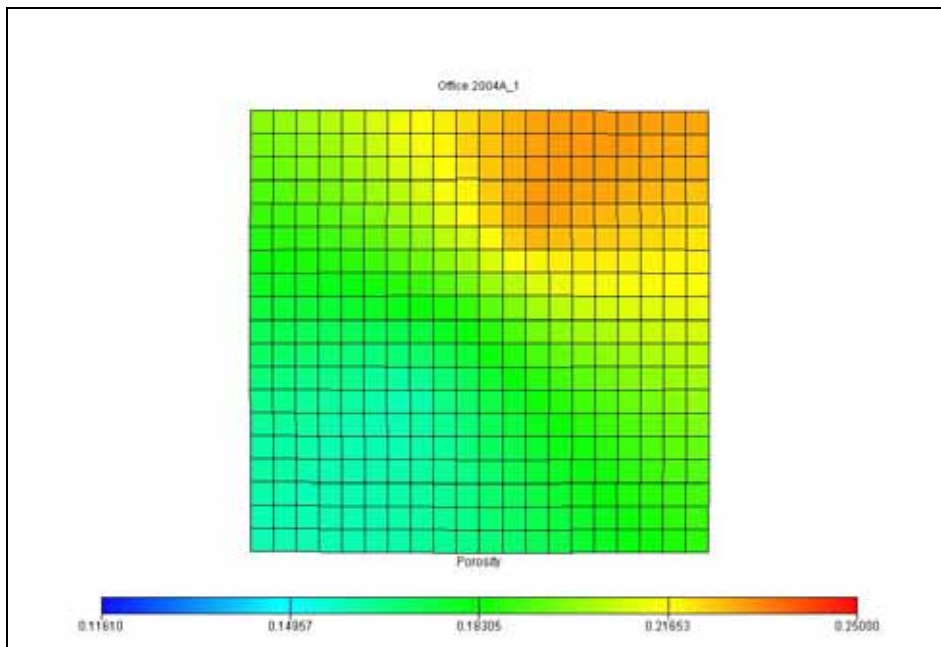


**Figure A-4** Porosity distribution of fourth layer.

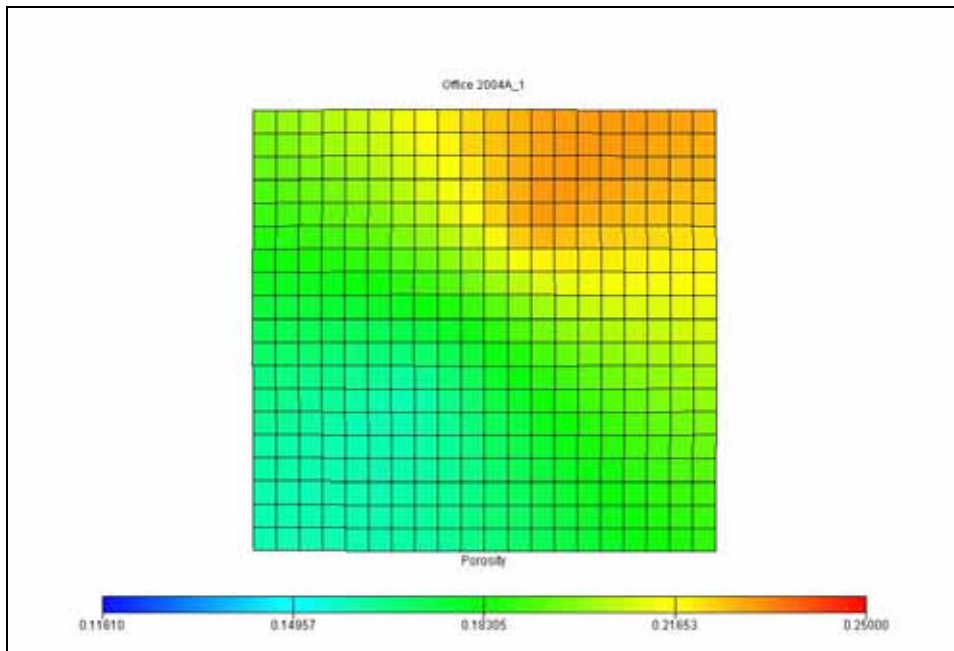


**Figure A-5** Porosity distribution of fifth layer.

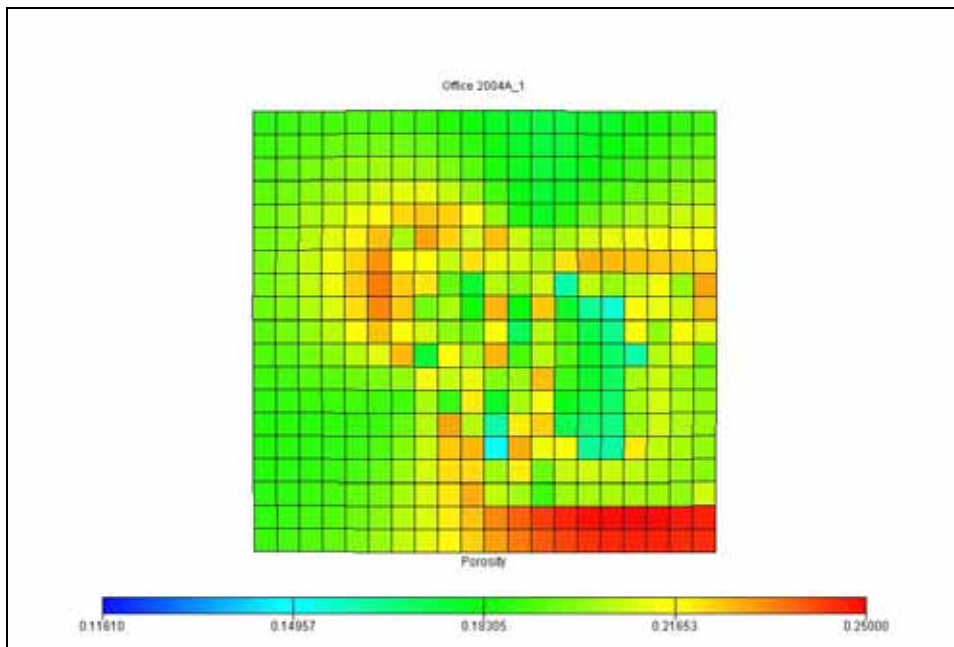


**Figure A-6** Porosity distribution of sixth layer.



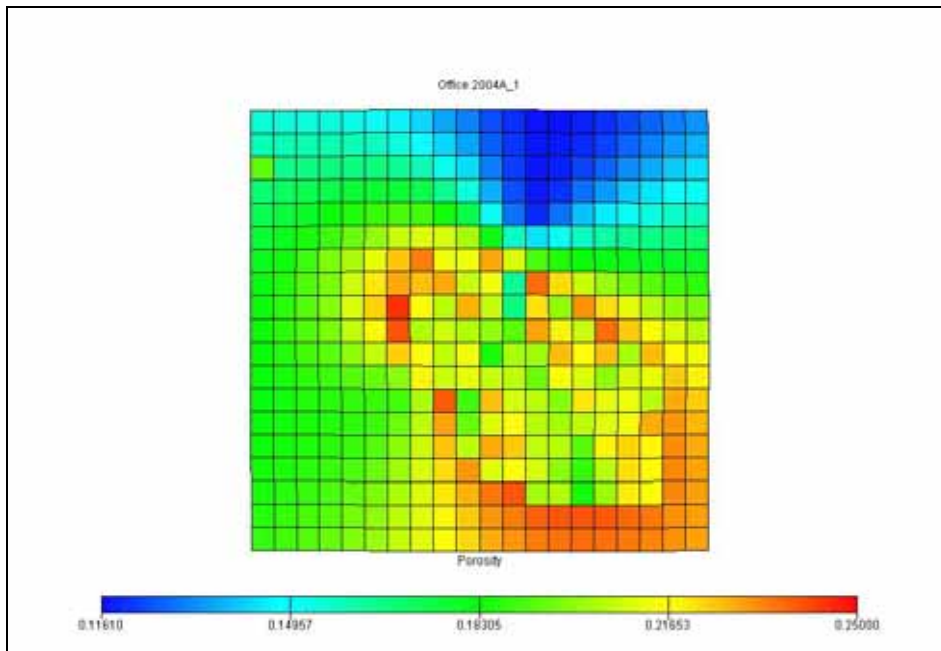


**Figure A-7** Porosity distribution of seventh layer.

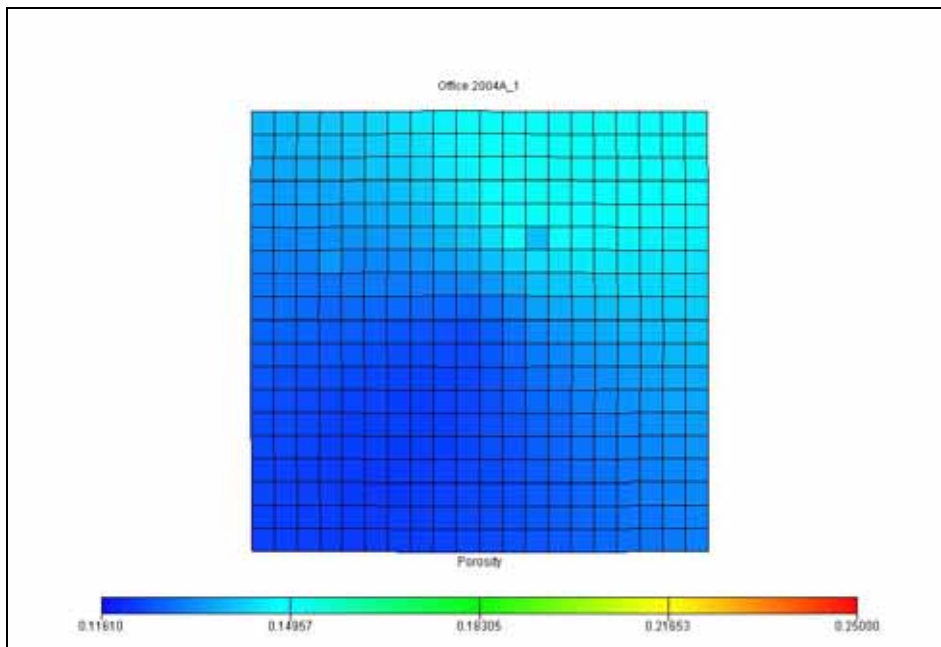


**Figure A-8** Porosity distribution of eighth layer.

APPENDIX B  
PERMEABILITY DISTRIBUTION IN X. Y  
AND Z DIRECTION

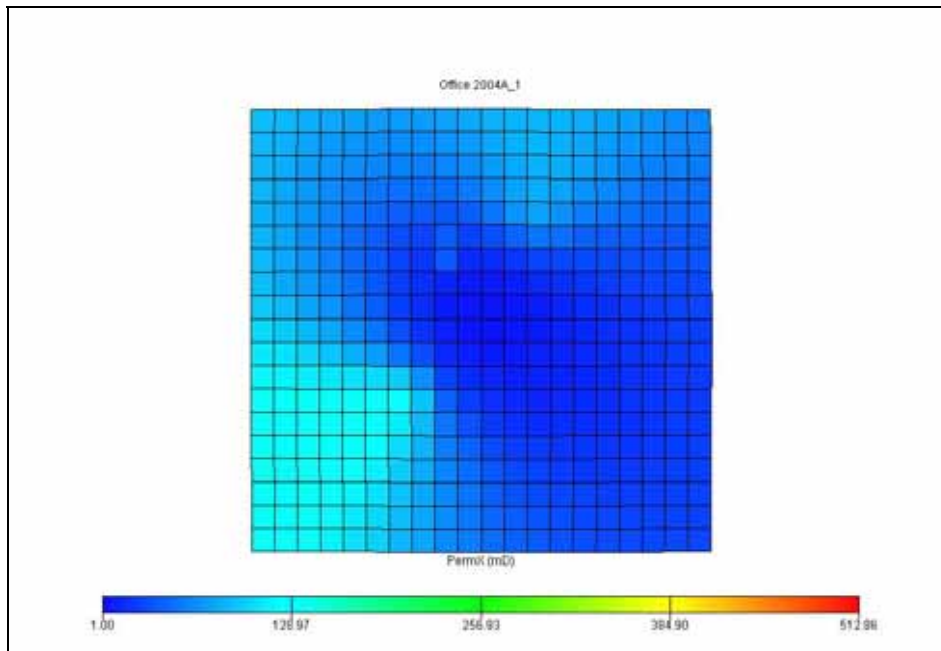


**Figure B-1** Permeability distribution in x and y direction of first layer.

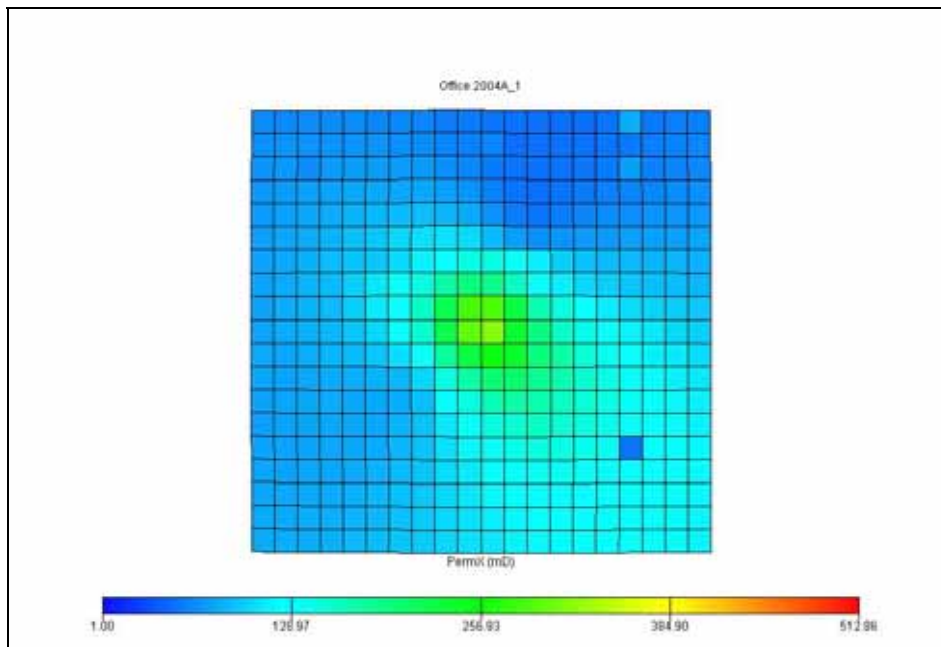


**Figure B-2** Permeability distribution in x and y direction of second layer.

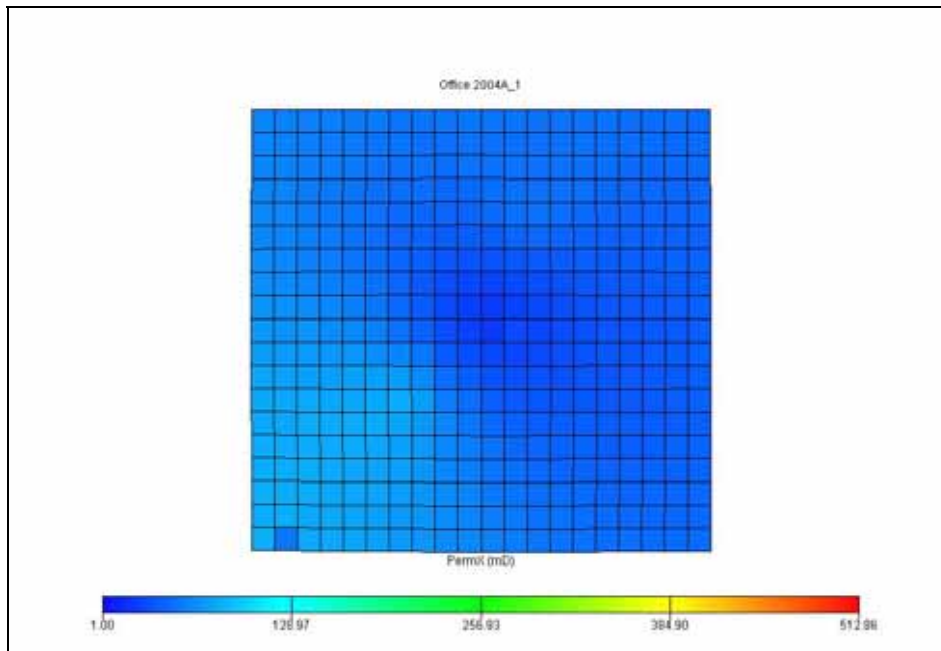


**Figure B-3** Permeability distribution in x and y direction of third layer.

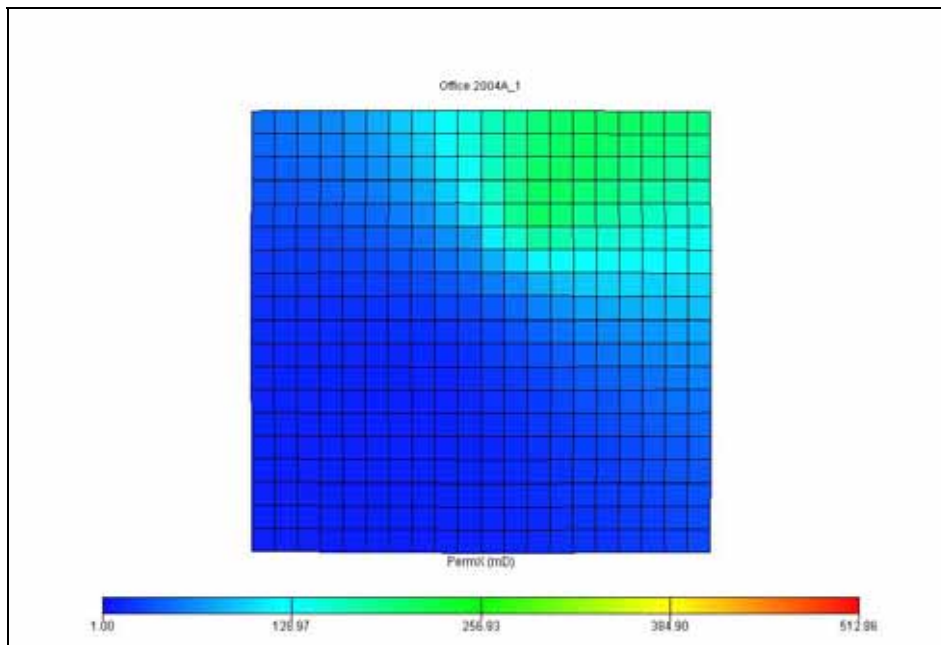


**Figure B-4** Permeability distribution in x and y direction of fourth layer.

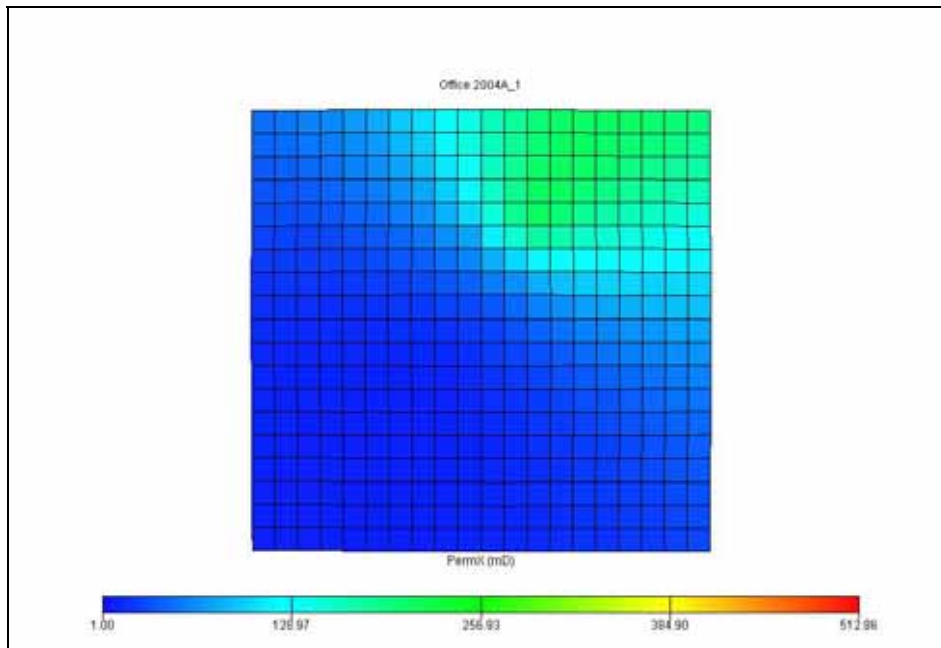


**Figure B-5** Permeability distribution in x and y direction of fifth layer.

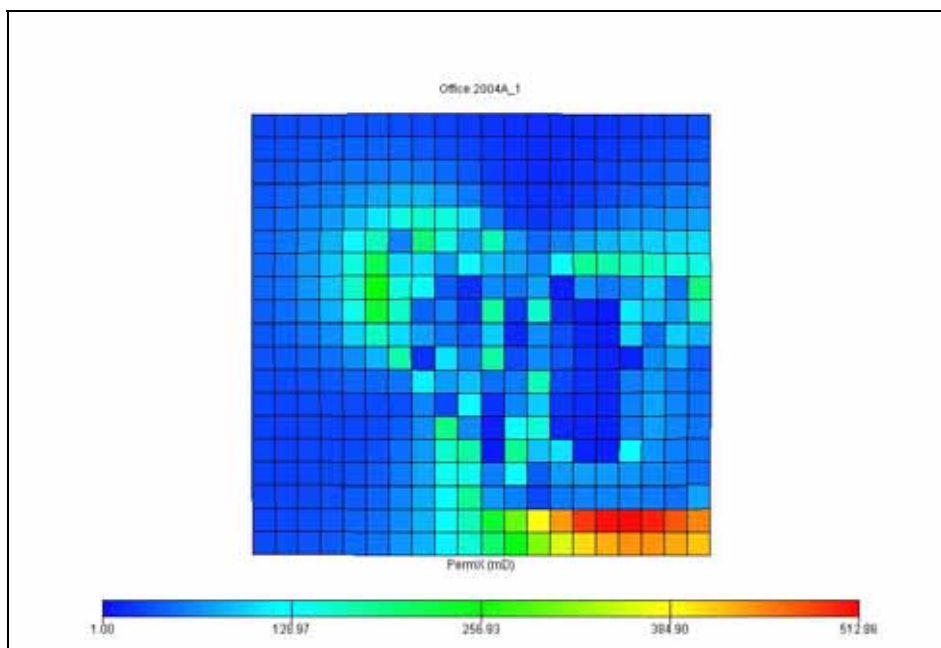


**Figure B-6** Permeability distribution in x and y direction of sixth layer.

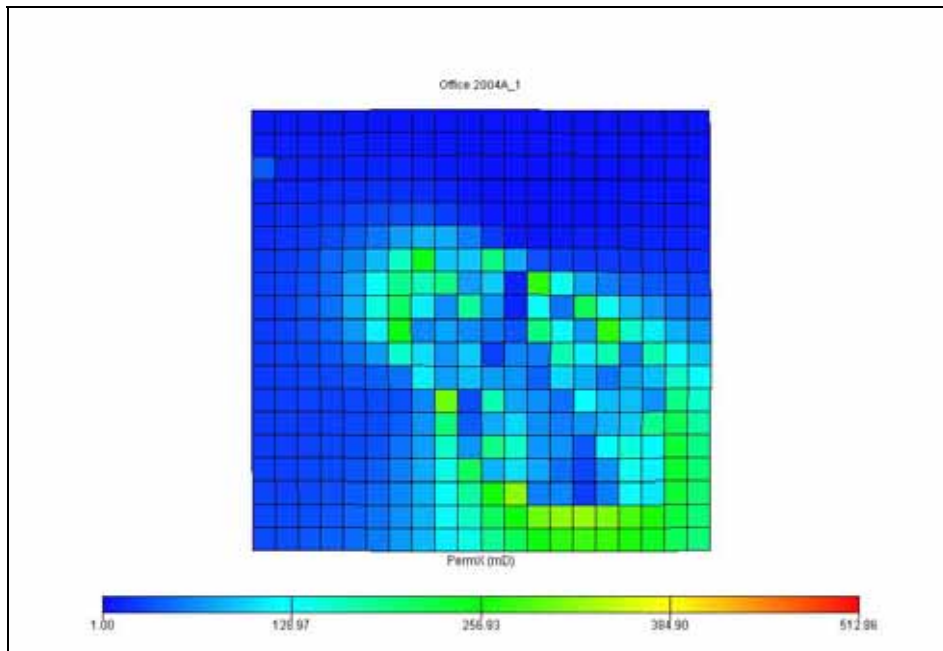


**Figure B-7** Permeability distribution in x and y direction of seventh layer.

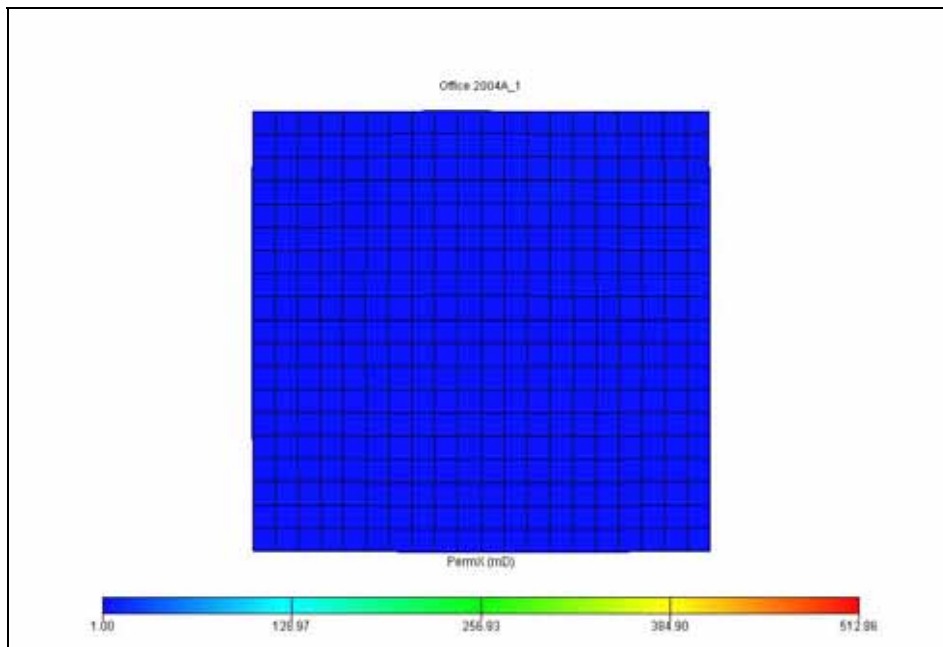


**Figure B-8** Permeability distribution in x and y direction of eighth layer.

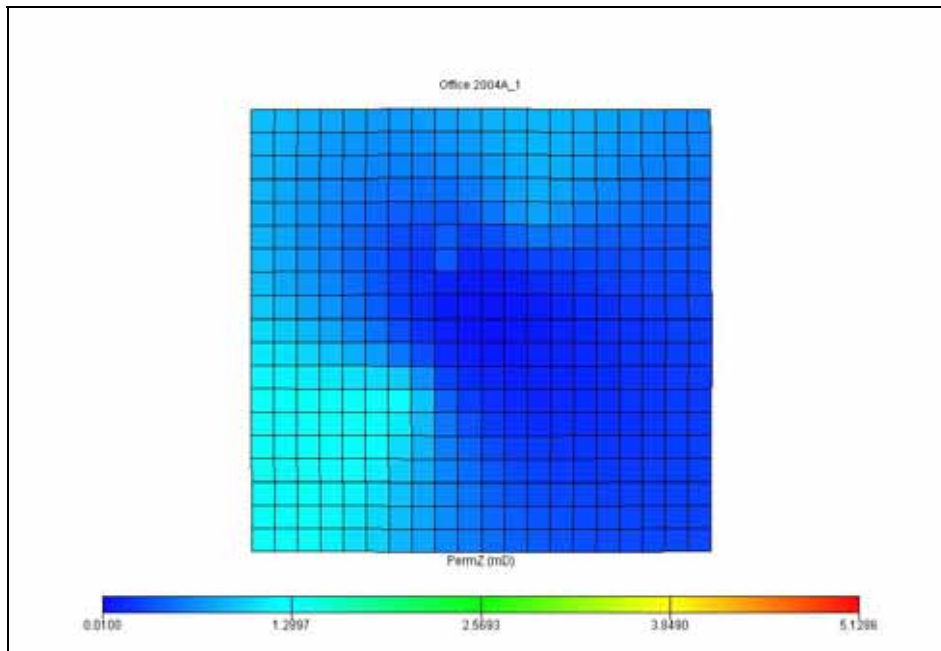


**Figure B-9** Permeability distribution in z direction of first layer.

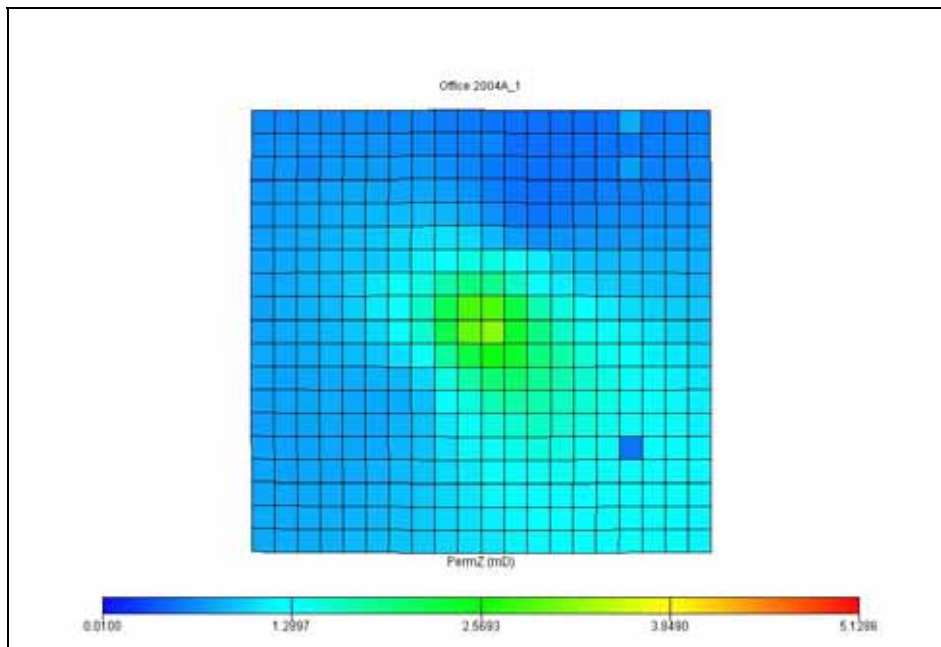


**Figure B-10** Permeability distribution in z direction of second layer.

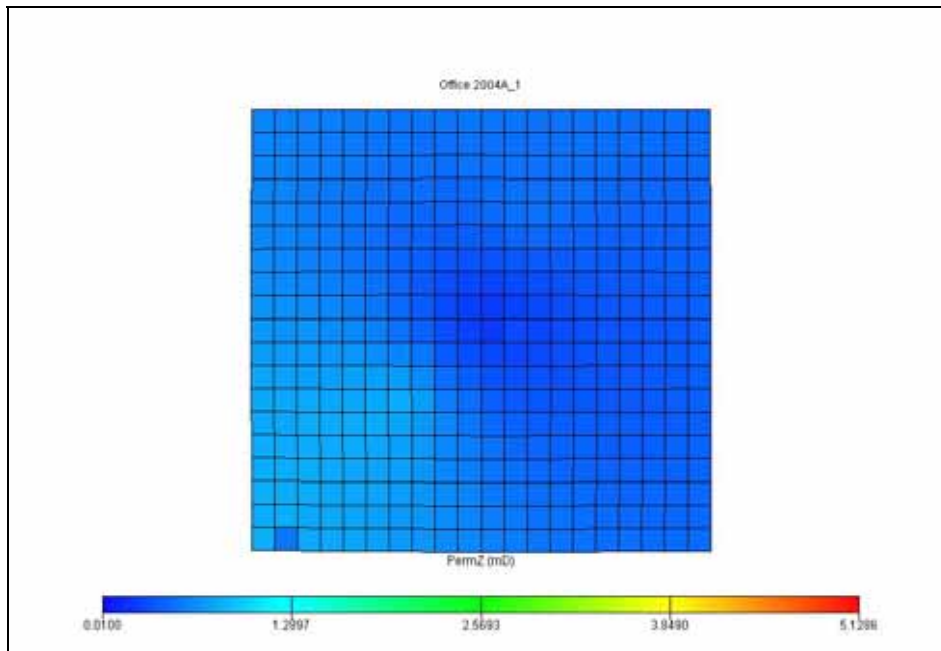


**Figure B-11** Permeability distribution in z direction of third layer.

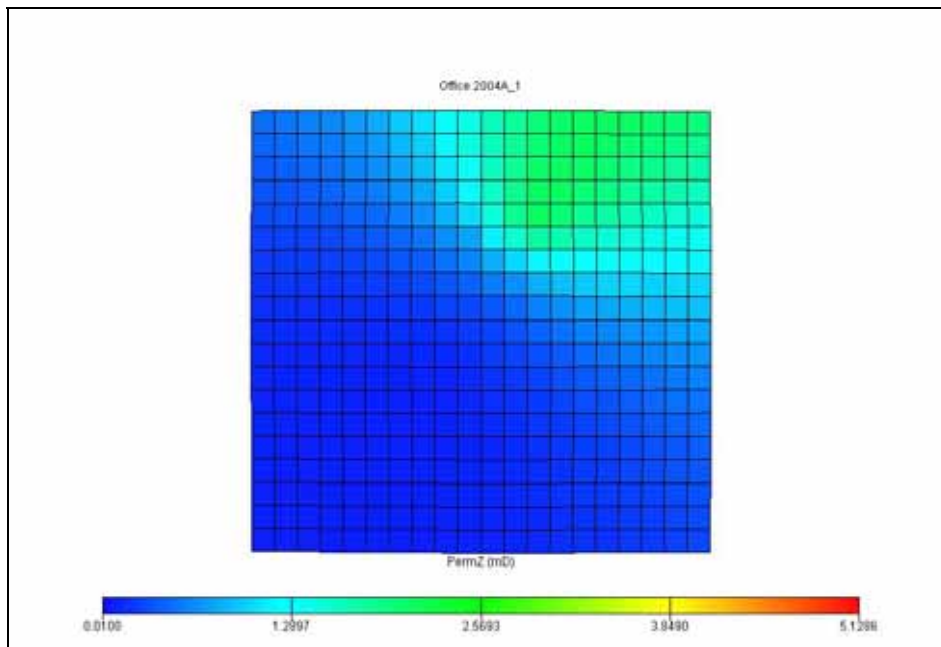


**Figure B-12** Permeability distribution in z direction of fourth layer.



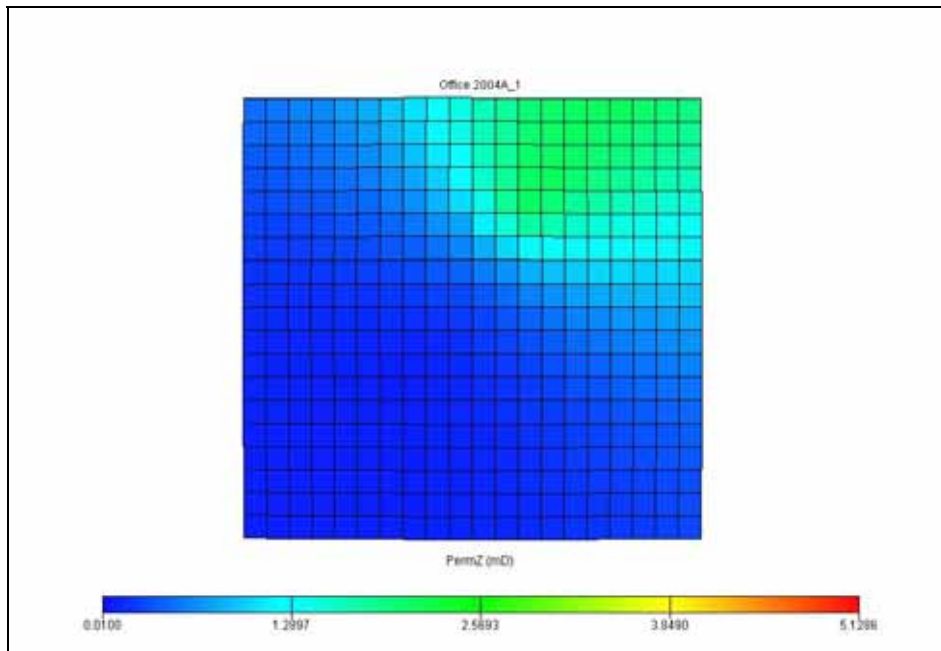


**Figure B-13** Permeability distribution in z direction of fifth layer.

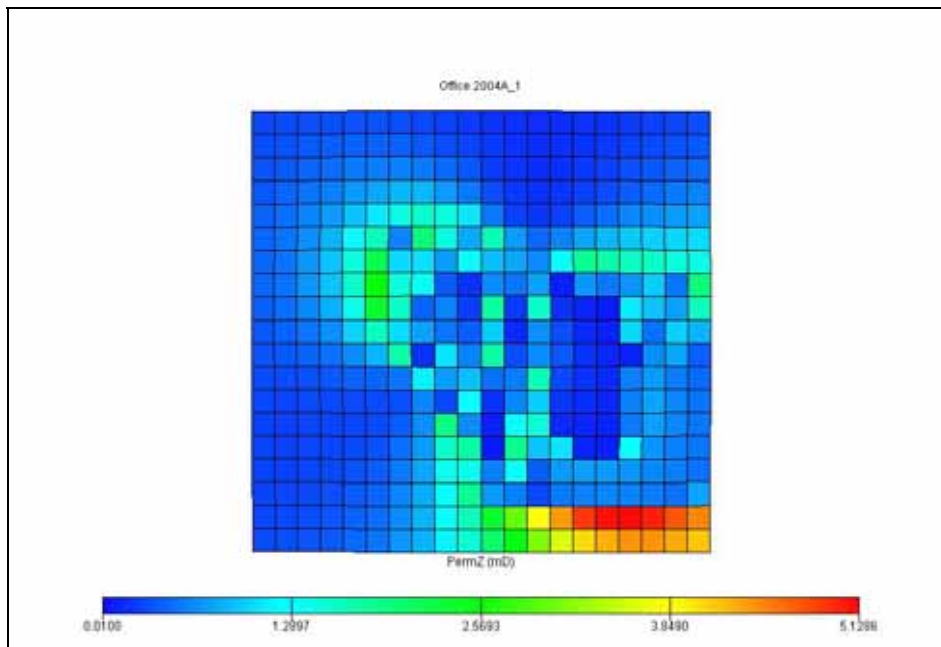


**Figure B-14** Permeability distribution in z direction of sixth layer.

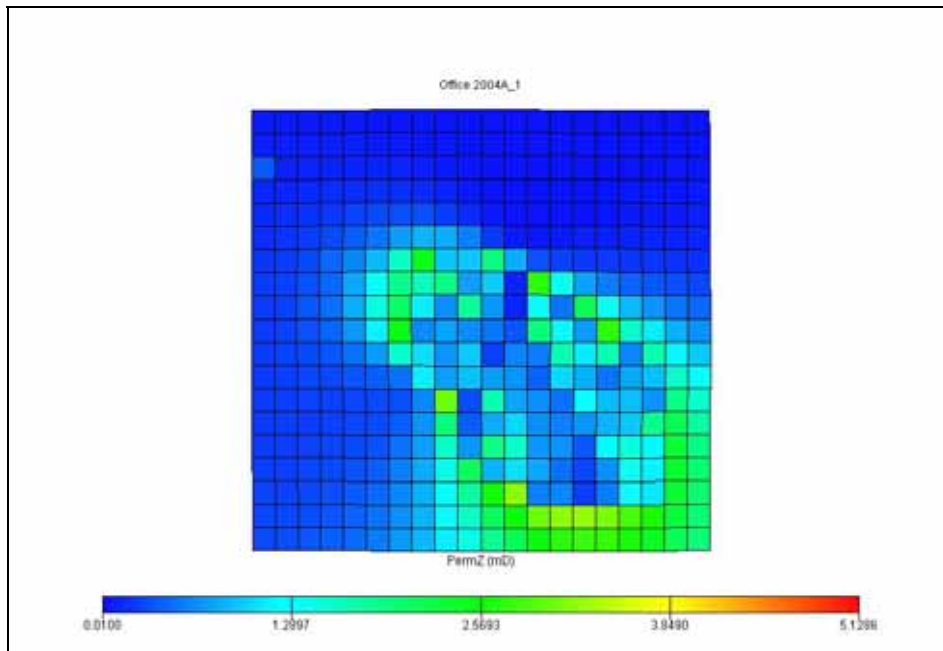


**Figure B-15** Permeability distribution in z direction of seventh layer.

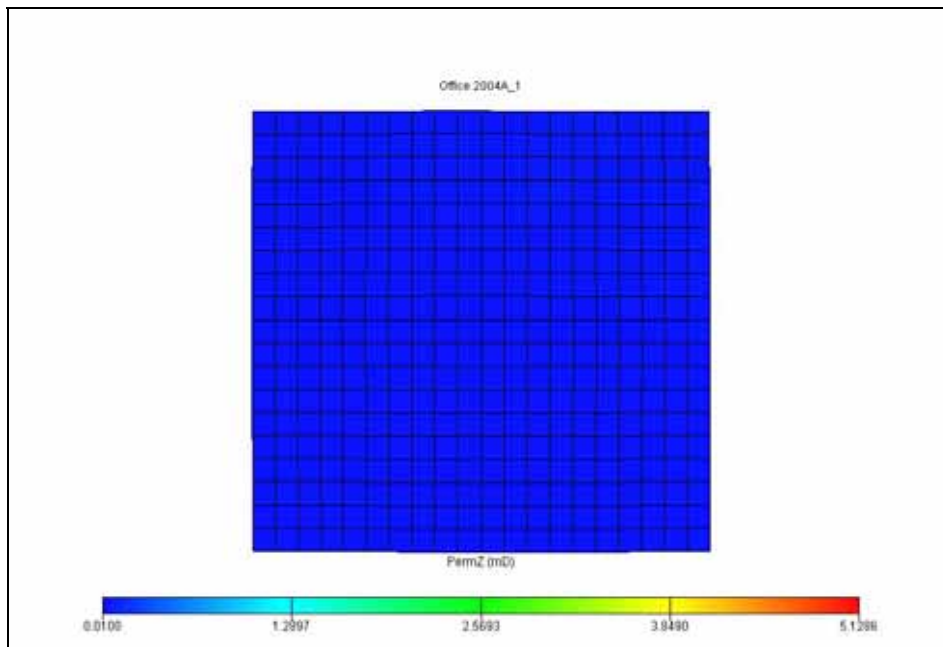


**Figure B-16** Permeability distribution in z direction of eighth layer.

## APPENDIX C

### DISTRIBUTION OF OIL SATURATION : CASE 1

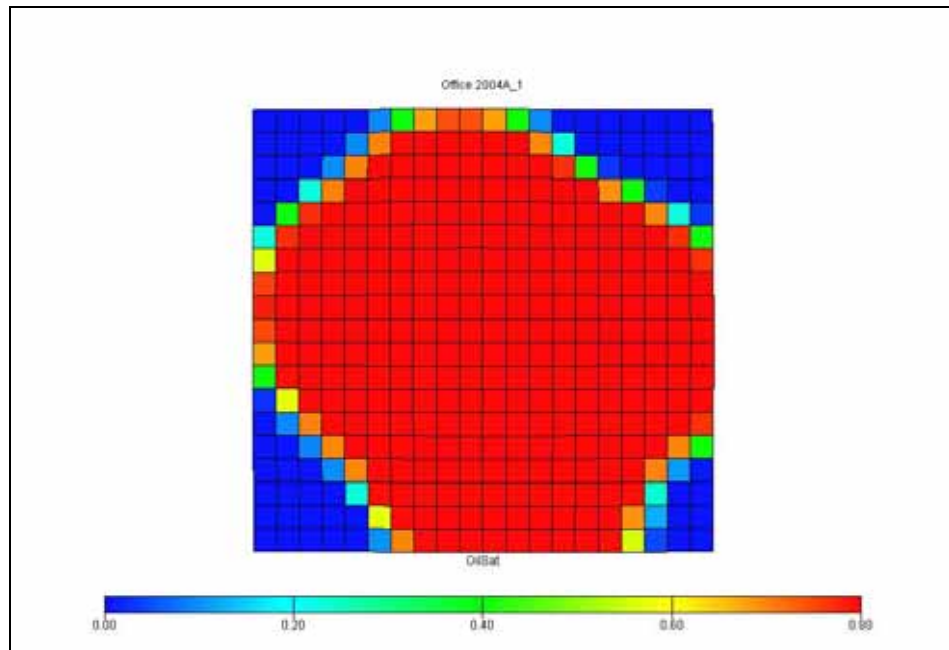


**Figure C-1** Distribution of oil saturation in July 1991.

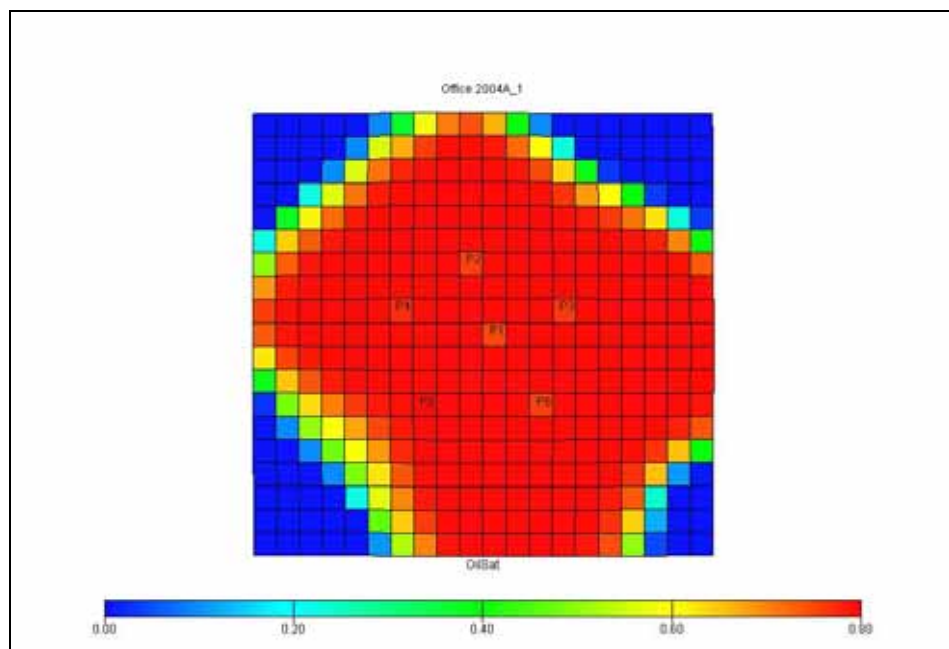


**Figure C-2** Distribution of oil saturation in January 1993.

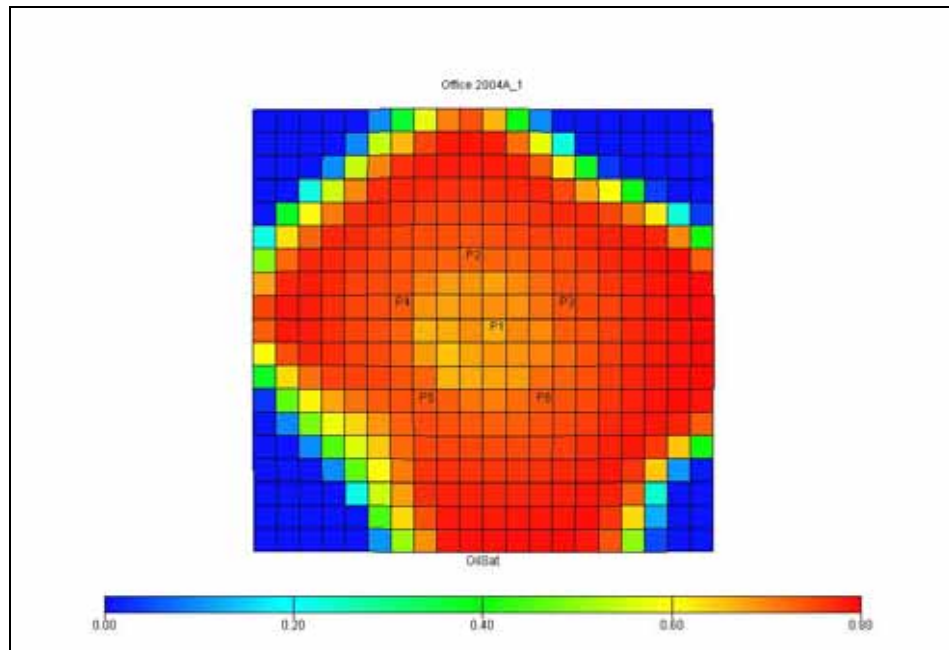


**Figure C-3** Distribution of oil saturation in January 1995.

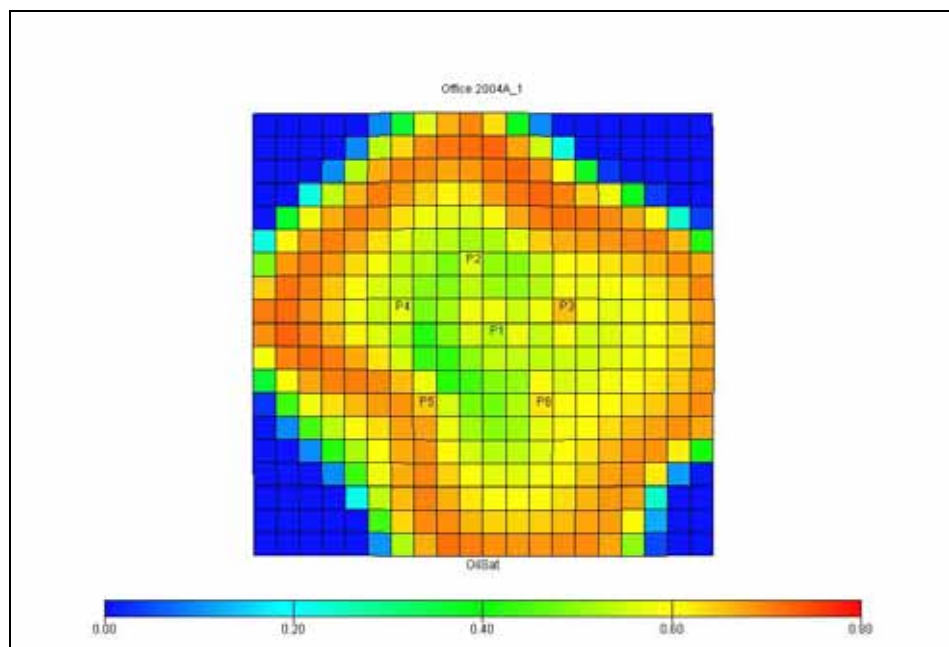


**Figure C-4** Distribution of oil saturation in January 2000.

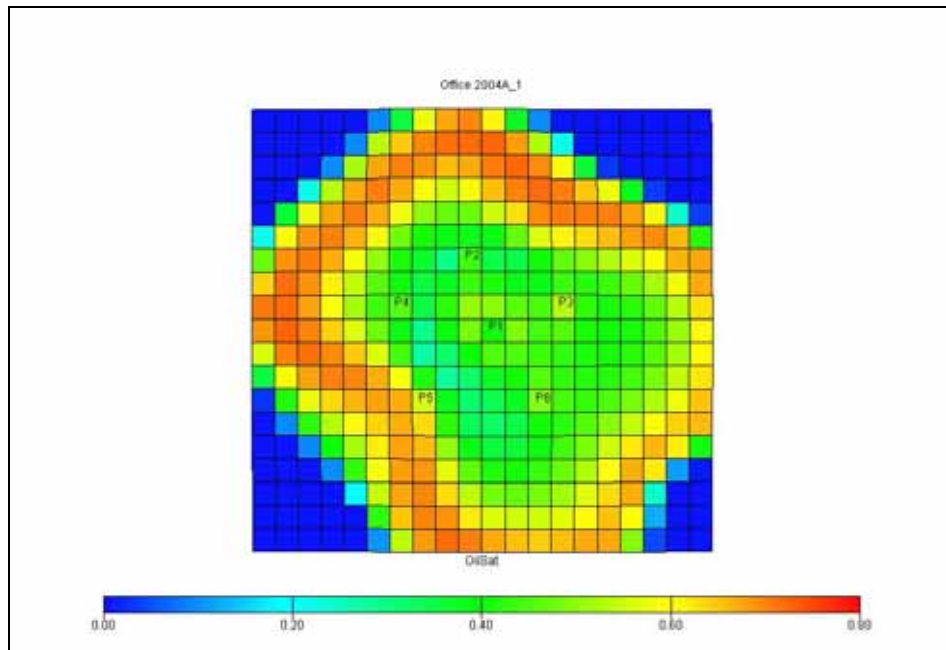


**Figure C-5** Distribution of oil saturation in January 2005.

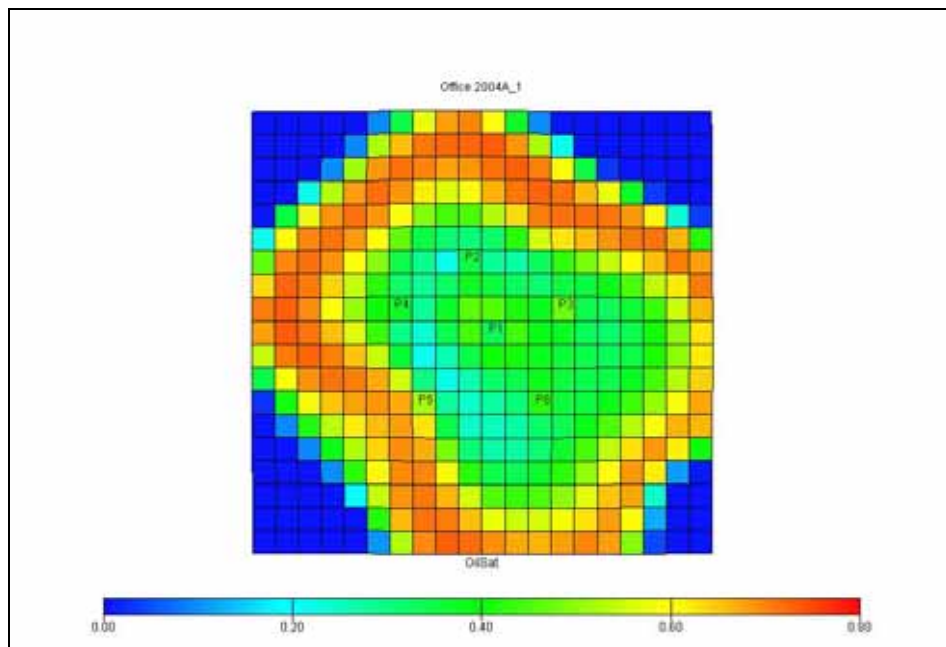


**Figure C-6** Distribution of oil saturation in January 2009.

## APPENDIX D

### DISTRIBUTION OF OIL SATURATION : CASE 2

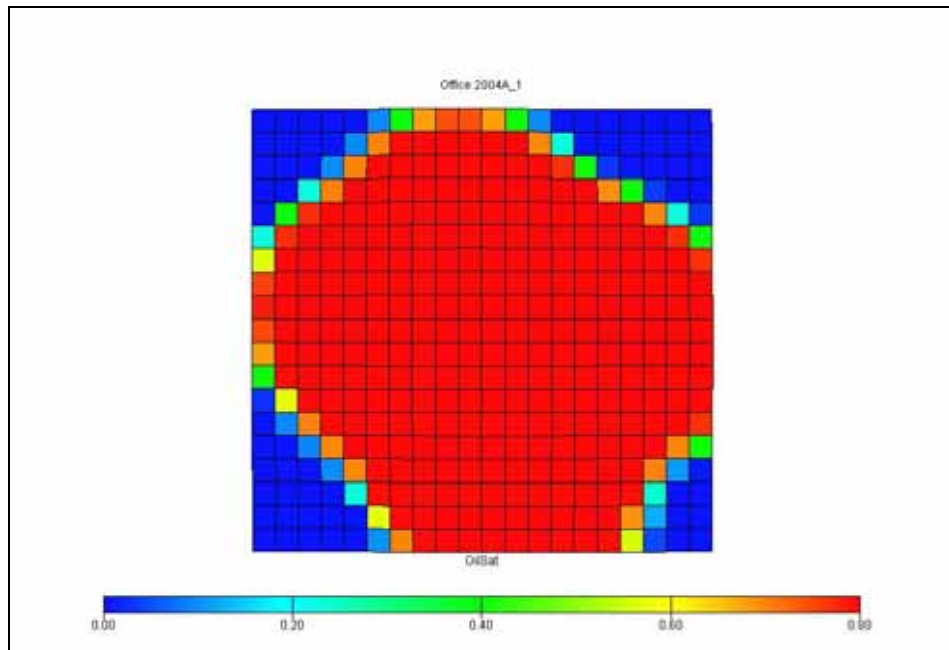


**Figure D-1** Distribution of oil saturation in July 1991.

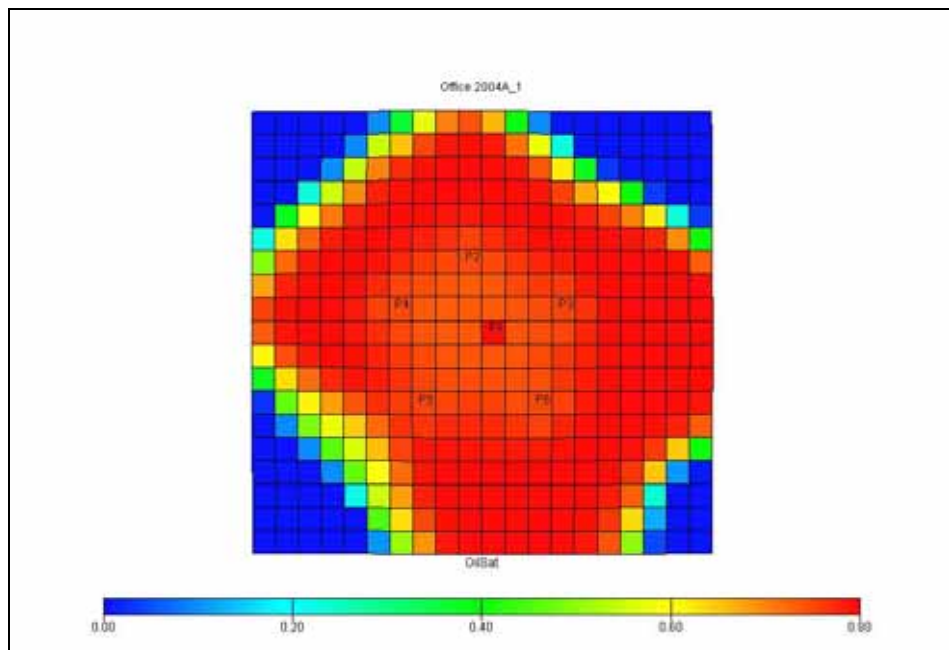


**Figure D-2** Distribution of oil saturation in December 1993.



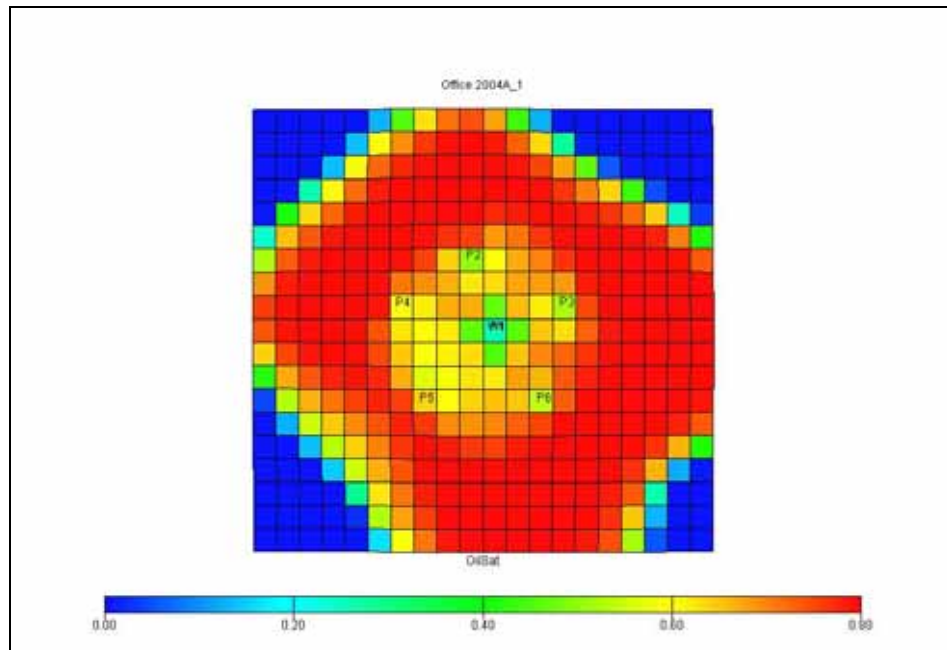


**Figure D-3** Distribution of oil saturation in January 1995.

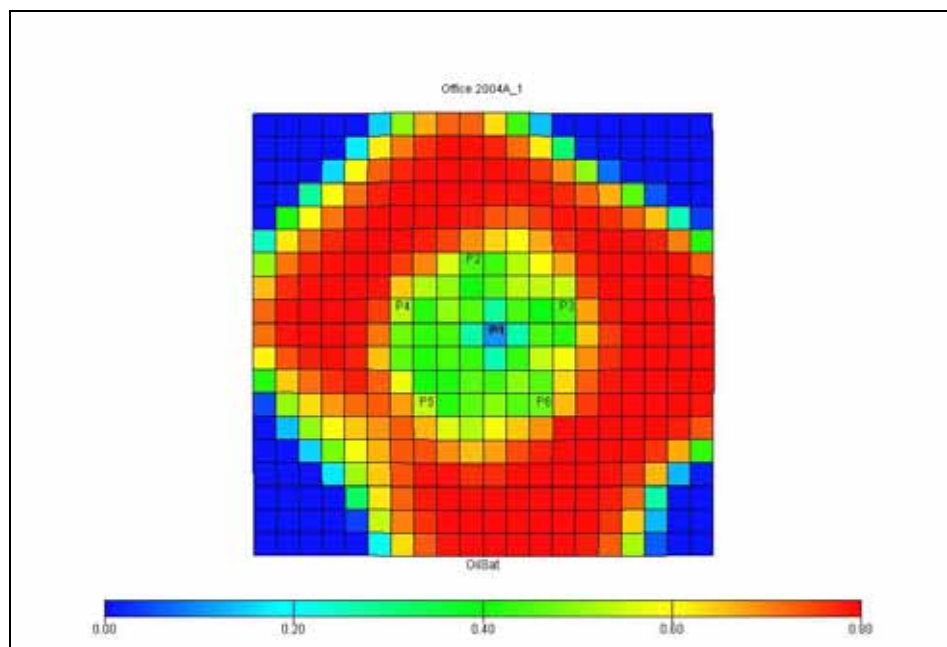


**Figure D-4** Distribution of oil saturation in January 2000.

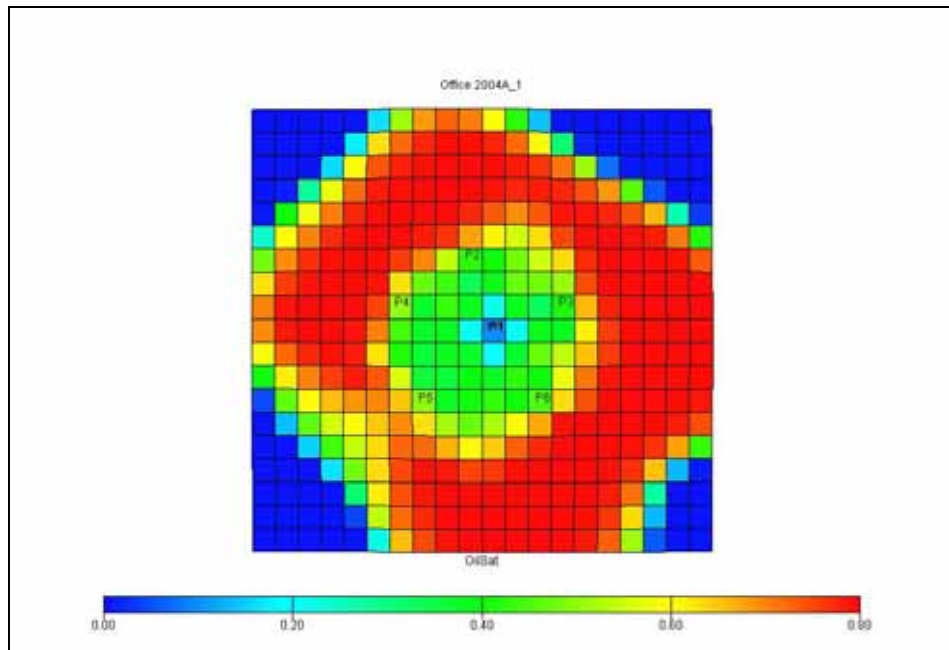


**Figure D-5** Distribution of oil saturation in January 2005.

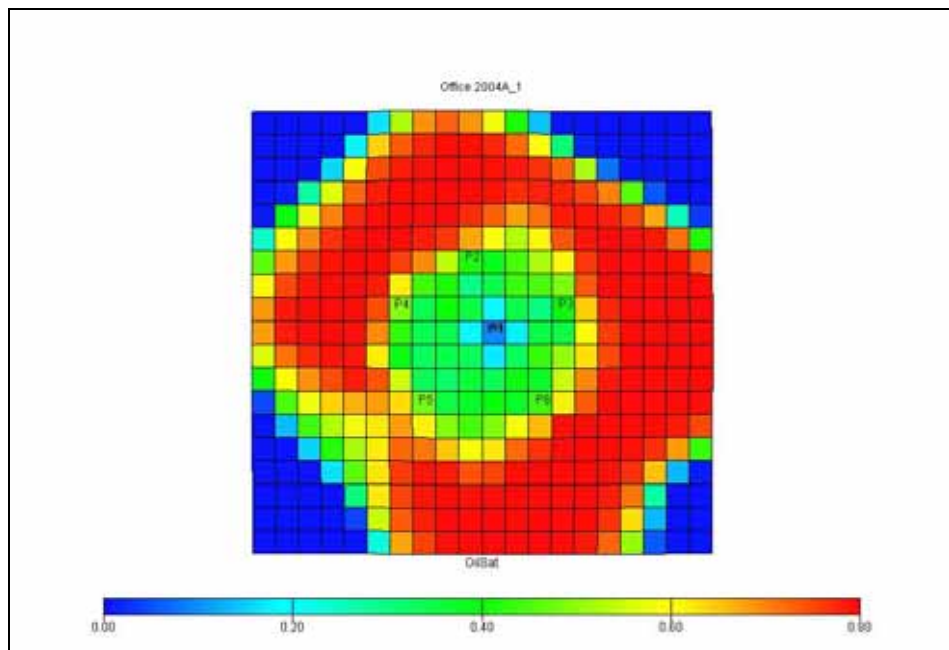


**Figure D-6** Distribution of oil saturation in January 2009.80

## APPENDIX E

### DISTRIBUTION OF OIL SATURATION : CASE 3

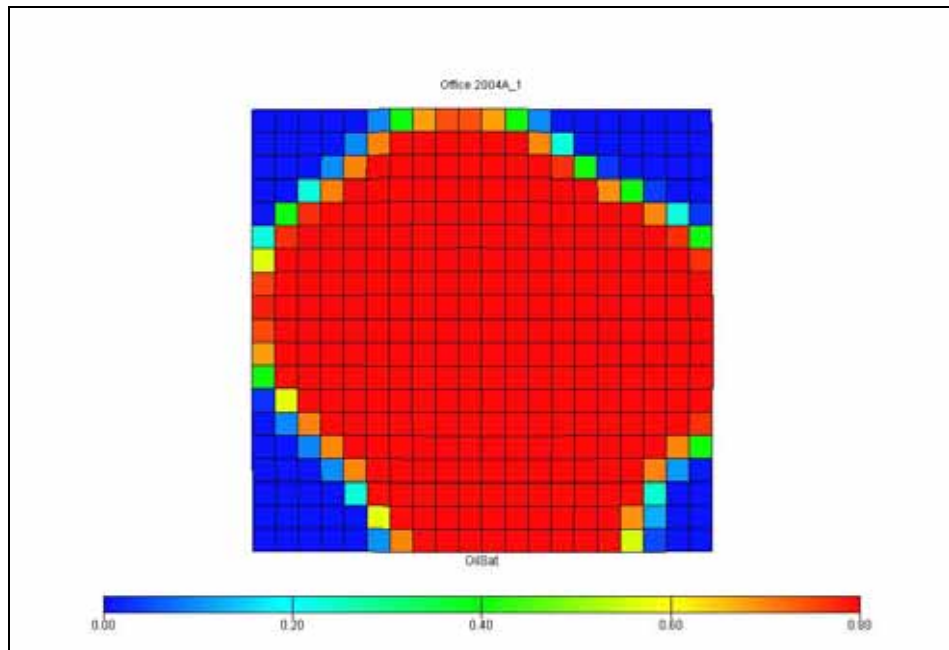


**Figure E-1** Distribution of oil saturation in July 1991.

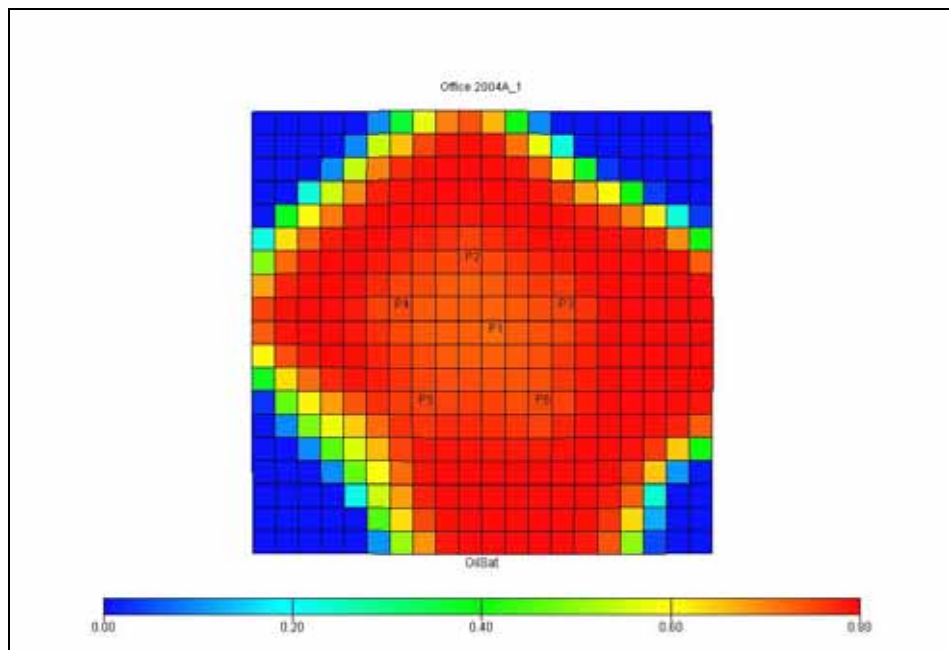


**Figure E-2** Distribution of oil saturation in December 1993.

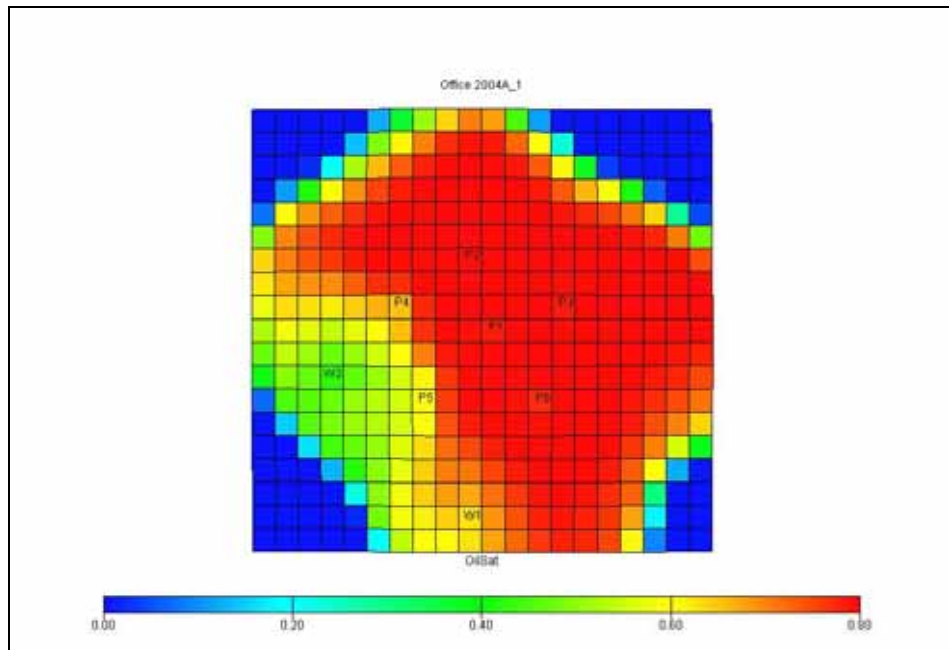


**Figure E-3** Distribution of oil saturation in January 1996.

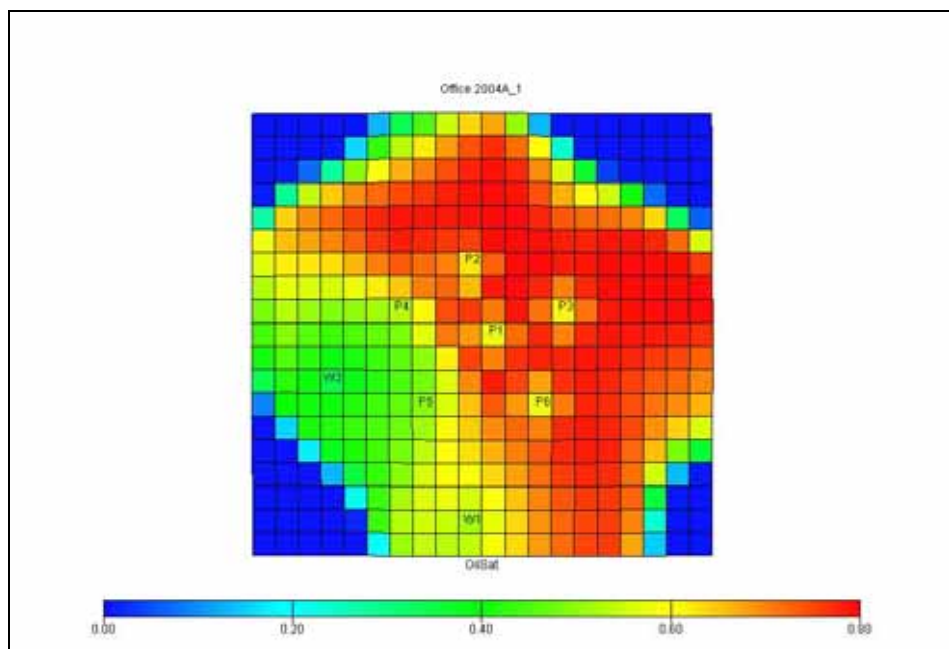


**Figure E-4** Distribution of oil saturation in January 2000.

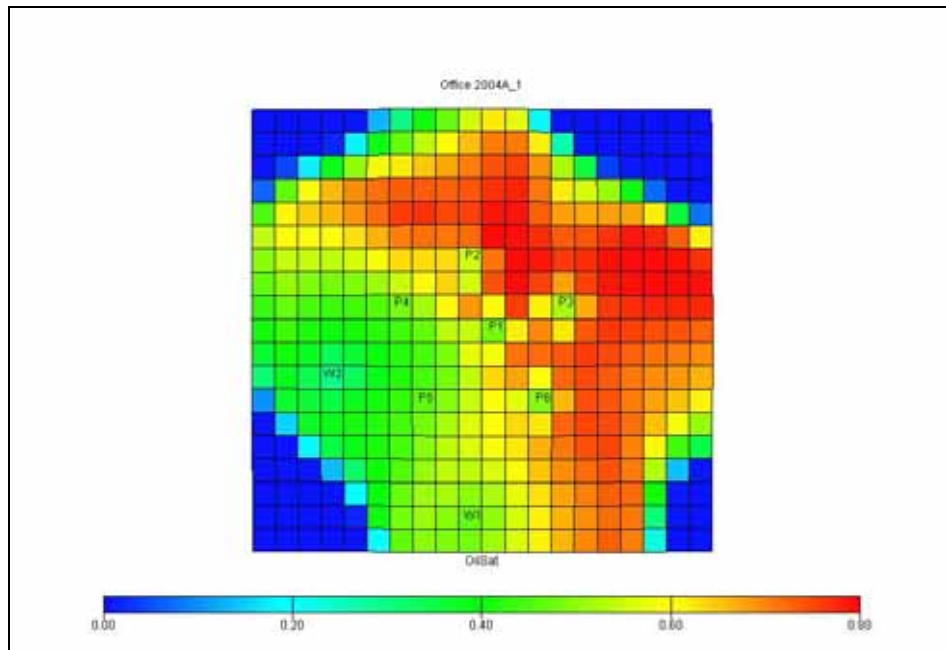


**Figure E-5** Distribution of oil saturation in January 2005.

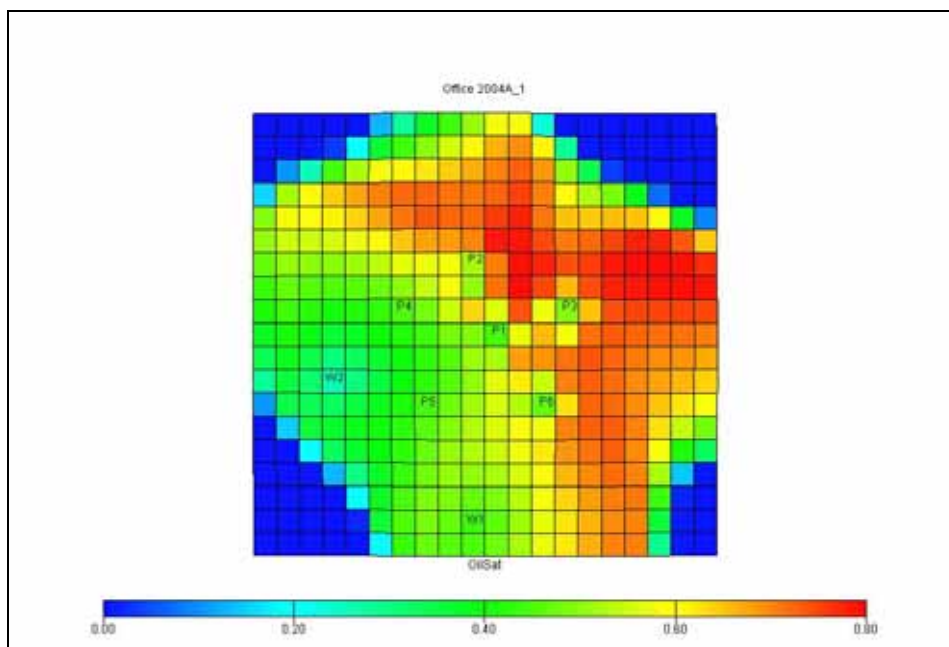


**Figure E-6** Distribution of oil saturation in January 2009.

## APPENDIX F

### DISTRIBUTION OF OIL SATURATION : CASE 4

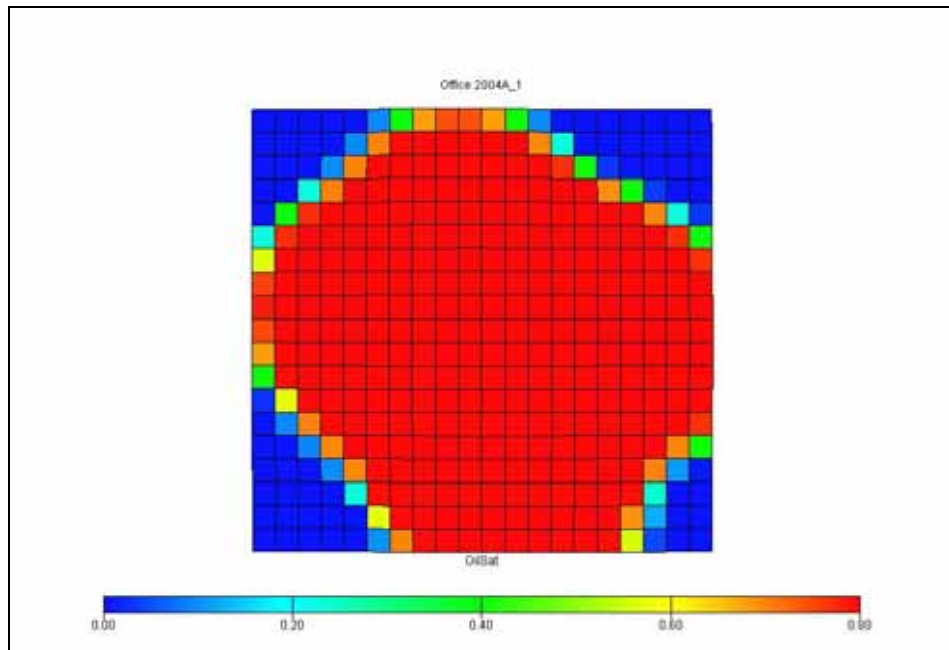


**Figure F-1** Distribution of oil saturation in July 1991.

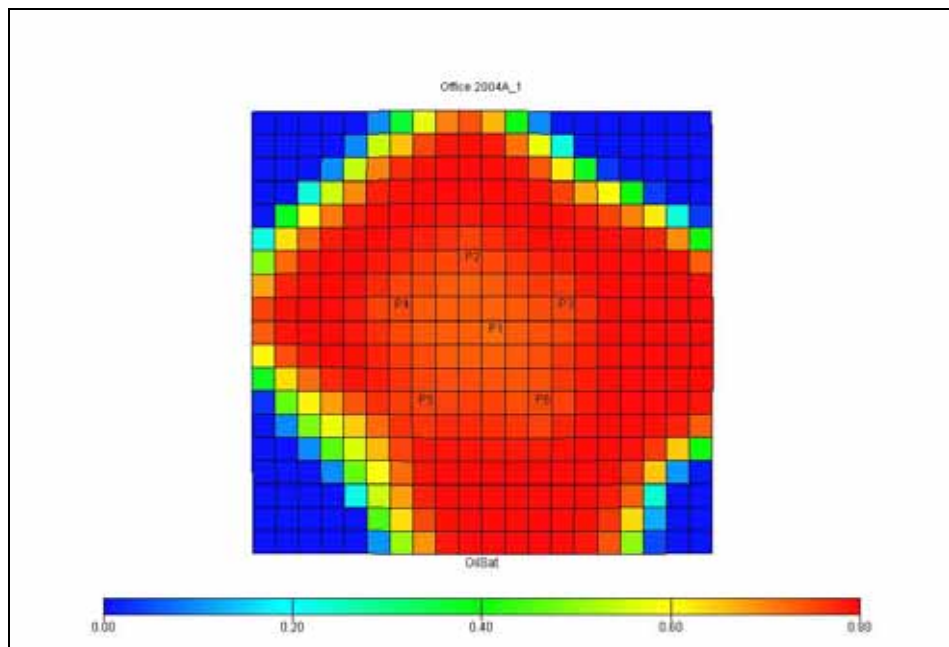


**Figure F-2** Distribution of oil saturation in December 1993.



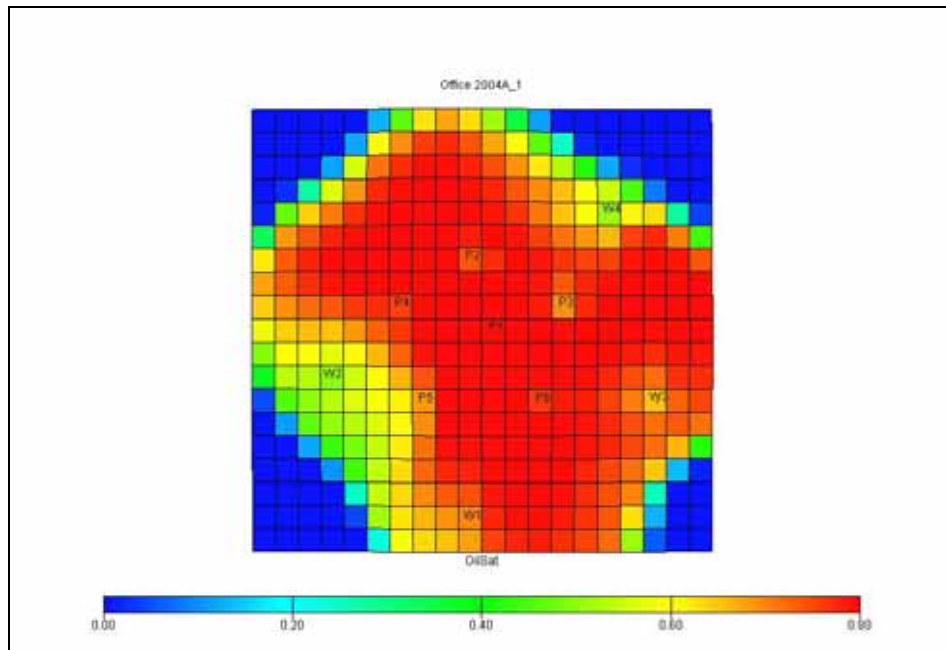


**Figure F-3** Distribution of oil saturation in January 1996.

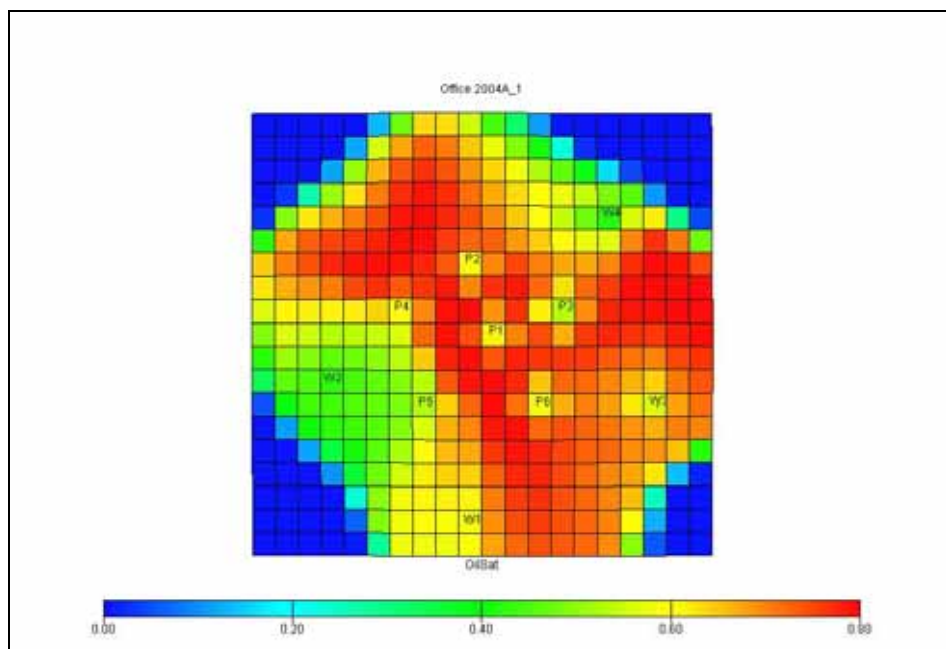


**Figure F-4** Distribution of oil saturation in January 2000.

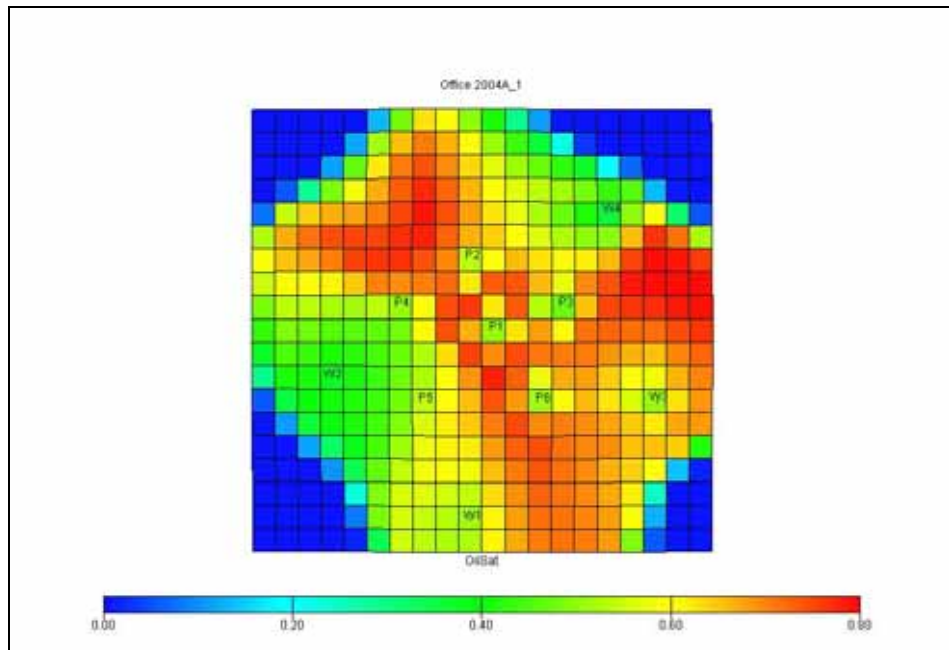


**Figure F-5** Distribution of oil saturation in January 2005.

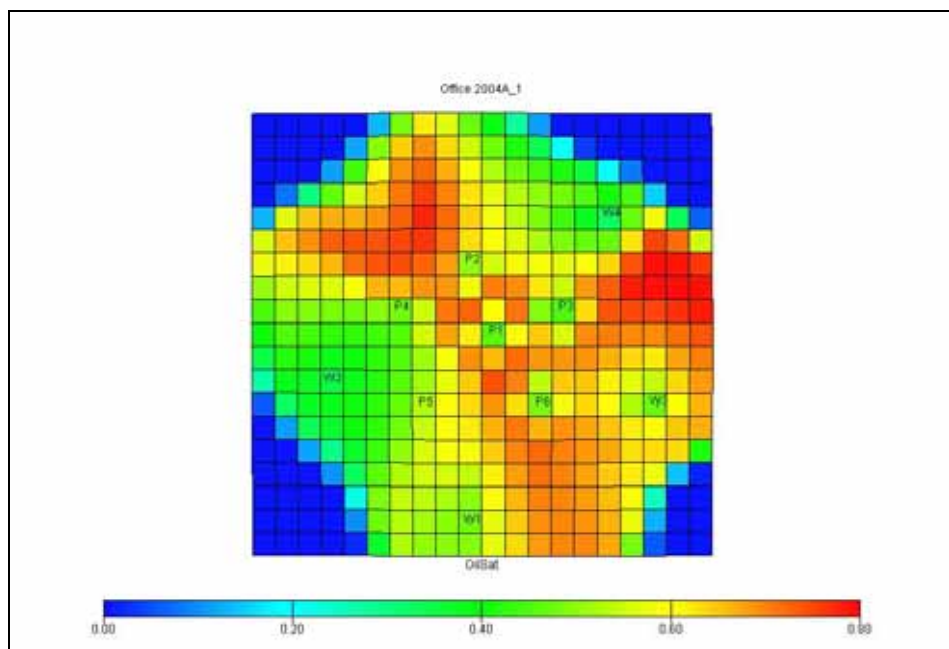


**Figure F-6** Distribution of oil saturation in January 2009.

## APPENDIX G

### DISTRIBUTION OF OIL SATURATION : CASE 5

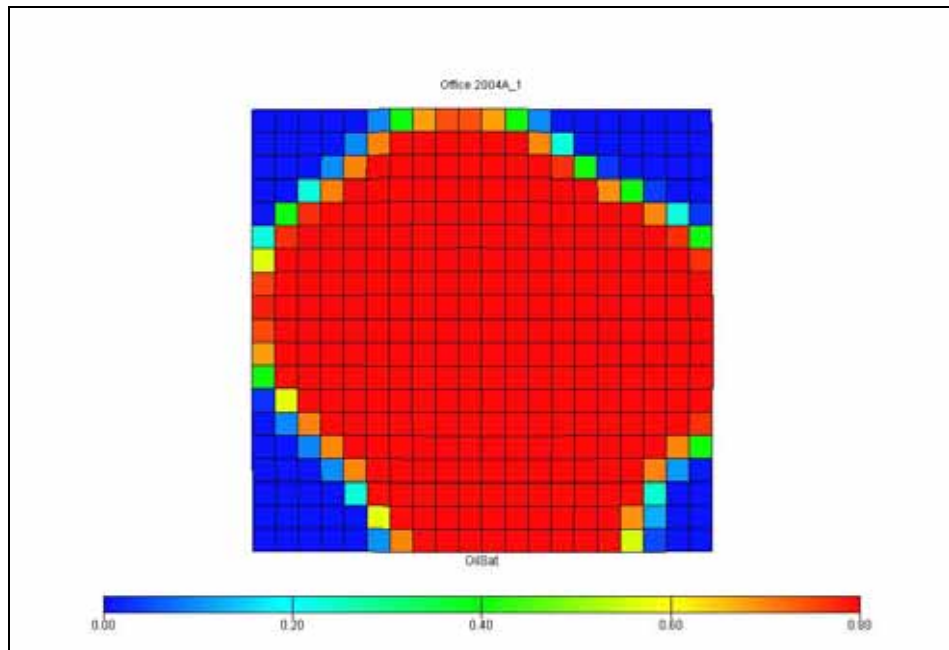


**Figure G-1** Distribution of oil saturation in July 1991.

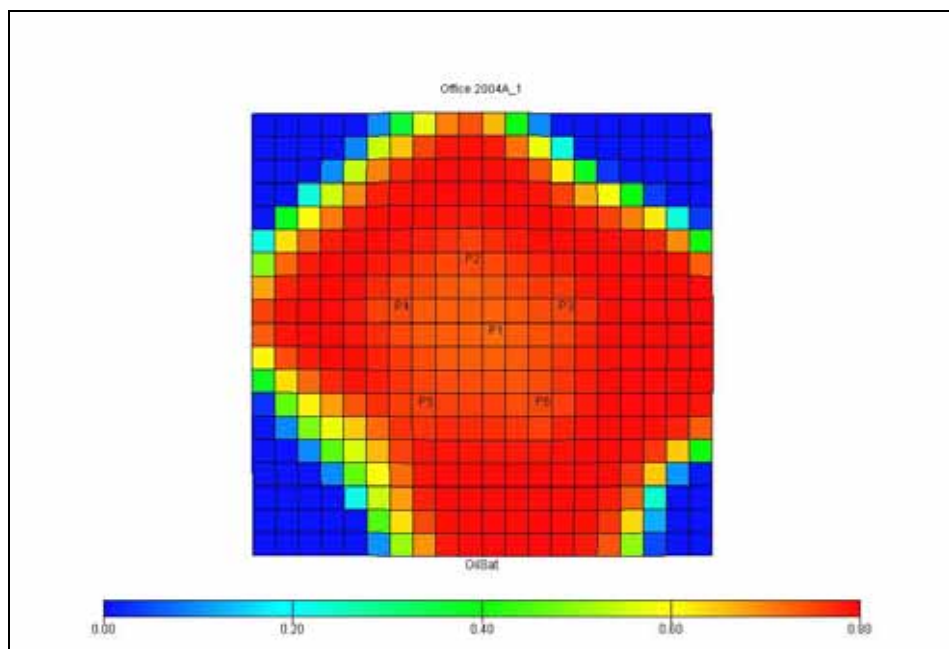


**Figure G-2** Distribution of oil saturation in December 1993.

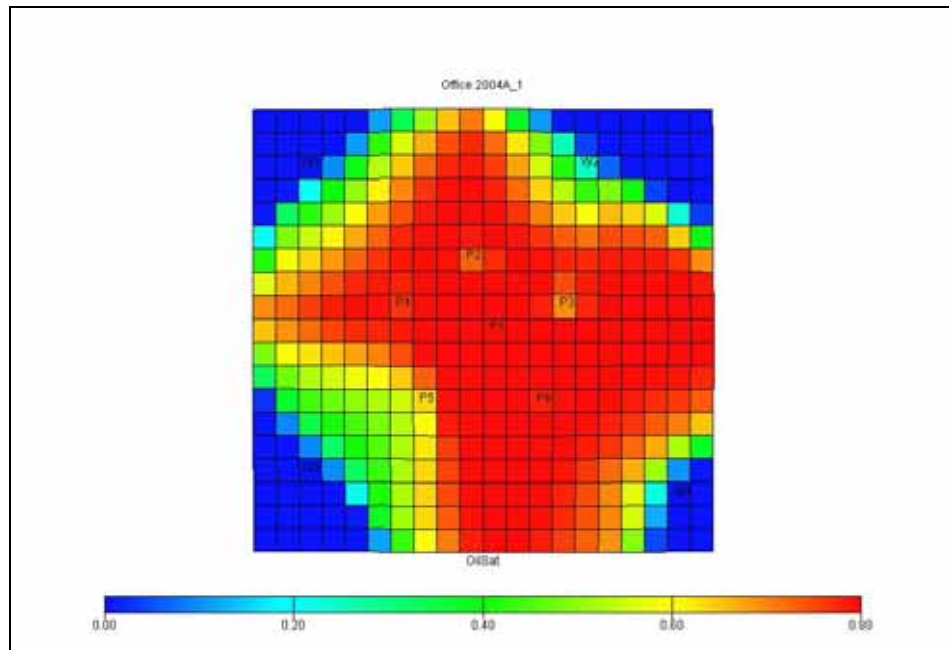


**Figure G-3** Distribution of oil saturation in January 1996.

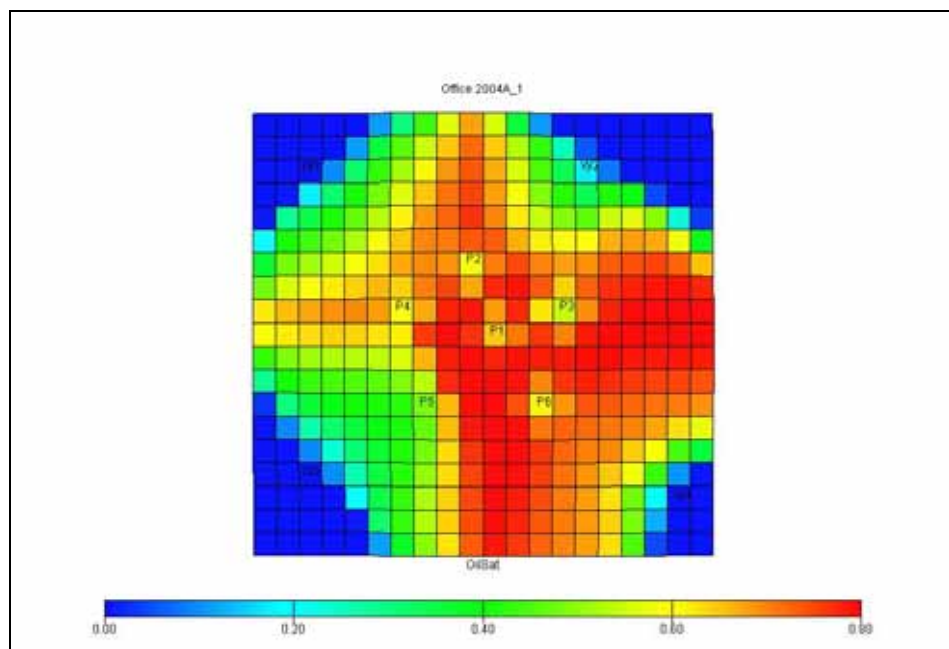


**Figure G-4** Distribution of oil saturation in January 2000.

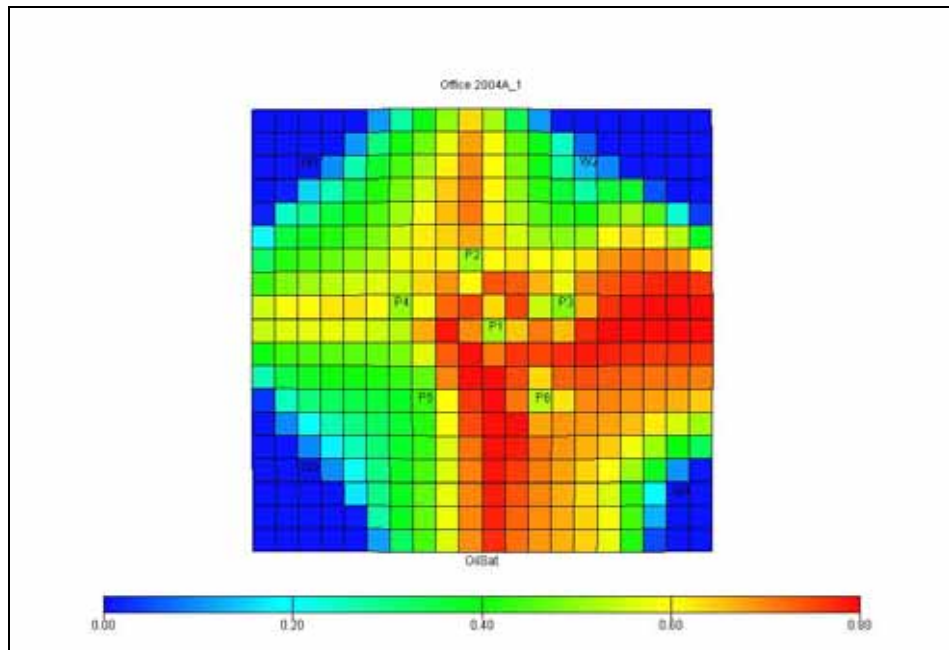


**Figure G-5** Distribution of oil saturation in January 2005.

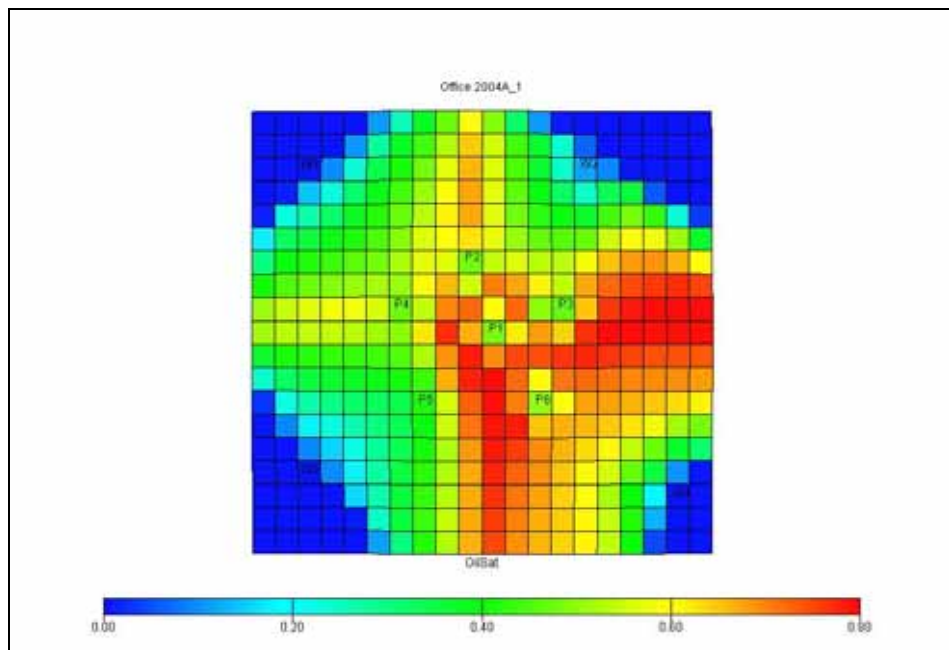


**Figure G-6** Distribution of oil saturation in January 2009.

APPENDIX H

WELL RESULTS OF CASE 1

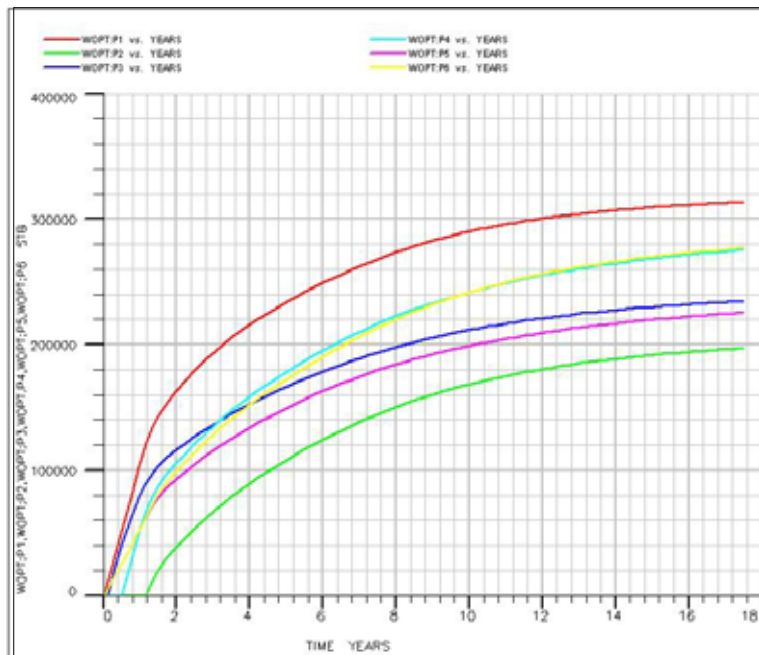


**Figure H-1** Cumulative Oil Production versus Time.

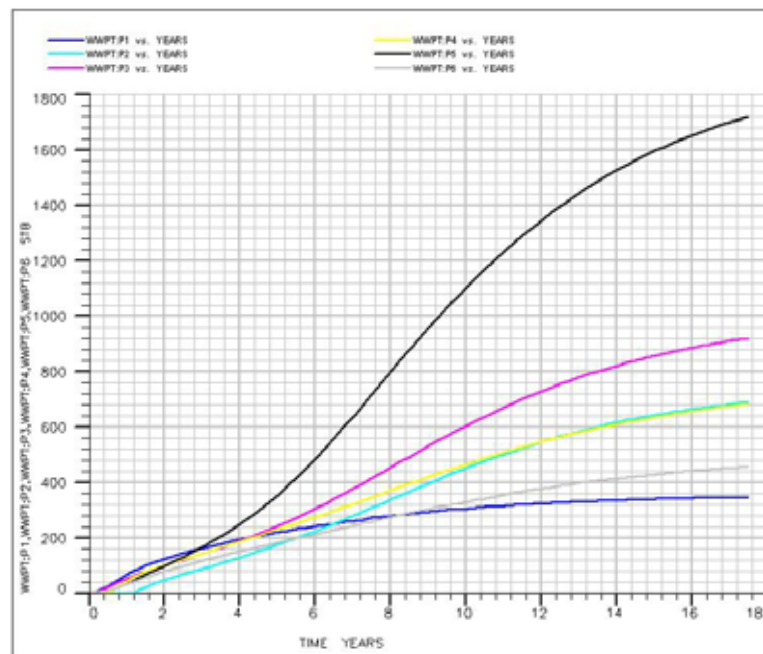


**Figure H-2** Cumulative Water Production versus Time.



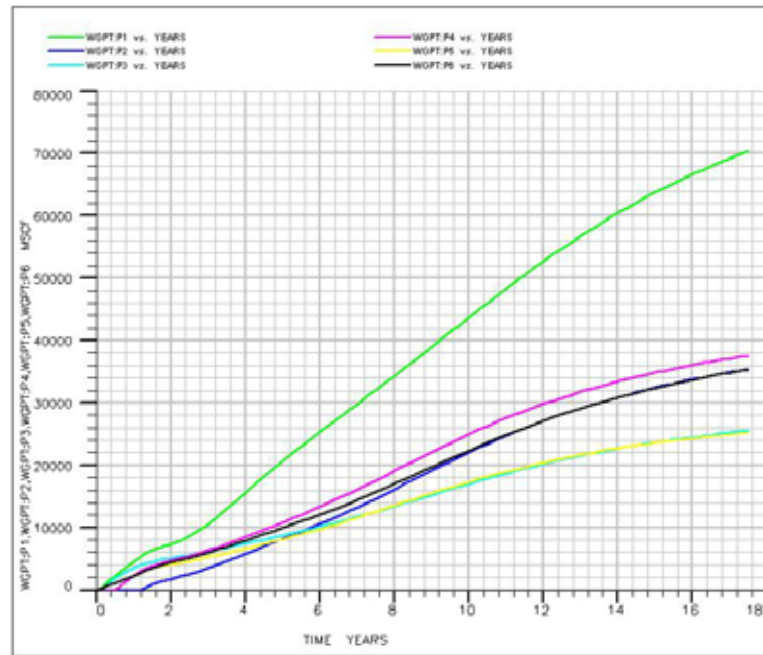


**Figure H-3** Cumulative Gas Production versus Time.

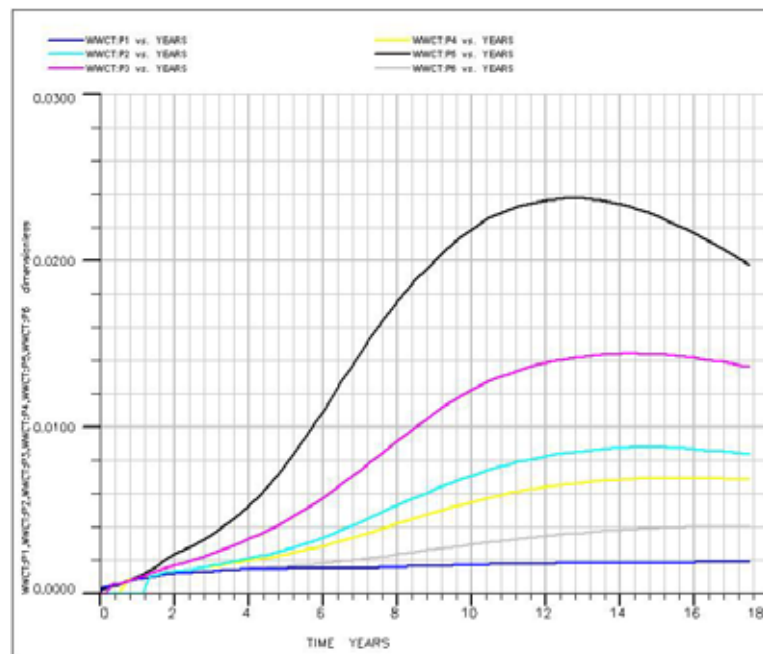


**Figure H-4** Water Cut versus Time.

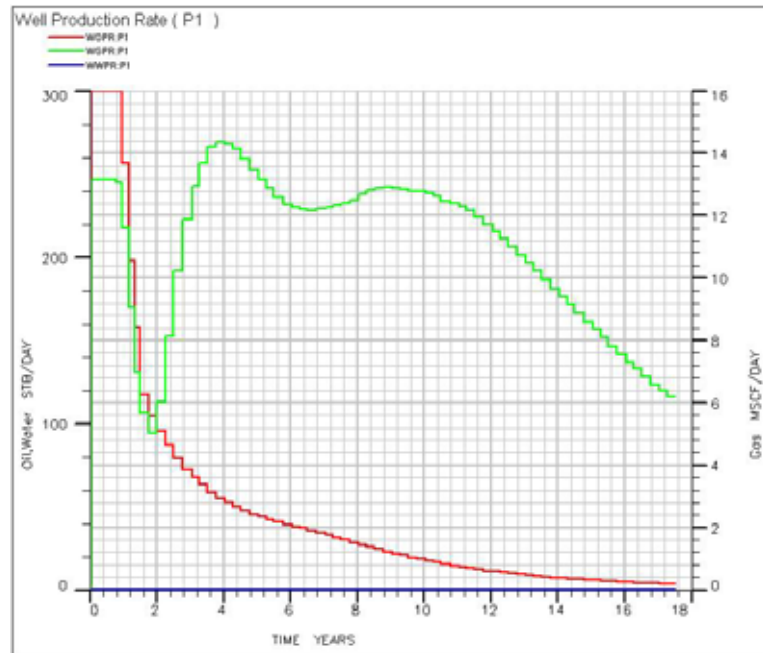


**Figure H-5** Oil, Water, and Gas Production Rate of Well P1 versus Time.

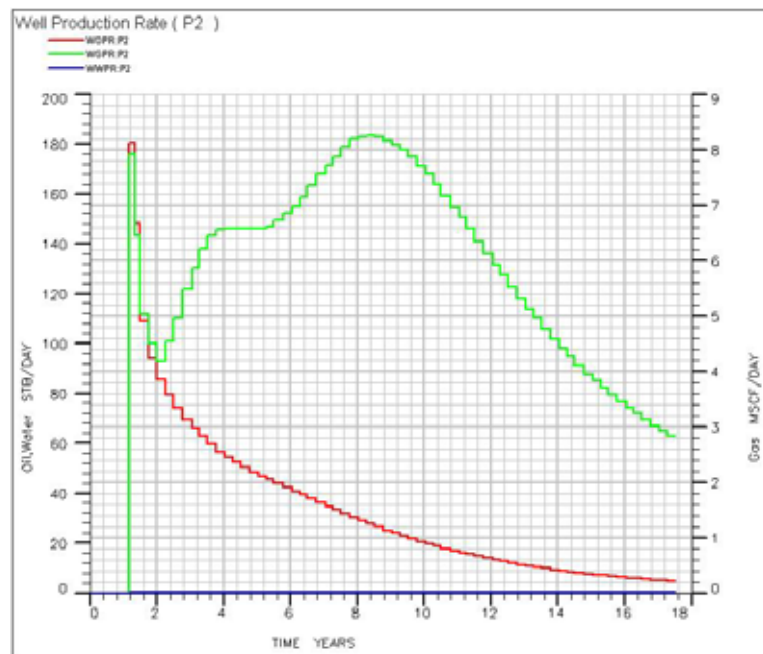


**Figure H-6** Oil, Water, and Gas Production Rate of Well P2 versus Time.

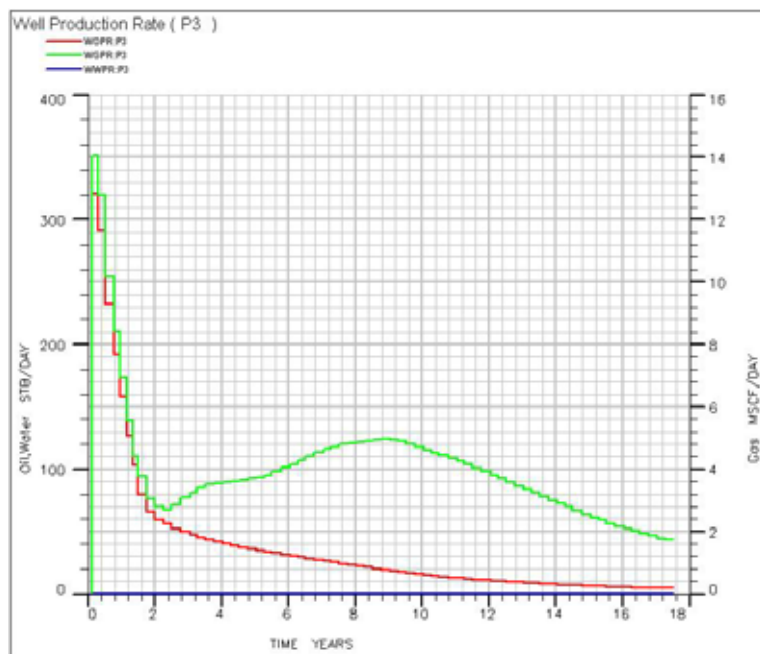


**Figure H-7** Oil, Water, and Gas Production Rate of Well P3 versus Time.

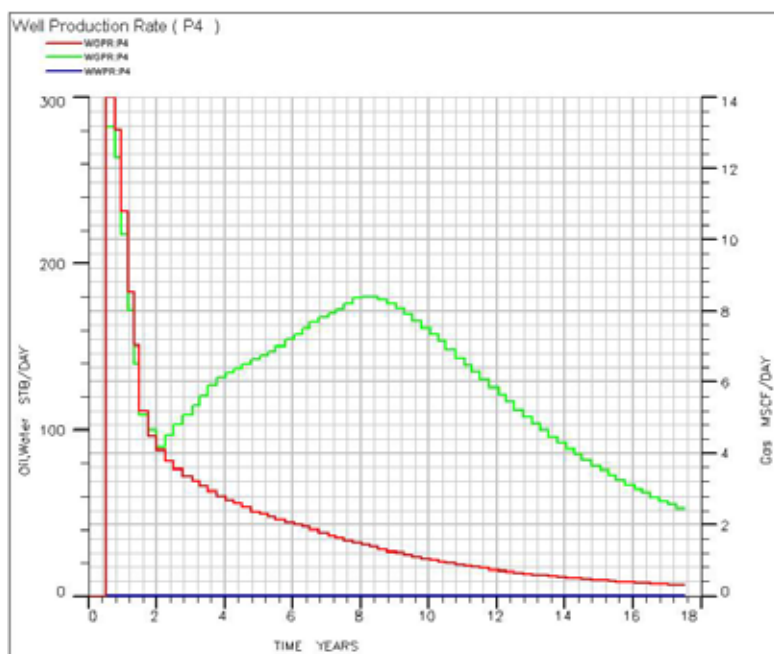


**Figure H-8** Oil, Water, and Gas Production Rate of Well P4 versus Time.

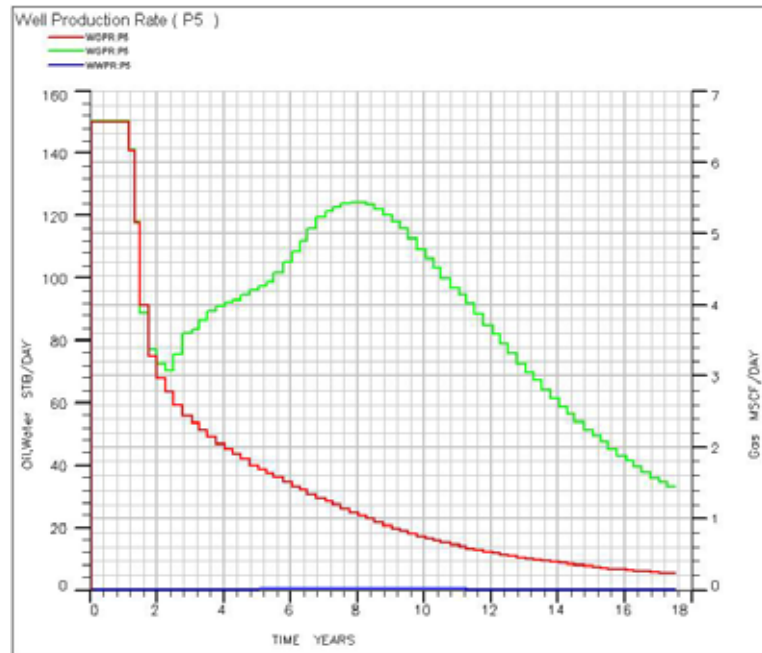


**Figure H-9** Oil, Water, and Gas Production Rate of Well P5 versus Time.

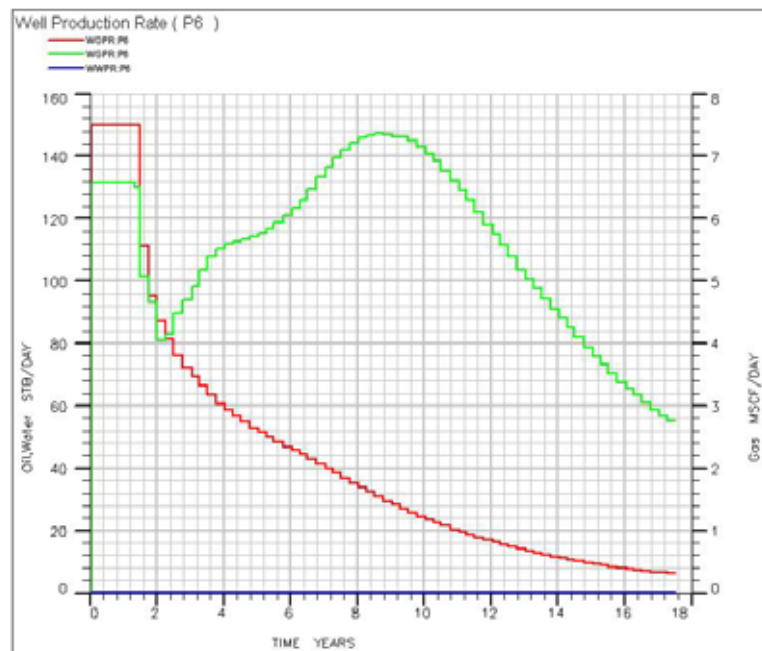


**Figure H-10** Oil, Water, and Gas Production Rate of Well P6 versus Time.

APPENDIX I

WELL RESULTS OF CASE 2

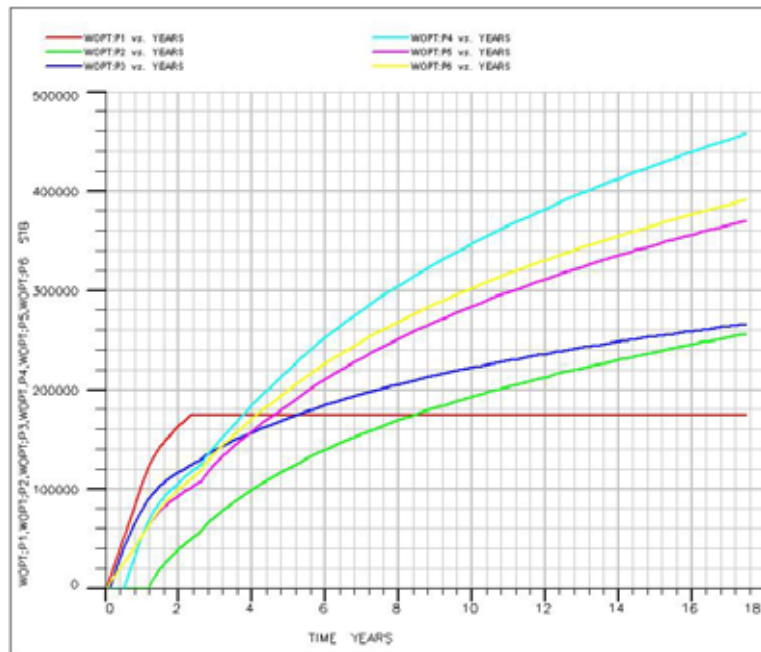


**Figure I-1** Cumulative Oil Production versus Time.

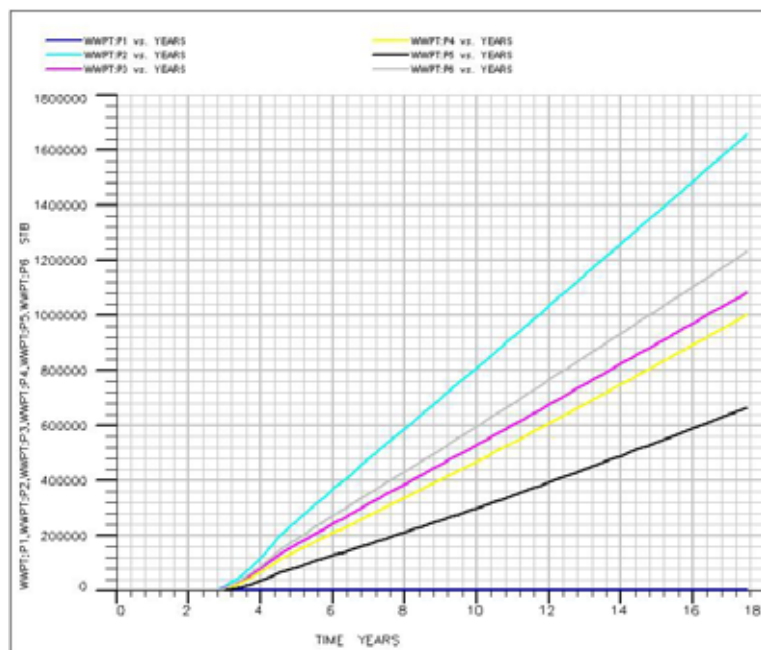


**Figure I-2** Cumulative Water Production versus Time.

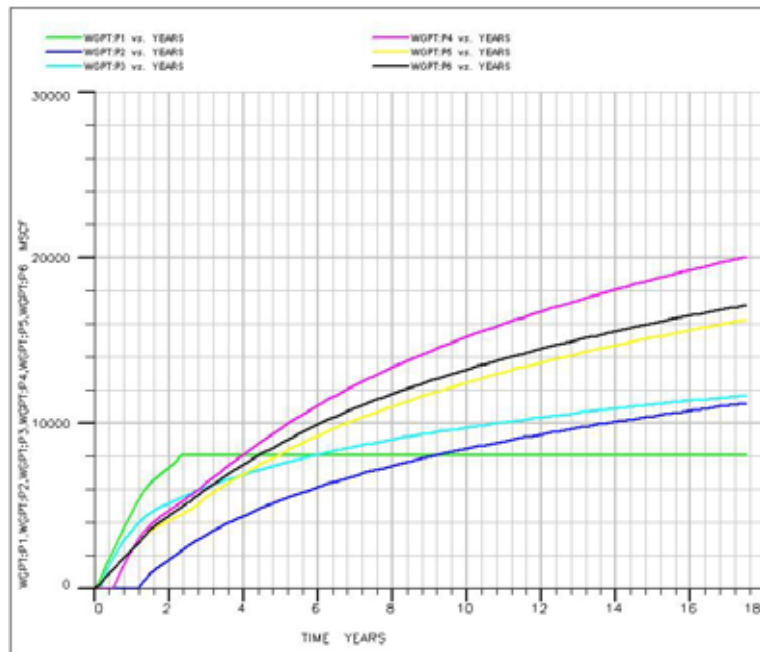


**Figure I-3** Cumulative Gas Production versus Time.

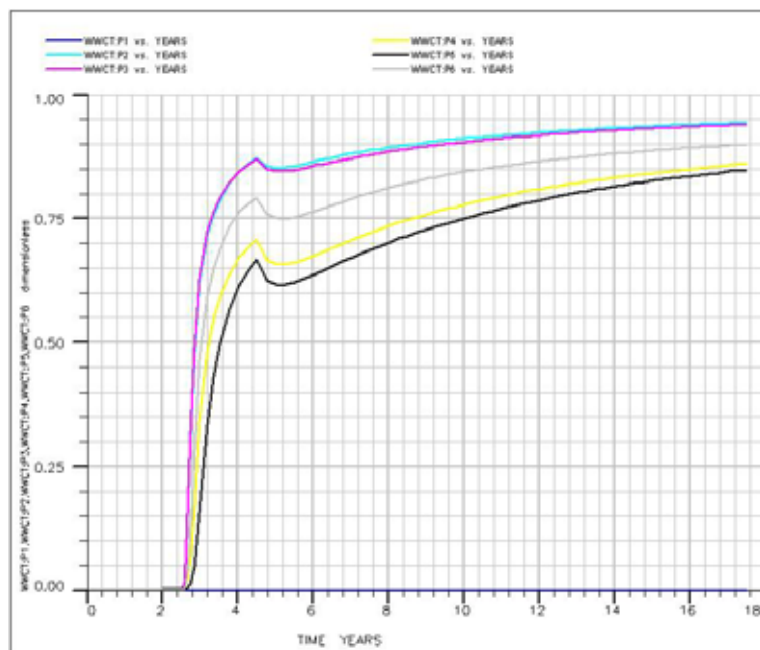


**Figure I-4** Water Cut versus Time.

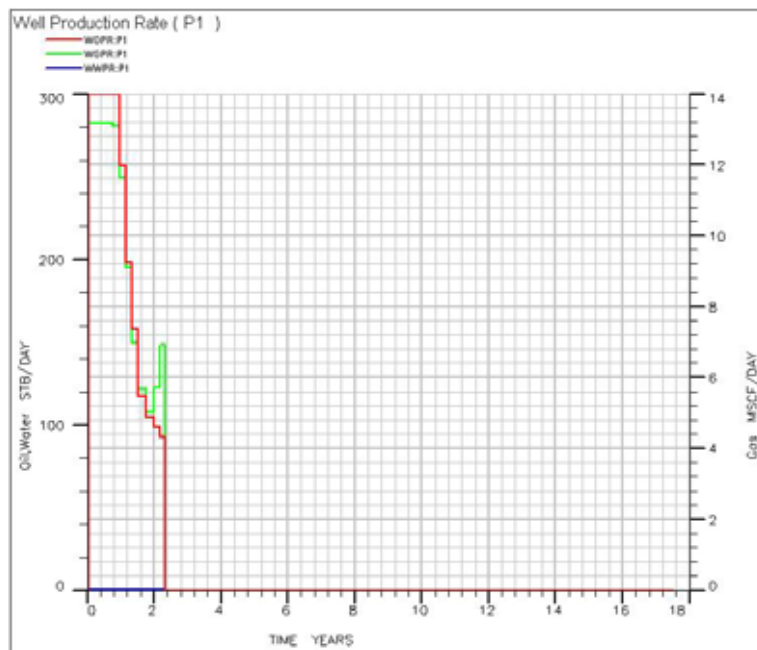


**Figure I-5** Oil, Water, and Gas Production Rate of Well P1 versus Time.

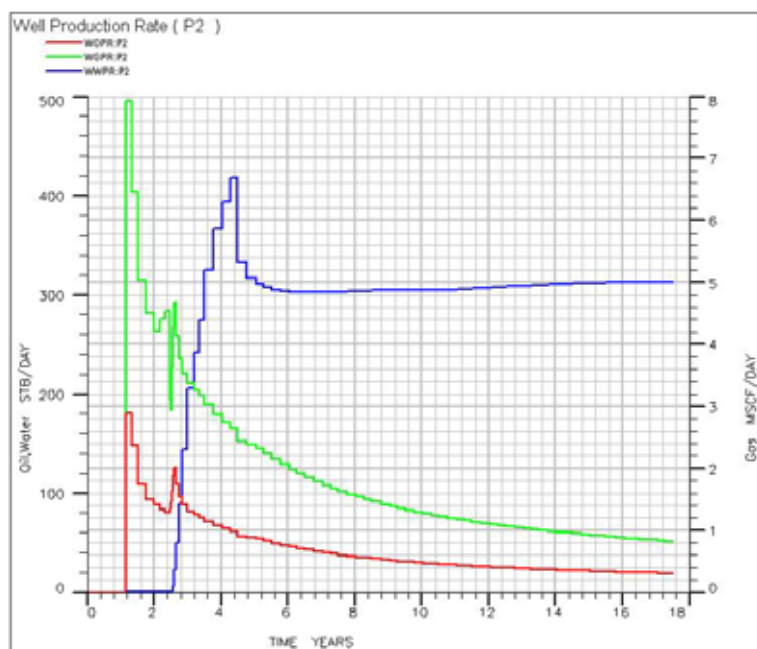


**Figure I-6** Oil, Water, and Gas Production Rate of Well P2 versus Time.



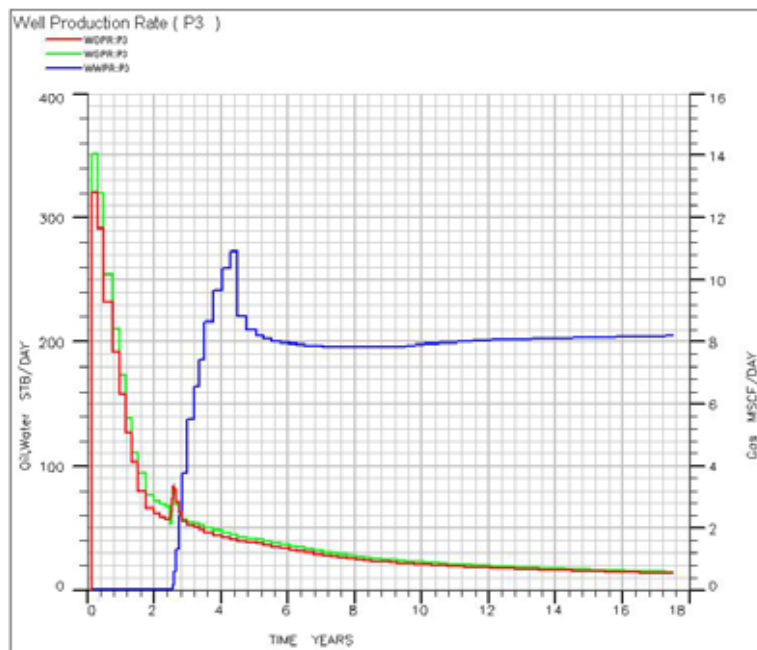


**Figure I-7** Oil, Water, and Gas Production Rate of Well P3 versus Time.

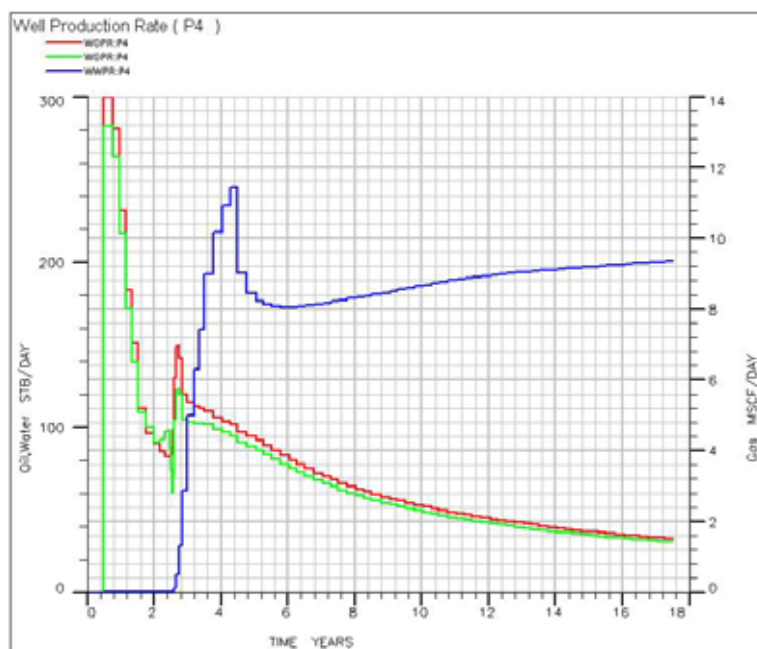


**Figure I-8** Oil, Water, and Gas Production Rate of Well P4 versus Time.

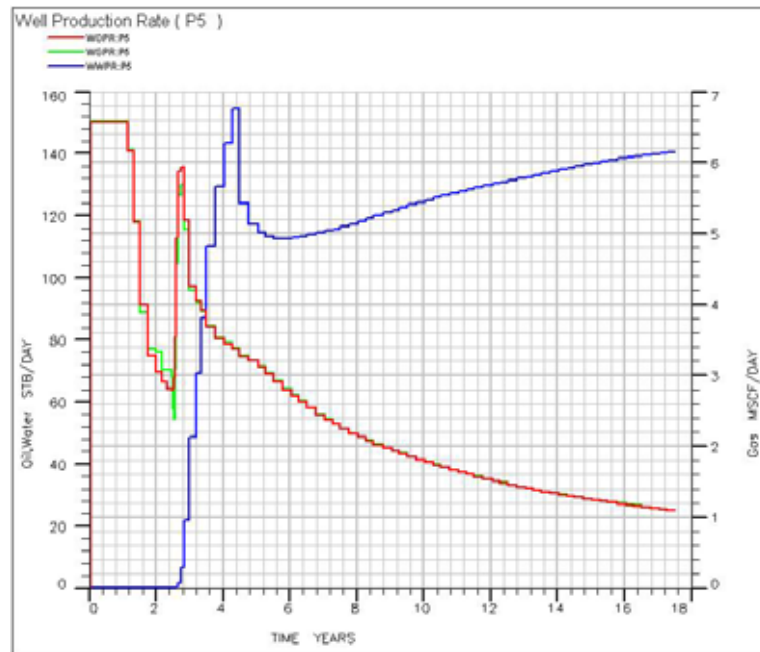


**Figure I-9** Oil, Water, and Gas Production Rate of Well P5 versus Time.

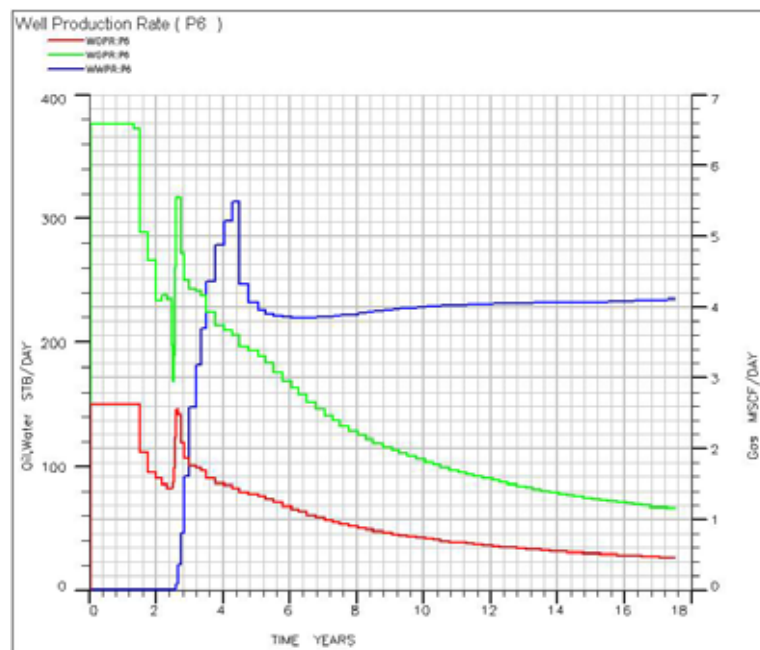


**Figure I-10** Oil, Water, and Gas Production Rate of Well P6 versus Time.

APPENDIX J

WELL RESULTS OF CASE 3

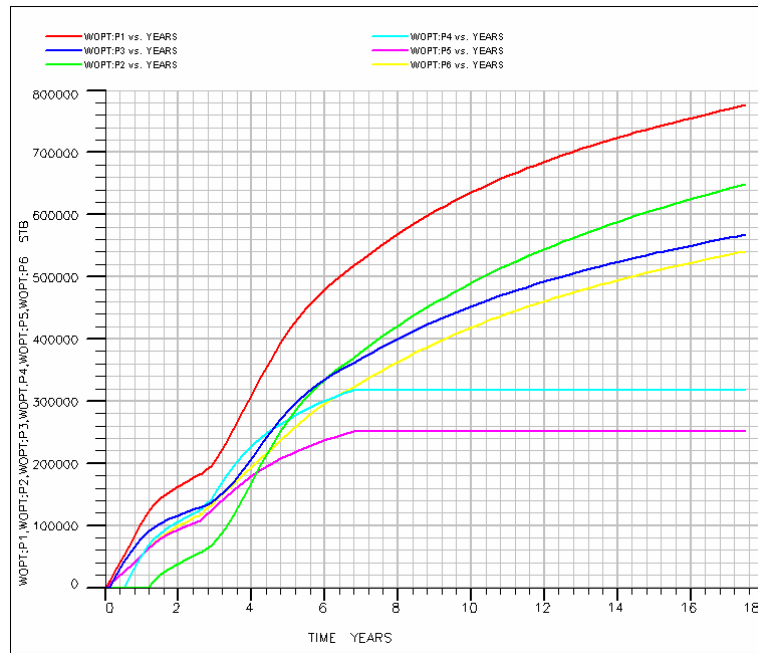


**Figure J-1** Cumulative Oil Production versus Time.

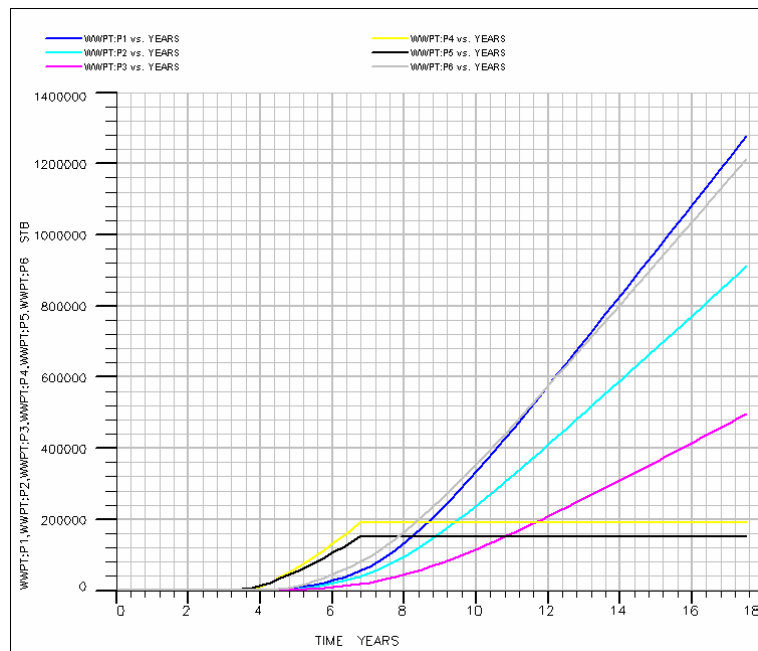


**Figure J-2** Cumulative Water Production versus Time.

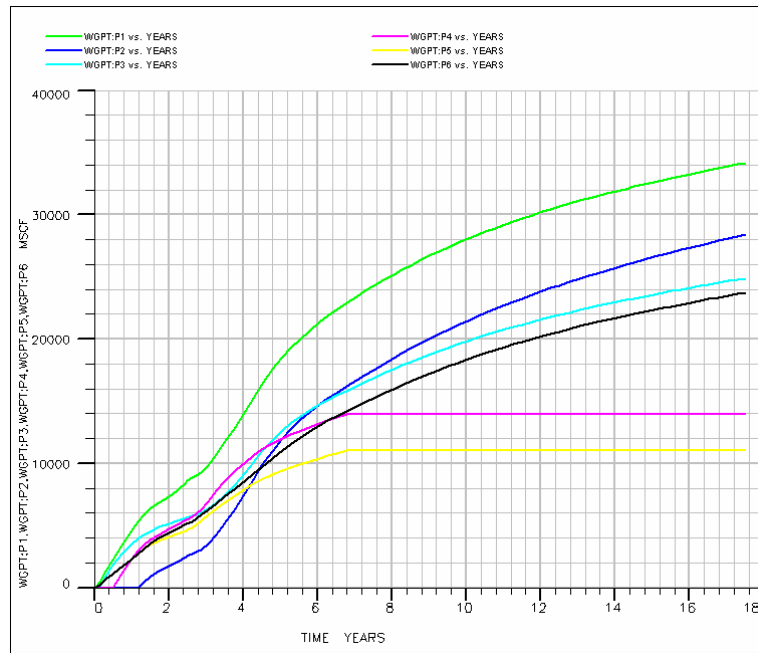


**Figure J-3** Cumulative Gas Production versus Time.

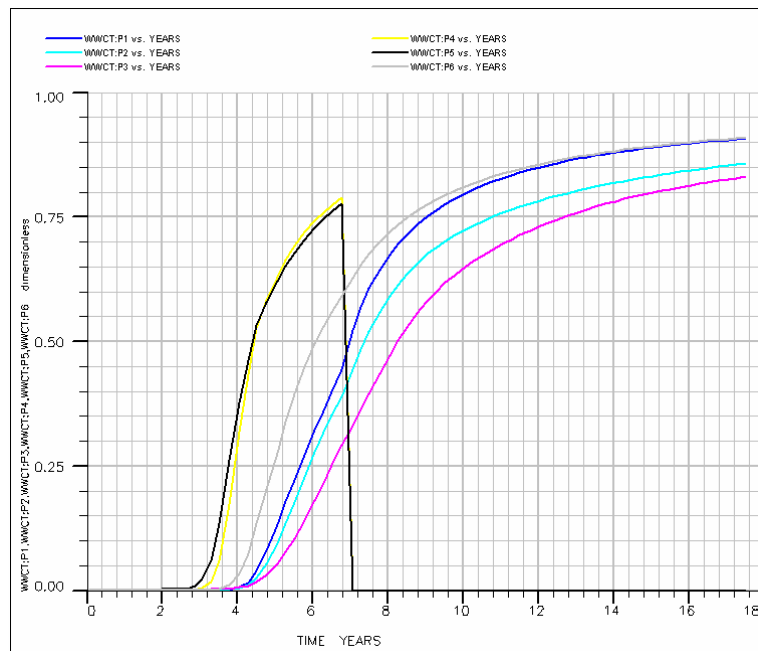


**Figure J-4** Water Cut versus Time.

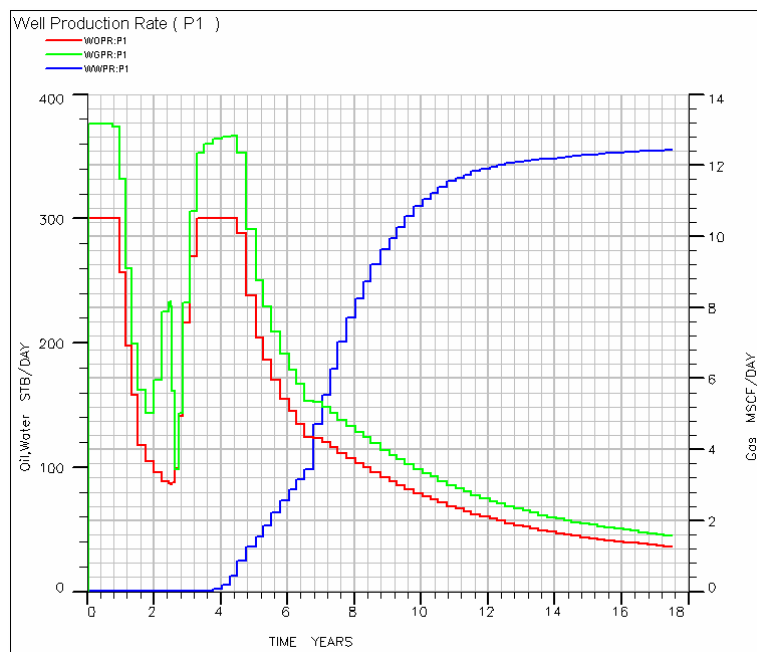


**Figure J-5** Oil, Water, and Gas Production Rate of Well P1 versus Time.

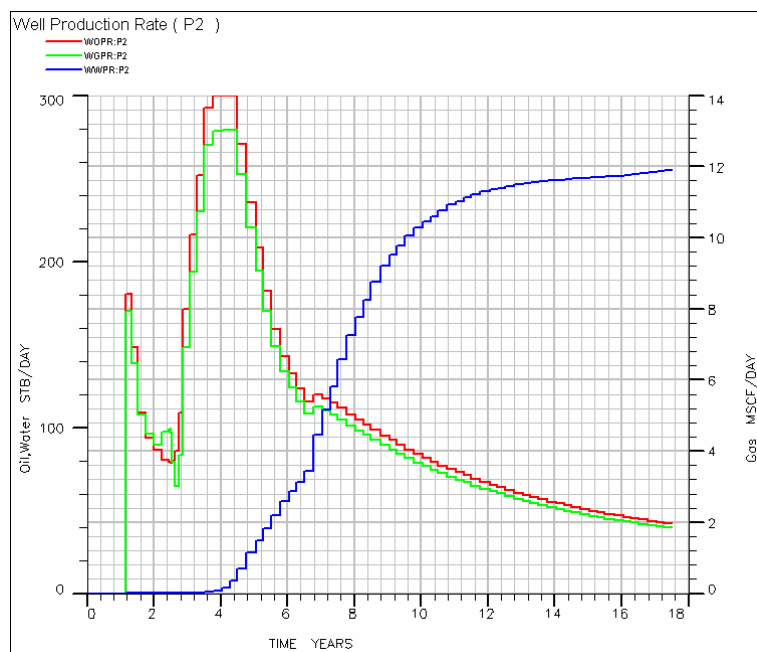


**Figure J-6** Oil, Water, and Gas Production Rate of Well P2 versus Time.

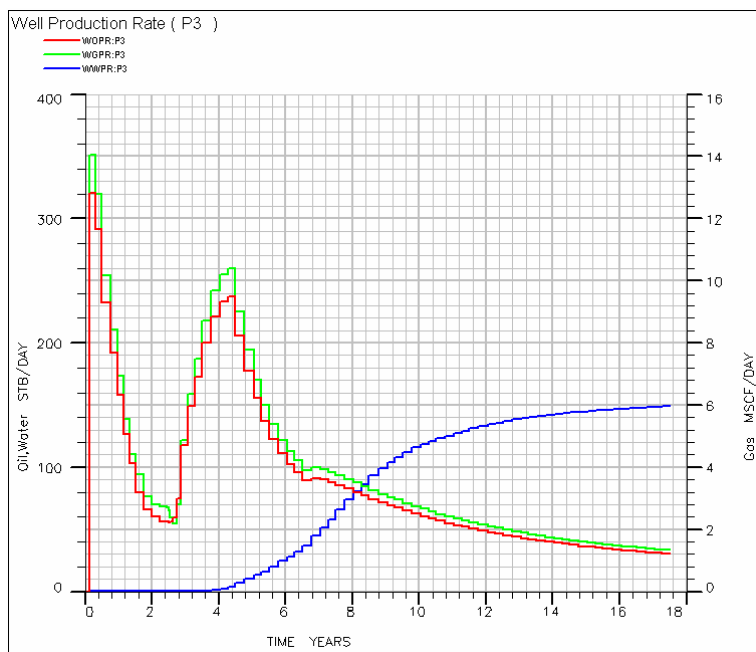


Figure J-7 Oil, Water, and Gas Production Rate of Well 31 versus Time.

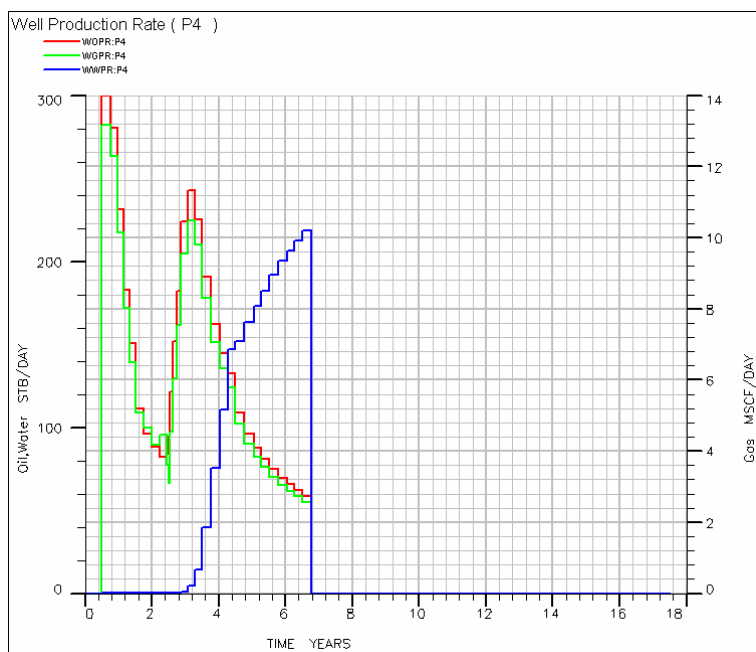
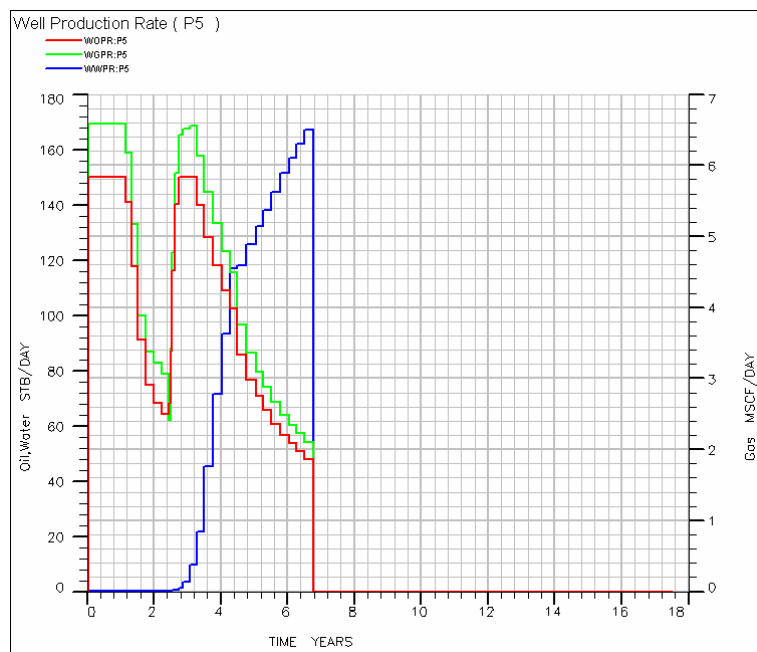
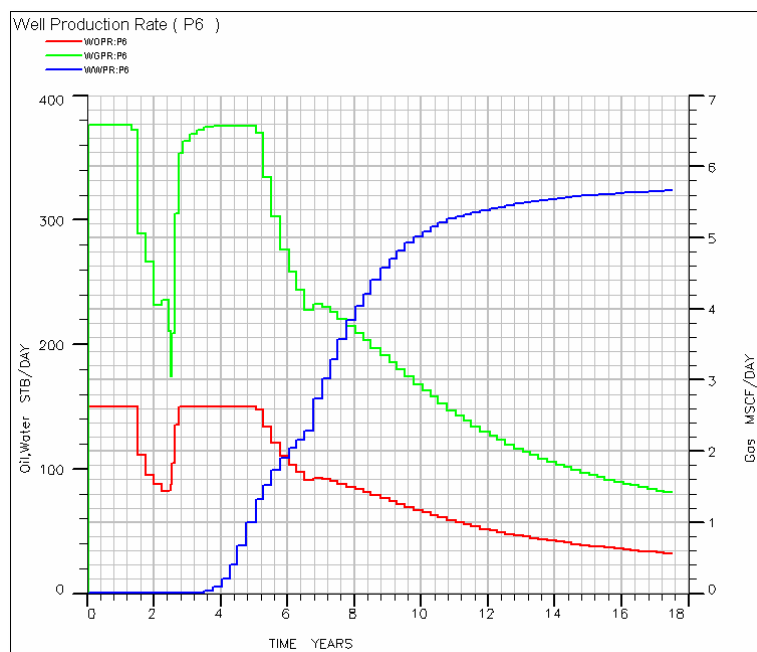


Figure J-8 Oil, Water, and Gas Production Rate of Well P1 versus Time.



**Figure J-9** Oil, Water, and Gas Production Rate of Well P5 versus Time.



**Figure J-10** Oil, Water, and Gas Production Rate of Well P6 versus Time.



APPENDIX K

WELL RESULTS OF CASE 4

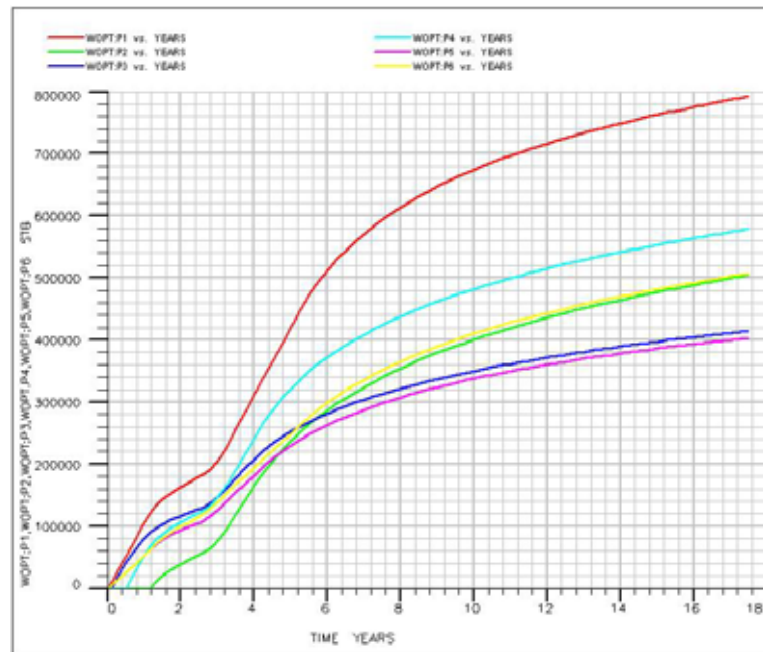


Figure K-1 Cumulative Oil Production Rate versus Time.

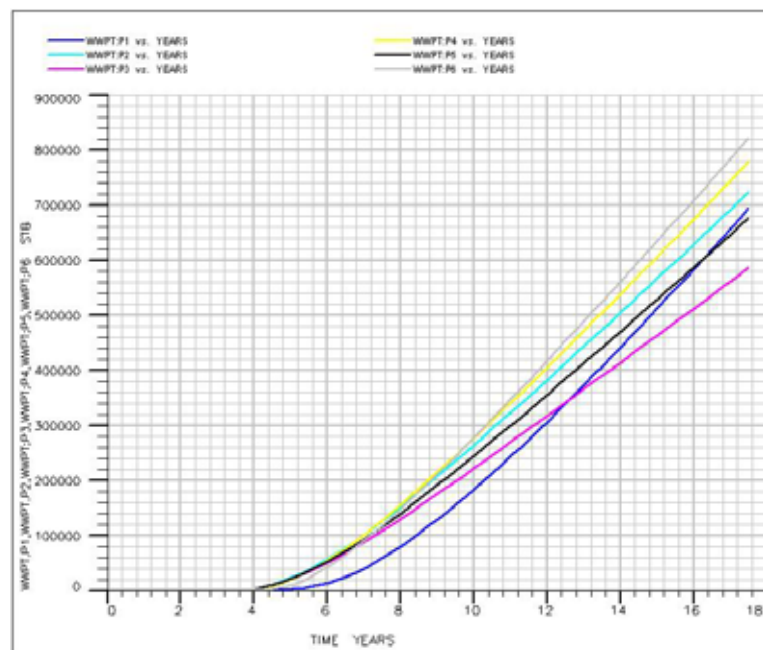
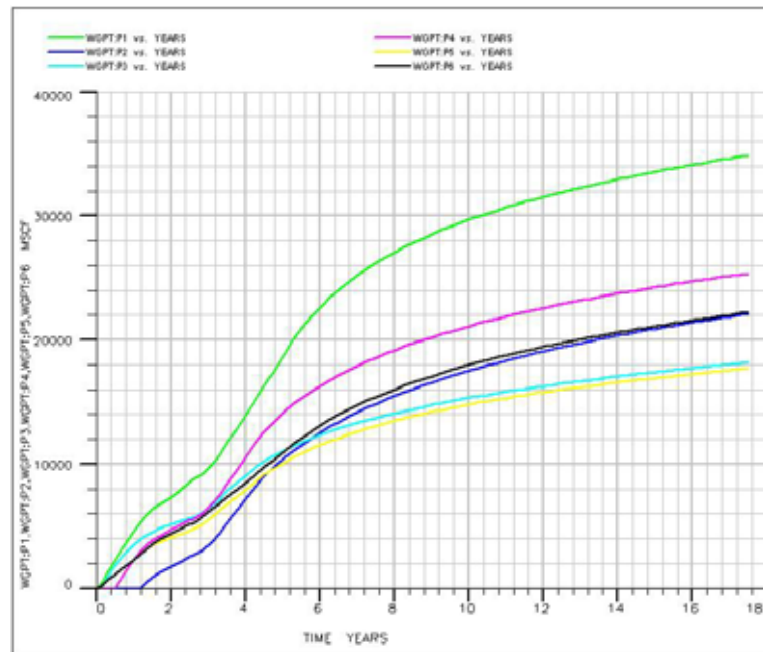
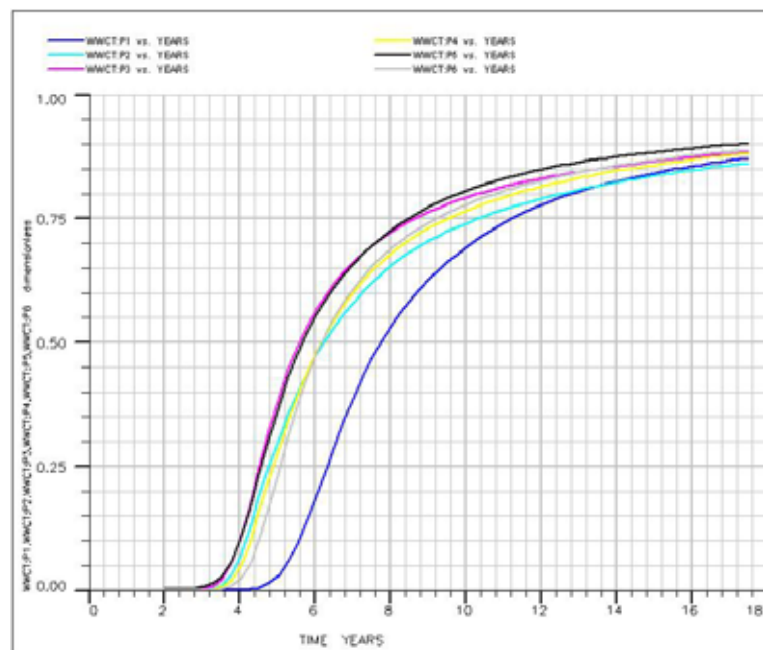


Figure K-2 Cumulative Water Production Rate versus Time.



**Figure K-3** Cumulative Gas Production Rate versus Time.



**Figure K-4** Water Cut versus Time.

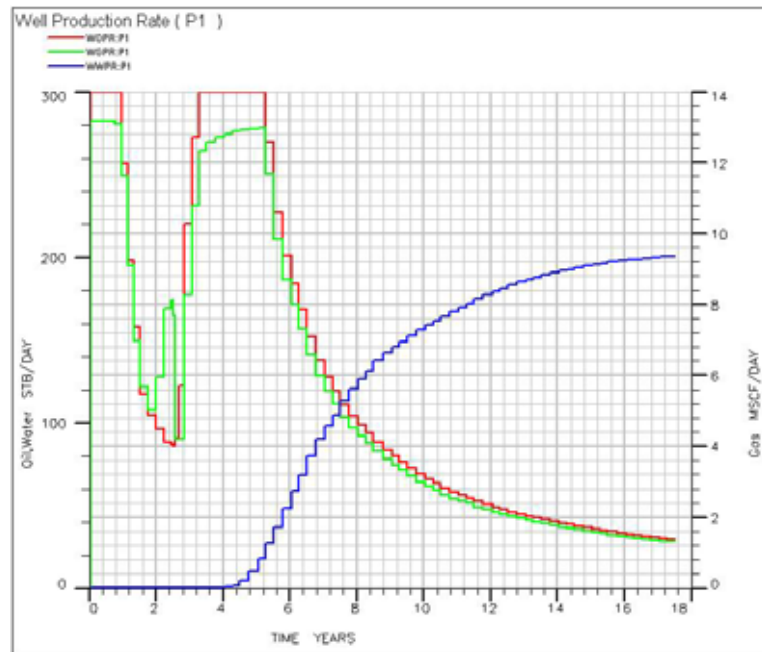


**Figure K-5** Oil, Water, and Gas Production Rate of Well P1 versus Time.

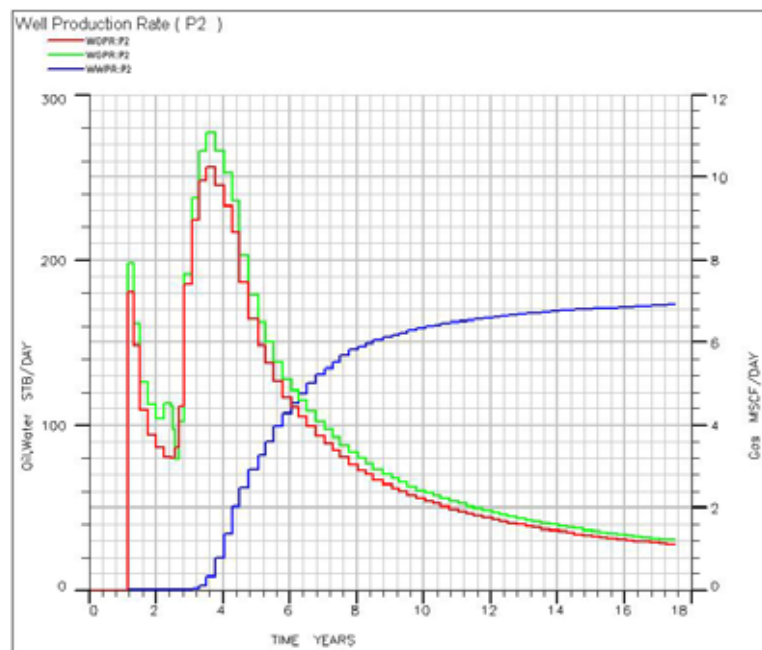


**Figure K-6** Oil, Water, and Gas Production Rate of Well P2 versus Time.

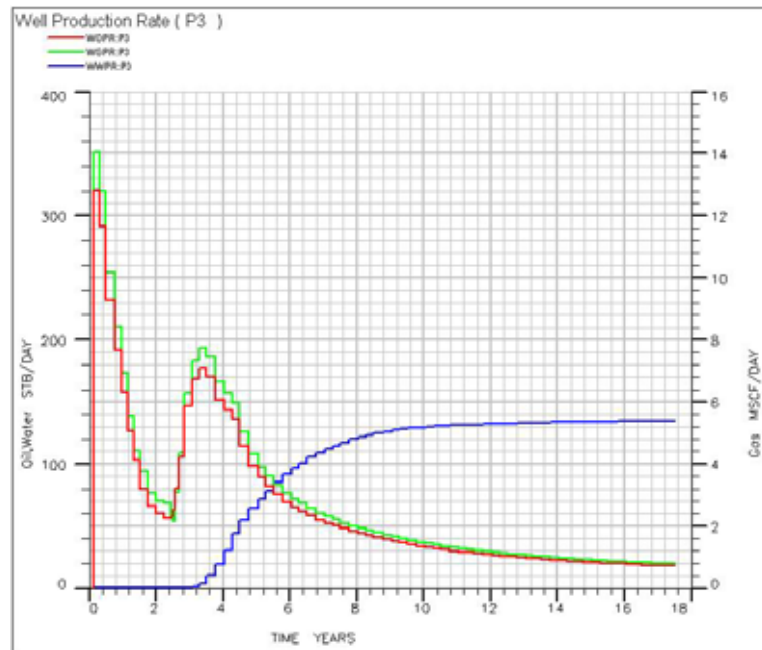


**Figure K-7** Oil, Water, and Gas Production Rate of Well P3 versus Time.

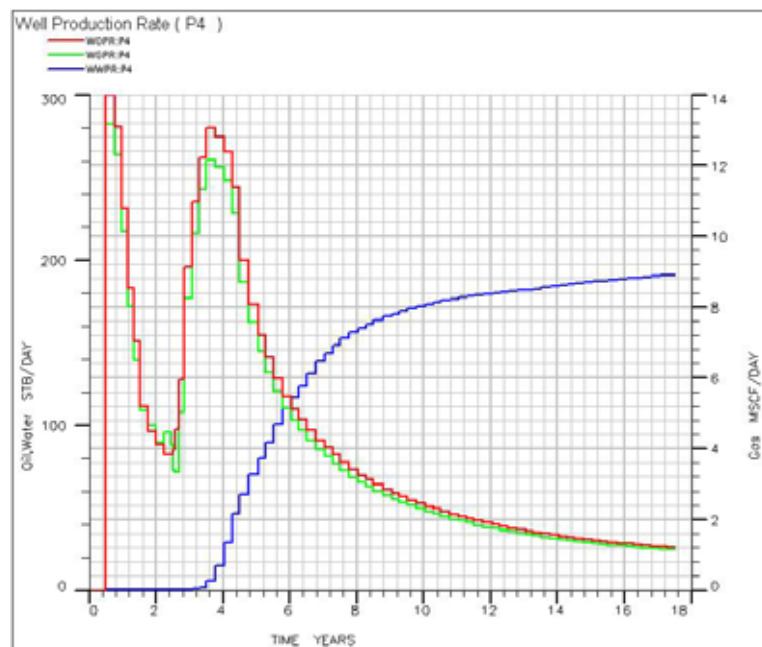


**Figure K-8** Oil, Water, and Gas Production Rate of Well P4 versus Time.

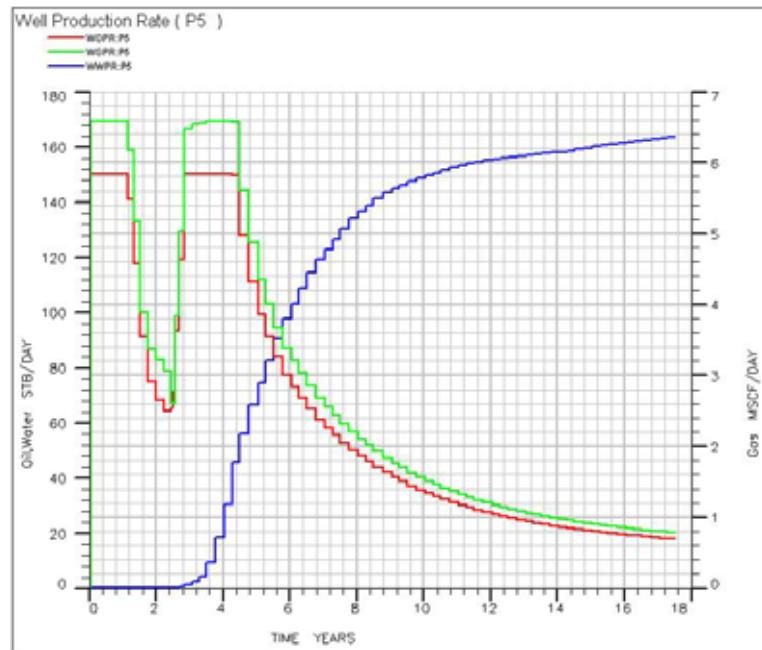


**Figure K-9** Oil, Water, and Gas Production Rate of Well P5 versus Time.

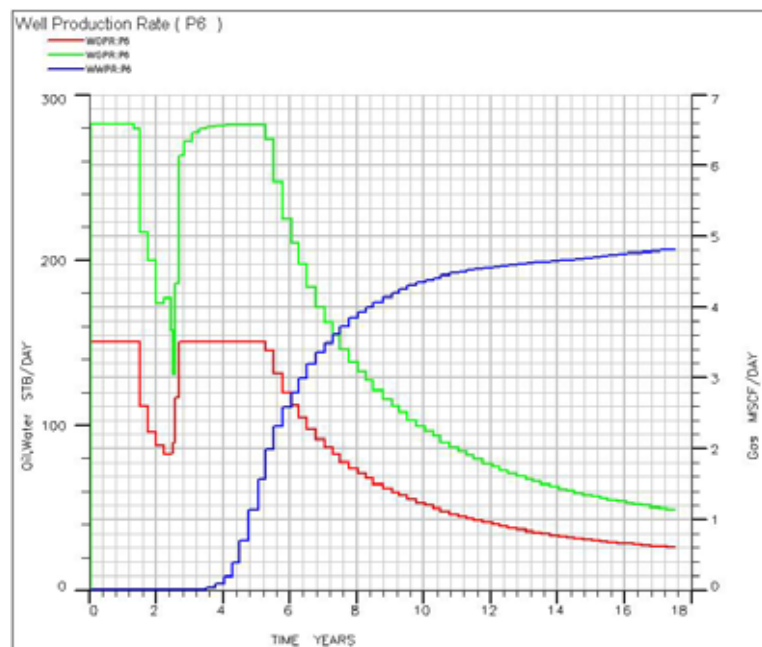


**Figure K-10** Oil, Water, and Gas Production Rate of Well P6 versus Time.

APPENDIX L

WELL RESULTS OF CASE 5

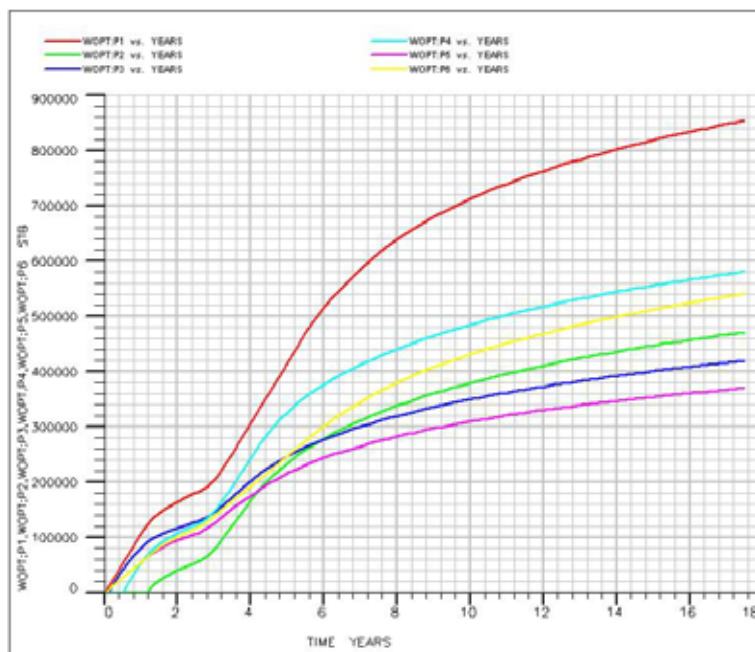


**Figure L-1** Cumulative Oil Production versus Time.

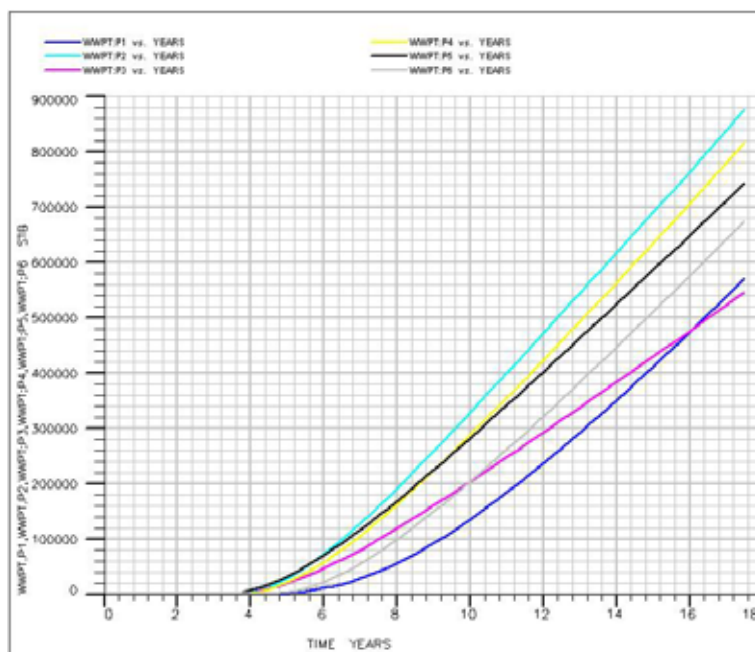


**Figure L-2** Cumulative Water Production versus Time.



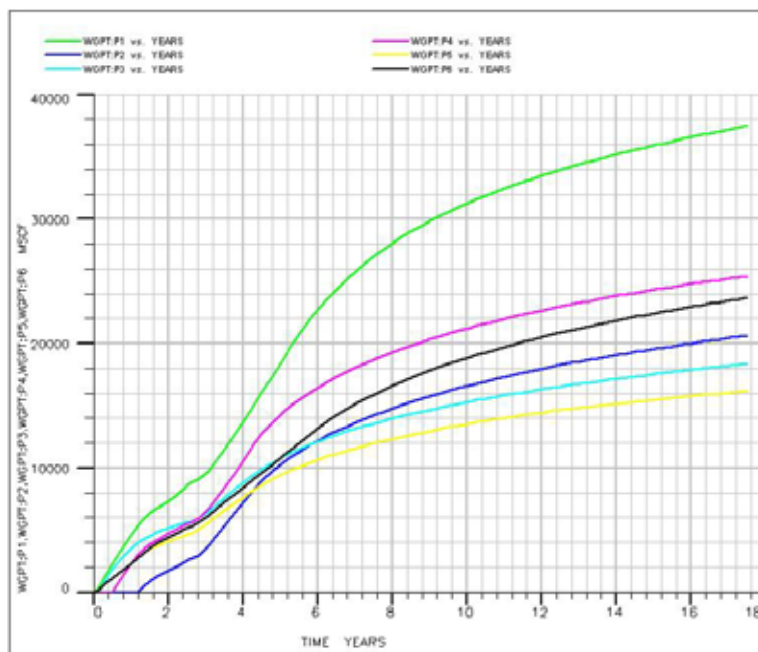


**Figure L-3** Cumulative Gas Production versus Time.

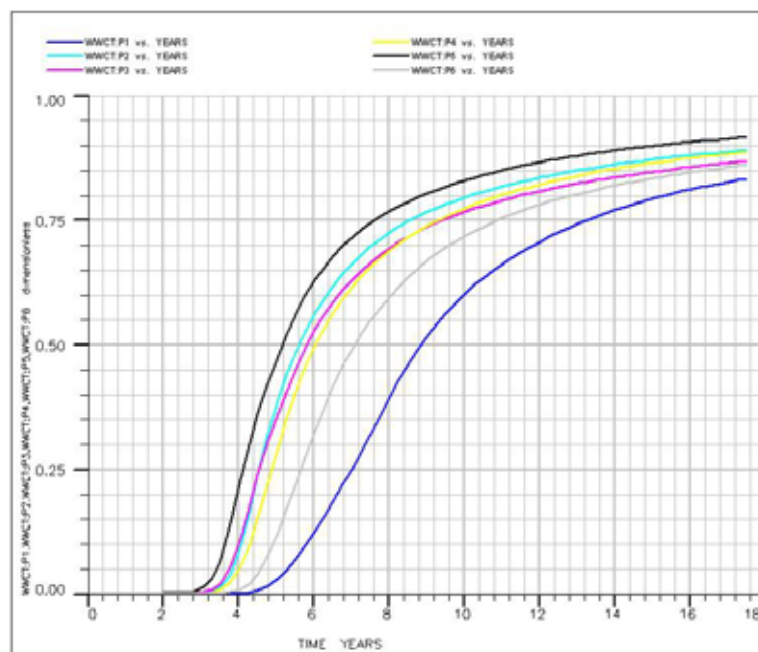


**Figure L-4** Water Cut versus Time.

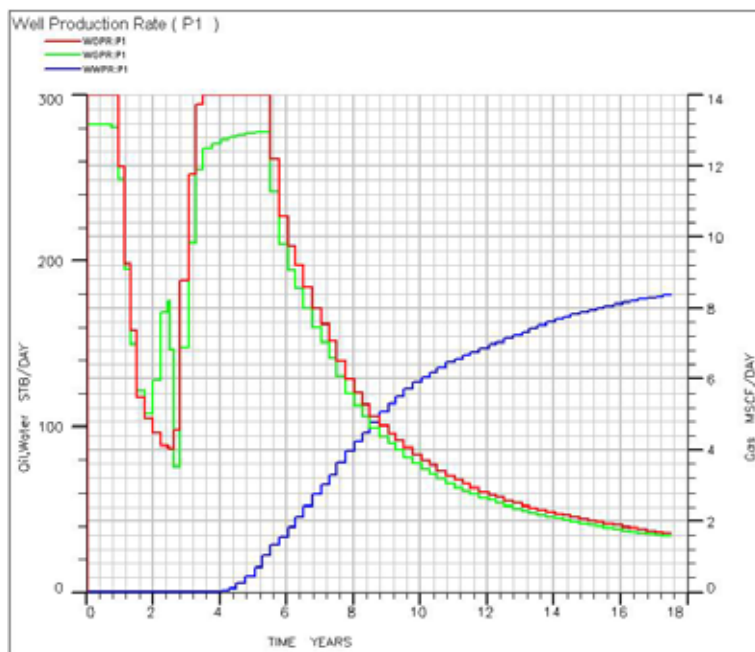


**Figure L-5** Oil, Water, and Gas Production Rate of Well P1 versus Time.

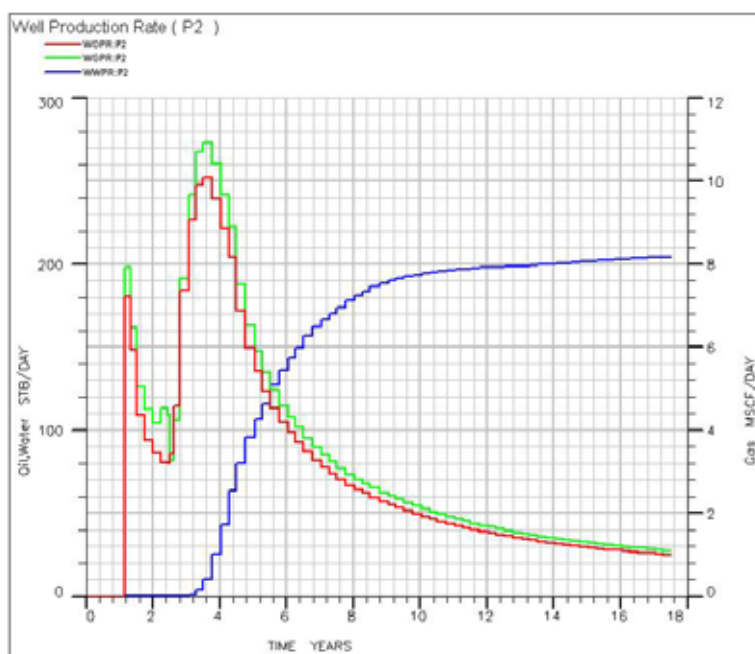


**Figure L-6** Oil, Water, and Gas Production Rate of Well P2 versus Time.

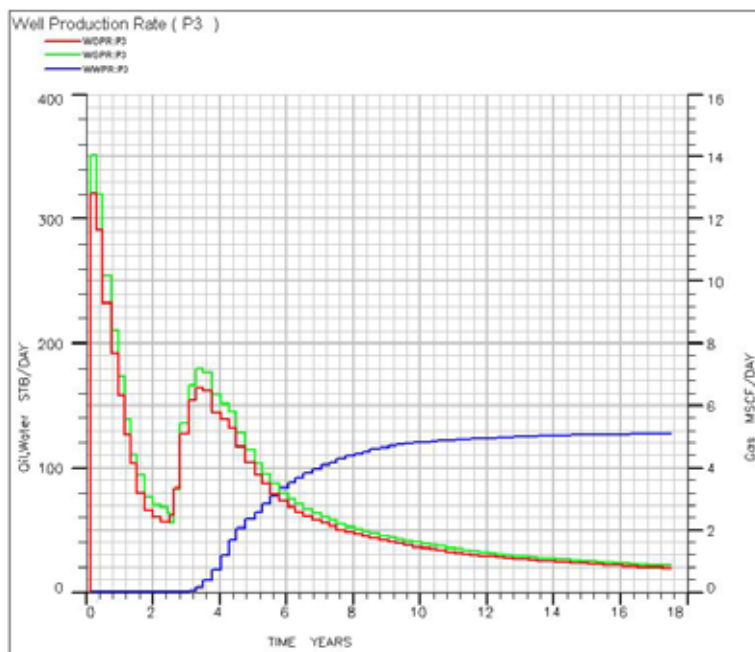


**Figure L-7** Oil, Water, and Gas Production Rate of Well P3 versus Time.

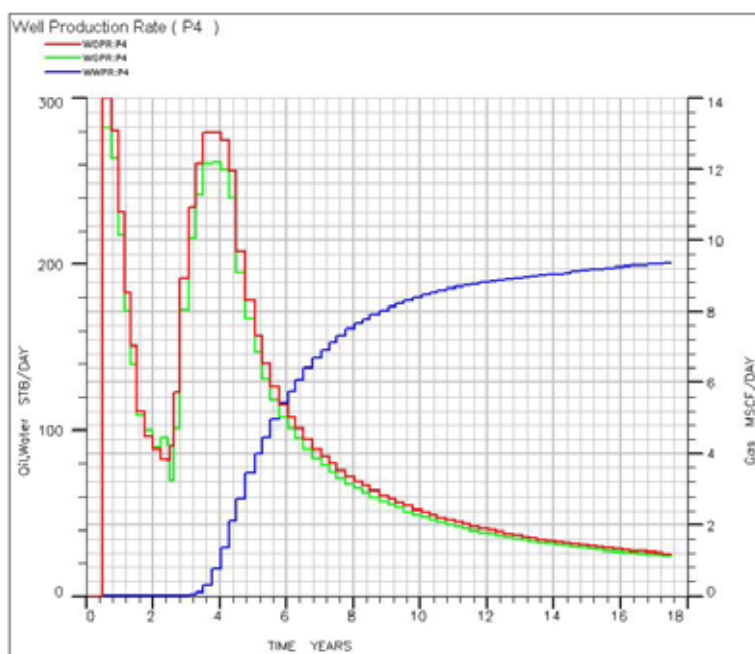


**Figure L-8** Oil, Water, and Gas Production Rate of Well P4 versus Time.

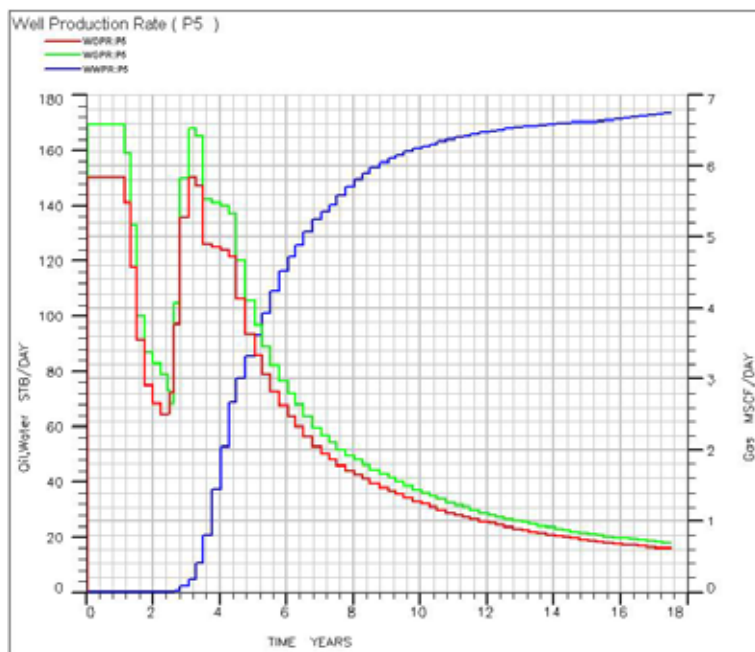


**Figure L-9** Oil, Water, and Gas Production Rate of Well P5 versus Time.

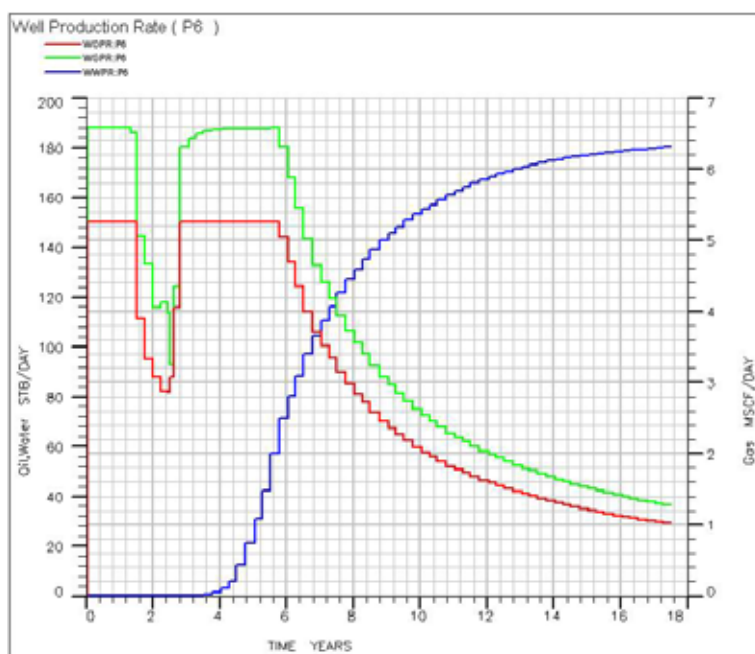


**Figure L-10** Oil, Water, and Gas Production Rate of Well P6 versus Time.

## **BIOGRAPHY**

Miss. Suwannee Rattanapranudej was born on the 19<sup>th</sup> of July 1977 in Nakhon Ratchasima province. She earned her Bachelor's Degree in Petroleum Engineering from Suranaree University of Technology (SUT) in 2000. After graduation, she continued with her master's degree in the School of Geotechnology, Institute of Engineering at SUT with the major in Petroleum Engineering. During 2001-2003, she was a teaching assistant and research assistant at SUT. Her strong background is in the areas of waterflooding, reservoir simulation, and reservoir management.